

**The use of (nano)oxides for metal
and metalloid stabilization in
contaminated soils**

PhD Thesis

Thesis supervisor: Prof. Dr. Michael Komárek

Thesis reviewers: Prof. Dr. Jurate Kumpiene
(Luleå University of Technology, Luleå)

Dr. Luke Beesley
(The James Hutton Institute, Aberdeen)

Dr. Petr Drahota
(Charles University, Prague)

Czech University of Life Sciences Prague

Faculty of Environmental Sciences

Department of Environmental Geosciences

Prague, 2016

The use of (nano)oxides for metal and metalloid stabilization in contaminated soils

Zuzana Michálková

Thesis

This thesis is submitted in fulfillment of the requirements for the PhD degree at the Czech University of Life Sciences Prague, Faculty of Environmental Sciences.

The use of (nano)oxides for metal and metalloid stabilization in contaminated soils.

Zuzana Michálková

Czech Univesity of Life Sciences Prague (2016)

Acknowledgement

First of all, I would like to thank to my supervisor Prof. Michael Komárek for giving me the trust and opportunity to work at the Department of Environmental Geosciences. I really appreciate his guidance, motivation, willingness and manager skills that were supporting me during the whole time of my study. I also wish to thank all my colleagues at the Department. I am very grateful for the team spirit and cooperation we can share and for so many friends. My thanks also go to Prof. Vojtěch Ettler for his valuable advices and consultations. I also wish to thank to Dr. Radek Fajgar and Dr. Zuzana Korbelová for their analytical work and shared knowledge. Finally, I would like to thank my parents and family for their love, background and support during all that long school years. The very last of my thanks goes to my beloved husband and children for filling my life with love and joy.

The experimental work included in this PhD thesis was funded by the following research projects:

P503/11/0840 (Czech Science Foundation)
GA14-01866S (Czech Science Foundation)
15-07117S (Czech Science Foundation)
CIGA 20134209 (Czech University of Life Sciences)
CIGA 20154202 (Czech University of Life Sciences)
IGA 4240013123159 (Internal Grant Agency of the Faculty of Environmental Sciences, CULS Prague)

Abstract

The main objective of the thesis was to evaluate the potential of selected Mn and Fe (nano)oxides for the stabilization of metals and metalloids in contaminated soils. The research was focused basically on three materials - commercial nanomaghemite (Fe III), nanomagnetite (Fe II,III) and a synthetic amorphous Mn oxide (AMO). The main aim of the work was to provide a complex view on the chosen stabilizing amendments regarding not just their direct influence on contaminants mobility and stabilization mechanisms, but also their stability and alterations in soil conditions together with influence on soil microorganisms and higher plants. Firstly, adsorption properties of the tested materials towards Cd, Cu, Pb and As were investigated. In this context, the most effective material showed to be the AMO reaching one to two orders of magnitude higher adsorption capacities than Fe III and Fe II,III under given experimental conditions. Interestingly, the rate of As(V) adsorption onto AMO was increasing with increasing pH as a result of high pH_{zpc} of the AMO (8.1) and significant dissolution of this phase at lower pH values. As a next step, the influence of (nano)oxides on metal(loid)s mobility and other physico-chemical soil characteristics after application to contaminated soil was examined. Again, the AMO proved to be the most efficient in reducing mobile pools of Cd, Cu, Pb, Zn and As. On the other hand, Fe III and Fe II,III addition had generally less significant effects on contaminants mobility. AMO application further resulted in an increase of soil pH connected with AMO dissolution and unwanted decomposition of soil organic matter. When (nano)oxides alterations in soil conditions were observed, $MnCO_3$ coatings were identified on AMO surface while no significant changes were recorded for Fe III and Fe II,III. As the $MnCO_3$ formation was connected with increased AMO stability, AMO particles synthetically covered with $MnCO_3$ coating (denoted as SM-AMO) were prepared. Although the SM-AMO had a lower mass loss in soil than pure AMO, the stabilizing efficiency was almost the same for both materials. The differences in surface composition of both materials were decreasing with time as $MnCO_3$ naturally precipitated on the AMO surface in soils while the SM-AMO coating was gradually dissolving. When investigating the effect on soil microbiota, AMO efficiently promoted soil microbial activity while no significant changes were observed in the case of Fe III and Fe II,III. The AMO was also able to reduce the uptake of Cd, Pb and Zn by sunflower (*Helianthus annuus* L.), eliminate Zn phytotoxicity symptoms and increase biomass yield. On the other hand, toxic levels of Mn released from the AMO in an acidic soil were found in sunflower tissues. AMO application is thus recommended for contaminated neutral or slightly alkaline pH with a higher cation exchange capacity in order to avoid unwanted release of Mn. Finally, various types of AMO-biochar composite sorbents were recently prepared and field experiment focused on stabilization of Cd, Pb, Zn and As using studied materials is currently under preparation. The combined results from the thesis highlight the importance of a complex experimental approach dealing with all parts of the contaminated soil environment in order to obtain complete information about the efficiency and usefulness of any newly developed stabilizing amendment.

Abstrakt

Hlavním cílem předkládané dizertační práce bylo zhodnocení potenciálu vybraných (nano)oxidů Fe a Mn pro stabilizaci kovů a polokovů v kontaminovaných půdách. Výzkum byl zaměřen především na tři materiály – komerční nanomaghemit (Fe III) a nanomagnetit (Fe II,III) a nově syntetizovaný amorfní oxid Mn (AMO). Hlavním cílem práce bylo poskytnout komplexní pohled na vybraná stabilizační činidla, přičemž důraz nebyl kladen pouze na jejich přímý vliv na mobilitu kontaminantů, ale též na jejich stabilitu a transformace v půdním prostředí, spolu s vlivem na půdní mikroorganismy a vyšší rostliny. Nejprve byly u testovaných materiálů zjištěny jejich adsorpční vlastnosti. V tomto případě se jako nejúčinnější ukázal AMO, který za daných experimentálních podmínek vykazoval o 1 až 2 řády vyšší adsorpční kapacity než Fe III a Fe II,III. Míra adsorpce As(V) na AMO se zvyšovala se zvyšujícím pH, což je v případě AMO způsobeno jeho vysokým pH_{zpc} (8,1) a vyšší rozpustností při nižších hodnotách pH. Dále byl sledován vliv aplikace (nano)oxidů na mobilitu kovů a polokovů v půdě a další fyzikálně-chemické vlastnosti. Zde se AMO opět prokázal jako nejúčinnější činidlo pro snížení mobilní frakce Cd, Cu, Pb, Zn a As. Aplikace činidel Fe III a Fe II,III měla naproti tomu jen minimální či žádný efekt. Aplikace AMO dále vedla ke zvýšení půdního pH spojeného s rozpouštěním samotného materiálu a nežádoucí degradací půdní organické hmoty. Při studiu transformací (nano)oxidů v půdním prostředí byl na povrchu AMO identifikován nově vzniklý $MnCO_3$, zatímco na povrchu Fe III a Fe II,III nebyly pozorovány žádné významné změny. Vzhledem k tomu, že pozorovaná formace $MnCO_3$ byla spojená se vzrůstem stability AMO, byly uměle připraveny částice AMO pokryté vrstvou $MnCO_3$ (SM-AMO). Přestože SM-AMO prokázal v půdě menší hmotnostní ztrátu než AMO, stabilizační účinnost byla u obou materiálů téměř stejná. Rozdíly ve složení povrchů u obou materiálů v čase klesaly, neboť na povrchu AMO docházelo k precipitaci $MnCO_3$, zatímco povlak na SM-AMO se postupně rozpouštěl. Při zjišťování vlivu na půdní organismy AMO účinně podpořil půdní mikrobiální aktivitu, zatímco v případě Fe III a Fe II,III nebyly pozorovány žádné významné změny. AMO byl též schopen snížit koncentrace Cd, Pb a Zn přijaté slunečnicí (*Helianthus annuus* L.), eliminovat symptomy fyto toxicity Zn a zvýšit výnos biomasy. Na druhou stranu byly ve tkáních slunečnice zaznamenány toxické koncentrace Mn uvolněného z aplikovaného AMO. V závislosti na výsledcích této práce tedy doporučujeme aplikace AMO do kontaminovaných neutrálních až alkalických půd. Dále byly před nedávnem připraveny různé typy kompozitních sorbentů na bázi AMO a biocharu a v současné době je v přípravě polní experiment zaměřený na stabilizaci Cd, Pb, Zn a As v kontaminované půdě pomocí studovaných stabilizačních činidel. Výsledky této práce vyzdvihují důležitost použití komplexního experimentálního přístupu zahrnujícího všechny složky půdního systému při studiu nových stabilizačních činidel.

Table of contents

Chapter I	General introduction	1
Chapter II	Evaluating the potential of three Fe- and Mn-(nano)oxides for the stabilization of Cd, Cu and Pb in contaminated soils	37
Chapter III	Selected Fe and Mn (nano)oxides as perspective amendments for the stabilization of As in contaminated soils	61
Chapter IV	The pH-dependent long-term stability of an amorphous manganese oxide in smelter-polluted soils: Implication for chemical stabilization of metals and metalloids	87
Chapter V	Stability, transformations and stabilizing potential of an amorphous manganese oxide and its surface-modified form in contaminated soils	107
Chapter VI	The application of an amorphous manganese oxide effectively reduces metal(loid) uptake by sunflower (<i>Helianthus annuus</i> L.)	135
Chapter VII	Biochar coated by amorphous manganese oxide efficiently removes various metal(loid)s from aqueous solution	153
Chapter VIII	Summary	175
References		181
Curriculum vitae & List of publications		205

Chapter I

General introduction

Content

Problem outline	3
Metals and metalloids – sources and toxicity	3
Speciation, bioavailability and bioaccessibility of metal(loid)s	5
Factors influencing speciation and fractionation of metal(loid)s in soil	7
Surface charge and pH_{pzc}	7
Adsorption	9
Cation and anion exchange	16
Living organisms and speciation of metal(loid)s in soil	17
Determining the speciation and fractionation of metals and metalloids	18
Instrumental methods	18
Extraction methods	19
Speciation and fractionation in solid phase	21
Stabilization of metals and metalloids in contaminated soils	22
Iron and manganese oxides as stabilizing amendments	23
Iron oxides	23
Manganese oxides	31

Problem outline

Common methods for treating contaminated soils (e.g. soil excavation, encapsulation, in situ and ex situ washing/flushing, vitrification etc.) are not only costly and energy demanding but are also disruptive in the context of natural site conditions. With regard to limited monetary means provided for soil remediation and with emphasis on the environment and landscape protection, research into stabilization methods has increased (Kumpiene et al., 2008; Komárek et al., 2013). Oxides of Fe and Mn are an indigenous part of the soil environment with significant sorption properties (Essington, 2004). Research focused on nanomaterials, their utilization and general characterization is very progressive nowadays and research projects concerning this topic are widely supported. Nanoparticles of Fe and Mn oxides seem to be an efficient sorbent for risk elements due to their large active surface. However, further understanding of the mechanisms influencing behavior and stability of these particles in complex soil environments is needed (Komárek et al., 2013).

Metals and metalloids - sources and toxicity

This thesis deals with remediation of soils contaminated with metals and metalloids. As these materials are not able to degrade in the environment (in contrast to e.g., organic contaminants such as oil compounds, polychlorinated biphenyls etc.), they accumulate in time in soils and can only transform, migrate or be accepted by living organisms. Of these materials, we usually deal in remediation practice with the so called group of “risky elements”. This term is usually used for metals and metalloids occurring in the soil at trace concentrations (i.e., less than 0.01%) whose increased levels after reaching a toxicological threshold can pose a potential risk to living organisms. Although the most serious contamination is often caused by non-essential elements (As, Cd, Hg, Pb), essential elements (e.g. Cu, Cr, Zn) might also pose a potential risk at elevated concentrations (Adriano, 2001). Potential phytotoxicity and toxicity for soil microorganisms may also play a role in the degradation of vegetation cover exposing the soil to wind and water erosion. Thus this process can promote further mobility and spread of the pollution (Liphadzi and Kirkham, 2005). Elevated concentrations of potentially risk elements in soils can be

both of natural (geogenic) and anthropogenic origin. The main anthropogenic sources are summarized in **Table 1.1**.

Table 1.1

Main anthropogenic sources of risky elements (Alloway, 2013).

Risk element	Contamination source
Arsenic (As)	Ore processing, fossil fuels combustion, glass additives, agriculture (fertilizers, insecticides), veterinary medicals, wood preservatives
Cadmium (Cd)	Smelting industry (associated metal in Zn and Pb ores), agriculture (phosphate fertilizers), dye and plastic pigments, batteries, fossil fuels combusting, wood preservatives, ceramics
Copper (Cu)	Electrochemical material, alloys (brass, bronze), waste disposal, chemical industry, agriculture (fungicides), copper wires and plates, livestock manure
Chromium (Cr)	steel works, chemical industry, dye pigments, wood preservatives, tanning industry, metal coating, alloys, fossil fuels combusting
Mercury (Hg)	Ore processing, agriculture (herbicides, fungicides), electrochemistry, batteries, medicine (thermometers, dental amalgams), fossil fuels combusting
Lead (Pb)	Smelters, refineries, chemical industry, accumulators, pigments, lead glass, ceramics, agriculture (fertilizers, pesticides), fossil fuels combusting, leaded petrol, shooting and military activities
Zinc (Zn)	galvanization and corrosion of galvanized materials, smelting industry, dye and ceramic glaze pigments, alloys (brass, bronze), agriculture (pesticides), communal waste, livestock manure, battery manufacture, catalysts, printing and graphics

From the toxicological point of view, lipophilicity is a crucial property of potentially risky elements implicating their ability to accumulate in living organisms, especially in intestines and bones (Jorgensen et al., 2010). For example, Pb accumulates in bones, disrupts hemoglobin synthesis and harms the nervous system. Its ability to permeate the placental barrier can also lead to teratogenic effects. Lead is treated as a human carcinogen (United Nations, 1998). Cadmium has a strong tendency to accumulate in the human body and has a long biological half-time, which is supposed

to vary between 10 and 20 years (Salt et al., 1997). The Itai itai disease was the most famous case of chronic Cd poisoning emerging in the Jinzu river basin (Japan) after the Second World War (Inaba et al., 2005; Shuto, 2005). As Cd accumulates in renal tubules, it harms their function and thus it affects calcium metabolism. Calcium is then mobilized from the skeletal stores causing decalcination of the skeleton leading to osteomalacia (Massaro et al., 1997). Exposure to As takes place predominantly through drinking water. Soluble inorganic As compounds are commonly more toxic than the organic ones (Villaescusa and Bollinger, 2008). The As(III) was classified as a human carcinogen harming the nervous system. Mutagenic and teratogenic effects were also demonstrated (Adriano, 2001). The cases of acute or chronic intoxication with Cu in mammals (including humans) are quite rare due to a high Cu tolerance and the liver and kidney biochemical systems able to detoxify excess Cu. The majority of problems with accumulation of Cu in human body thus arise precisely in the cases of genetic metabolic disorders, such as Wilson's disease (Wright and Welbourn, 2002). On the other hand, Cu is extremely toxic to many aquatic and marine organisms, such as algae or phytoplankton, and also to microorganisms like bacteria or fungi (Jorgensen et al., 2010).

Speciation, bioavailability and bioaccessibility of metal(loid)s

Adriano (2001) defines bioavailability as a potential for living organisms to take up chemicals from food or from the abiotic environment to the extent that the chemicals may become involved in the metabolism of an organism. Vangronsveld and Cunningham (1998) refer to the fraction of the total chemical that can interact with a biological target. Due to the lack of uniformity of the term "bioavailability" across various scientific (e.g., toxicology versus biogeochemistry) fields, Semple et al. (2004) suggested a distinction between bioavailable and bioaccessible compounds: the term bioavailable represents a substance which is "freely available to cross an organism's cellular membrane from the medium to the organism at a given time." Bioaccessibility thus should correspond to the compound that is "available to cross an organism's cellular membrane from the environment, if the organism has access to the chemical." Reeder et al. (2006) in their review generalized bioaccessibility as a process including solubilization of metals from geomaterials and bioavailability as an absorption across the biological membrane.

Bioavailability/bioaccessibility of targeted compound can thus be influenced both by the nature of accepting organism and the chemical itself (physical-chemical properties, concentration etc.), both by the environmental factors (in soil e.g., pH, cation exchange capacity, type and the concentration of organic matter, redox potential, amount of Fe, Mn oxides and clay minerals etc.). Processes influencing the speciation and distribution of trace elements in soil are schematically described in **Fig. 1.1** (Adriano, 2001).

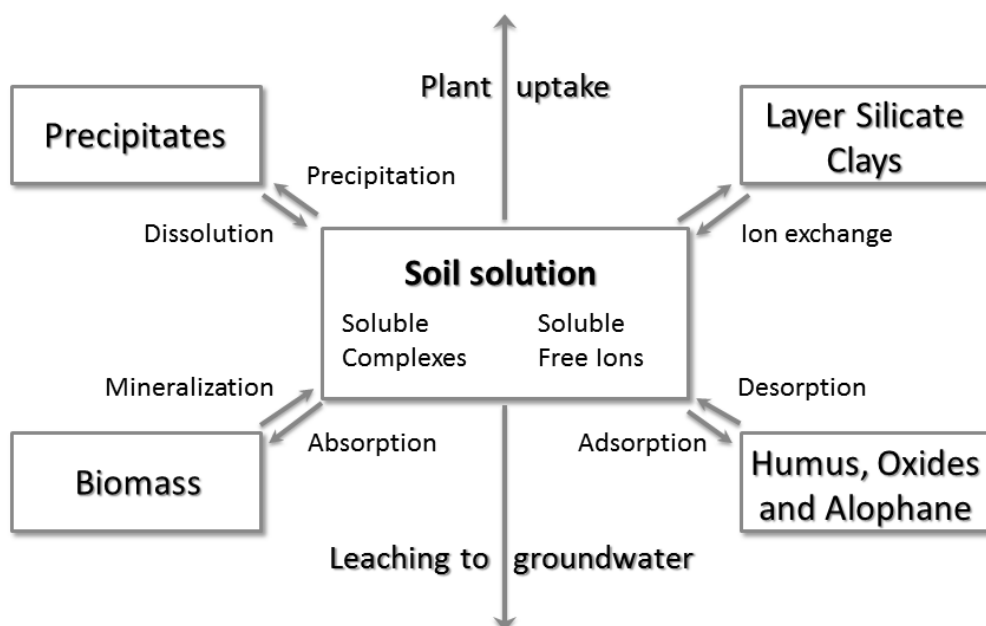


Figure 1.1

Diagram of main processes affecting trace elements behavior and distribution in soil conditions; adapted according to Adriano (2001).

Bioavailability/bioaccessibility of a given metal(loid) is closely connected with its speciation as it gives information on distribution of an element amongst defined chemical species (i.e., specific forms of an element differing in oxidation state, stoichiometry, coordination, complexation, association with other phases etc.) in a system (Templeton et al., 2000). These properties govern chemical behavior and mobility of targeted species both in the environment and living organisms and play

the main role in a potential element toxicity (Reeder et al., 2006). Even so, determination of a direct chemical species in environmental matrices is often complicated or even impossible. For this reason, the chemical species of a given element can be sorted into fractions based on their chemical (e.g., bonding, reactivity) or physical (e.g., size, solubility) properties. In this case, we thus speak about fractionation of a given element (Templeton et al., 2000). Fractionation analyses present a widespread and useful tool in environmental practice and will be described in more detail further in text.

Factors influencing speciation and fractionation of metal(loid)s in soil

Surface charge and pH_{pzc}

Electric charge on the surface of soil particles originates from two main mechanisms. The first one is the isomorphic substitution in crystal lattice of clay minerals when the ion with higher valence is exchanged with the ion with lower valence (e.g., octahedral Al^{3+} can be replaced with Mg^{2+} , tetrahedral Si^{4+} with Al^{3+}). Lack of protons thus generates on the mineral surface a permanent negative charge (Sposito, 2008). The degree of this exchange depends on the size and valence of the ions involved and it occurs only when the ions are of comparable size (Tan, 2011). The second mechanism relates to the dissociation (deprotonation) of the hydroxyl (OH-) functional groups present on the surface of Al octahedral and Si tetrahedral layers in crystal lattice of clay minerals and on the surfaces of Fe, Mn and Al oxides. The dissociation reaction is pH-dependent, increasing at higher pH and decreasing at lower pH. This type of surface charge is thus pH-dependent and variable (Adriano, 2001).

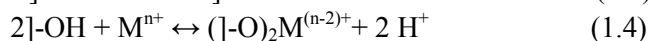
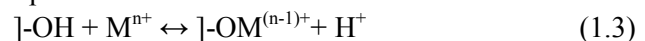
The protonation reaction at low pH runs as follows:



The deprotonation reaction at high pH runs as follows:



This type of charge is important for 1:1 clay minerals, Fe and Al oxide clays, and organic colloids (Tan, 2011). Dissociated surface hydroxyl functional groups can act as a Lewis base towards metal cations (McBride, 1994). Metals can form complexes with one or two deprotonated groups as follows:



As the exposed OH⁻ groups on clay surfaces can be protonated in acidic conditions due to proton (H⁺) addition from the soil solution, sorption of a large amount of H⁺ leads to a positive surface charge. Increased adsorption of metal ions at higher pH is thus a result of both the increasing density of negative surface charge and of the increasing concentration of M-OH⁺ species in the soil (Adriano, 2001). The electric charge is usually expressed in moles of charge per kilogram (mol_c kg⁻¹). It is possible to distinguish four different types of surface charge which together form the *net total particle charge*, denoted as σ_p (Essington, 2004). Each of these partial charges can be positive, zero, or negative, depending on the chemical conditions. *Structural (permanent) charge* (σ_0) arises as a result of isomorphous substitution of 2:1 clay minerals and cation vacancies on the Mn oxides surfaces. The *net proton charge* (σ_H) is inherent to soil humus and is defined as the difference between the moles of the protons and hydroxide ions complexed with surface functional groups (Sposito, 2008). The sum of the structural and net proton charge gives the *intrinsic charge* (σ_{in}) (Tan, 2011):

$$\sigma_{in} = \sigma_0 + \sigma_H \quad (1.5)$$

This charge represents only partial charges arising solely from the adsorbent structure.

The *net adsorbed ion charge* (Δq) is defined as follows:

$$\Delta q = \sigma_{IS} + \sigma_{OS} + \sigma_d \quad (1.6)$$

This charge includes the net charge of ions adsorbed as *inner-sphere complexes* (σ_{IS}), *outer-sphere complexes* (σ_{OS}) and the *diffuse-ion swarm* (σ_d). As Eq. (6) can be used only when the experimental distinction between inner- and outer-sphere complexes is possible, Eq. (6) can be simplified as:

$$\Delta q = \sigma_s + \sigma_d \quad (1.7)$$

where σ_s denotes as Stern layer charge, described as all adsorbed ions that do not belong to diffuse-ion swarm. The net total particle charge can thus be written as:

$$\sigma_p = \sigma_{in} + \sigma_s \quad (1.8)$$

consisting of a charge inherent to the adsorbent structure and a charge of adsorbed ions bound in surface complexes and thus not involved in diffusive motions. The net total particle charge (σ_p) is balanced with a charge of ions in a diffuse-ion swarm:

$$\sigma_p + \sigma_d = 0 \quad (1.9)$$

In order to maintain electroneutrality of the system, the structural charge and charge arising from the surface complexed protons or hydroxide ions is balanced with an equal counterion charge of all other adsorbed ions and H⁺ and OH⁻ in diffuse-ion swarm (Sposito, 2008).

Points of zero charge (pH_{pzc}) are defined as pH values at which one of the parts of a total net particle charge denoted in Eqs. (1.8) and (1.9) is equal to zero under the given conditions (temperature, pressure, solution chemism). Three standard definitions are summarized in **Table 1.2**.

Table 1.2

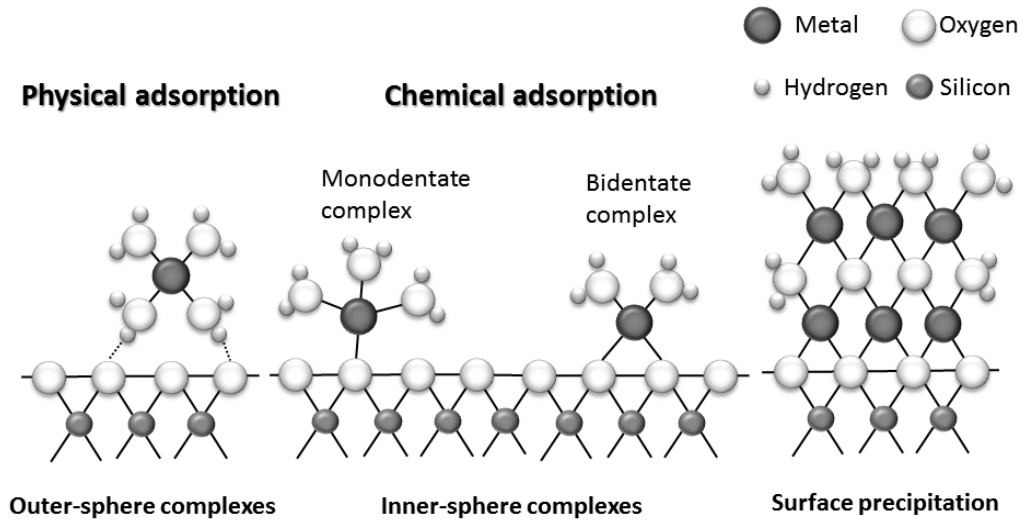
Definitions of distinct types of points of zero charge; adapted according to Sposito (2008).

Symbol	Name	Definition
p.z.c.	Point of zero charge	$\sigma_p = 0$
p.z.n.c.	Point of zero net charge	$\Delta q = 0$
p.z.n.p.c.	Point of zero net proton charge	$\sigma_H = 0$

The most widely used is the point of zero charge pHpzc , i.e., pH value at which σ_p (and also complementary σ_d) value equals zero. When the pH of a solution is lower than pH_{pzc} , the mineral surface bears a positive net charge. If the pH of a solution is higher, the mineral surface bears a negative net charge. Soil minerals with low pH_{pzc} (e.g., SiO_2) have a stronger ability to attract and bind cations over wide pH spectra than those with higher pHpzc due to their negative surface charge under common soil conditions. On the other hand, minerals with high pHpzc (e.g., $\alpha\text{-Al}_2\text{O}_3$) are better in binding anions over a wide pH range (Essington, 2004).

Adsorption

Adsorption is generally the most important physical-chemical process controlling the retention of organic and inorganic compounds in soil. It can be defined as a process occurring on soil particles surfaces resulting in accumulation of dissolved compounds (adsorbate) at the interface of solid (adsorbent) and aqueous phases (Adriano, 2001). Adsorption also differs from precipitation, i.e., a process in which the volume of a compound increases due to the three dimensional growth of a specific crystalline structure. Organic and inorganic compounds can be bound due to absorption as well. In this process, a compound diffuses into the three dimensional structure of a certain soil phase. This mechanism is often involved in retention of organic compounds by soil organic matter (SOM) (Essington, 2004).

**Figure 1.2**

Schematic representation of surface adsorption complexes; adapted according to Brown (1990).

Surface complexes originate when the surface functional group reacts with an ion or a molecule dissolved in the soil solution. There exist two types of surface complexes: the inner- and the outer-sphere complexes (**Fig. 1.2**). If an adsorbed ion is bound directly to the surface ligand, it is denoted as an inner-sphere complex. If there is at least one water molecule between an adsorbed ion and adsorbent surface, it is denoted as an outer-sphere complex (or non-specific or physical sorption) (Sposito, 2008). Outer-sphere complexes are bound to the surface with relatively weak electrostatic binds and are not significantly adsorbate-selective. Inner-sphere complexation is also denoted as specific or chemical sorption. This bond has a covalent character and a relatively high degree of structural configuration. It is possible to make a distinction between two types of inner-sphere complexes: monodentate and bidentate. A complex is denoted as monodentate, if one position in the coordination sphere of adsorbate is occupied by one surface functional group of adsorbent. If two positions are occupied, we speak about a bidentate complex (**Fig. 1.2**) (Essington, 2004). Specific adsorption is strongly pH-dependent and is connected with metal ions hydrolysis (Reeder et al., 2006). Metals easily forming hydroxy complexes are also bound with strong specific adsorption forces. For that reason, equilibrium reaction constant (pK) indicates adsorption behavior of a targeted metal (M):



A specific adsorption rate rises with an increasing pK value. In the case of Pb and Cu with equal pK values, Pb is adsorbed more strongly due to a larger ionic radius (Alloway, 1995). According to Tiller et al. (1984), the strength of specific adsorption of risk elements towards soil clay particles increases in the following order: Cd (pK = 10.1) < Ni (pK = 9.9) < Co (pK = 9.7) < Zn (pK = 9.0) << Cu (pK = 7.7) < Pb (pK = 7.7) < Hg (pK = 3.4). Hydrated Al, Fe and Mn oxides are considered to be the main elements involved in specific adsorption reactions.

Adsorption isotherms are a common tool used for describing the adsorption of various compounds (Limousin et al., 2007). Adsorption isotherms are non-mechanistic empirical models describing the partitioning of adsorbate between the solid and liquid phases as the dependence of an adsorbed amount per unit of adsorbent (q , units mmol kg^{-1} or mg kg^{-1}) on equilibrium concentration of adsorbate in solution (c_{eq} , units mmol L^{-1} or mg L^{-1}). Temperature, pressure and solution composition (pH and ionic strength) are considered to be constant (Essington, 2004). There exist 4 main curve types of adsorption isotherms (**Fig. 1.3**).

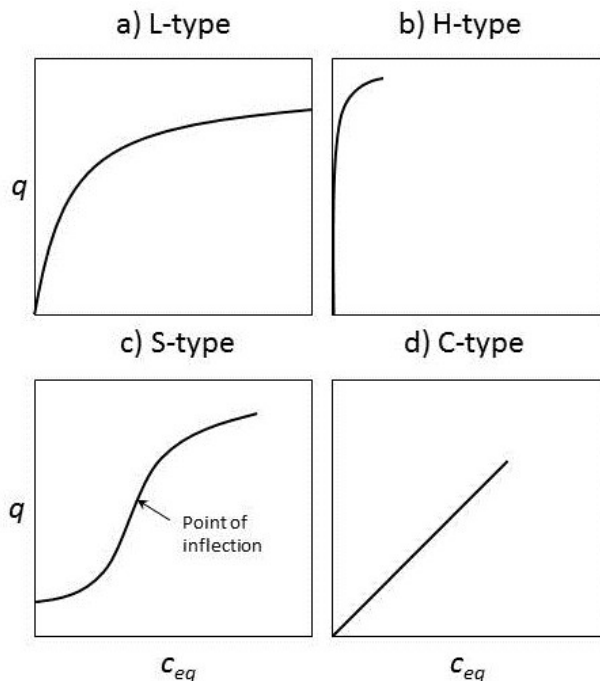


Figure 1.3

The most common shapes of isotherm curves in soil chemistry; adapted from Essington (2004) and Limousin et al. (2007).

L-curve isotherm is the most abundant type in soil chemistry. It is related to relatively high affinity of adsorbate to adsorbent surface at low surface coverage, decreasing with increasing coverage and thus suggesting progressive saturation of the solid (Limousin et al., 2007). **H-type** curve is an extreme case of L-isotherm characterized with a very steep initial slope (i.e., very high affinity). It is usually considered to mark occurrence of inner-sphere complexes (Essington, 2004). Adsorption of trace elements and non-polar organic compounds in the soil can be described by an **S-curve** isotherm. This curve is sigmoidal and thus owing a point of inflection (Limousin et al., 2007). Concerning metals, this curve type is usually observed in soils with high amounts of dissolved organic matter. If the concentration of adsorbate is low, the sorption is also low due to the competition between solid and aqueous phases. As an example, the adsorption of Cu in soil can be mentioned. If the concentration of Cu²⁺ ions is low, they become the subject of competition between soluble organic ligands and free adsorption sites on the soil sorption complex. When full saturation of soluble organic ligands is reached, preferential adsorption onto soil surfaces starts (i.e. point of inflection). Affinity towards the adsorbent increases significantly and the isotherm continues as an L-type (Essington, 2004). The initial slope of **C-curve** isotherm remains independent of the surface coverage or adsorbate concentration until certain adsorption maximum is reached. This adsorption behavior is typical for nonpolar hydrophobic compounds and is also termed as constant partitioning (Essington, 2004; Sposito, 2008).

Several mathematic models were developed for the description of adsorption isotherms. The simplest one is modeling using a distribution coefficient (K_d , units L kg⁻¹), describing constant partitioning of adsorbate between solid and aqueous phases:

$$K_d = q/c_{eq} \quad (1.11)$$

where q is the amount adsorbed per gram of adsorbent at equilibrium and c_{eq} is adsorbate concentration in the solution at equilibrium (Essington, 2004). Distribution coefficient is suitable for adsorption modelling of constant partitioning or when a very low concentration of adsorbate is present in the solution (Limousin et al., 2007).

Under soil conditions, concave adsorption curves (L- and H-type) are met most frequently. The most common models used for L- and H-isotherm modeling are the Langmuir (Langmuir, 1918) and Freundlich (Freundlich, 1909) models. The main difference between these two models is in inclusion of maximum sorption capacity in the case of Langmuir model. That is defined with the following equation:

$$q = b K_L c_{eq} / (1 + K_L c_{eq}) \quad (1.12)$$

where q is the amount adsorbed per weight unit of adsorbent (mmol kg^{-1} or mg kg^{-1}), b is maximal adsorbed amount (units are the same as for q), and K_L is the rate of adsorbate/adsorbent affinity (Essington, 2004). Langmuir model assumes that: i) all adsorption sites are identical, ii) each adsorption site binds one molecule of adsorbate and iii) all sites are energetically independent of adsorbate concentration (Limousin et al., 2007).

Freundlich empirical model is often used for L-, H- and C- curves, describing adsorbed amount (q) as a function of adsorbate concentration in a solution at equilibrium (c_{eq}):

$$q = F c_{eq}^n \quad (1.13)$$

where F (L kg^{-1}) and n (dimensionless, $0 < n < 1$) are positive constants (Essington, 2004; Limousin et al., 2007). It is usually assumed that these constants do not possess any specific physical meaning. Despite this, it was mathematically demonstrated that the n value can be treated as a marker of adsorption sites heterogeneity on adsorbent surface. Adsorption sites heterogeneity arises as n approaches zero. Conversely, as n approaches 1, homogeneity of adsorption sites arises (Sposito, 2008).

In order to properly construct adsorption isotherms, equilibrium adsorption time under given conditions has to be known. Additionally, information on the adsorption kinetics rate can provide additional information on the prevailing adsorption mechanism type in a given system (Febrianto et al., 2009). Several adsorption kinetic models have been proposed. Amongst them, pseudo-first and pseudo-second order kinetic models are the most widely used for the description of metals/metalloids adsorption onto adsorbents for environmental cleanup (Febrianto et al., 2009; Gupta and Bhattacharyya, 2011; Ho, 2004; 2006).

Probably the first known example describing the rate of adsorption in the liquid-phase system is the Lagergren pseudo-first order model (Lagergren, 1898). In its integrated form, it can be written as:

$$\ln(q_e - q_t) = \ln q_e - k_1 t \quad (1.14)$$

where q_e and q_t are the amounts of adsorbate adsorbed per unit mass at equilibrium and at given time t . The pseudo-first order kinetic rate (k_1) can be calculated from the slope of the linear plot of $\ln(q_e - q_t)$ versus t (Gupta and Bhattacharyya, 2011). Although widely used, discrepancies in a pseudo-first

order kinetic model occur in most systems and higher order kinetic models thus have to be tested (Febrianto et al., 2009; Gupta and Bhattacharyya, 2011; McKay et al., 1999).

The pseudo-second order equation was found to be more suitable in most studies for fitting the experimental data rather than the pseudo-first order equation (Febrianto et al., 2009). It can be integrated and linearized to:

$$t/q_t = 1/(k_2q_e^2) + (1/q_e) \cdot t \quad (1.15)$$

where k_2 is the second order kinetic rate and q_e and q_t are the amounts of adsorbate adsorbed per unit mass at equilibrium and at a given time t . Based on theoretical estimates and published results, it seems that the k_2 value usually depends on the initial adsorbate concentration when it increases with the decreasing initial adsorbate concentration (Gupta and Bhattacharyya, 2011; Rudzinski and Plazinski, 2006).

Surface complexation models (SCMs) were developed as a tool for describing chemical reactions and associated equilibrium constants involved in adsorption (Essington, 2004). In contrast to empirical model such as adsorption isotherms, the “intrinsic” equilibrium constants (K^{int}) obtained from SCMs are much less system-dependent. The derived K^{int} values usually depend solely on the type of the solid and adsorbate, in some models also on ionic strength, but not on the pH or adsorbate concentration as in the case of empirical models (Koretsky, 2000). However, the strength of the SCMs is in their ability to predict the distribution of the compound between the adsorbed and aqueous phase (Essington, 2004).

Many various types of SCMs exist according to the treatment of the electrostatic layer. The most commonly used are the constant capacitance model (CCM), the diffuse layer model (DLM) and the triple layer model (TLM), all of them using the so called 2-pK approach (Lützenkirchen, 1998). The 2-pK models are based on reactive surface hydroxyl groups (SOH) undergoing both protonation (Eq. 1.16) and deprotonation (Eq. 1.17) reactions (Goldberg, 2013):



Another concept of SCM is referred as the 1-pK approach and is originally based on Stern model. Here, surface functional groups bind either one or two protons, i.e., SOH

or SOH_2 , respectively. Surface charging can be thus expressed with one reaction (Goldberg, 2013):



The major advantage of the 1-pK model over the 2-pK model is a reduction of adjustable parameters as the stability constant from Eq. (1.18) ($K=10^{\text{PPZC}}$) can be experimentally determined as the pristine point of zero charge (PPZC) of a solid (Lützenkirchen, 1998).

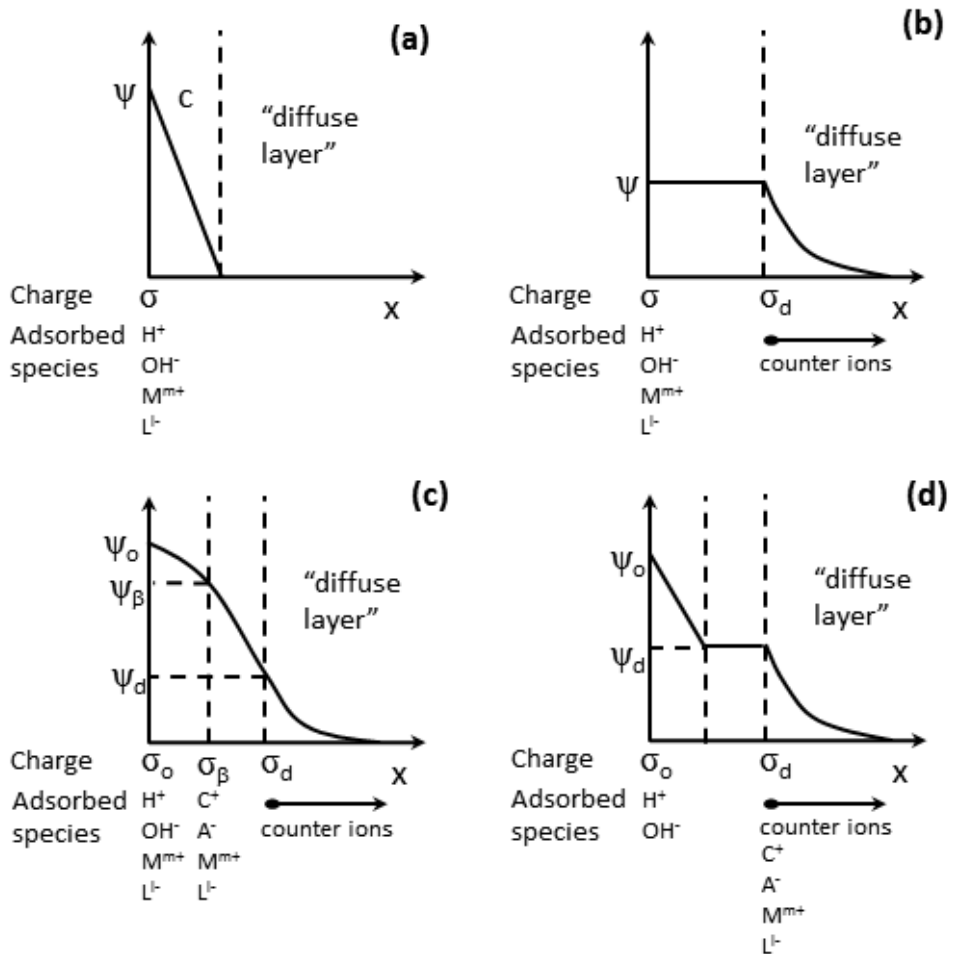


Figure 1.4

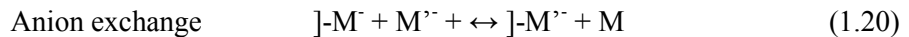
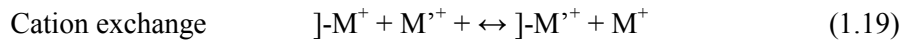
Location of ions, potentials and charges in the constant capacitance model (a), diffuse-layer model (b), triple-layer model (c) and 1-pK model (d); adapted according to Goldberg (2013) and Koretsky (2000). Ψ : electric potential, x : distance from the surface, M^{m+} : metal ion of the charge m^+ , L^- : ligand of the charge l^- , C^+ : cation, A^- : anion.

Various SCMs differ in their assumptions concerning the location and surface configuration of the adsorbed ions (**Fig. 1.4**). In the constant capacitance model (**Fig. 1.4a**) and diffuse-layer model (**Fig. 1.4b**), all surface complexes are bound as inner-sphere in a single surface plane. Additionally, the diffuse-layer model contains a diffuse layer extending from a d-plane to solution. In the case of the triple-layer model (**Fig. 1.4c**), inner-sphere complexes are located in a surface o-plane, while the outer-sphere complexes are located in the β -plane situated between the o-plane and the d-plane. In the 1-pK model based on Stern model (**Fig. 1.4d**), inner-sphere complexes are formed by protons and hydroxyls in the o-plane, while all other ions bound as outer-sphere complexes adsorb in the d-plane (Goldberg, 2013).

Most SCMs assume that all surface hydroxyl groups of a given adsorbent to be completely homogenous (i.e., so called single-site models). Yet, in reality, many types of surface hydroxyl groups with different reactivity may be found on a single mineral plane. To cope with this problem, differences in site reactivities are in single-site SCMs averaged to the equilibrium constants. The disadvantage of this approach thus lies in limiting the applicability of such constants to materials with similar morphology and surface composition as those from which the constants were experimentally derived (Koretsky, 2000). For this reason, the multi site complexation models, such as MUSIC model (Hiemstra et al., 1989a,b), have been proposed. In this case, the model operates with six types of surface groups – singly, doubly or triply coordinated surface oxygen atoms bound to one or two surface protons. Although still simplified, this model presents an improvement compared to simple-site models. The difficulties may rise in multi-site models from the large number of fitting parameters needed to use experimental data to determine equilibrium constants for each site type (Koretsky, 2000).

Cation and anion exchange

Cation (anion) exchange refers to a process when, for the aim of sustaining the electroneutrality, ions adsorbed in inner-sphere and diffuse-ion swarm are bound to particle surface with electrostatic forces. The binding force is in this case directly proportional to the ion charge/radius ratio (i.e., ionic potential). These ions can be exchanged with free ions in solution (Essington, 2004). If the soil pH drops below the pH_{pzc} of clay particles, a positive charge arises and particles are able to bind anions. Cation (anion) exchange can be described as:



Cation exchange is stoichiometric (i.e., two Na^+ ions exchanges with one Ca^{2+} ion), fast and reversible. The order of exchange depends on the ratio of ion affinity towards the charged surface site or water molecules. The most abundant cations in soil solution (i.e., Ca^{2+} , Mg^{2+} , K^+ , Na^+) are generally only weakly bound in soils. By contrast, most trace elements are bound in soil much strongly. Bond stability generally decreases in the following order: $\text{Al}^{3+} > \text{H}^+ > \text{Ca}^{2+} > \text{Mg}^{2+} > \text{K}^+ > \text{NH}_4^+ > \text{Na}^+$ (Adriano, 2001). Soil cation exchange capacity (CEC) is defined as the maximum moles of charge of adsorbed ions, which can be desorbed under given conditions (temperature, pressure, soil solution chemistry and solid/liquid ratio). It is usually denoted in moles (centimoles) of charge per kilogram ($\text{cmol}_c \text{ kg}^{-1}$) (Sposito, 2008).

Living organisms and speciation of metal(loid)s in soil

Many various species of microorganisms and invertebrates occurring in soils play a irreplaceable role in the soil system dynamics. They accelerate degradation of organic matter, mineralization and humification processes and participate in the transport of elements through the soil profile (Paul et al., 2007). Microorganisms are also able to mediate transformations of certain metal(oids) (e.g. As, Cr, Hg, Mn, Se, Sn) due to oxidation-reduction and methylation demethylation reactions. An important feature is their association with plant roots. Microbial populations in rhizosphere are 10-100 times more abundant than in bulk soil. That is caused by easily available energy sources originating from root exudates. Specific associations of plants and microbes as vesicular-arbuscular mycorrhiza or ectomycorrhiza play a major role in plant nutrition and trace elements uptake (Adriano, 2001).

Organic carbon, especially dissolved organic carbon (DOC) is an important compound for many biogeochemical processes, e.g. erosion, mobility, availability and transport of metals or acid-base reactions (Sposito, 2008). The DOC in soil can be divided into two main groups: i) low-molecular organic compounds (e.g. polyphenols, amino acids, sugars etc.) and ii) water soluble humic and fulvic acids. Humic and fulvic acids are usually prevalent in soil with only the exception of rhizosphere where low-molecular organic compounds originating from root exudates prevail. Root exudates contain wide spectra of aliphatic organic acids from whom many are able to form complexes with metals (Adriano, 2001). The most common organic acids

identified in root exudates are citric, fumaric, malic, malonic, tartaric and succinic acid (Chang et al., 2004). Exudation of organic compounds can influence the solubility and metal uptake by plant in direct (acidification, chelation, precipitation, changes in redox conditions) or in indirect ways (stimulation of microbial activity, influence on physical properties of rhizosphere and dynamics of root growth) (Adriano, 2001).

Chemical reactivity of humus can be estimated according to its total acidity which is the sum of titration acidity of carboxylic (-COOH) and phenolic (-OH) functional groups. Protons from carboxylic groups start to dissociate around pH 3 producing a negative charge. This charge elevates together with increasing pH and around pH 9, phenolic groups start to dissociate too. This phenomenon is the reason of variable (pH-dependent) charge of humus polymers. This charge enables adsorption of cations, complexation with metals and association with clay minerals and oxides (Adriano, 2001).

Determining the speciation and fractionation of metals and metalloids

Several methods exist for the determination of metal(loid)s speciation and fractionation both in liquid, solid and gaseous phases. The choice of suitable technique depends predominantly on the type and phase of a targeted element and the analysis purpose.

Instrumental methods

High performance liquid chromatography (HPLC) methods with various modifications are probably the most widely used techniques for speciation assessment of As, Se and Sb. This separation technique is based on the different velocity of analytes passing through the column that is caused by different adsorption abilities, solubility or other properties between mobile and stationary phases. Separated analytes are finally eluted at different characteristic retention times and analyzed using a sensitive detector such as inductively-coupled plasma mass spectrometer (ICP-MS), inductively-coupled plasma optical emission spectrometer (ICP-OES) or fluorescence spectroscopy (AFS) (Komorowicz and Barańkiewicz, 2011; Wu and Sun, 2016).

Besides chromatographic methods, hydrid generation (HG) presents another wide-spread separation technique often used for As speciation in environmental samples (González et al., 2003; Koh et al., 2005; Matos Reyes et al., 2008). The method is based on the reaction of As compounds with tetrahydroborate in acidic medium that produces various arsines differing according to initial As species. These generated arsines can be subsequently separated due to different boiling points. The HG unit is usually coupled with suitable detector as atomic absorption spectrometer (AAS), AFS, ICP-MS or ICP-OES (Anawar, 2012). Although hyphenated techniques became very popular in speciation analyses, traditional chemistry-based separation methods are still useful and robust as well. We can name e.g., liquid-liquid extraction (LLE), when the different species are separated based on their solubility in two immiscible liquids, cloud-point extraction (CPE), when the analytes are selectively extracted by non-ionic surfactant separated from aqueous phase above specific critical temperature or solid-phase extraction (SPE), when the analytes pass, interact and retain on the stationary phase, from where are subsequently eluted with specific solvent (Wu and Sun, 2016).

Extraction methods

In spite of certain drawbacks such as low selectivity of extracting agents, readsorption or precipitation, the simple and sequential extraction methods remain an irreplaceable technique used for determination of metals and metalloids in soils and sediments (Adriano, 2001; Gleyzes et al., 2002, Reeder et al., 2006). It gives information on the partitioning of metal(loid) among distinct soil phases and can be thus useful for observing metal(loid) fluxes among these phases (e.g., before and after remediation) (Adriano, 2001). The general principle of sequential extraction techniques lies in a stepwise extraction of one sample with more extracting agents in the order ranging from less to more aggressive. The extractant should be selective, i.e., able to release only defined metal(loid) fraction attached to a specific soil phase. Many various extraction schemes with different numbers of extraction steps (usually 4-7) have been developed. Probably the most widely used method (including its variations) remains the basic scheme developed by Tessier et al. (1979) more than 30 years ago. That consists of a targeted element partitioning into 5 operationally-defined fractions: exchangeable, bound to carbonates (acid soluble), bound to Fe and Mn oxides (reducible), bound to organic matter (oxidizable) and residual (Adriano, 2001; Gleyzes et al., 2002).

Exchangeable fraction involves weakly sorbed metal species, especially those bound to particle surface with relatively weak electrostatic bonds or released by ion exchange (Gleyzes, 2002). Agents used for extracting this fraction are electrolytes in aqueous solution (e.g., MgCl_2 , $\text{CH}_3\text{COONH}_4$, CaCl_2 , KNO_3) at pH 7 (Rauret, 1998). **Carbonate-bound fraction** is sensitive to pH changes and its release occurs at pH close to 5. A buffered acetic acid/sodium acetate solution is generally used (Gleyzes, 2002). Under these conditions, metals coprecipitated with carbonates, but also specifically sorbed to certain sites on clay, SOM and Fe/Mn oxides surfaces are released (Pickering, 1986). **Reducible fraction** aims to represent metal fraction bound to hydrated Fe, Mn and Al oxides. By controlling the extractant pH and Eh, all or just certain metal phases bound to oxides can be dissolved (Gleyzes, 2002). The most effective agents targeting total reducible fraction are those containing both a reducing agent and a ligand able to maintain the released ions in soluble form. The most widely used extractants are hydroxylamine, oxalate/oxalic acid buffered solution and sodium dithionite (Pickering, 1986; Gleyzes, 2002). **Oxidizable fraction** relates to metal fraction bound to various forms of organic matter, including living organisms, organic coatings on inorganic particles or organic detritus. However, the main metal portion is bound to polymer humic compounds, less to sugars, proteins, amino acids, fats, waxes (Pickering, 1986). These materials degrade in oxidizing conditions releasing adsorbed ions. Oxidizing agents as H_2O_2 or NaClO are used in this case (Gleyzes, 2002). **Residual fraction** consists of primary and secondary minerals containing targeted metals in their crystalline lattice. For its destruction, digestion with strong acids (e.g. HF , HClO_4 , HCl a HNO_3) is used. Some authors use for calculation of this fraction also the difference between the total element concentration and the sum of fractions extracted in previous steps (Rauret et al., 2000; Gleyzes, 2002).

Although these extraction schemes were originally developed to determine fractionation of cationic species, they were also applied to anionic species, such as As or Se (Karak et al., 2011). However, the feasibility of applying such schemes for anionic species has been questioned. As these elements can exist in different oxidation states possessing particular properties, application of reducing/oxidizing extracting agents can induce a change of oxidation state and thus also extraction results (Gleyzes et al., 2002). Gruebel et al. (1988) examined the feasibility of two common steps of sequential extraction, the reductive dissolution of amorphous iron oxides by hydroxylamine, and the oxidation of organic matter by H_2O_2 and NaClO , for determining As and Se fractionation. They found these steps inappropriate for metalloids due to partial release, redistribution and readsorption of dissolved

metalloids. Specific extraction schemes targeting oxyanions as As thus have been proposed. Based on the chemical similarity of As and P, extraction protocols for P were adopted for As (Woolson et al., 1971). Wenzel et al. (2001a) developed an improved sequential extraction procedure for As distinguishing 5 fractions: (1) non-specifically sorbed (2) specifically-sorbed, (3) bound to amorphous and poorly-crystalline hydrous oxides of Fe and Al, (4) bound to well-crystallized hydrous oxides of Fe and Al, and (5) residual.

Originally, methods of sequential extraction were widely criticized mainly for insufficient selectivity of chosen extractants, readsorption and redistribution of metals dissolved during extraction, sample preparation or general methodology and the result dependence on operation precision. There exists no universal extraction scheme, each possesses its own advantages and drawbacks and suits a certain type of analyzed material. Interpretation of results thus should not be based on a specific mineralogical fraction but rather on the type of used reagent (Adriano, 2001; Gleyzes, 2002; Reeder et al., 2006).

Speciation and fractionation in solid phase

Besides the widely used techniques determining speciation of the elements in liquid phase, there also exist many instrumental techniques working directly with solid samples. The largest group of these methods is based on X-rays. Here, we can name X ray fluorescence (XRF). In this case, the characteristic X-rays are produced when the atomic element is irradiated with a radiation of sufficient energy, which can be, e.g., an electron beam in the scanning electron microscope (SEM). The SEM-EDS (energy dispersive spectrometry) makes it possible to identify the elements in a sample based on the energy level of characteristic X-rays while the element concentration corresponds to X-rays intensity. It can also provide maps showing the spatial distribution of specific chemical elements in a sample (Wang and Mulligan, 2008). Another nondestructive surface analysis method is called X ray photoelectron spectroscopy (XPS) that provides information on the chemical composition of the thin surface layer (0.2-0.5 nm) of the sample. Conversely to XRF, this method uses X-rays to knock the electrons out of the inner-shell orbitals. The emitted photoelectrons possess specific kinetic energies which depend on the nature of emitting atoms and their binding states. This analysis thus can be used for identification of the oxidation state and ligands of an atom (Verma, 2007). The X-ray absorption spectroscopy (XAS) enables the characterization of element-specific electronic configurations at the surface of both amorphous and crystalline samples

(Wang and Mulligan, 2008). Due to the element-specificity of XAS, it is useful to speciate trace elements (e.g., As) adsorbed to pure minerals, soils and sediments (Wilkin and Ford, 2006). The XAS spectrum divides to extended X-ray absorption fine structure (EXAFS) and X-ray absorption near edge structure (XANES). While the EXAFS gives information on the coordination number and interatomic distance together with the nature and position of the neighboring atoms in the coordination shell of the adsorbed ion, the XANES provides the electronic and structural information with respect to the adsorbed ion and can be used for the determination of the oxidation state and local electronic structure (Teo, 1986; Wang and Mulligan, 2008).

Stabilization of metals and metalloids in contaminated soils

As was shown, apart from the total concentration of a particular element in the environment, there are many other factors driving its mobility, bioavailability, bioaccessibility and overall hazards in the soil. When dealing with contamination with metals/metalloids, two basic approaches can be chosen: i) removing the contaminants from the soil and thus decreasing their total concentration, or ii) decreasing the mobility (and thus also the bioavailability and bioaccessibility) of the contaminants while the total concentration remains the same (Bolan et al., 2014). In the first case, various physico chemical or biological methods can be used, e.g., soil washing (Dermont et al., 2008), electrokinetic methods (Kim et al., 2011), phytoextraction (Bhargava et al., 2012) or bioremediation (Chen et al., 2015). In contrast to these methods based on removing the metals/metalloids from the soil, immobilization methods have a potential to be cheaper, less disturbing and easier to perform (Kumpiene et al., 2008).

Metals/metalloids in soil can be stabilized (i.e., their mobility and bioavailability can be decreased) by means of various stabilizing amendments (so called chemical stabilization), activity of living plants and associated microbial communities (i.e., phytostabilization) or combination of both (i.e., aided phytostabilization) (Komárek et al., 2013). Metal(loid)s can be immobilized in the soil as a result of adsorption processes on mineral surfaces, formation of stable complexes with organic ligands, surface complexation, ion exchange and (co)precipitation. These processes

can be influenced by many factors, such as pH, redox potential, cation exchange capacity, size and type of soil particles, concentration and type of organic matter etc. (Kumpiene et al., 2008). This type of soil amendment is not novel, in fact, lime or organic and phosphate fertilizers have been used for hundreds years to ameliorate soil fertility, supply nutrients or decrease phytotoxicity and bioavailability of various toxic substances (Adriano, 2001; Bolan et al., 2003).

Iron and manganese oxides as stabilizing amendments

Various types of materials can be used for chemical stabilization. It is possible to categorize them in several main groups: alkaline materials (milled limestone, dolomite), clay minerals and zeolites, organic matter and organic-based industrial waste products (compost, sewage and paper mill sludge), inorganic industrial waste- and by-products (gypsum- and lime-rich industrial by-products, by-products from aluminum and iron industry) or Fe, Mn and Al oxides (Komárek et al., 2013; Kumpiene et al., 2008).

Iron oxides (including hydroxides and oxyhydroxides) together with Mn oxides occur naturally as erosion products in almost all soil types mainly as coatings on soil particles and pores or in the form of concretions and nodules. Although not so abundant, they possess significant sorption properties due to the extent and reactivity of their specific surface and present thus an important sink of risk elements in soil conditions (Essington, 2004; Sposito, 2008). Another advantage favoring the use of oxides for soil remediation is their natural occurrence in the soil environment. This means that possible additional contamination by, for instance, impurities in composts, ashes, sludges etc., is avoided (Komárek et al., 2013).

Iron oxides

Amongst Fe oxides, goethite (α -FeOOH) is the most common stable Fe oxide in the soil occurring in virtually all soil types, in larger quantities especially at places with a cool and humid climate. Other Fe minerals, hematite (α -Fe₂O₃) and lepidocrocite (γ -FeOOH), often occur in association with goethite (Sposito, 2008). Hematite forms predominantly in regions with warm climate (tropics and subtropics) and its formation is favored by a slightly alkaline pH. Lepidocrocite, a polymorph of goethite, forms from precipitated Fe²⁺ hydroxides under seasonally anaerobic conditions that can be found in gleys and pseudogleys. In calcareous soils, however, it

is replaced by goethite (Breemen and Buurman, 2002; Essington, 2004). Ferrihydrite ($\text{Fe}_2\text{O}_3 \cdot n\text{H}_2\text{O}$) is a poorly ordered (usually nanosized) iron hydroxide occurring in fresh precipitates that transforms with time to more stable and better crystalline phases (Breemen and Buurman, 2002; Cornell and Schwertmann, 2003). Due to its large specific surface, ferrihydrite presents an important part of the soil sorption complex (Sposito, 2008).

In this PhD thesis, the use of nanosized magnetite and maghemite was investigated. Magnetite (Fe_3O_4) present in soils is lithogenic in principle (i.e., inherited from the parent rock) rather than pedogenic (Essington, 2004). The structure of the magnetite is that of an inverse spinel with a face-centered cubic unit cell (**Fig. 1.5**). In contrast to most of other Fe oxides, magnetite contains both Fe(II) and Fe(III) in the structure when about one third of Fe in magnetite is Fe(II) in octahedral coordination while Fe(III) is present both in octahedral and tetrahedral coordinations (Cornell and Schwertmann, 2003; Essington, 2004). The maghemite (*magnetite-hematite*) ($\gamma\text{-Fe}_2\text{O}_3$), a hematite polymorph isostructural with magnetite, forms as a result of partial or complete oxidation of Fe(II) in magnetite structure. It can be found in highly weathered soils of tropics and subtropics. Maghemite may also transform from goethite (or ferrihydrite) at high temperatures (300 to 425°C) in presence of organic matter. These conditions can be met during forest or bush fires (which are most common in tropical and subtropical climate) making the maghemite widespread in soils (Breemen and Buurman, 2002; Cornell and Schwertmann, 2003; Essington, 2004).

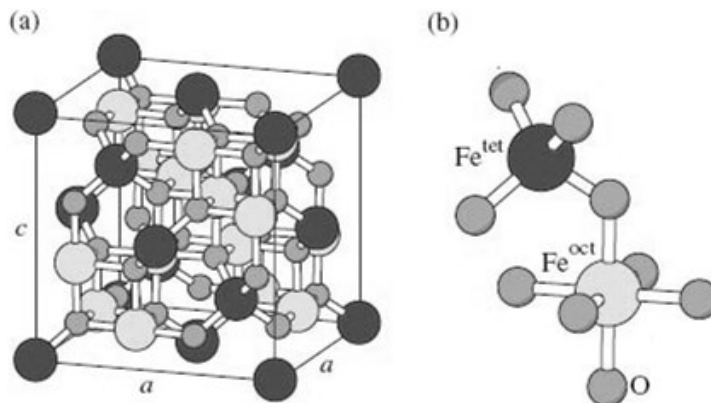


Figure 1.5

Face-centered cubic spinel unit of magnetite (a) with magnification of one tetrahedron (Fe^{tet}) and one adjacent octahedron (Fe^{oct}) sharing an oxygen atom (O) (b); adapted from Friák et al. (2007).

In remediation practices, Fe oxides are often applied in the form of their precursors or industrial waste or by-products rather than the final materials. An overview of some studies dealing with these materials during the last decade (2006-2016) is given in **Table 1.3**. The precursors of Fe oxides include Fe sulfates or elemental iron (i.e., also various Fe based waste materials like iron grit, iron filings, steel abrasive) and nano zerovalent iron (nZVI) (Komárek et al., 2013; Zhao et al., 2016). Furthermore, industrial by products or waste materials containing Fe oxides were used, e.g., contaminant stabilization using water treatment residues (Garau et al., 2014; Nielsen et al., 2011), furnace slags (Lee et al., 2011; Matsumoto et al., 2016), red mud (Garau et al., 2014; Lee et al., 2011) or iron rich acid mine drainage sludge (Ko et al., 2015).

Although the Fe(II) contained in Fe sulfates is readily available for immobilizing reactions and these materials proved to be efficient in stabilization of As in contaminated soils (Warren et al., 2003; Xenidis et al., 2010) or in reduction and immobilization of Cr(IV) (Di Palma et al., 2015), the presence of sulfate anions leads to unwanted soil acidification and potential release of cationic contaminants, such as Pb, Cd and Zn (Di Palma et al., 2015; Xenidis et al., 2010). The Fe sulfate application thus should be accompanied by additional liming (Contin et al., 2008).

The advantage of using various industrial by-products or waste materials is their cost and availability in large amounts. On the other hand, attention has to be paid to the composition of these materials as they themselves may be the source of additional contamination. But in fact, the sole presence of contaminants in stabilizing agent composition does not always indicate an increased risk under real conditions. For example, Lee et al. (2011) used red mud containing 62 mg kg⁻¹ As for stabilization of As, Cd, Pb and Zn in contaminated soil. In their case, combined treatment with limestone and red mud resulted in a reduction of Ca(NO₃)₂-extractable As, Cd, Pb, and Zn and uptake by lettuce (*Lactuca sativa* L.). It thus seems that in this case, potential risk posed by increased As content in red mud was overcome by the stabilizing efficiency of the used treatment. Conversely, Oustriere et al. (2016) tested poultry manure-derived biochar alone and in combination with iron grit for stabilization of Cu in contaminated soil. This biochar contained increased levels of Cu (362 mg kg⁻¹), Zn (1100 mg kg⁻¹) and PAHs (20 mg kg⁻¹). All treatments using this biochar resulted in a 4- to 10-fold increase of Cu in pore water compared to control. This observation was explained by significantly increased levels of DOM (dissolved organic matter) in pore water in biochar-amended variants, as the DOM is able to complex and mobilize Cu in the soil. Yet, the Cu contained in material itself might

also contribute to increased Cu levels. Additionally, the biomass yield of roots and shoots of dwarf bean (*Phaseolus vulgaris* L.) significantly decreased when the biochar was used. One of the possible reasons proposed by the authors is the phytotoxicity of contained PAHs together with increased levels of Cu in soil pore water. Unfortunately, the content of other trace elements in the soil and plants (e.g., Zn in the context of this biochar) is not mentioned in the paper, as the potential phytotoxic effects may also arise from increased levels of these elements.

When elemental Fe is applied to soil, it oxidizes forming firstly amorphous/slightly crystalline Fe oxides (e.g. ferrihydrite) (Komárek et al., 2013). These oxidation reactions are not as fast as in the case of Fe sulfates, but they appear more efficient in the long term perspective with no undesirable influence on soil pH (Kumpiene et al., 2006; 2008). For example, Matsumoto et al. (2016) successfully used Fe metal powder (content of Fe(0) > 90%) for the stabilization of As in paddy field soils. In this case, both mobile As pool in the soil together with its concentration in rice (*Oriza sativa* L.) grains decreased in correlation with the increased content of poorly amorphous Fe oxides formed after Fe metal powder addition. The nZVI presents a special case of elemental Fe amendment while being one of the most extensively studied materials for environmental cleanup over the past 20 years (Zhao et al., 2016). This highly reactive reductant can be used both for binding and/or reduction of metals and metalloids, but also for degradation of organic pollutants. Due to the broad extent of research dealing with nZVI, it is not the subject of this brief overview. Yet, many extensive reviews are available (Fu et al., 2014; Noubactep, 2015; Stefaniuk et al., 2016; Tosco et al., 2014; Yirsaw et al., 2016; Zhao et al., 2016).

Besides the application of their precursors, “pure” Fe oxides have also been tested for remediation purposes. Since the Fe oxides are supposed to be the main sink of As in soils (Wang and Mulligan, 2008), they were widely tested for immobilization of this metalloid. In the study of Bagherifam et al. (2014) dealing with the stabilization of As using various naturally occurring metal oxides, a goethite-based amendment proved to be the most efficient in decreasing exchangeable fraction of As together with its bioavailability while being also the most efficient in supporting barley (*Hordeum vulgare* L.) growth. García-Sánchez et al. (2002) tested various natural Fe oxyhydroxides, clay minerals and synthetic Al hydroxide and FeOOH for adsorption of As(V) and its immobilization in two contaminated soils. Here, generally the best results were obtained for synthetic FeOOH (5%, w/w), that was able to decrease the water-extractable As content in model soils by nearly 100% and 79%. Yet, the Fe oxides were successfully used not only for the stabilization of As, but also

for immobilization of other metals. Hartley and Lepp (2008) tested the application of lime, goethite, iron grit and Fe(II) and Fe(III) sulfates. In their study, goethite proved as the most effective in decreasing both As and Cu and Zn uptake by spinach (*Spinacea oleracea* L.) reducing their contents in biomass by 99%, 95% and 97%, respectively. In a complex study of Friesl et al. (2006) including batch, pot and field experiments and 15 different amendments, ferrihydrite bearing amendments proved in pot experiments to be the most effective treatment in reducing both the Cd and Pb uptake and transport in the test plants (various barley cultivars). In field experiment, however, ferrihydrite was replaced with red mud due to the problems with supply. The results obtained from the field did not support in this case those from the pot experiment as while the uptake of Pb and Zn decreased in most variants, the uptake of Cd remained the same or had even increased. Authors thus point out the difficulties connected with the transfer of the results from laboratory to the field and the importance of correct amendment applications under field conditions.

To date, most of the studies dealing with Fe-based nanomaterials have focused mainly on the treatment of contaminated water (Hu et al., 2004; 2005; Tang and Lo, 2013), where Fe based adsorbents can be easily separated using magnetic field. However, soil applications are still rather scarce and deal usually with composite or surface-coated nanoparticles rather than “pure” nanooxides. Liu and Zhao (2007a,b) examined the influence of the novel CMC (sodium carboxymethyl cellulose)-stabilized iron phosphate nanoparticles on the leachability and bioaccessibility of Cu and Pb in contaminated soils. At higher doses of the amendment ($3 \text{ mg PO}_4^{3-} \text{ kg}^{-1}$), the Cu and Pb leachability was reduced by 63-87% and 85-95%, respectively, while the Cu and Pb bioaccessibility decreased by 54-69% and 31-47%. In the study of Kim et al. (2012), nano-sized zero valent iron (nZVI) coated by sodium dodecyl sulfate (SDS-nZVI) and nano-sized magnetite coated by sodium dodecyl sulfate (SDS-nMGT) (0.34% Fe, w/w) proved efficient when decreasing extracted amount of As by 73.94% (SDS-nMGT) and 52.25% (SDS-nZVI), respectively. Starch-stabilized magnetite nanoparticles also proved feasible in immobilization of As(V) in sandy loam soil. Additionally, once delivered, the particles remained virtually immobile under the soil conditions, thus avoiding the risk of possible unwanted migration (Liang and Zhao, 2014). On the other hand, in our studies (Micháľková et al., 2014; 2016), we tested adsorption properties and the stabilizing potential of nanomagnetite and nanomaghemite towards Cd, Cu, Pb, Zn and As in contaminated soils. Although the recorded adsorption capacity towards targeted metals/metalloids reached approx. 10 mg g^{-1} , we did not observe any significant changes in contaminants mobility/extractability when applied directly to contaminated soils.

Table 1.3

Overview of selected studies dealing with Fe oxides or their precursors published in the last 10 years (2006-2016).

Metal(loid) concentration (mg kg⁻¹)	Treatment (wt.%)	Effect	Reference
As (1033) Cr (371)	water treatment residue (mainly ferrihydrite) (5%)	- leaching of As and Cr reduced by 98% and 91%, respectively	Nielsen et al. (2011)
Sb (40-123) Pb (356-1112)	ferric oxyhydroxide powder (2%) + limestone (1%)	- decrease of Sb and Pb in pore water by 66% and 97%, respectively - stable over 4 years	Okkenhaug et al. (2016)
As (V) (60)	iron filings (33% and 50%)	- after 4 hours 31% (wt.33%) and 51% (wt.50%) reduction in As release - after 24 hours 16% (wt.33%) and 70% (wt.50%) reduction in As release	Tyrovola and Nikolaidis (2009)
Pb (6973) As (840) Zn (5775)	Ca(H ₂ PO ₄) ₂ ·H ₂ O (0-1.06%) + FeSO ₄ ·H ₂ O (0-6.16%)	- simultaneous immobilization of both Pb and As only when mixture of stabilizing agents was applied - addition of phosphate (0.64%) + Fe sulfate (3.08%) decreased the concentration in extracts under EU drinking water standards - significant acidification of soil and mobilization of Zn and Cd after treatment	Xenidis et al. (2010)
Cd (7-54) Cu (75-642) Ni (43-389) Pb (468-2712) Zn (1117-13 341)	iron rich waste (FeW) (0-2.5%) + organic waste (OW) (0-5%)	- exchangeable Zn reduced by 50 and 90% in both soils by FeW(2.5%) + OW(5%) - DTPA-extractable fraction (i.e., phytoavailable) of Cd, Cu and Zn decreased after 1 to 3 redox cycles by 88-95%, 93-98% and 36-65%, respectively; Pb and Ni availability increased	Contin et al. (2007)
As (40)	metal Fe powder, Fe oxide (mainly ferrihydrite), converter furnace slag; all (1 kg m ⁻²)	- the lowest As concentration in soil solution reached using Fe powder - Fe powder and Fe oxide significantly reduced phytoavailable As -application of Fe materials very effectively reduced As in rice (<i>Oriza sativa</i> L.) grains	Matsumoto et al. (2016)

As (132)	iron rich acid mine drainage sludge (AMDS) (0-5%)	<ul style="list-style-type: none"> - optimum mixing ratio of 3% AMDS - in field, As concentration in pore water decreased from 11.6 to 4.9 $\mu\text{g L}^{-1}$ - AMDS decreased As transport to rice grain by 92% 	Ko et al. (2015)
As (222; low OM content) As (89; high OM content)	steel abrasive (SA; 97% Fe^0) (1%), oxygen scarfing granulate (OSG; 69% Fe_3O_4) (8%)	<ul style="list-style-type: none"> - SA and OSG decreased As concentration in pore water by 68% and 92%, respectively, in soil with low OM content and by 30% in soil with high OM content 	Lidelöw et al. (2007)
As (20) Pb (117) Zn (233)	red mud (23% Feox), furnace slag (19% Feox), limestone; all 2 and 5%	<ul style="list-style-type: none"> - combined treatment with red mud (2%) and limestone (2%) reduced $\text{Ca}(\text{NO}_3)_2$-extractable As, Cd, Pb, and Zn by 58%, 98%, 98%, and 99%, respectively - microbial activity increased and plant uptake decreased after treatment 	Lee et al. (2011)
As (2105) Cd (18) Cu (264) Pb (710) Zn (522)	red mud (RM), hematite (H), Fe rich water treatment residue (WTR), all 3%	<ul style="list-style-type: none"> - after 6 months, H and WTR reduced water-soluble fraction of contaminants - despite the highest bioavailability of contaminants in RM amended soil, microbiological indicators were significantly higher - RM addition completely inhibited bean germination 	Garau et al. (2014)
Cu (964)	iron grit (IG) (1%)	<ul style="list-style-type: none"> - application of IG or in combination with pine bark-derived biochar resulted in the lowest total amount of Cu in soil pore water - iron grit application has no significant influence on beans biomass yield 	Oustriere et al. (2016)
As (50)	hematite, goethite; all 2% and 5%	<ul style="list-style-type: none"> - goethite (5%) application was the most effective in decreasing exchangeable and bioaccessible fractions of As together with supporting the grown of barley 	Bagherifam et al. (2014)
Cr(VI) (94)	Fe sulfate; $\text{Fe(II):Cr(VI)}=5; 10; 30$ with/without oxygen stripping	<ul style="list-style-type: none"> - the amount of Cr(VI) after 16 hours below the limit of industrial reuse (Italian Environmental Regulation), after 45 hours complete removal of Cr(VI)- need for oxygen stripping before reagent addition - mobilization of other metals due to soil acidification 	Di Palma et al. (2015)

As (20-580)	soluble Fe(II) (0.5-2.5%), Fe(II)-modified zeolite (Fe-Z) (0.05-0.2%-loaded Fe)	- at 200 mg As kg ⁻¹ soil and 600 minute shaking time, the immobilization of As(III) with Fe(II) and Fe-Z was 90.6% and 81.4%, respectively	Naseri et al. (2014)
As(V) (32)	starched magnetite nanoparticles (2.4% and 9.4%)	- water-leachable As(V) was reduced by 93% and the TCPL (Toxicity Characteristic Leaching Procedure) leachability by 83%	Liang and Zhao (2014)
As(III) (104)	polysaccharide stabilized Fe-Mn oxide nanoparticles (CMC-Fe-Mn) (Fe:As-6.5-39)	- treatment with CMC-Fe-Mn reduced water leachable As by 91-96%, TCLP leachability was reduced by 94-98% - once delivered, particles remain virtually immobile in soil	An and Zhao (2012)
Cd (33) Pb (702) Zn (2090)	iron grit (3.2%)	- iron grit reduced strongly the leaching of Cd and Pb, but doubled the concentrations of Cd and Pb in shoots of white lupin (<i>Lupinus albus</i> L.)	Houben et al. (2012)
Cu (33-508) Zn (69-118) As (60-78)	goethite, iron grit, Fe(II) and Fe(III) sulfates + lime; all 1%	- goethite showed the best results from tested amendments concerning the effect on biomass of spinach and tomato and reduced plant uptake	Hartley and Lepp (2008)
Cu (666, 639, 459) Pb (24, 62, 139)	Fe phosphate nanoparticles (0.61 and 3.01 mg PO ₄ g ⁻¹ soil)	- at higher dose of amendment, the Cu leachability was reduced by 63–87% and Cu concentrations in TCLP extract decreased from 1.74–13.33 mg L ⁻¹ to 0.23–2.55 mg L ⁻¹ - TCLP leachability was reduced by 85-95% - Cu and Pb bioaccessibility was reduced by 54-69% and 31-47%, respectively	Liu and Zhao (2007a,b)
Cd (7), Cu (75) Ni (43) Pb (468) Zn (1117)	0.1M FeSO ₄ + Ca(OH) ₂ (3.35 g Fe kg ⁻¹ soil for each treatment cycle- 8 cycles)	- after 8th cycle, exchangeable fractions of Cd, Cu, Pb and Zn decreased by 70%, 87.7%, 73.5% and 49.8% respectively - soil treatment effectively reduced toxicity of metals to microorganisms	Contin et al. (2008)
As (9-26)	iron oxide (80% magnetite and 20% hematite) (0,5%, 1%, 2%)	- addition of iron oxide (2%) significantly reduced grain-As concentrations from 0.161 to 0.053 mg kg ⁻¹ and from 1.407 to 0.796 mg kg ⁻¹ , respectively - treatment had minimal impact on grain accumulation of other elements	Farrow et al. (2015)

Manganese oxides

Compared to Fe oxides, the content of Mn oxides in soils is generally lower but these materials appear more efficient in immobilization of some metals (Dong et al., 2000; O'Reilly and Hochella, 2003). This can be caused by their large specific surface and usually low pH_{pzc} , which is the reason for their negative surface charge under usual soil conditions (Essington, 2004). Manganese oxides commonly occur in the form of coatings and fine grained aggregates. Although the main Mn mineral reported in soils is birnessite (Sposito, 2008), these materials are often not classified due to their poorly-crystalline (even amorphous) structure. The basic building unit of most of the Mn oxides is the MnO_6 octahedron. These octahedra can be coordinated by sharing edges and/or corners in a wide variety of structural arrangements falling usually into two major groups: chain (or tunnel) structures and layer structures (**Fig. 1.6**). The structure of the tunnel Mn oxides (e.g., pyrolusite, ramsdellite, hollandite, romanechite, todorokite, manganite etc.) consists of single, double, or triple chains of edge-sharing MnO_6 octahedra that share edges with each other to form a framework with the tunnels with square or rectangular cross sections. The larger tunnels may also accommodate water molecules and/or cations. The layer Mn oxides (e.g., lithiophorite, birnessite, chalcophanite, vernadite etc.) are formed of stacks of sheets (layers) of edge-sharing MnO_6 octahedra. The interlayer regions can be filled with water molecules and a wide range of cations (Post, 1999).

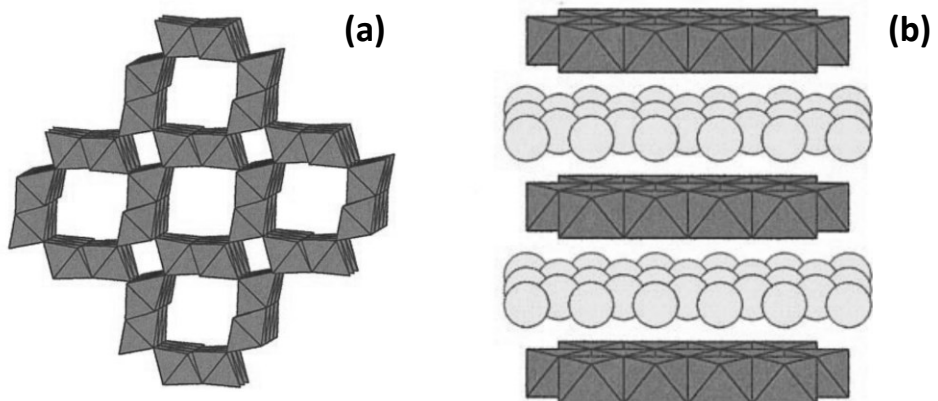


Figure 1.6

Illustrative depiction of tunnel (hollandite) (a) and layer (Na-rich birnessite with disordered $\text{H}_2\text{O}/\text{Na}$ sites (circles)) (b) crystal structures; adapted according to Post (1999).

Manganese oxides have strong oxidative properties and therefore play part in many oxidation-reduction and cation exchange reactions. For that reason, these oxides are not suitable amendments for soils contaminated with Cr as they are able to readily oxidize Cr(III) to more mobile and toxic Cr(VI) (Fandeur et al., 2009; Feng et al., 2006). On the other hand, this oxidizing nature can be benefit in case of contamination with As, as Mn oxides are known to be efficient in oxidizing more mobile and toxic As(III) to As(V) (Chen et al., 2006; Driehaus et al., 1995; Villalobos et al., 2014; Watanabe et al., 2013; Zhu et al., 2009). Due to their promising properties, many studies focused on the synthesis and testing of engineered Mn (nano)oxides, that can be, in addition to other possible applications, used as a potential agent for environmental cleanup. Manganese oxide nanoparticles can be prepared both by the classical chemical route (Naderi et al., 2013; Simenyuk et al., 2015; Singh et al., 2010; Zhang et al., 2015) and by biotechnological way, using the oxidizing activity of microorganisms like bacteria or fungi (Miyata et al., 2007; Villalobos et al., 2005b; Zhou et al., 2015). In fact, biogenic oxidation of Mn(II) also presents the prevailing way of the formation of the Mn oxides in soils (Droz et al., 2015). Although thermodynamically favored, Mn(II) oxidation in the environment solely by the chemical means is very slow. Hence, when the process is microbially-mediated, the reaction rate can be elevated by several orders of magnitude (Morgan, 2000; Tebo et al., 1997).

To date, there is just a limited number of studies dealing directly with the application of Mn oxides for the stabilization of metals/metalloids in contaminated soils. Instead, many more studies dealing with this type of materials are in the first phase focused mainly on the synthesis, characterization or adsorption properties in relation to the targeted compounds, i.e., metals/metalloids in this case (**Table 1.4**). Based on these data, possible applications including remediation purposes can be proposed.

Table 1.4
Adsorption capacities of chosen Mn-based materials.

Material	Targeted metal(loid)	Maximum adsorption capacity	Reference
Ce-incorporated Mn oxide	As (V)	19 mg g ⁻¹	Gupta et al. (2011)
Mn-immobilized activated carbon	Cu	0.89 mg g ⁻¹	Lalhmunsiana et al. (2013)
	Pb	4.32 mg g ⁻¹	
Birnessite	Cu	0.72 mol Cu mol ⁻¹ Mn	Peña et al. (2015)
Mn oxide produced by <i>Leptothrix discophora</i> SS-1	Pb	0.55 mol Pb mol ⁻¹ Mn	Nelson et al. (1999)
Mn oxide- biochar composite	Pb	14.4 mg g ⁻¹	Yu et al. (2015)
Mn oxide produced by <i>Pseudomonas putida</i> strain MnB1	Pb	21 mmol g ⁻¹	Zhou et al. (2015)
	Cd	14.6 mmol g ⁻¹	
	Zn	14.2 mmol g ⁻¹	
Birnessite	Pb	2.8 mmol g ⁻¹	Zhou et al. (2015)
	Cd	1.7 mmol g ⁻¹	
	Zn	1.8 mmol g ⁻¹	
Hydrogel-supported hydrous Mn dioxide	Pb	0.48 mmol g ⁻¹	Zhu and Li (2015)
	Cu	0.57 mmol g ⁻¹	
	Cd	0.47 mmol g ⁻¹	
	Ni	0.41 mmol g ⁻¹	
Hydrous Mn dioxide	Pb	0.45 mmol g ⁻¹	Zhu and Li (2015)
	Cu	0.53 mmol g ⁻¹	
	Cd	0.39 mmol g ⁻¹	
	Ni	0.37 mmol g ⁻¹	
Amorphous Mn oxide	Cd	2.24 mmol g ⁻¹	Micháľková et al. (2014)
	Cu	0.52 mmol g ⁻¹	
	Pb	4.02 mmol g ⁻¹	
	As (V)	1.79 mmol g ⁻¹	Micháľková et al. (2016)
	Zn	0.46 mmol g ⁻¹	Della Puppa et al. (2013)
Birnessite	Cd	0.50 mmol g ⁻¹	Della Puppa et al. (2013)
	Cu	0.50 mmol g ⁻¹	
	Pb	0.55 mmol g ⁻¹	
	Zn	0.48 mmol g ⁻¹	

In one of the first published studies, a hydrous Mn oxide proved efficient in decreasing the mobility and plant uptake of Cd, Pb and Zn in the soil contaminated by smelting industry (Mench et al., 1994). Hettiarachchi et al. (2000) tested the influence of phosphorus (as triple superphosphate or phosphate rock) and/or cryptomelane addition on Pb mobility/bioaccessibility in five contaminated soils or mine spoils. According to their results, both phosphorus and cryptomelane proved efficient, yet the best results were obtained when both amendments were applied together. In this case, the highest formation of low soluble pyromorphite-like minerals was observed. Chen et al. (2000b) evaluated the changes in speciation and extractability of Cd and Pb together with the phytoavailability to wheat (*Triticum aestivum* L.) after the addition of various stabilizing agents. Here, generally the calcium carbonate, Mn oxide (non-specified) and zeolite proved the most efficient in decreasing the observed markers and transforming both contaminants to unavailable forms. In the study of McCann et al. (2015), Mn oxide waste water residue was applied as a stabilizing amendment to historically Pb contaminated soil. In this case, unexpected contamination heterogeneity at the place almost disallowed the comparison of the results obtained from the control and amended soils. Yet, the adsorption capacity observed for Pb for this material ($346 \pm 14 \text{ mg g}^{-1}$) was one of the highest reported to date.

On the other hand, application of Mn oxides has not been fully successful in all cases. Bagherifam et al. (2014) tested the potential of six naturally occurring metal oxides including three Mn oxides. Natural Mn oxide (non-specified), braunite and bixbyte were able to reduce the exchangeable fraction of As by 71%, 49% and 50%, respectively. By contrast, only the braunite and bixbyte efficiently decreased As bioaccessibility. All Mn-based amendments also significantly decreased As concentrations in stems and supported barley biomass production. Despite the mentioned positive effects, the most effective amendment concerning the targeted markers proved to be the goethite. In the study of McBride and Martínez (2000), a K-saturated birnessite together with other amendments were tested for the stabilization of Cu (3430 mg kg^{-1} soil) and other metals/metalloids (Pb, Zn, Cd and As) in a contaminated soil. The Mn oxide application resulted in this case in an increase of pH from 6.8 (control) to 7.4 and connected with a 7.5-fold increase of DOC in the soil solution. As the DOC content is strongly associated with fractionation of Cu in the soil due to its ability to form soluble complexes with Cu (and also other metals/metalloids), the amount of Cu, Cd, As, Pb, Ni and Cr in soil solution significantly increased after Mn oxide addition. Although the Mn oxide proved to be the most efficient in decreasing free Cu^{2+} ion concentration, the pool of

total soluble and labile Cu remained 4 to 5 orders of magnitude higher, thus also exceeding the values recorded from the control. Even though the Mn oxide was able to slightly decrease the Cu content in maize (*Zea mays* L.) (from 23 to 17 mg kg⁻¹), simultaneous increase of As and Cd content was observed.

Della Puppa et al. (2013) together with Michálková et al. (2014; 2016) and Ettler et al. (2015) investigated the adsorption properties and stabilizing potential of the novel amorphous Mn oxide (AMO) with respect to Cd, Cu, Pb, Zn and As in contaminated soils. In these studies, AMO proved as a highly efficient adsorbent for targeted metals reaching adsorption maxima of 2.24, 0.52, 4.02, 0.46 and 1.79 mmol g⁻¹, respectively. After application to contaminated soils, AMO was able to decrease significantly the amount of targeted metals/metalloids in soil solution. On the other hand, higher dissolution of this agent in acidic conditions associated with the rise of pH and unwanted oxidation and dissolution of soil organic matter was recorded similarly as in the study of McBride and Martínez (2000). For that reason, AMO appears as a suitable amendment for neutral and slightly alkaline soils. Studies dealing with the AMO as well as the nanomaghemite and nanomagnetite are the subject of this PhD thesis and are described in detail in following chapters.

When speaking about nanooxides (and nanomaterials generally), questions concerning their potential environmental hazards and the need for reliable risk assessment arise. Regarding this context, application of Mn nanooxides for soil remediation appears as relatively safe as nanoscale biogenic Mn oxides are natural and ubiquitous soil components. No harmful effect on soil microbiota was also reported in some stabilization studies (McCann et al., 2015; Michálková et al., 2014).

Chapter II

Evaluating the potential of three Fe- and Mn-(nano)oxides for the stabilization of Cd, Cu and Pb in contaminated soils

Z. Michálková, M. Komárek, H. Šillerová, L. Della Puppa, E. Joussein, F. Bordas, A. Vaněk, O. Vaněk, V. Ettler

Adapted from Journal of Environmental Management 146 (2014): 226-234

Content

Abstract	39
Introduction	40
Materials and methods	41
Soil properties	41
Properties of the studied (nano)oxides	42
Incubation experiments	43
Column experiments	44
Effect of (nano)oxides on soil microbiological activity	45
Statistical analysis	45
Results and discussion	45
Soil properties	45
Metal adsorption on (nano)oxides	47
Batch incubations	55
Column experiments	57
Effect of (nano)oxides on soil microbiological activity	57
Conclusions	59

Abstract

The potential of three Fe- and Mn-(nano)oxides for stabilizing Cd, Cu and Pb in contaminated soils was investigated using batch and column experiments, adsorption tests and tests of soil microbial activity. A novel synthetic amorphous Mn oxide (AMO), which was recently proposed as a stabilizing amendment, proved to be the most efficient in decreasing the mobility of the studied metals compared to nanomaghemite and nano-magnetite. Its application resulted in significant decreases of exchangeable metal fractions (92%, 92% and 93% decreases of Cd, Cu and Pb concentrations, respectively). The adsorption capacity of the AMO was an order of magnitude higher than those recorded for the other amendments. It was also the most efficient treatment for reducing Cu concentrations in the soil solution. No negative effects on soil microorganisms were recorded. On the other hand, the AMO was able to dissolve soil organic matter to some extent.

Introduction

Commonly used methods of contaminated soil remediation, such as soil excavation, encapsulation, in situ and ex situ washing/flushing, vitrification etc., are not only costly and energy demanding, but also disruptive for the soil in the context of natural site conditions (Kumpiene et al., 2008; Tsang et al., 2007; Tsang and Yip, 2014). Due to the limited funding available for soil remediation and with the emphasis on environmental and landscape protection, research on the stabilization of metals in contaminated soils has become a high priority (Bolan et al., 2014; Geebelen et al., 2006; Komárek et al., 2013; Kumpiene et al., 2008; Mench et al., 2006a,b; Renella et al., 2008). Stabilization of metals and metalloids by decreasing their mobility, bioavailability and bioaccessibility in soils can be achieved using living plants and associated microbial communities in the root zone (phytostabilization), application of various immobilizing amendments (chemical stabilization) or using a combination of both (aided phytostabilization) (Komárek et al., 2013; Kumpiene et al., 2008).

Nano-sized oxides (particle size of 1e100 nm) act as important scavengers for contaminants in soils, mainly due to their high reactivity and large specific surface area (Klaine et al., 2008). To date, research on the use of engineered nanoparticles for remediation purposes has focused mainly on the treatment of contaminated water (Hashim et al., 2011; Tang and Lo, 2013). For example, nano-sized particles of γ -Fe₂O₃ and Fe₃O₄ were successfully used for the removal of anionic metal/metalloid species (e.g., Cr(VI) and As(V)) from water (Hu et al., 2004, 2005). Although numerous studies have been published on the use of nanoparticles for water treatment, research on their application in soil remediation is still scarce. Komárek et al. (2013) reviewed recently the use of metal oxides in general for the stabilization of metals and As in contaminated soils and even though the remediation potential of some naturally occurring or synthetic metal oxides has been already tested, these data cannot be easily extrapolated as oxide particles have unique properties on the nano-scale (Mueller and Nowack, 2010; Tratnyek and Johnson, 2006). On the other hand, Mn-oxides were found to be more efficient for adsorbing Pb and Cd compared to Fe-oxides (Dong et al., 2000; O'Reilly and Hochella, 2003). A new amorphous Mn oxide (AMO) has been previously synthesized and tested as a promising amendment for chemical stabilization of metals in soils due to its good adsorption properties and simple preparation (Della Puppa et al., 2013; Ettler et al., 2014).

Environmental effects of engineered nanoparticles are still not much known, as the up-to-date research has been largely limited to their ecotoxicity (Nowack and Bucheli, 2007). Their bioavailability and potential ecotoxicity depends on many factors, such as speciation (dissolved, colloidal or particulate phase) (Klaine et al., 2008), size (Madden et al., 2006), shape (Pal et al., 2007) and surface properties (Yang and Watts, 2005) etc. Auffan et al. (2008) observed a strong impact of the Fe oxidation state on the oxidative stress (and associated cytotoxic effect) towards *Escheria coli*, as nano zerovalent Fe (nZVI) and magnetite (Fe_3O_4) generated reactive oxygen species. On the other hand, maghemite ($\gamma\text{-Fe}_2\text{O}_3$) particles did not cause any cytotoxicity. In vitro experiments are useful tools for elucidating toxicity interactions at the molecular level, yet the behavior and ecotoxicity in complex soil environments is difficult to predict. Nevertheless, simple toxicity tests are useful for a fast evaluation of potential toxicity of stabilizing amendments. The aim of this work was thus to evaluate the potential of two selected Fe nanooxides (maghemite and magnetite) and one amorphous Mn oxide (AMO, Della Puppa et al., 2013) to stabilize metals (Cd, Cu, Pb) in two contaminated soils and examine the interactions of these (nano)oxides in soil environments including their influence on soil microbiota.

Materials and methods

Soil properties

Two soils from the vicinity of a Pb (Haplic Udept) and Cu smelter (Dystric Udept) were chosen for the experiment, mainly due to their increased content of Pb, Cd and Cu and varying characteristics. Soil samples were collected from the superficial layer (0-20 cm), air-dried, homogenized and sieved through a 2-mm stainless sieve. Particle size distribution was determined using the hydrometer method (Gee and Bauder, 1986). Soil pH was measured in suspension using a 1:2.5 (w/v) ratio of soil and deionized water and 1 M KCl (ISO 10390:1994). Total organic carbon content (TOC) was determined using the carbon analyzer TOC-L CPH (Shimadzu, Japan). Cation exchange capacity (CEC) was evaluated using the 0.1 M BaCl_2 extraction method (ISO 11260:1994). Pseudo total concentrations of Al, Cd, Cu, Fe, Mn, Pb and Zn were determined using the US EPA aqua regia extraction method (US EPA method 3051a) with microwave digestion (SPD-Discover, CEM, USA) and ICP-OES analysis (Agilent 730, Agilent Technologies, USA). Chemical fractionation of metals in the soils was determined using the modified BCR sequential extraction procedure by

Rauret et al. (2000). The standard reference materials 2710a Montana Soil I (NIST, USA) and CRM 483 (Institute for Reference Materials and Measurements, EU) were used for QA/QC of the determination of total metal concentrations and their fractionation. Accuracy of metal recovery for Cd, Cu and Pb reached 97.1, 93.9 and 99.3% for SRM 2710a and 91.3, 95.5, 94.9% (step 1), 93.7, 90.1, 91.9% (step 2) and 95.0, 92.4, 88.5% (step 3) for CRM 483. Detection limits were 0.0002 mg L⁻¹ (Cd), 0.001 mg L⁻¹ (Cu) and 0.001 mg L⁻¹ (Pb). All chemicals used were of analytical grade.

Properties of the studied (nano)oxides

Three different metal oxides were tested in order to evaluate their potential to immobilize Cd, Cu and Pb in the soils: (i) nanosized γ -Fe₂O₃ - maghemite (Fe III), (ii) nano-sized Fe₃O₄ - magnetite (Fe II,III) and (iii) an amorphous manganese oxide (AMO) (particle size distribution follows a Gaussian curve, 600-1200 nm, with a maximum at 1000 nm) synthesized according to Della Puppa et al. (2013). The Fe-nanooxides were purchased from Sigma Aldrich (Germany). Properties of the tested amendments are summarized in **Table 2.1**. The particle size was determined using transmission electron microscopy (TEM, JEOL JEM 1230, USA). The pH of the studied oxides was measured in deionized water at 1:10 w/v, pH_{zpc} was determined using the immersion technique (Fiol and Villaescusa, 2009) at 1.25:100 w/v. The specific surface was determined using the Brunauer-Emmett-Teller (BET) method and a Nova e-Series analyzer (Quantachrome Instruments, USA).

Table 2.1

Properties of the tested (nano)oxides.

	Chemical formula	Particle size (nm)	pH	pH_{zpc}	BET (m² g⁻¹)
AMO ^a	δ -MnO ₂	600-1200	8.1	8.3	76.5
Fe III	γ -Fe ₂ O ₃	20-100	3.0	7.4	46.6
Fe II,III	Fe ₃ O ₄	20-100	4.9	6.9	36.6

AMO - amorphous manganese oxide; Fe III - maghemite; Fe II,III - magnetite

^a Della Puppa et al. (2013)

Adsorption experiments were performed in order to evaluate the adsorption kinetics of the targeted metals (Cd, Cu, Pb) for the tested (nano)oxides and to construct

corresponding adsorption isotherms. The pH values for the kinetic and equilibrium batch experiments were maintained to the respective soil pH values: pH 4.25 for Cu and 5.85 for Cd and Pb, respectively. The pH was controlled and manually adjusted using 0.1 M and 0.1 M HNO₃ and NaOH throughout the experiment. The adsorption kinetic experiment was performed in duplicates in HD-PE bottles with 0.249 L of background electrolyte (0.01 M NaNO₃) and 2 g L⁻¹ of the (nano)oxides. Adsorption of each metal was studied in separate batches. Subsequently, 1 mL of 0.025 M solutions of Cd (as Cd(NO₃)₂•4H₂O), Cu (as Cu(NO₃)₂•3H₂O) and Pb (as Pb(NO₃)₂) were added in order to reach the maximum concentration of 0.1 mM L⁻¹. Five mL of the suspensions were collected after each step in duplicate and filtered immediately through a 0.45 µm nylon syringe filter and subsequently through a 0.22 µm filter. Metal concentrations in solutions were determined using ICP-OES. The difference between the measured metal concentration of the batch without the added (nano)oxide and with the (nano)oxide suspension yielded the adsorbed concentration.

Adsorption isotherm experiments at equilibrium were performed using the same experimental setup as in the kinetic experiments. Solutions of Cd, Cu and Pb in concentrations varying from 0.02 to 3 mM were left to equilibrate in suspension for 1 h. Langmuir and Freundlich models were used to describe experimental data and adsorption isotherm parameters were calculated using the Bolster and Hornberger (2007) spreadsheets.

Incubation experiments

In order to evaluate the interactions of the (nano)oxides with the soil solutions, the following experiment was conducted: both studied soils were put into pots, kept at 23 ± 1°C and watered with deionized water for 14 days in order to maintain ~60-70% of the water holding capacity. Soil solutions were collected using rhizon soil solution samplers (mean pore volume size 0.15 µm; Rhizosphere Research Products, Netherlands). The tested oxides were mixed with the soil solutions at a w/v ratio of 1:20 and agitated for 28 days in dark. Suspensions were then centrifuged (3000 rpm, 10 min), decanted and dried at 30°C. Oxide morphology changes were investigated using scanning electron microscopy coupled with an X-ray microanalyser (SEM-EDS, Philips XL 30, 20 kV, SERMIEL). Samples were Au-Pd-coated before analysis.

Another set of batch incubation experiments was performed in order to evaluate the influence of the (nano)oxides on the fractionation and mobility of metals in

the studied soils, pH and dissolved organic carbon (DOC) content. The experiment was performed in triplicates for both the soils with different treatments: C (control), AMO, Fe III and Fe II,III at concentrations of 1 and 2% (w/w). Soil weighing equivalent to 100 g air-dried weight was added to PET pots and watered continuously with deionized water in order to maintain ~60-70% of the water holding capacity. No leaching was allowed during this experiment. After 7, 14, 28 and 62 days of incubation, soil solution was collected using rhizon samplers and the concentrations of Pb, Cu, Cd, Fe, Al, Mn and Zn were analyzed without filtration (as the soil solution has been already filtered through the rhizon) using ICP-OES. The concentration of DOC in the soil solution samples was determined using the carbon analyzer in order to evaluate the possible effects of the amendments on soil organic matter (SOM) dissolution. The pH of the soil solution was monitored throughout the experiment and soil pH values were determined after 62 days when the experiment ended. The sequential extraction procedure (Rauret et al., 2000) and two simple extractions with 0.05 M EDTA and 0.01 M CaCl₂ (Quevauviller, 1998) were performed in order to evaluate the influence of the stabilizing agents on metals fractionation and potential availability after 62 days of the experiment.

Column experiment

Column experiments were performed to evaluate the effect of the (nano)oxides under dynamic conditions in contrast to the static batch experiments. Only Dystric Udept was used in the experiment, because of intensive column clogging with fine particles of the Haplic Udept, which hindered solution flow through column. Two different leaching solutions were used: (i) solution from the SPLP (Synthetic Precipitation Leaching Procedure, pH 5.0; US EPA Method 1312. 2000) and (ii) solution of 6.5 mM Cu(NO₃)₂•3H₂O in 0.01 M NaNO₃ (pH 4.8) for determining Cu breakthrough. Both feeding solutions were applied to separate columns. Prior to the column experiment, soils amended by AMO, Fe III and Fe II,III at concentrations of 2% (w/w) and without the (nano)oxides (Control) were equilibrated for one month at ~60-70% of the water holding capacity. Forty grams of air-dried soil were placed into columns (12.5 cm height, 2.5 cm in diameter; Bio-Rad, Canada) and washed with the leaching solutions. The leaching solutions were applied to separate columns, which were operated in a down-flow mode. A relatively low flow rate (0.2 mL min⁻¹) was chosen in order to minimize potential effects of preferential flow. The flow rate was controlled using a peristaltic pump and the samples were continuously collected using an automated sampling device (FC 204, Gilson, USA). The leachates were

analyzed for metal and DOC concentrations, pH and Eh (Multi 3420, WTW, Germany).

Effect of (nano)oxides on soil microbiological activity

Changes in soil microbiological activity after metal oxides addition were evaluated using simple enzymatic and soil respiration tests. The dehydrogenase activity of both studied soils was determined using the modified triphenyltetrazolium chloride (TCC) test by Rogers and Li (1985). Soil dehydrogenase activity was defined as the amount of TPF (triphenylformazan) formed in the soil per 1 h. The soil dehydrogenase test was chosen for its nonspecific nature, which enables capturing changes in the whole microbial community (Carbonell et al., 2000). Soil respiration was measured in closed PET bottles using the static alkali absorption method (Yim et al., 2002). All samples were processed in triplicates.

Statistical analysis

All statistical treatments of the data were performed using SigmaPlot 12.5 (StatSoft Inc., USA). The experimental data were evaluated using analysis of variance (ANOVA) at $P < 0.05$ using the Tukey test.

Results and discussion

Soil properties

Basic physico-chemical properties and metal contents in the studied soils are summarized in **Table 2.2**. Dystric Udept has a coarse texture (62% sand, 30% silt and 8% clay), has a lower pH value and a higher SOM content compared to the Haplic Udept. Concentrations of trace elements exceeded their limit values for agricultural soils set by the Ministry of the Environment of the Czech Republic (1994) in the case of Pb and Cd in the Haplic Udept and Cu and Cd in the Dystric Udept. According to the sequential extraction (**Table 2.3**), most Cu (about 50%) in the Dystric Udept and Pb (about 80%) in the Haplic Udept is present in the reducible fraction, which is roughly related to metals associated with oxides in soils. A relatively high content of exchangeable Cu (23%) in the Dystric Udept is probably due to the low pH value of the soil, whereas about 27% of Cu was present in the oxidizable fraction (strongly associated with SOM), which is in accordance with the high affinity of Cu for SOM, even at lower pH values. Cadmium was mainly associated with the most available

exchangeable fraction in both soils (49% and 66% for the Haplic Udept and the Dystric Udept, respectively).

Table 2.2
Basic physico-chemical characteristics of the studied soils.

	Dystric Udept	Haplic Udept
pH _{H2O}	4.25	5.85
pH _{KCl}	3.62	5.47
CEC (cmol kg ⁻¹)	14.2	15.1
TOC (mg kg ⁻¹)	6.01	2.16
Particle size distribution (%)		
Clay (%)	7.55	12.75
Silt (%)	30.18	52.24
Sand (%)	62.27	35.01
Texture	Sandy loam	Silt loam
Total metal concentrations (mg kg ⁻¹) (n = 3)		
Pb	170 ± 9	1515 ± 29
Cu	396 ± 10	24.4 ± 0.9
Cd	4.1 ± 1.0	8.4 ± 0.4
Fe	15 501 ± 204	20 376 ± 210
Mn	293 ± 21	2 048 ± 31
Zn	86.0 ± 5.7	244 ± 2
Al	24 725 ± 967	22 646 ± 315

Table 2.3
Fractionation of the metals in the studied soils. Data presented are means ± SD (n = 3).

	FA: exchangeable	FB: reducible	FC: oxidizable	FD: residual phases
Dystric Udept				
Cu (%)	27.2 ± 0.3	45.7 ± 1.4	20.2 ± 1.2	7.0
Cd (%)	64.9 ± 0.9	19.1 ± 1.0	5.0 ± 0.3	10.9
Pb (%)	10.9 ± 0.1	58.5 ± 1.1	5.1 ± 0.3	25.5
Haplic Udept				
Cu (%)	6.4 ± 0.1	39.2 ± 2.2	15.6 ± 0.6	38.8
Cd (%)	47.7 ± 1.3	34.3 ± 2.0	2.9 ± 0.1	5.4
Pb (%)	15.3 ± 0.3	77.8 ± 4.6	2.8 ± 0.2	4.0

Metal adsorption on (nano)oxides

Adsorption kinetics of Cd, Cu and Pb onto the (nano)oxides are shown in **Fig. 2.1**. The adsorption process was relatively fast, reaching equilibrium in less than 30 min. Although the adsorption of Cu and Cd onto Fe III and Fe II,III was very fast (reaching equilibrium in nearly 1 min), the adsorbed metal concentration was low. On the other hand, Pb adsorption onto AMO was the highest and even for Fe III and Fe II,III it reached 100% of the adsorbed amount (**Fig. 2.1**).

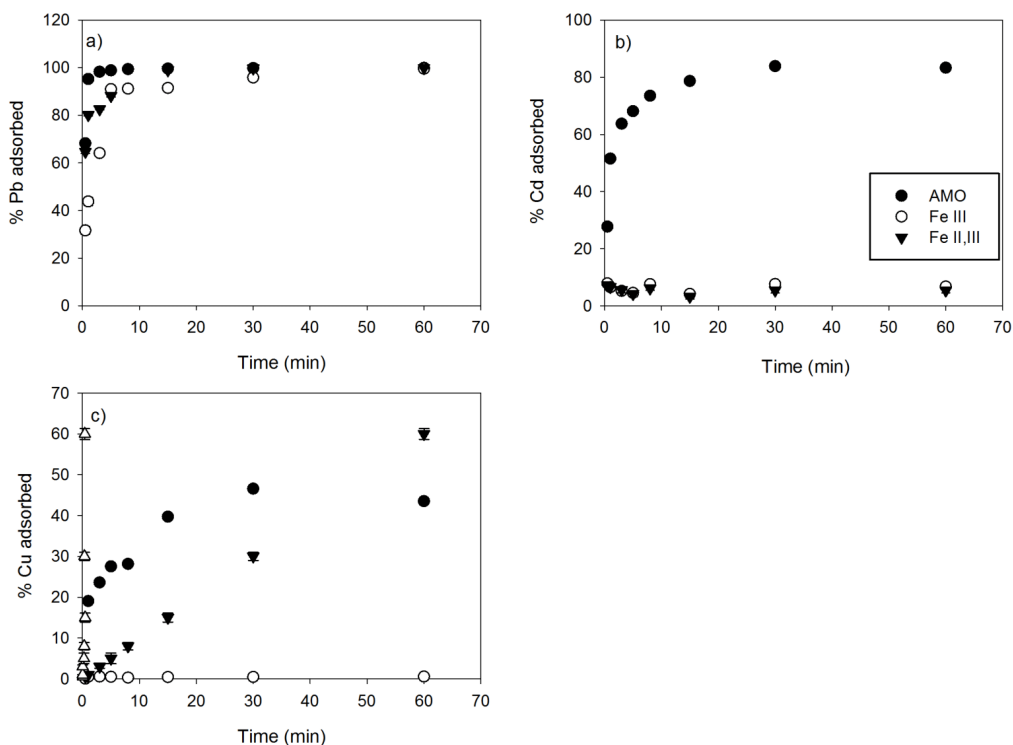


Figure 2.1

Kinetics of Pb (a), Cd (b) and Cu (c) adsorption onto the studied (nano)oxides at pH 4.25 (Cu) and 5.85 (Cd and Pb) (n = 2).

AMO: amorphous Mn oxide, Fe III: maghemite, Fe II,III: magnetite.

Almost all obtained adsorption isotherms (**Fig. 2.2**) fitted better the Langmuir model with the only exception of Pb adsorption onto Fe III and Fe II,III (**Table 2.4**). The calculated adsorption isotherm parameters corresponded well to the results from batch and column experiments (see Section 3.3). The AMO showed the highest affinity (K parameter) for the targeted metals (**Fig. 2.2, Table 2.4**). The calculated S_{\max} (maximal adsorbed metal mass) again highlights AMO as the most efficient sorbent for the studied metals and retained 2.24, 0.52 and 4.02 mmol g^{-1} for Cd, Cu and Pb, respectively. The observed adsorption of Cu and Cd onto Fe III and Fe II,III was significantly lower compared to the AMO. As values of pH_{zpc} of all studied materials (**Table 2.1**) should theoretically favor the adsorption of anionic species under given experimental conditions, it is possible to suggest the major role of chemisorption as the main process involved in metal retention. Higher Pb adsorption

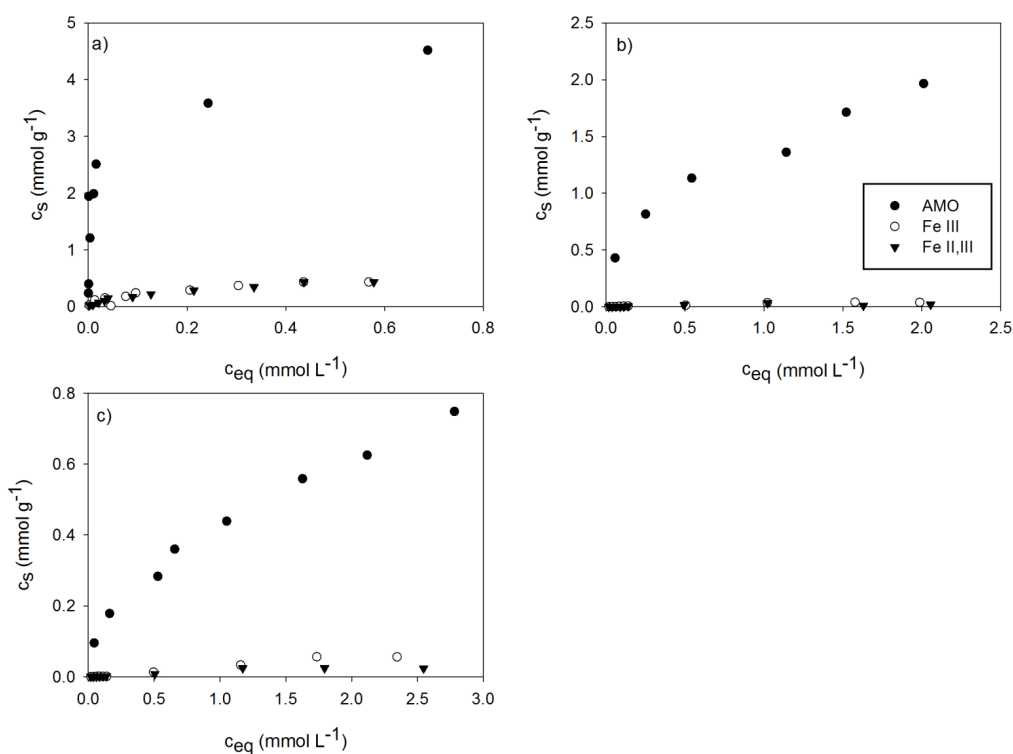


Figure 2.2

Isotherms of Pb (a), Cd (b) and Cu (c) adsorption onto the studied (nano)oxides at pH 4.25 (Cu) and 5.85 (Cd and Pb) ($n = 2$).

AMO: amorphous Mn oxide, Fe III: maghemite, Fe II,III: magnetite.

onto Mn oxides compared to other metals can be generally explained by different occupancy of binding sites, when Pb^{2+} is able to enter the Mn oxide structure (O'Reilly and Hochella, 2003) and to occupy both interlayer and surface edge sites of the Mn oxide in contrast to other metals (Cd^{2+} , Cu^{2+} and Zn^{2+}) occupying mostly interlayer sites (Wang et al., 2011b).

Table 2.4

Modeled Langmuir and Freundlich isotherm parameters (S_{max} , K) and model efficiency (E) describing the adsorption of Cd, Cu and Pb onto amorphous Mn oxide (AMO), maghemite (Fe III) and magnetite (Fe II,III) at pH values of the studied soils (4.25 for Cu and 5.85 for Cd and Pb). Isotherm models with $E < 0.50$ were considered as not fitting.

		Langmuir			Freundlich		
		S_{max} (mmol g ⁻¹)	K (L mmol ⁻¹)	R ²	n	K (L mmol ⁻¹)	R ²
AMO	Cd	2.243	2.057	0.93	n.a.	n.a.	< 0.50
	Cu	0.522	0.762	0.97	n.a.	n.a.	< 0.50
	Pb	4.019	135.32	0.82	n.a.	n.a.	< 0.50
Fe III	Cd	0.088	0.505	0.98	0.706	0.028	0.96
	Cu	0.156	0.250	0.97	0.562	0.035	0.93
	Pb	n.a.	n.a.	< 0.50	0.458	0.633	0.99
Fe II,III	Cd	0.100	0.445	0.99	n.a.	n.a.	< 0.50
	Cu	0.066	0.373	0.96	0.764	0.017	0.94
	Pb	n.a.	n.a.	< 0.50	0.543	0.658	0.99

AMO: amorphous manganese oxide, Fe III: maghemite, Fe II,III: magnetite.

Batch experiments

Interactions of the (nano)oxides with the soil solutions were studied using SEM coupled with EDS analysis (Fig. 2.3). The analysis identified the partial transformation of the AMO to rhodochrosite ($MnCO_3$), stabilizing to some extent the AMO in the soils (Ettler et al., 2014). No significant observable changes were identified for the Fe nanooxides. In the study of Ettler et al. (2014), 90-days incubation of the AMO in soil samples resulted not only in the formation of rhodochrosite, kutnahorite ($CaMnCO_3$) and scacchite ($MnCl_2$), but also to observable particle aggregation, decreasing thus the amount of particles smaller than 5 mm from

78% to 9-18%. The application of the studied (nano)oxides had no effect on soil pH, except for AMO in the Dystric Udept where its addition increased soil $\text{pH}_{\text{H}_2\text{O}}$ from 4.25 up to 5.54 (1% AMO, w/w) and to 6.47 (2% AMO, w/w), respectively. The effect on pH of Haplic Udept was negligible (increasing from 5.77 (Control) to 5.92 (1% AMO, w/w) and 5.94 (2% AMO, w/w)). The pH increases observed after AMO application were greater in acidic soils in general mainly due to the high pH value (8.1) of the phase and its acidic dissolution (Della Puppa et al., 2013; Ettler et al., 2014).

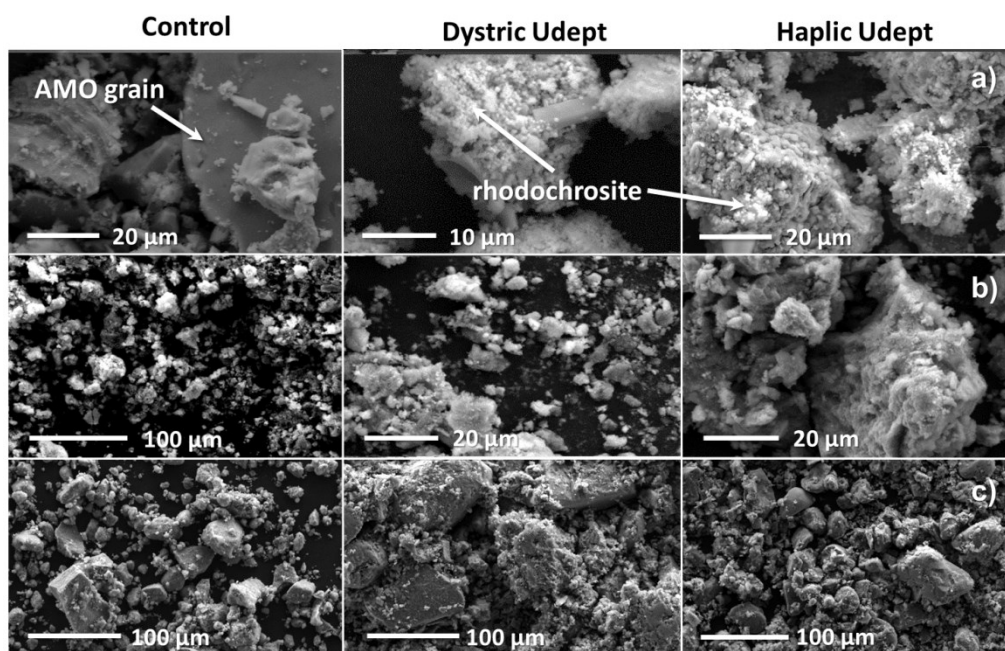


Figure 2.3

SEM images of AMO: amorphous Mn oxide (a), Fe III: maghemite (b), Fe II,III: magnetite (c) (nano)particles before (Control) and after incubation in soil solutions from the studied soils.

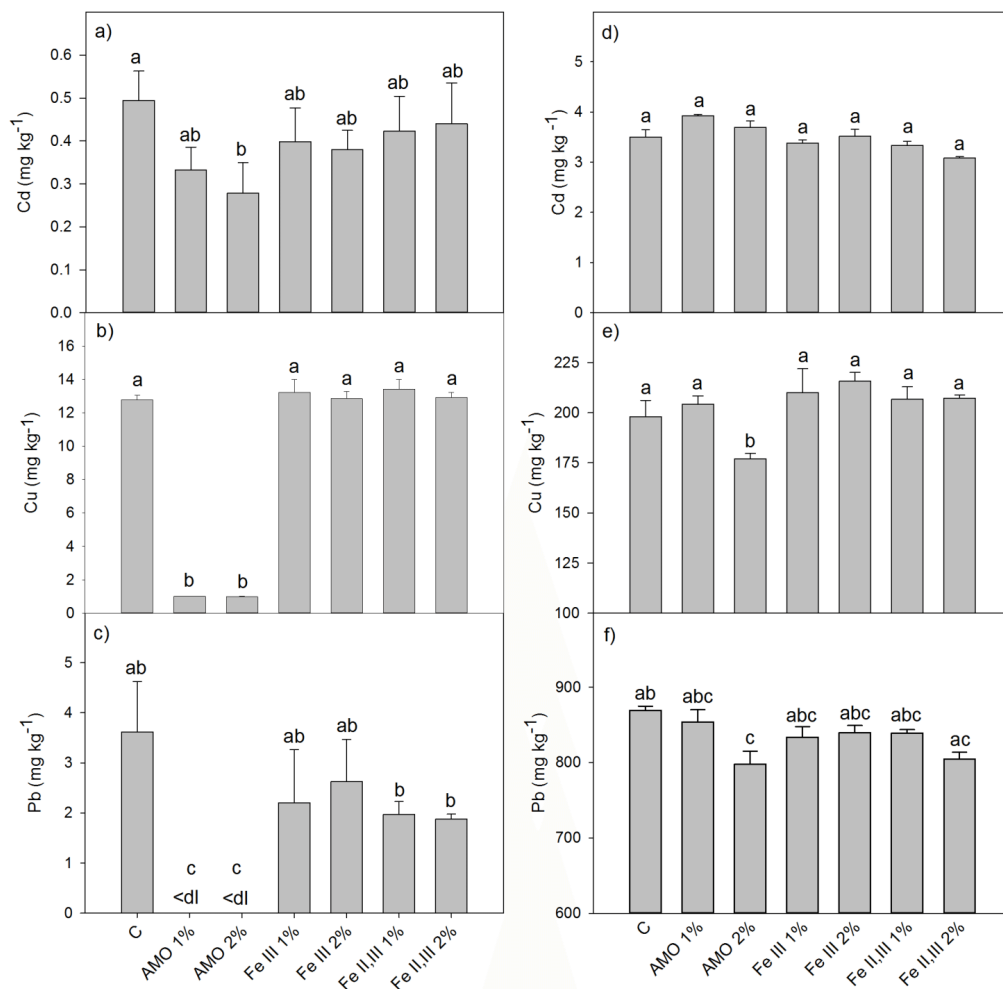


Figure 2.4

Results from the 0.01 M CaCl₂ extraction of Haplic Udept (a) and Dystric Udept (b, c) and from the 0.05 M EDTA extraction of Haplic Udept (d, f) and Dystric Udept (e), performed after 62 days of incubation (n = 3).

bdl: below detection limit; *C*: control; *AMO*: amorphous Mn oxide, *Fe III*: maghemite, *Fe II,III*: magnetite.

Data with the same letter represent statistically identical values (P < 0.05).

Analyses of metal and DOC concentrations in soil solutions coupled with simple and sequential extraction procedures were applied to determine the influence of the tested (nano)oxides on the availability and mobility of the metals and to observe changes in their fractionation. In general, the most observable effects were recorded for the AMO (Figs. 2.4 and, 2.5, 2.6). Results obtained from the sequential extraction (Fig. 2.6) performed after 62 days of incubation imply that after two months, AMO was able to decrease the amount of exchangeable Cu and Pb down to 43% and 13% of the control, respectively, with a simultaneous increase in the reducible and oxidizable metal fractions. Similar results were described by Kumpiene et al. (2006) where the application of ZVI decreased the exchangeable fraction of Cu and increased its oxidizable and especially reducible fraction. A less pronounced decrease of exchangeable metals was observed even in the control treatment and can be explained by the leaching of the most mobile fraction during 62 days of the experiment.

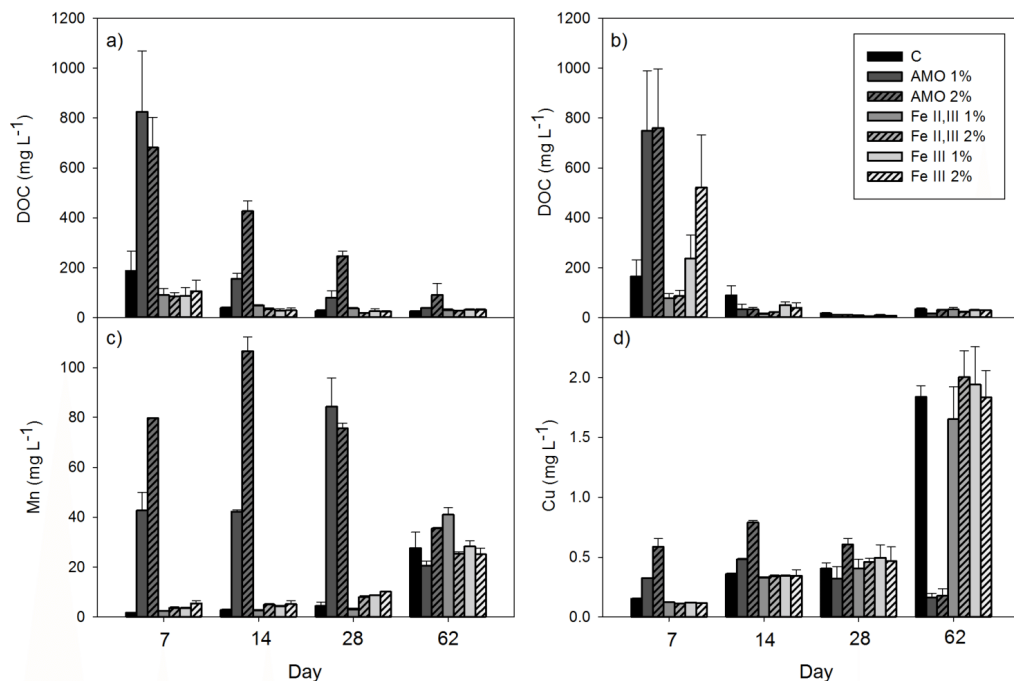


Figure 2.5

DOC concentrations in soil solutions from rhizons from Dystric Udept (a) and Haplic Udept (b) and Mn (c) and Cu (d) from Dystric Udept (n = 3).

C: control, AMO: amorphous Mn oxide (2%, w/w), Fe III: maghemite (2%, w/w), Fe II,III: magnetite (2%, w/w).

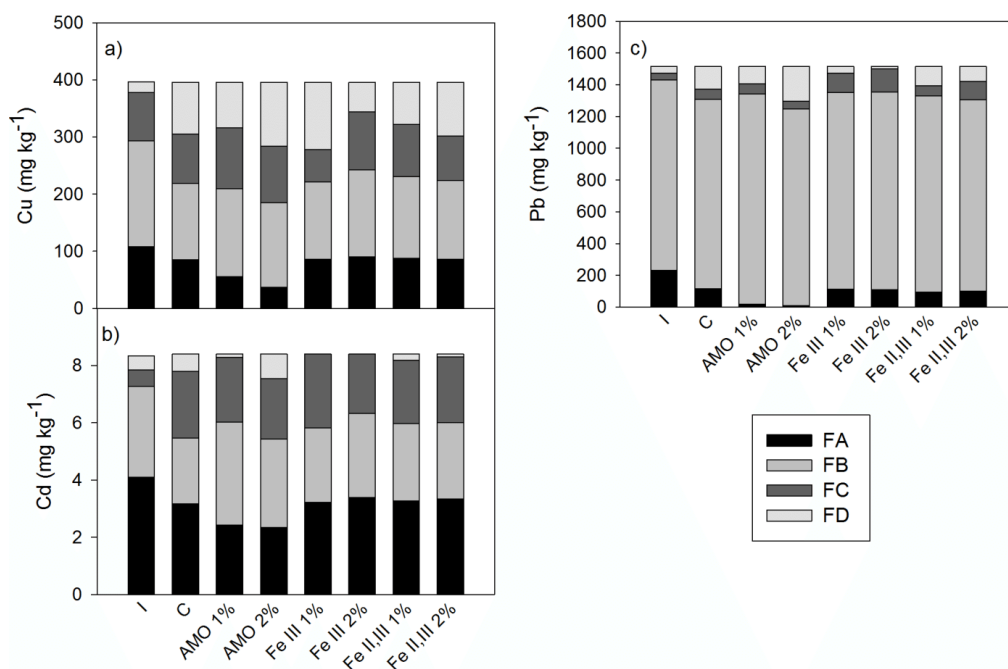


Figure 2.6

Results from the sequential extraction for the Dystric Udept (a) and Haplic Udept (b, c) performed after 62 days of incubation ($n = 3$).

Fractions: FA - exchangeable, FB oxidizable, FC - reducible, FD - residual.

I: original soil, C: control, AMO: amorphous Mn oxide, Fe III: maghemite, Fe II,III: magnetite.

Data from the CaCl_2 extraction (Fig. 2.4a, b, c) showed similar results. Both Cu and Pb concentrations decreased significantly after AMO application (down to 8% of the control in the case of Cu and below the limit of detection, i.e., 0.001 mg L^{-1}). A statistically significant decrease of CaCl_2 -extractable Cd was observed only in the soil amended with AMO (2%, w/w). Similar results were observed after the application of amorphous alumina (5%, w/w) and ferrihydrite (10%, w/w) with a significant decrease of 0.01 M CaCl_2 -extractable Cu and Pb by 23% and 8%, respectively (McBride and Martínez, 2000). On the other hand, birnessite application (10%, w/w) resulted in the abovementioned study into a 3- and 2.6-fold increase of 0.01 M CaCl_2 -extractable Cu and Pb, respectively, released due to SOM oxidation, which could be the case for the AMO application as well (see next paragraph). Differences in results obtained from the extraction with EDTA (Fig. 2.4d, e, f) are not as apparent as EDTA is a much stronger extracting (chelating) agent compared to

CaCl₂. It should be pointed out that EDTA caused a significant release of Mn originated from AMO dissolution (data not shown). Manganese concentrations were 10 times higher in the AMO-amended Haplic Udept and 70 times higher in the Dystric Udept compared to the control. Interestingly, this trend was not observed for Fe in soils amended with Fe III and Fe II,III, despite the higher affinity of trivalent Fe for EDTA compared to Mn ($\log K_{\text{FeEDTA}} = 27.2$; $\log K_{\text{MnEDTA}} = 15.6$; Martell et al., 2001). This is probably caused by the stronger AMO dissolution (lower stability) due to its amorphous/poorly crystalline character.

Soil solution samples collected using rhizons were analyzed in order to observe directly the changes of metal concentrations and DOC contents during two months after the addition of the (nano) oxides (**Fig. 2.5**). The AMO (2%, w/w) proved again to be the most efficient amendment in decreasing metal contents in soil solutions. However, in accordance with Ettler et al. (2014), AMO also significantly increased DOC concentrations in the soil solution, especially at the beginning of the experiment, together with significant increase of pH of the Dystric Udept. This was probably caused by AMO-induced SOM dissolution coupled with the release of surface glucose/oxalate residues originated from AMO synthesis. Based on SEM/TEM/XRD analysis and studies of newly formed phases, hydrolytic dissolution of AMO in the presence of SOM could result into oxidation of SOM coupled with Mn reduction connected with a release of OH⁻ ions (Ettler et al., 2014). Manganese(II) then precipitates with CO₃²⁻ as rhodochrosite. This process can be accelerated by microbial respiration producing CO₂ and lead to the stabilization of the AMO surface by formation of rhodochrosite coatings (Ettler et al., 2014; Ying et al., 2011). The observed increased DOC concentrations were associated with increased Cu concentrations as significant amounts of Cu bound with SOM were probably released due to its oxidation by AMO. Similar results were observed when birnessite (10%, w/w) was applied to a Cu-contaminated soil, which caused a 7.5-fold increase in DOC content associated with a 3-fold increase in 0.01 M CaCl₂-extractable Cu (McBride and Martínez, 2000). Correlation between DOC and Cu concentrations in soil solution was also observed after the application of red mud (2%, w/w), which was attributed to increased DOC dissolution promoted by this amendment (Lombi et al., 2002).

The addition of AMO resulted into significant amounts of Mn released to the soil solution, especially at the beginning of the experiment. This release was significantly higher in the more acidic Dystric Udept compared to the Haplic Udept (by 2 orders of magnitude). Because the total Mn concentration in the Dystric Udept was 7 times

lower than in the Haplic Udept (**Table 2.2**), it is possible to assume that Mn ions supposedly originated from AMO dissolution or from weakly adsorbed unidentified surface Mn species originating from AMO synthesis. In the study of Ettler et al. (2014), the highest Mn mass loss from the AMO was recorded during the first 15 days. Nevertheless, total mass loss during 90 days of experiment reached 18% in an acidic forest soil (pH 4.2) and 13% in a slightly acidic agricultural soil (pH 5.4).

Column experiments

Results from the column experiments provided additional information to those from the static batches. Metal and DOC concentrations (**Figs. 2.7a and b**) were measured in the leachate from the Dystric Udept after the SPLP (pH 5.0) treatment. Changes in pH and redox status are depicted in **Fig. 2.8**. AMO proved to be the most effective treatment for decreasing Cu content in the leachate during the first 1000 min, but it also caused a significant increase in pH. Due to the one-month equilibration period prior to the column experiment, no intensive dissolution of SOM induced by the AMO as in the case of incubation experiments was observed. Nevertheless, the treatment with AMO led to the highest DOC content in the leachate (associated with the highest pH level) compared to other amendments but all the treatments resulted into the stabilization of the SOM in soils. Spuller et al. (2007) observed in their column leaching an apparent correlation between DOC and Cu contents in the leachate as the mobilization of organic matter favors leaching of mobile Cu-DOC complexes.

Breakthrough curves (**Fig. 2.7c**) were constructed in order to describe the ability of the studied (nano)oxides to retain/stabilize additional Cu added to the soil, which simulates to some extent, a reactive stabilizing layer for Cu migrating downward from upper soil layers. The curves were constructed as a ratio of Cu in leachate and Cu in the original leaching solution. At the beginning of the experiment (up to 600 min), the highest concentration of Cu was observed in the unamended control soil. For the first 2 h, Fe II,III was able to maintain Cu concentrations in the leachates below 1% of the total inflow concentrations, until the concentration started to increase constantly, while Fe III started at a concentration of ~4% with a constant increase reaching 80% (Fe II,III) and 60% (Fe III) after 24 h, respectively. The best results were obtained with the AMO addition; the AMO was able to maintain Cu concentrations below 1% of total inflow concentration for the first 6 h and reached 40% at the end of the experiment. Increase of pH in the leachates by 1.5-2 units after the application of AMO has been observed during the experiment (**Fig. 2.8**) and it is

clearly an important factor influencing its stabilization potential. Additionally, no significant redox changes that would influence metal and oxide geochemistry were observed (**Fig. 2.8**).

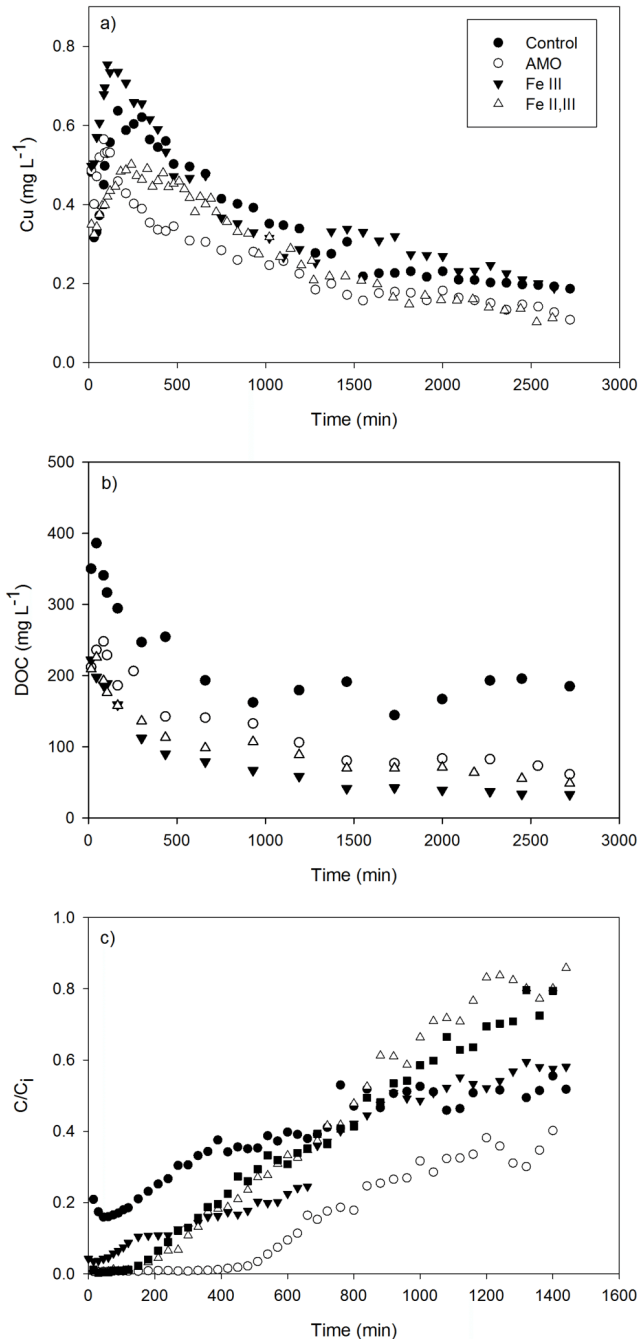


Figure 2.7

Cu (a) and DOC (b) concentrations in SPLP leachate from column experiments with Dystric Udept and breakthrough curve of Cu after the application of Cu nitrate (c).

C: control, AMO: amorphous Mn oxide (2%, w/w), Fe III: maghemite (2%, w/w), Fe II,III: magnetite (2%, w/w).

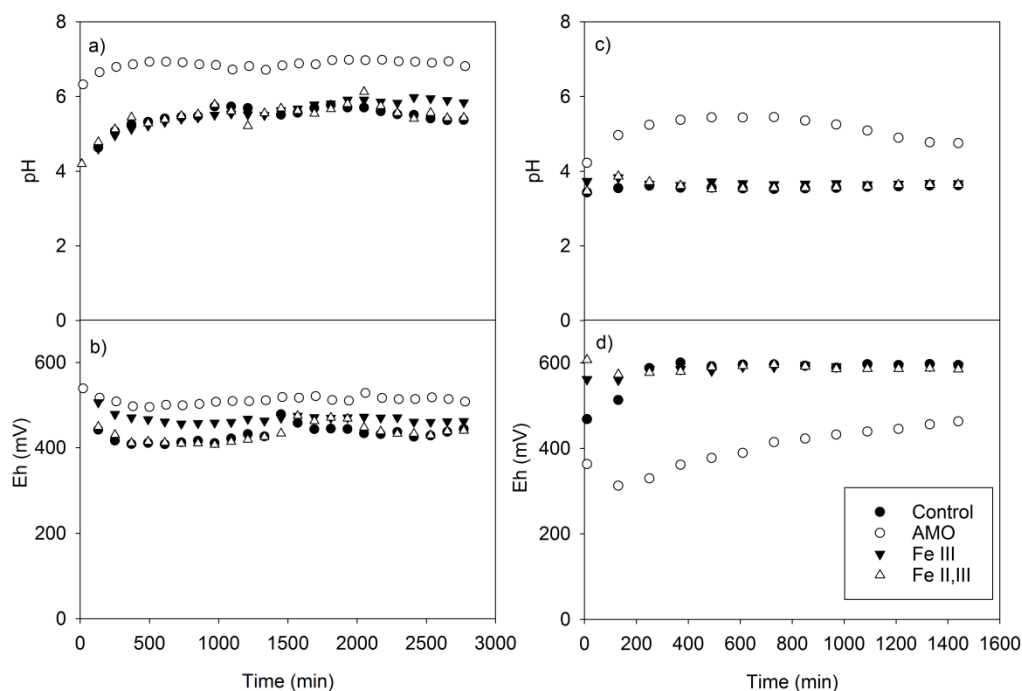


Figure 2.8

The pH and Eh values measured in eluate after column leaching with SPLP, pH 5.0 (a, b) and Cu nitrate (c, d) (Dystric Udept).

AMO: amorphous Mn oxide (2%, w/w), Fe III: maghemite (2%, w/w), Fe II,III: magnetite (2%, w/w).

Effect of (nano)oxides on soil microbiological activity

Simple enzymatic and soil respiration tests were performed for evaluating the influence of the stabilizing amendments on microorganism activity in the treated soils. In general, the AMO had the highest influence on measured parameters in both soils (**Fig. 2.9**) while other treatments proved to have no effect. The TPF production was supposed to correspond to the respiration rate as dehydrogenase is involved in the respiratory chain (Kandeler, 2007). The TPF production in the Haplic Udept after AMO addition was significantly higher than in other cases, yet the respiration rate was not significantly higher. In the case of Dystric Udept, the soil respiration rate increased significantly after AMO addition by 75% compared to the control. However, as it is known that the TCC test is not the best choice for soils with high Cu concentrations and it should be taken into account that the obtained results could be

overestimated due to the abiotic reaction of TPF with free Cu species (Chander and Brookes, 1991). The increased microbial activity after soil remediation is commonly interpreted as a proof of decreased mobile/bioavailable metal fractions and restoration of indigenous soil environments (Kumpiene et al., 2006; Lee et al., 2011). Yet in this case, it was probably also the effect of increased DOC amount that supported microbial activity. The decrease in the directly available metal species (e.g., free Cu^{2+}) as a result of AMO application was perhaps related to decreased cytotoxicity and increased amounts of low-weight organic compounds originating from SOM dissolution and organic residues from AMO synthesis serving as additional substrate for soil microorganisms (Della Puppa et al., 2013; Ettler et al., 2014).

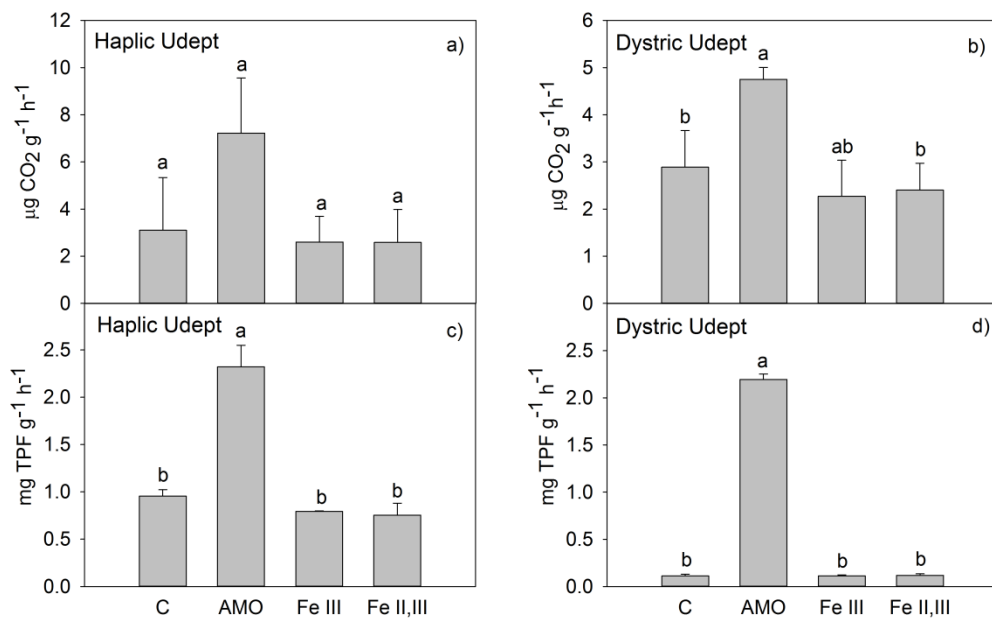


Figure 2.9

Results from soil respiration tests in Haplic Udept (a) and Dystric Udept (b) and from soil dehydrogenase tests in Haplic Udept (c) and Dystric Udept (d) ($n = 3$).

C: control, AMO: amorphous Mn oxide (2%, w/w), Fe III: maghemite (2%, w/w), Fe II,III: magnetite (2%, w/w).

Data with the same letter represent statistically identical values ($P < 0.05$).

Conclusions

Results from batch and column experiments coupled with adsorption tests proved that the AMO was the most effective treatment for the stabilization of metals in the studied soil samples at the given w/w ratios (1 and 2%, w/w). Metal stabilization resulted from combined specific adsorption onto the AMO surface together with an increase in soil pH promoting the adsorption of metallic cations. On the other hand, no impact on soil pH was found for the Fe oxides. Furthermore, the AMO had a positive influence on the activity of soil microorganisms, although this was partially caused by the increased DOC concentration originating from SOM dissolution. Nevertheless, the strongly oxidizing properties of the AMO has to be taken into account as it is able to promote SOM dissolution associated with the (re)mobilization of adsorbed metals. Results obtained for the AMO during laboratory experiments (the longest experiment in soil conditions took 3 months; Ettler et al., 2014) highlight the necessity of long-term field studies addressing important questions concerning its transformation and stability in the soil environment. Further information about the importance of resulting pH alterations compared to specific metal adsorption onto the AMO and its transformation products are also needed.

Chapter III

Selected Fe and Mn (nano)oxides as perspective amendments for the stabilization of As in contaminated soils

Z. Michálková, M. Komárek, V. Veselská, S. Číhalová

Adapted from *Environmental Science and Pollution Research* 23 (2016):
10841-10854.

Content

Abstract	63
Introduction	64
Materials and methods	66
Properties of studied soils and oxides	66
Arsenic adsorption onto Fe and Mn (nano)oxides	68
Adsorption kinetics and isotherms	68
XPS analyses	69
Incubation batch experiments	69
pH-static leaching experiments	70
Statistical analysis	70
Results and discussion	70
Characterization of the studied soils	70
Arsenic adsorption study	73
Adsorption kinetics and isotherms	73
XPS analyses	76
Incubation batch experiments	79
pH-static leaching experiments	82
Conclusions	84

Abstract

An amorphous Mn oxide (AMO), nanomaghemite, and nanomagnetite were used as potential amendments reducing the mobility of As in three contrasting contaminated soils differing in origin of As contamination. Adsorption experiments and XPS analyses combined with incubation batch experiments and pH-static leaching tests were used. The AMO showed excellent adsorption capacity for As(V) reaching a maximum of 1.79 mmol g⁻¹ at pH 7 and 8. Interestingly, the adsorption capacity in this case decreases with decreasing pH, probably as a result of AMO dissolution at lower pH values. Chemical sorption of As(V) onto AMO was further confirmed with XPS. Both Fe nano-oxides proved the highest adsorption capacity at pH 4 reaching 11 mg g⁻¹ of adsorbed As(V). The AMO was also the most efficient amendment for decreasing As concentrations in soil solutions during 8 weeks of incubation. Additionally, pH-static leaching tests were performed at pH 4, 5, 6, 7, and natural pH (not adjusted) and AMO again proved the highest ability to decrease As content in leachate. On the other hand, strong dissolution of this amendment at lower pH values (especially pH 4) was observed. For that reason, AMO appears as a promising stabilizing agent for As, especially in neutral, alkaline, or slightly acidic soils, where As(V) species are expected to be more mobile.

Introduction

Arsenic is ubiquitous in the environment being ranked as the 20th most abundant element in the earth's crust (Mandal and Suzuki, 2002). It occurs mainly in four oxidation states - arsenate As(V), arsenite As(III), elemental arsenic As(0), and arsine As(-III), differing in their mobility, bioavailability, and toxicity (Sharma and Sohn, 2009). In general, inorganic As species are more toxic than organic ones and As(III) is usually more toxic and mobile than As(V) (Duker et al., 2005; Singh et al., 2015). Among the mentioned possible oxidation states, As(V) is the prevailing form in oxidizing environmental conditions including oxidic soil horizons (Cancès et al., 2008; Duker et al., 2005; Giral et al., 2010; Shi et al., 2003). Occurrence of As in the environment and its potential entrance into the food chain are of great public concern as As has shown to be a proven human carcinogen causing skin, brain, liver, kidney, and stomach cancer (Ng, 2005; Smith et al., 1992). Additionally, As species are phytotoxic with the ability to accumulate within the plants (Farrow et al., 2015; Meharg et al., 2008). The main source of As in the environment is usually considered to be its release from As-enriched minerals. Yet, many anthropogenic activities, such as mining and smelting, coal combustion, use of insecticides, pesticides, phosphate fertilizers, and timber preservatives, play an important role in the input and propagation of As in the environment (Singh et al., 2015). The main pathway of human intoxication with As is through drinking water (Villaescusa and Bollinger, 2008) and consumption of food (predominantly rice) with increased As levels (Rahman and Hasegawa, 2011). For that reason, considerable effort is put into developing efficient and sustainable methods of remediation of As-contaminated soils and waters.

The use of Fe and Mn (nano)oxides for chemical stabilization/immobilization of As in contaminated soils have the potential to be more cost-effective and less disruptive compared to traditional methods of remediation (Kumpiene et al., 2008; Komárek et al., 2013). Iron and Mn oxides are naturally occurring soil components that can be found virtually in most types of soils. Due to their large and reactive surface, they possess considerable sorption properties and are playing thus a significant role in nutrient and contaminant cycling in soils (Sposito, 2008). Because of their high abundance and high isoelectric point, Fe (hydr)oxides possess a strong affinity toward As and are thus considered to be the main sink of As in soils (Wang and Mulligan, 2008). For that reason, they are also the most extensively studied amendments for As stabilization (Kumpiene et al., 2008) that can be applied both directly (Bagherifam et

al., 2014) and in the form of their precursors, e.g., ferrous sulfate (Warren et al., 2003), zerovalent iron (Kumpiene et al., 2006), iron grit (Hartley et al., 2004), or various industrial by-products (e.g., red mud, water treatment residue) (Gray et al., 2006; Nagar et al., 2014). In the study of Bagherifam et al. (2014) dealing with stabilization of As using various naturally occurring metal oxides, a goethite-based amendment proved to be the most efficient in decreasing exchangeable fraction of As together with its bioavailability and was also the most efficient for supporting plant growth (*Hordeum vulgare* L.). The adsorption capacity of Fe and Mn oxides highly depends on the particle size. As the particle size decreases, the specific surface area increases, providing thus more active sites ready for adsorption (Bujňáková et al., 2013; Yean et al., 2005). When the size further decreases down to the nanoscale, particles obtain unique properties inherited from their size, i.e., so called nano-effect (Charlet et al., 2011). For example, Auffan et al. (2007) recorded that 11-nm diameter magnetite was able to adsorb three times more As per nm² than 20- and 300-nm diameter magnetite. Manganese oxides, on the other hand, usually possess a relatively low p*H*_{zpc} (Kosmulski, 2004) and bear thus a net negative charge in common soil conditions, suggesting that they would not be good adsorbents for negatively charged As(V) species (Scott and Morgan, 1995; Wang and Mulligan, 2006). In spite of this, Mn oxides are able to stabilize As in soil through the oxidation of more mobile and toxic As(III) to As(V) connected with reductive dissolution of the Mn-bearing phase (Manning et al., 2002; Scott and Morgan, 1995). Nevertheless, Mn oxides are not suitable amendments for soils contaminated with Cr as they are also able to oxidize Cr(III) to more mobile and toxic Cr(VI) (Feng et al., 2006; Pansar-Kallio et al., 2001).

This paper focuses on the evaluation of an amorphous Mn oxide (AMO), nanomaghemite, and nanomagnetite for their potential use as stabilizing agents for As in contaminated soils. In our previous studies, the AMO has proved its excellent ability to adsorb Cd, Cu, and Pb, reaching the adsorption maxima of 1-2 orders of magnitude higher than those recorded for nanomaghemite and nanomagnetite. In addition, this oxide was also the most efficient in binding/immobilizing contaminants directly in contaminated soils and appears thus as promising and cheap amendment for environmental cleanup (Della Puppa et al., 2013; Micháľková et al., 2014; Ettler et al., 2015). Due to the unusually high p*H*_{zpc} of the AMO (8.3) (Della Puppa et al., 2013), together with the expected high affinity of As for nano-sized Fe oxides, these amendments are interesting candidates for the remediation of As-contaminated soils. The main objectives of the present study were thus to determine the adsorption properties of tested Fe and Mn oxides toward As and

subsequently examine their effect on As mobility in contaminated soils together with their influence on soil characteristics.

Materials and methods

Properties of the studied soils and oxides

Three different Fe and Mn (nano)oxides were used in our study to evaluate their influence on the mobility of As and other risk elements in contaminated soils: (i) nano-sized γ -Fe₂O₃ - maghemite; (ii) nano-sized Fe₃O₄ - magnetite, both purchased from Sigma-Aldrich (Germany); and (iii) an amorphous manganese oxide (AMO) synthesized according to Della Puppa et al. (2013). The specific surface area of the AMO was determined using the Brunauer-Emmett-Teller (BET) method and the ASAP 2050 instrument (Micrometrics Instrument Corporation, USA). The pH of the studied oxides was measured in deionized water at 1:10 (w/v), and the pH_{zpc} was determined using the immersion technique (Fiol and Villaescusa, 2009) at 1:10 (w/v). Properties of the tested amendments are summarized in **Table 3.1**.

Table 3.1

Properties of the tested (nano)oxides

	Chemical formula	Particle size (nm)	pH	pH _{zpc}	BET (m ² g ⁻¹)
AMO ^a	δ -MnO ₂	600-1200	8.1	8.3	134.9 ^b
Fe III ^c	γ -Fe ₂ O ₃	20-100	3.0	7.4	46.6
Fe II,III ^c	Fe ₃ O ₄	20-100	4.9	6.9	36.6

AMO: amorphous manganese oxide; Fe III: maghemite; Fe II,III: magnetite

^a Della Puppa et al. (2013)

^b This study

^c Michálková et al. (2014)

Three contrasting soils with varying As sources were used in this study. The first soil (Fluvisol) was collected from a river alluvium polluted by occasional floods as the stream was heavily contaminated due to the infiltration of rainwater through the historical slag heaps from nearby Pb-processing smelter in Příbram (Czech Republic). The second soil (Cambisol) was sampled at the Mokrsko gold deposit (Czech Republic), where As occurs naturally in a form of As-bearing minerals, predominantly as arsenopyrite (FeAsS) (Drahota et al., 2009). The last soil (Chernozem) was collected in Prague-Suchdol (Czech Republic) as an uncontaminated soil that was subsequently artificially spiked with As(V) (see below). This artificially spiked soil was used for experimental purposes in addition to field contaminated samples as, in spite of high total concentrations, the easily mobilizable fraction of As in these soils was relatively low (see “Characterization of the studied soils,” **Table 3.3**).

Soil samples were collected from the superficial layer (0-20 cm), air-dried, homogenized, and sieved through a 2-mm stainless sieve. The Chernozem soil was mixed with a solution of As(V) (as $\text{Na}_2\text{HAsO}_4 \cdot 7\text{H}_2\text{O}$) in order to reach As content in soil of approximately 1000 mg kg^{-1} (i.e., similarly to the Cambisol), left to equilibrate for 2 months maintaining ~60-70 % of the water-holding capacity (WHC) and subsequently air-dried again. Particle size distribution was determined according to Gee and Or (2002). Soil pH was measured in suspension using a 1:2.5 (w/v) ratio of soil/deionized water or 1 M KCl (ISO 10390:1994). Total organic carbon content (TOC) was determined using the carbon analyzer TOC-L CPH (Shimadzu, Japan). Cation exchange capacity (CEC) was determined according to Carter and Gregorich (2008). Pseudo-total concentrations of elements were determined using the US EPA aqua regia extraction method (US EPA method 3051a) with microwave digestion (SPD-Discover, CEM, USA) and ICP-OES analysis (Agilent 730, Agilent Technologies, USA). The fractionation of metals was determined using the modified BCR sequential extraction procedure by Rauret et al. (2000), and the fractionation of As was determined according to Wenzel et al. (2001a). The standard reference materials 2710a Montana Soil I (NIST, USA) and CRM 483 (Institute for Reference Materials and Measurements, EU) were used for QA/QC. All chemicals used were of analytical grade.

Arsenic adsorption onto Fe and Mn (nano)oxides

Adsorption kinetics and isotherms

Adsorption experiments were used to evaluate the kinetics of As(V) adsorption onto the tested (nano)oxides and to construct corresponding adsorption isotherms prior to their application to soils. This study was focused solely on As. The adsorption of metallic contaminants, such as Cd, Cu, Pb, and Zn, was already the objective of our previous studies (Della Puppa et al., 2013; Micháľková et al., 2014). Arsenate was chosen for our study as the chosen (nano)oxides were further tested as potential stabilizing amendments for oxidic (upper) soil horizons where As(V) occurs as the predominant species (Cancès et al., 2008). All adsorption experiments were performed in 0.01 M NaNO₃ as background electrolyte. The kinetic study was performed in a suspension of 1 g L⁻¹ of the (nano)oxides and 10 mg L⁻¹ As(V) (added as Na₂HAsO₄•7H₂O) at pH 6. A separate batch was used for each (nano)oxide. The suspension was then agitated for up to 4 days, and the pH was controlled using NaOH/HNO₃ and an automatic titration device (TitroLine alpha plus, SI Analytics, Germany). Five milliliters of the suspensions were collected after each time step in duplicate, filtered immediately through a 0.45-μm nylon syringe filter and subsequently through a 0.22-μm filter to ensure effective separation of solid particles. The filtration efficiency was controlled by analyzing Fe and Mn in the filtrates. Metal concentrations in solutions were determined using ICP-OES (720 Series, Agilent Technologies, USA). The obtained kinetic data were further modeled using pseudo-second-order equation, which is a common model used for these adsorption studies (Kalantari et al., 2015; Karami, 2013; Markovski et al., 2014; Mohan et al., 2011; Wang et al., 2015e; Yari et al., 2015).

Adsorption isotherm experiments at equilibrium were performed at pH 4, 5, 6, 7, and 8 for each (nano)oxide with As(V) concentrations varying from 2 to 300 mg L⁻¹. Equilibrium time was set according to the results of previous kinetic experiments (see “Arsenic adsorption study”, page 73) at 10 h for AMO and 72 and 48 h for nanomagemite and nanomagnetite, respectively. Langmuir and Freundlich models were subsequently used to describe experimental data and to calculate adsorption isotherm parameters (Bolster and Hornberger, 2007).

XPS analyses

The adsorption mechanisms of As(V) onto the AMO were further examined using XPS. The XPS analyses of nanomaghemite and nanomagnetite were not performed as the mechanisms of As(V) adsorption onto these solids are already well known (Dixit and Hering, 2003; Jönsson and Sherman, 2008; Liu et al., 2015; Morin et al., 2008; Wang et al., 2011a). The samples were prepared under the same conditions as in adsorption experiments by mixing the AMO in 3 mM As(V) solution for 10 h at pH 7. The solid fraction was filtered, washed with deionized water, and dried at room temperature, and the concentrations of elements in filtrates were analyzed using ICP-OES. The XPS analyses were carried out using the ESCA 3400 instrument (Kratos, UK) with Mg K α energy source (1253.6 eV). Pulverized samples of original (i.e., before sorption) and As-treated (i.e., after sorption) AMO were applied on carbon layer in thin film and cleared by Ar ion bombardment. Samples were measured in the range of kinetic energies from 0 to 800 eV with sample step of 0.1 eV (review spectra) and then in Cr2p bands (570-595 eV) with 0.05 eV step. The obtained spectra were identified using NIST X-ray Photoelectron Spectroscopy Database (NIST Standard Reference Database 20, version 4.1).

Incubation batch experiments

Incubation batch experiments were performed in order to investigate the changes in soil solution characteristics and mobility of As and metals in the contaminated soils after the addition of the tested amendments. The experiment was performed in triplicate using the Fluvisol and Chernozem soils in variants: C (control), AMO, nanomaghemite and nanomagnetite at concentrations of 1 % (w/w) (Micháľková et al., 2014). The Cambisol was not suitable for this experiment as the amount of As in unamended soil solution in preliminary experiment remained below the limit of detection (data not shown). The amount of 125 g of air-dried soil was placed in pots and watered continuously with deionized water in order to maintain ~60-70 % of the WHC. No leaching was allowed during this experiment. The incubation experiment was performed in separate pots for 1, 4, and 8 weeks. After these periods, soil solution was directly collected using rhizon samplers (mean pore volume size 0.15 μ m; Rhizosphere Research Products, Netherlands) and metals, As and DOC concentrations were analyzed using ICP-OES and TOC/ DOC analyzer, respectively. The pH of the soil solution was monitored throughout the experiment. Finally, As fractionation in soil samples incubated for 8 weeks was determined using the sequential extraction by Wenzel et al. (2001a).

pH-static leaching experiments

The pH-static leaching tests were performed in order to evaluate the influence of pH on the stabilizing potential of the studied amendments. Prior to the experiment, the air-dried soil was mixed with the amendments as follows: C (control), AMO, nanomaghemite, and nanomagnetite at concentrations of 1 % (w/w) and maintained at ~60-70 % of the WHC for 1 month. The amount of 1.5 g of dry soil was then watered with 15 mL of deionized water and leached for 48 h (Van Herreweghe et al., 2002) at pH 4, 5, 6, and 7. The pH was continuously controlled and adjusted using NaOH/HNO₃. A variant with natural soil pH (i.e., without pH adjusting) was included. All experiments were performed in triplicates. After the end of experiment, the pH of samples without pH adjustments was determined. All samples were then centrifuged (5000 rpm, 10 min) and filtered through 0.45- μ m nylon syringe filters. The Eh value was measured in filtrate. Metals, As, and DOC concentrations in leachates were measured using ICP-OES and TOC/DOC analyzer, respectively.

Statistical analysis

All statistical analyses were performed using SigmaPlot 12.5 (StatSoft Inc., USA). The experimental data were evaluated using analysis of variance (ANOVA) at $P < 0.05$ using the Tukey test.

Results and discussion

Characterization of the studied soils

Basic physicochemical properties of the studied soils are summarized in **Table 3.2**. The pH of both the Fluvisol and Cambisol are slightly acidic, whereas the pH of the artificially As-spiked Chernozem is alkaline. The Fluvisol and Cambisol have also a coarser texture than the Chernozem. The highest TOC content was observed in the case of Fluvisol, but it was also the soil with the lowest CEC. While elevated contents of As, Cd, Pb, and Zn were observed only in the Fluvisol originating from the smelting industry, As was the only major contaminant in the Cambisol and Chernozem. The concentrations of metals and As in the Fluvisol highly exceed limits set for agricultural soils set by the Ministry of the Environment of the Czech Republic (Act No. 13/1994) (**Table 3.2**). The predominant valence state of As in sampled soils

is supposed to be As(V) as the soil was sampled from the upper aerated layer. Additionally, the pH-Eh conditions in all the sampled soils favor strongly the presence of As(V).

Table 3.2
Basic physico-chemical characteristics of studied soils.

	Fluvisol	Cambisol	Chernozem	
pH _{H2O}	5.95	6.05	8.01	
pH _{KCl}	4.97	4.43	7.05	
CEC (cmol kg ⁻¹)	9.10 ± 0.49	35.9 ± 4.7	36.3 ± 9.1	
TOC (mg kg ⁻¹)	2.35	1.10	2.07	
Particle size distribution (%)				
Clay (%)	5	2	17	
Silt (%)	20	26	65	
Sand (%)	75	72	18	
Texture	Loamy sand/sandy loam	Sandy loam	Silt loam	
Total metal concentrations (mg kg⁻¹) (n = 3)				Limit concentrations (mg kg⁻¹)
As	332 ± 20	878 ± 26	1046 ± 9	30
Pb	4234 ± 429	12 ± 2	28 ± 0.1	140
Cd	42 ± 2	2.95 ± 0.3	2.04 ± 0.10	1
Zn	4107 ± 179	65 ± 7	86 ± 3	200
Cu	72 ± 3	21 ± 2	25 ± 0.5	100
Fe	36 563 ± 1120	40 104 ± 4381	24 991 ± 1117	no limit
Mn	4785 ± 581	690 ± 67	665 ± 18	no limit

Limit concentrations of metals/metalloids in agricultural soils are set according to the Ministry of the Environment of the Czech Republic (Act No. 13/1994).

The fractionation and mobility of As (as determined according to the sequential extraction) in original (unamended) soils differ predominantly according to the origin of As contamination (**Table 3.3**). In the artificially spiked Chernozem, the major portion of As was present in the two most labile fractions, i.e., extracted by 0.05 M (NH₄)₂SO₄ (36 %) and 0.05 M NH₄H₂PO₄ (36 %), that are usually related to

nonspecifically and specifically bound As. In the case of the Fluvisol contaminated by the smelting industry, the largest fraction of As (65 %) was present in the 0.2 M NH_4^+ -oxalate buffer extractable fraction associated with amorphous and poorly crystalline hydrous oxides of Fe, Mn, and Al. On the other hand, the geogenic origin of As in the Cambisol resulted in most of the As (50 %) to be bound to well-crystalline hydrous Fe, Mn, and Al oxides (i.e., 0.2 M NH_4^+ -oxalate buffer + ascorbic acid-extractable fraction). The fractionation results thus indicate that except artificially spiked soil, As is predominantly bound to secondary soil oxides (especially Fe oxides) (Lee et al., 2015). The major part of Cd and Zn in Fluvisol was present in the most mobile exchangeable fraction (57 and 44 %, respectively), while Pb was found mainly in the reducible fraction (51 %), usually associated with metals bound to Fe, Mn, and Al oxides.

Table 3.3

Fractionation of As, Cd, Pb and Zn in studied soils.

Fractionation of As (sequential extraction by Wenzel et al., 2001a) (mg kg⁻¹) (n=3)					
	FA: nonspecifically sorbed	FB: specifically adsorbed	FC: bound to amorphous and poorly crystalline hydrous oxides of Fe, Al and Mn	FD: bound to well- crystallized hydrous oxides of Fe, Al and Mn	FE: residual phases
Chernozem	374 ± 3	380 ± 7	152 ± 14	45.7 ± 8.5	95
Cambisol	2.69 ± 0.08	43.6 ± 1.9	247 ± 31	442 ± 21	144
Fluvisol	0.16 ± 0.02	20.2 ± 0.1	214 ± 4	45.9 ± 8.4	51

Fractionation of Cd, Pb and Zn in the Fluvisol (sequential extraction by Rauret et al., 2000) (mg kg⁻¹) (n=3)				
	FA: exchangeable	FB: reducible	FC: oxidizable	FD: residual phases
Cd	24.0 ± 0.3	8.0 ± 1.1	1.3 ± 0.2	9
Pb	281 ± 11	2165 ± 176	705 ± 93	1083
Zn	1822 ± 50	816 ± 45	298 ± 32	1171

Arsenic adsorption study

Adsorption kinetics and isotherms

The kinetic adsorption study (**Fig. 3.1**) was performed at pH 6 corresponding to the pH values of the Fluvisol and Cambisol with initial As(V) concentration of 10 mg L^{-1} . The fastest adsorption process was recorded for the AMO, reaching equilibrium after $\sim 8 \text{ h}$ while adsorbing $\sim 87 \%$ of As(V) from solution. On the other hand, both Fe oxides proved a similar behavior, reaching equilibrium after $\sim 48 \text{ h}$ (nanomagnetite) and $\sim 72 \text{ h}$ (nanomaghemite) while adsorbing $\sim 50 \%$ of As(V). These equilibrium times are in accordance with those previously recorded for natural magnetite (Giménez et al., 2007) and commercial maghemite (Tuutijärvi et al., 2009). The decrease of As adsorption onto AMO after 20 h has been probably caused by AMO dissolution in experimental conditions when the amount of Mn released to solution increased from 85 mg g^{-1} (9 h) to 130 mg g^{-1} (99 h). In all cases, the adsorption kinetics fitted very well the pseudo-second-order equation (**Table 3.4**), roughly indicating that chemisorption as the main process controlling the adsorption of As(V) onto the studied oxides (Giménez et al., 2007).

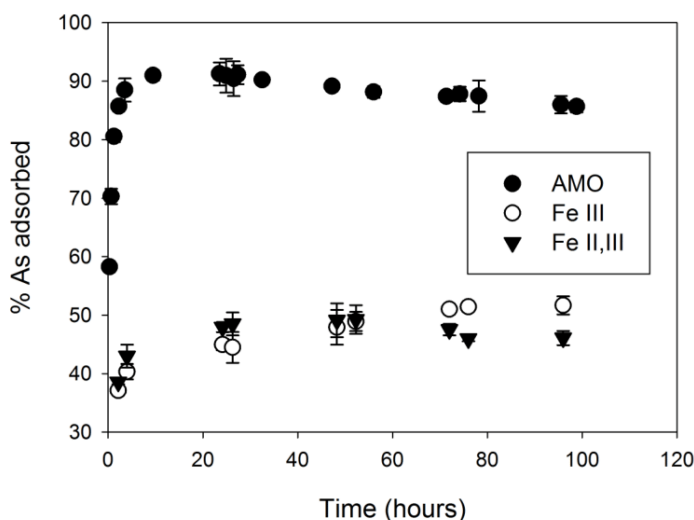


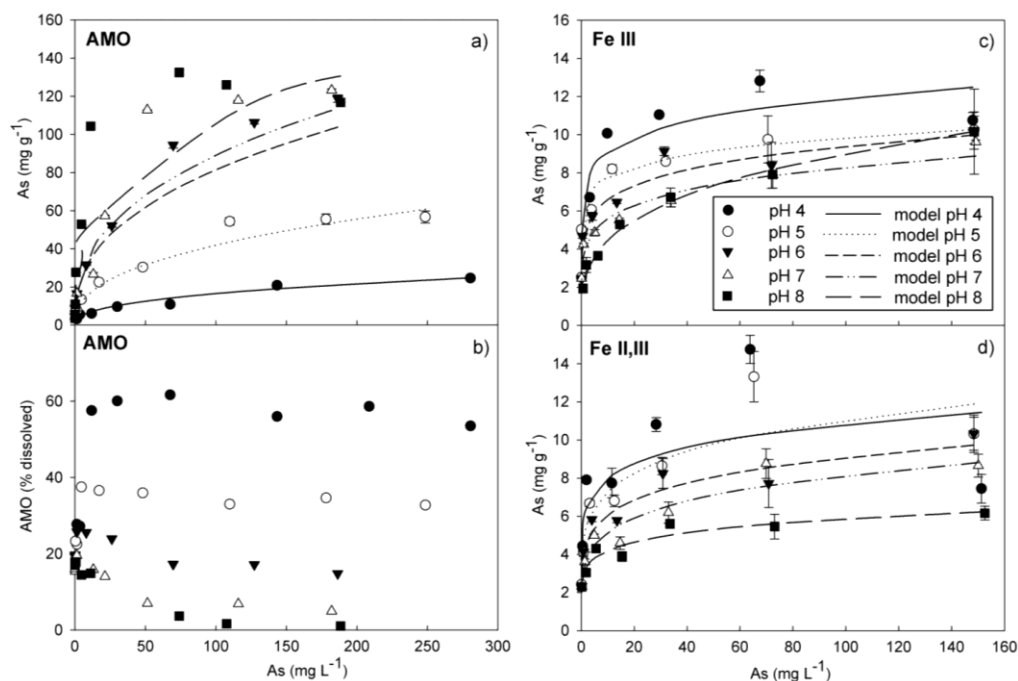
Figure 3.1

Kinetics of As adsorption onto the amorphous manganese oxide (AMO), nanomaghemite (Fe III), and nanomagnetite (Fe II,III) at pH 6, initial As concentration 10 mg L^{-1} ($n=2$).

Table 3.4

Pseudo-second-order kinetic parameters obtained for adsorption of As(V) onto amorphous Mn oxide (AMO), maghemite (Fe III), and magnetite (Fe II,III) at pH 6.

	k_2 ($\text{g mg}^{-1} \text{min}^{-1}$)	q_e (mg g^{-1})	R^2
AMO	0.0112	9.40	1.00
Fe III	0.0011	5.99	1.00
Fe II,III	0.0150	5.43	1.00

**Figure 3.2**

Adsorption isotherms of As onto the amorphous manganese oxide (AMO) (a), nanomaghemite (Fe III) (c), and nanomagnetite (Fe II,III) (d) at pH 4, 5, 6, 7, and 8 with modeled Freundlich isotherms and amount of AMO dissolved during the experiment (b) (n=2).

According to the obtained adsorption isotherms (**Fig. 3.2**) and corresponding isotherm parameters (**Table 3.5**), the AMO showed the highest adsorption capacity for As(V), exceeding the maximum capacity of both Fe nano-oxides by an order of magnitude. The highest concentration of As(V) adsorbed by AMO (S_{\max}) exceeds 130 mg g^{-1} at pH 7 and 8, while adsorption maxima for nanomaghemite and nanomagnetite reached only 11.3 and 10.5 mg g^{-1} at pH 4 and 5, respectively.

Table 3.5

Parameters of Langmuir and Freundlich isotherms of As adsorption.

		Langmuir			Freundlich		
		S_{\max} (mg g^{-1})	K (L kg^{-1})	R^2	n	K (L kg^{-1})	R^2
AMO	pH 4	27.9	0.019	0.856	0.395	2681	0.954
	pH 5	61.1	0.038	0.550	0.406	6489	0.958
	pH 6	123	0.042	0.319	0.390	13 518	0.927
	pH 7	134	0.045	0.368	0.389	14 886	0.849
	pH 8	134	0.214	0.479	0.320	24 469	0.825
Fe III	pH 4	11.3	0.810	0.595	0.119	6878	0.898
	pH 5	9.91	0.429	0.328	0.107	6009	0.947
	pH 6	8.22	3.458	0.728	0.153	4638	0.931
	pH 7	7.30	1.415	0.572	0.170	3789	0.963
	pH 8	10.1	0.091	0.857	0.304	2224	0.991
Fe II,III	pH 4	10.4	1.747	0.623	0.132	5899	0.548
	pH 5	10.5	0.561	0.720	0.180	4833	0.835
	pH 6	8.13	1.215	0.744	0.174	4071	0.931
	pH 7	7.61	0.464	0.645	0.197	3281	0.921
	pH 8	5.33	1.133	0.606	0.145	3012	0.920

AMO: amorphous manganese oxide, *Fe III*: maghemite, *Fe II,III*: magnetite

When compared to other studies dealing with Fe- and Mn-based materials (**Table 3.6**), AMO appears as one of the most efficient materials, and to the best of our knowledge, such adsorption capacity is significantly higher than values reported for most Mn and Fe (hydr)oxides (**Table 3.6**). One possible explanation is probably the unusually basic pH_{zpc} of the AMO (8.3) (Della Puppa et al., 2013) that is considerably higher than values summarized for numerous Mn oxides by Kosmulski

(2004) and Prélôt et al. (2003). According to these overviews, the highest pH_{zpc} (7.7) was reported for $\beta\text{-MnO}_2$ by Prélôt et al. (2003), which is still lower than the value obtained in our study. Interestingly, while the adsorption of As onto the Fe nanooxides increased with decreasing pH, AMO showed the opposite trend, increasing the adsorption with increasing pH. While the former is the behavior commonly supposed for anionic species and already confirmed both for magnetite (Yean et al., 2005; Giménez et al., 2007) and maghemite (Tuutijärvi et al., 2009), the opposite trend recorded for the AMO could be explained by the pH-dependent dissolution of this phase (**Fig. 3.2b**) as up to 60 % of total AMO was dissolved at pH 4 compared to 17 % at pH 8. Additionally, the amount of released Mn was found to closely negatively correlate with the S_{max} of the AMO ($R^2 = -0.98$). When recalculated the amount of As bound to undissolved phase (data not shown), the adsorption of As onto AMO appears almost pH-independent which possibly indicate the formation of inner-sphere complexes.

XPS analyses

Concerning the original AMO samples (i.e., before sorption), the binding energy at the peak detected for Mn 2p 3/2 (642.5 eV) together with the peak splitting of Mn 2p 3/2 and Mn 2p 1/2 (11.7 eV) corresponds well to values tabulated for MnO_2 (McCann et al. 2015; Wagner et al. 1979). The Mn 2p spectra shows contributions of MnO_2 (642.8 eV) together with Mn bound to hydroxy groups (Mn-O-H) (645.9 eV) at the surface of the original material. In the case of AMO with adsorbed As(V), Mn is bound predominantly to oxygen atoms (**Fig. 3.3b**). The deconvolution of oxygen spectra further suggests Mn-O, Mn-O-H and probably adsorbed water as the main oxygen-bound surface complexes to the original AMO very similar to those observed by McCann et al. (2015) for their birnessite-type natural manganese oxide. The Ar ion bombardment proved almost no influence on obtained spectra.

Comparison of the spectra (**Fig. 3.3a**) generally confirms the presence of As on the surface of As-treated samples. The As 3d peak (46.95 eV) confirms As(V) as the only As species which was further confirmed by the deconvolution of As 3p 3/2 and As 3p 1/2 bands (**Fig. 3.3d**). The calculated surface stoichiometry (15 % Mn, 74 % O, and 11 % As) further indicates considerably high surface coverage with adsorbed As(V) being, e.g., 2 orders of magnitude higher than values reported for $\alpha\text{-MnO}_2$ nanorods (0.099 %) and $\delta\text{-MnO}_2$ nano-fiber clumps (0.021 %) treated with 6.7 mM As(V) (Singh et al. 2010). The As(V) is bound to the AMO surface through bonds with oxygen atoms (**Fig. 3.3c**) and together with previous adsorption

Table 3.6

Maximum As(V) adsorption capacities of selected Fe- and Mn-based materials.

Material	Maximum adsorption capacity for As(V) (mg g ⁻¹)	pH	BET surface area (m ² g ⁻¹)	Reference
<i>Fe-based materials</i>				
Nanomaghemite	11.3	4.0	46.6	present study
Nanomagnetite	10.5	5.0	36.6	present study
Magnetite	3.65	7.9	11.9	Bujňáková et al. (2013)
Amorphous FeOOH	55	6.9	247	Zhang et al. (2009)
Hematite	0.41	6.0	1.7	Mamindy-Pajany et al. (2011)
Goethite	1.22	6.0	11.6	Mamindy-Pajany et al. (2011)
Magnetite	0.85	6.0	1.6	Mamindy-Pajany et al. (2011)
Sodium dodecyl sulphate-goethit	60.6	7.0	293	Wu et al. (2014)
Maghemite commercial	16.7	3.0	51.0	Tuutijärvi et al. (2009)
Maghemite mechanochemical	50	3.0	203	Tuutijärvi et al. (2009)
Maghemite sol-gel	25	3.0	90.4	Tuutijärvi et al. (2009)
Magnetite 300 nm	1.1	4.8	3.7	Yean et al. (2005)
Magnetite 20 nm	11.4	4.8	60.0	Yean et al. (2005)
Magnetite 11.72 nm	46.7	8.0	98.8*	Yean et al. (2005)
<i>Mn-based materials</i>				
Amorphous manganese oxide	134	7	135	present study
δ-MnO ₂	19	3	114	Villalobos et al. (2014)
Acid birnessite	7.5	3	39	Villalobos et al. (2014)
MnO ₂	7.5	not specified	not specified	Lenoble et al. (2004)
MnO ₂	2	5		Ajith et al. (2013)
MnO ₂	60	7		Dalvi et al. (2015)
α-MnO ₂ nanorods	19.4	6.5		Singh et al. (2010)
δ-MnO ₂ nano-fiber clumps	15.3	6.5		Singh et al. (2010)
<i>Fe/Mn binary oxides</i>				
3:1 Fe:Mn binary oxide	60	6.9	265	Zhang et al. (2009)
6:1 Fe:Mn binary oxide	60	7.0	224	Zhang et al. (2012)
CMC-stabilized Fe-Mn binary oxide	372	3.0	not specified	An and Zhao (2012)
CMC-stabilized Fe-Mn binary oxide	272	5.0	not specified	An and Zhao (2012)
Fe-Mn binary oxide	69	5.0	265	Zhang et al. (2007)

*Surface area calculated from the mean particle diameter and magnetite density

experiments, this confirms the chemical sorption as the main mechanism involved in As(V) adsorption onto AMO. These results are in good accordance with previous studies dealing with As(V) adsorption mechanism onto AMO. These results are in good accordance with previous studies dealing with As(V) adsorption mechanism onto MnO₂-based materials (Foster et al., 2003; Manning et al., 2002; Singh et al., 2010; Villalobos et al., 2014) that consistently confirms specific adsorption of As(V) onto MnO₂ surface. Further spectroscopic investigations focused on geometry of surface complexes formed with As(V) on several types of birnessite revealed that As(V) is present mainly in a form of bidentate binuclear (bridging) complexes (Manning et al., 2002; Singh et al., 2010; Villalobos et al., 2014), which can be also expected for the AMO.

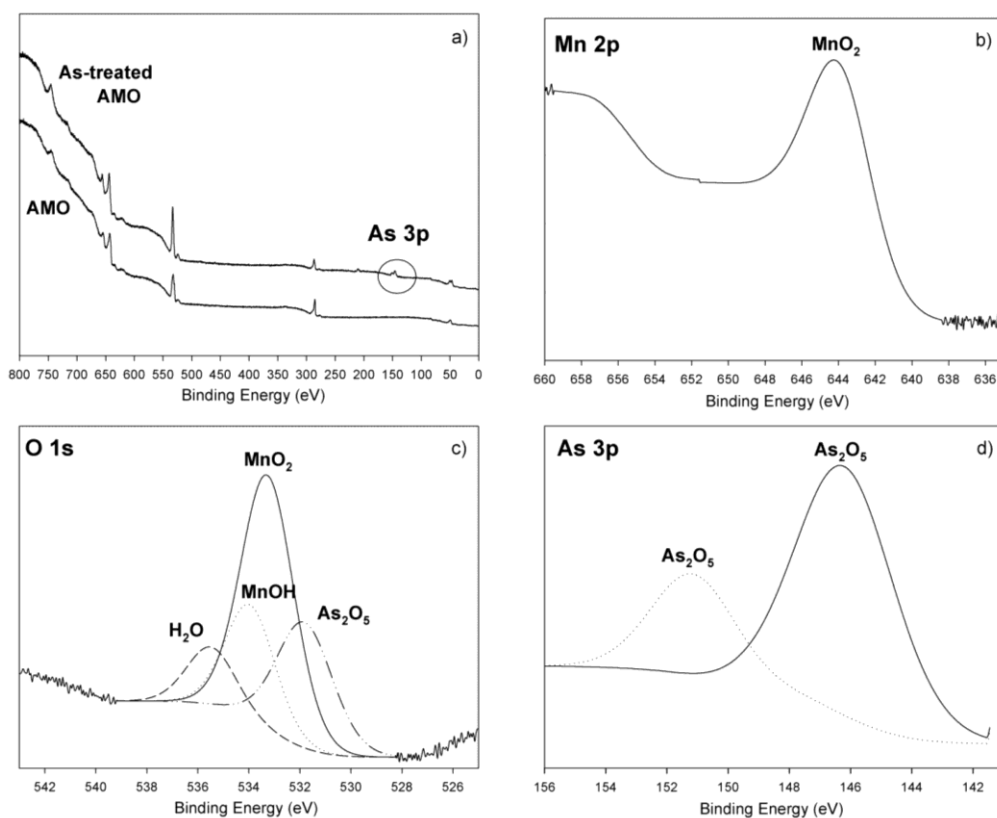


Figure 3.3

XPS spectra of the original AMO and AMO with adsorbed As(V) (a) and deconvolution of Mn 2p (b), O 1s (c), and As 3p (d) peaks from As-treated AMO spectra.

AMO: amorphous manganese oxide.

Incubation batch experiments

The time-dependent stability of the tested oxides in amended soils together with their effect on the mobility of As and metals was evaluated using incubation batch experiments (**Fig. 3.4**). The changes in pH of soil solution after the addition of the tested amendments (**Table 3.7**) were observed mainly in the Fluvisol. In this case, the most significant effect was recorded for the AMO as its application resulted into an increase of pH from 5.6 (control) to 6.1 after 4 weeks observed as well by Micháľková et al. (2014). The pH of other variants showed a decreasing trend in time decreasing from pH ~6.0 to ~5.5-5.6. In the case of the Chernozem, the effect of (nano)oxides application was not so pronounced because of an already high initial pH of the original soil (8.0). The AMO proved to be the most efficient amendment for stabilizing As in the Chernozem soil (**Fig. 3.4a**), being able to reduce the content of As in the soil solution after 1, 4, and 8 weeks to 7, 40, and 16 % of the control, respectively. On the other hand, almost no effect of nanomaghemite and nanomagnetite on the content of As in the Chernozem soil solution was observed (**Fig. 3.4a**), which is in accordance with their relatively low adsorption capacities at pH 8 (**Table 3.5**). Regarding the fractionation of As in the studied soils after 8 weeks of the experiment, the changes were much more pronounced in the Chernozem with the largest portion of labile As (**Table 3.8**). As visible, the influence of aging on As mobility during 8 weeks of experiment is still crucial in the artificially spiked soil regardless previous 2-month equilibration and highlights thus the drawback of using artificially spiked soils for stabilization studies (Ali et al., 2004; Liang et al., 2014; Smolders et al., 2015). From the tested amendments, the AMO was the most efficient in decreasing the most labile As fraction while increasing significantly those bound to amorphous and poorly crystalline oxides. On the other hand, the most effective in increasing the residual phase of As was nanomaghemite; however, the value was still lower than in the control. In the case of the Fluvisol, As and Pb in the soil solution were below the limit of detection for all the time intervals. The AMO was again the most efficient amendment for decreasing the mobility of other contaminants in this soil (i.e., Cd and Zn) (**Fig. 3.4b, c**). Eight weeks after AMO application, the concentration of Cd and Zn in the soil solution decreased 10 and 15 times compared to the control (from 0.32 to 0.03 mg kg⁻¹ and from 26.9 to 1.8 mg kg⁻¹, respectively). For both of these elements, a general trend of concentration increases in time was recorded, which was probably the consequence of the decreasing pH value. Increased concentrations of Mn in the soil solution from the AMO-amended Fluvisol suggest a partial dissolution of the AMO. On the other hand, no dissolution of Fe oxides was observed in any soil.

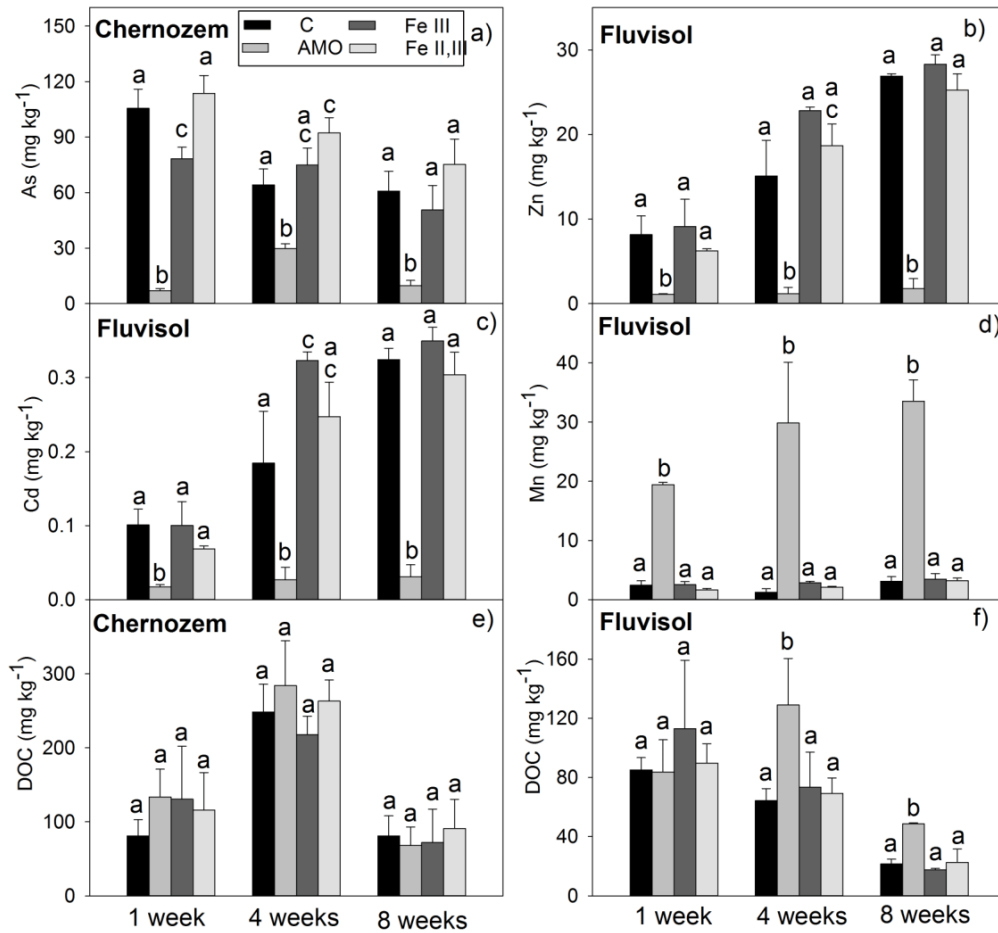


Figure 3.4

Characteristics of the soil solutions obtained during batch incubation experiment: As (a) and DOC concentrations (e) in soil solution from the Chernozem and Zn (b), Cd (c), Mn (d), and DOC (f) concentrations in soil solution from the Fluvisol soil.

C: control, AMO: amorphous manganese oxide (1 %, w/w), Fe III: maghemite (1 %, w/w), Fe II,III: magnetite (1 %, w/w).

Statistical analysis was performed separately for every single time interval; data with the same letter represent statistically identical values ($P < 0.05$) ($n=3$).

Table 3.7

Soil solution pH after 1, 4, and 8 weeks of incubation.

	Chernozem			Fluvisol		
	1 week	4 weeks	8 weeks	1 week	4 weeks	8 weeks
C	8.19 ± 0.10	7.96 ± 0.05	8.05 ± 0.11	5.96 ± 0.04	5.60 ± 0.01	5.51 ± 0.10
AMO	8.03 ± 0.24	8.00 ± 0.05	8.23 ± 0.03	6.04 ± 0.08	6.08 ± 0.10	6.02 ± 0.03
Fe III	8.00 ± 0.20	8.11 ± 0.06	8.10 ± 0.11	5.84 ± 0.18	5.72 ± 0.04	5.44 ± 0.05
Fe II,III	7.99 ± 0.01	8.11 ± 0.02	8.01 ± 0.03	5.95 ± 0.01	5.79 ± 0.15	5.60 ± 0.10

Table 3.8

Fractionation of As (mg kg⁻¹) in the Chernozem after 8 weeks of incubation using the sequential extraction by Wenzel et al. (2001a).

	FA: non-specifically sorbed	FB: specifically adsorbed	FC: bound to amorphous and poorly crystalline hydrous oxides of Fe, Al and Mn	FD: bound to well-crystallized hydrous oxides of Fe, Al and Mn	FE: residual phases
Initial	374 ± 3	380 ± 7	152 ± 14	46 ± 9	95
Control	180 ± 4	281 ± 4	165 ± 7	42 ± 2	378
AMO	153 ± 20	340 ± 0.3	297 ± 14	43 ± 6	214
Fe III	204 ± 4	301 ± 10	183 ± 8	38 ± 2	321
Fe II,III	209 ± 24	310 ± 4	193 ± 6	58 ± 6	277

AMO: amorphous manganese oxide (1 %, w/w), Fe III: nanomaghemite (1 %, w/w), Fe II,III: nanomagnetite (1 %, w/w).

Data shown are means ± SD, n=3.

Additionally, the influence of the tested amendments on the potential dissolution of soil organic matter (SOM) was evaluated as well, as the potential ability of AMO to oxidize/dissolve SOM was highlighted in our previous studies (Ettler et al., 2014; Michálková et al., 2014). In the present study, the influence of the applied amendments on SOM dissolution was not so pronounced and was statistically significant only in the case of AMO incubated in the Fluvisol for 4 and 8 weeks

(**Fig. 3.4f**). That could be caused by the higher pH values of soils used in this study compared to those used in previous works where the oxidizing nature of AMO toward SOM is generally more pronounced in more acidic conditions (Ettler et al., 2014; Micháľková et al., 2014).

The pH-static leaching experiment

The results from the pH-static leaching experiment are shown in **Fig. 3.5**. The pH of the soil leachate was influenced by the (nano)oxide addition only in the case of the Fluvisol where the AMO application resulted in a pH increase from 5.8 to 6.6. In the case of the Cambisol and Chernozem, the pH of all variants remained 5.9 and 7.7, respectively. A similar pattern was recorded for As release from the Fluvisol (**Fig. 3.5a**) and the Cambisol (**Fig. 3.5b**), reaching the maximum at the highest pH value (pH 7), which is a behavior commonly observed for As in contaminated soils (Cappuyns et al., 2002; Van Herreweghe et al., 2002). On the other hand, the release of As from the artificially contaminated soil showed an opposite trend when decreased As leachability with increasing pH. This behavior was caused probably by the artificial origin of As contamination supplied into soil in a form of a highly soluble As salt, highlighting thus the problems associated with experiments using artificially spiked soils even after a two month equilibration. The predominant As fractions in the Chernozem soil were thus nonspecifically (374 mg kg^{-1}) and specifically (380 mg kg^{-1}) sorbed species (**Table 3.3**). The AMO was again the most efficient amendment reducing As concentrations in the leachates, especially in the case of the Chernozem soil, despite the considerable dissolution of the AMO at lower pH values (**Fig. 3.5g**). This trend was similar for all soils (data not shown). We propose that the main reason why the AMO immobilizing potential was the most pronounced in the case of the artificially spiked soil dwells in the fractionation of As. To illustrate, the content of specifically and nonspecifically bound fractions (**Table 3.3**) of As in Chernozem was determined to be $\sim 750 \text{ mg kg}^{-1}$ compared to $\sim 46 \text{ mg kg}^{-1}$ in the Cambisol and $\sim 20 \text{ mg kg}^{-1}$ in the Fluvisol, while the content of the most labile fraction (nonspecifically sorbed) was $\sim 374 \text{ mg kg}^{-1}$ compared to ~ 2.7 and $\sim 0.16 \text{ mg kg}^{-1}$, respectively. We thus suppose that during the 1-month equilibrating period before the experiment, AMO in the artificially spiked soil was able to adsorb the highest portion of As due to its highest available amount available for adsorption in this soil. Despite the high efficiency of AMO for both cationic (Cd, Cu, Pb, Zn) and for anionic (As) contaminants, a potential drawback of this stabilizing agent remains its possible dissolution in acidic conditions coupled with

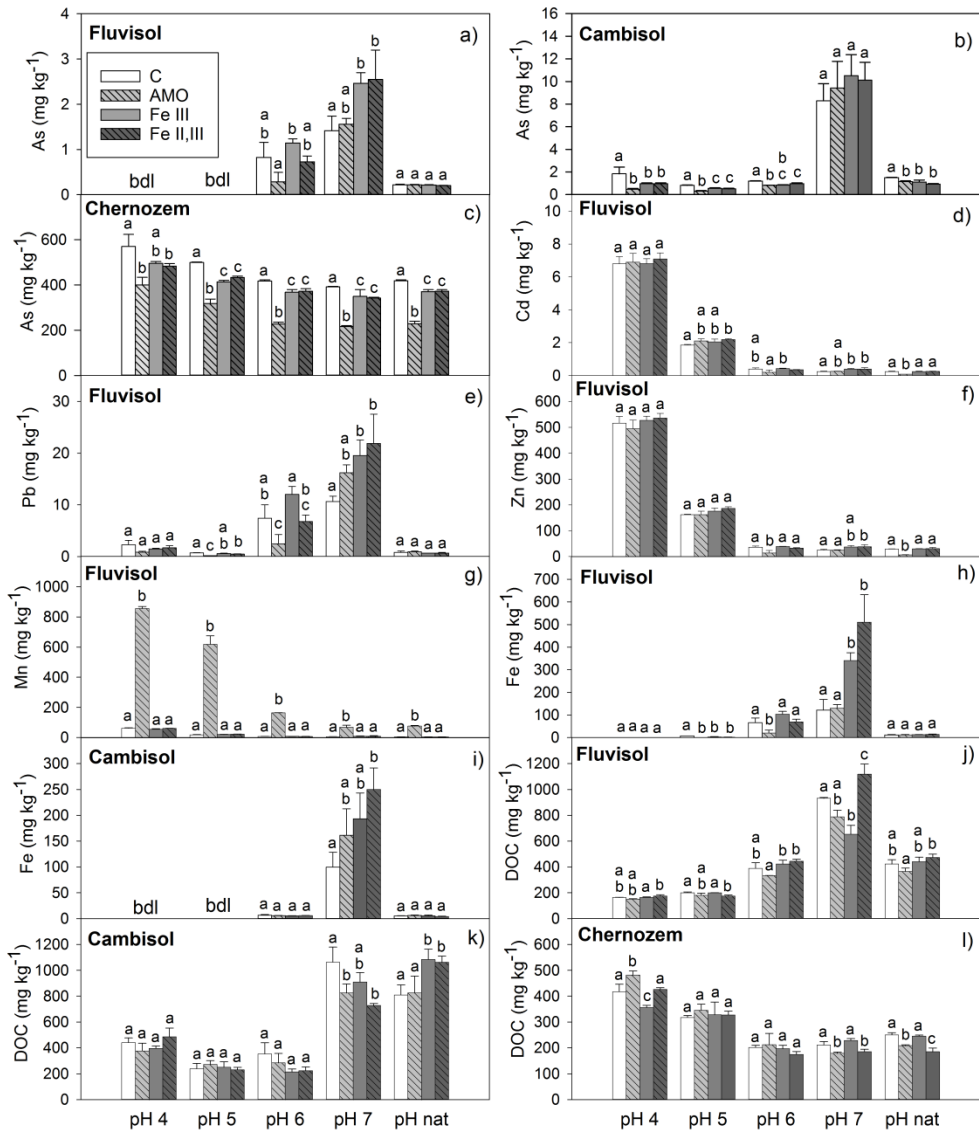


Figure 3.5

Results of the pH-static leaching experiment: As (a), Cd (d), Pb (e), Zn (f), Mn (g), Fe (h), and DOC (j) contents in Fluvisol extract; As (b), Fe (i), and DOC (k) contents in Cambisol extract; As (c) and DOC (l) contents in Chernozem extract.

C: control, AMO: amorphous manganese oxide (1 %, w/w), Fe III: maghemite (1 %, w/w), Fe II,III: magnetite (1 %, w/w), pH nat: variants with natural (nonadjusted) pH.

Statistical analysis was performed separately for every single pH value; data with the same letter represent statistically identical values ($P < 0.05$) ($n = 3$).

oxidation of SOM connected with potential remobilization of adsorbed metals. This shortcoming could be theoretically mitigated with a surface modification of AMO particles with a manganese carbonate layer as our previous studies suggest that during the aging in soil conditions, the surface of the AMO is naturally covered by manganese carbonate coatings, which decreases its solubility and oxidative properties towards SOM (Ettler et al., 2014; Michálková et al., 2014). Although many authors found Fe oxides to be highly effective in decreasing As mobility, bioaccessibility, and bioavailability in soils (Bagherifam et al., 2014; Farrow et al., 2015; Hartley and Lepp, 2008; Kim et al., 2012; Ko et al., 2015; Liang and Zhao, 2014), their effect was not as pronounced as in the case of AMO in our study. Besides, the already mentioned higher adsorption capacity of AMO toward As(V), another reason of the apparently lower stabilizing efficiency of the tested Fe oxides could also be the extremely high As concentrations in soils that are generally an order of magnitude higher than in former works. In the case of Cd (**Fig. 3.5d**) and Zn (**Fig. 3.5f**) in the Fluvisol, the effect of applied amendments was rather indistinctive being the most pronounced in the case of variants with AMO at natural (i.e., not adjusted) pH. An interesting trend was observed in the case of Pb (**Fig. 3.5e**), showing the lowest leachability at pH 5 and increasing significantly toward higher pH values. Lead in soils usually shows an opposite trend, decreases its leachability with increasing pH (Cerqueira et al., 2011; Houben et al., 2013). In our study, the increased amount of Pb released at pH 6 and pH 7 is supposed to be the consequence of increased dissolution of SOM (**Fig. 3.5j**) as $\sim 750 \text{ mg kg}^{-1}$ ($\sim 17 \%$) Pb was bound to the oxidizable fraction of the original soil (**Table 3.3**). The highest dissolution of Fe in neutral conditions (**Fig. 3.5h**) was also probably connected with the release of organically bound Fe ($\sim 3500 \text{ mg kg}^{-1}$ in the original soil).

Conclusions

The potential of an amorphous Mn oxide, nanomaghemite, and nanomagnetite to stabilize As in various contaminated soils was evaluated using adsorption and XPS study together with batch incubation and pH-static leaching experiments. The results of all experiments consistently highlight that the AMO is a promising and efficient amendment for As immobilization. The XPS analyses confirmed chemical sorption as the main process involved in As(V) binding onto the AMO surface. The adsorption capacity of the AMO for As(V) increased with increasing pH and reached a maximum of 134 mg kg^{-1} at pH 7-8 that is significantly more than reported for any other Mn (hydr)oxide. Such a high adsorption capacity at neutral/alkaline pH is even

more emphasized for As contaminated soils where the risk associated with As leaching is more pronounced at higher pH values (Sadiq, 1997). Considerable stabilization potential of the AMO shown in this study together with the unusually high pH_{zpc} of this material highlight its suitability for remediation of soils contaminated with As. A potential drawback of this agent, its possible dissolution in acidic conditions, could be theoretically reduced by its surface modification with a manganese carbonate layer which is currently under investigation. However, this is not the issue in neutral-alkaline soils contaminated with As.

Chapter IV

The pH-dependent long-term stability of an amorphous manganese oxide in smelter-polluted soils: Implication for chemical stabilization of metals and metalloids

V. Ettler, Z. Tomášová, M. Komárek, M. Mihaljevič, O. Šebek, Z. Michálková

Adapted from *Journal of Hazardous Materials* 286 (2015): 386-394, with permission of corresponding author (V. Ettler).

Content

Abstract	89
Introduction	91
Materials and methods	91
Amorphous manganese oxide and studied soils	91
Amorphous manganese oxide leaching	92
Chemical stabilization experiment	93
Data treatment	94
Results	95
Leaching of AMO	95
Chemical fractionation of contaminants in soil treated with AMO	97
The pH-dependent metal(loid) leaching	100
Discussion	103
Effect of L/S ratio and pH on the leaching of AMO	103
Effect of time and pH on metal(loid) stabilization	103
Conclusions	106

Abstract

An amorphous manganese oxide (AMO) and a Pb smelter-polluted agricultural soil amended with the AMO and incubated for 2 and 6 months were subjected to a pH-static leaching procedure (pH 3–8) to verify the chemical stabilization effect on metals and metalloids. The AMO stability in pure water was pH-dependent with the highest Mn release at pH 3 (47% dissolved) and the lowest at pH 8 (0.14% dissolved). Secondary rhodochrosite (MnCO_3) was formed at the AMO surfaces at $\text{pH} > 5$. The AMO dissolved significantly less after 6 months of incubation. Sequential extraction analysis indicated that “labile” fraction of As, Pb and Sb in soil significantly decreased after AMO amendment. The pH-static experiments indicated that no effect on leaching was observed for Cd and Zn after AMO treatments, whereas the leaching of As, Cu, Pb and Sb decreased down to 20%, 35%, 7% and 11% of the control, respectively. The remediation efficiency was more pronounced under acidic conditions and the time of incubation generally led to increased retention of the targeted contaminants. The AMO was found to be a promising agent for the chemical stabilization of polluted soils.

Introduction

Iron and manganese oxides are often tested for chemical stabilization of metals and metalloids in polluted soils mainly due to their sorption potential, which leads to a decrease in contaminant mobility and bioavailability (Bagherifam et al., 2014; Bolan et al., 2014; Komárek et al., 2013; Kumpiene et al., 2008). Comparison of the sorption efficiencies indicated that Mn-oxides can be much more efficient sorbents than Fe-oxides for some metals (e.g. Pb) (O'Reilly and Hochella, 2003; Wang et al., 2012a). Moreover, Mn oxides, through their dissolution, can change the redox speciation of contaminants, leading to their oxidation, which is not favorable in the case of Cr (Cr(III) to more mobile and toxic Cr(VI)) (Dai et al., 2009; Feng et al., 2006; Landrot et al., 2012a, b), but can be suitable for As (As^{III} oxidizes to less mobile and less toxic As^V) (Chen et al., 2006; Feng et al., 2007; Lafferty et al., 2010a,b; Manning et al., 2002; Villalobos et al., 2014; Ying et al., 2012).

Recently, a novel amorphous manganese oxide (AMO), prepared by a modified sol-gel procedure generally used for the birnessite synthesis but without the heating step, was tested as a new sorbent for metals and its sorption efficiency was found to be comparable with that of birnessite (Della Puppa et al., 2013). Despite the fact that 10-18% of AMO dissolved during the 90 days of exposure in contrasting soils, it was concluded that it is relatively stable and can be potentially used as an amendment for polluted soils (Ettler et al., 2014). The first experiments studying the chemical stabilization of Cd, Cu and Pb in polluted soils using AMO indicated that the adsorption capacity of AMO was an order of magnitude higher than those recorded for selected Fe-nanooxides (nano-maghemite, Fe₂O₃ and nano-magnetite, Fe₃O₄) (Michálková et al., 2014).

The influence of varying environmental conditions (where pH is the major driving force) on chemically stabilized metal(loid)s in soils is often overlooked in evaluation of the efficiency of a particular remediation technique. The adsorption efficiency of the AMO in soils is expected to be highly dependent on the pH and time of aging. For these reasons, the present study investigated (i) the AMO stability in aqueous environments as a function of the pH and liquid-to-solid (L/S) ratio used during the leaching experiments and (ii) the changes in chemical fractionations of inorganic contaminants and their pH-dependent leaching from an AMO-amended smelter-polluted agricultural soil.

Materials and methods

Amorphous manganese oxide and studied soil

The synthesis of a poorly crystalline or amorphous manganese oxide (AMO) was based on the methodology of Ching et al. (1997), generally used for birnessite synthesis, but without the heating step (details of the procedure are given in Della Puppa et al. (2013) and Ettler et al. (2014)). The specific surface area (SSA) of the AMO was measured by BET measurement using a Sorptomatic 1990 Thermo Electron instrument (ThermoFisher Scientific, USA) and corresponded to $14.8 \text{ m}^2\text{g}^{-1}$ (without degassing) or $157 \text{ m}^2\text{g}^{-1}$ (after degassing at 110°C). The average oxidation state of Mn was 2.52 (corresponding to the chemical formula $\text{MnO}_{1.26}$) (Della Puppa et al., 2013). The natural pH of AMO was obtained by acid neutralization capacity/base neutralization capacity measurement (ANC/BNC; details see below) and corresponded to 7.12. The granulometry of the AMO sample used in the present study was measured using a Sympatec particle size analyser equipped with a HELOS laser diffraction sensor and ultrasound sample treatment (Sympatec GmbH, Germany) and yielded the following results: $<1 \mu\text{m}$ (3.28%), $1\text{-}2.6 \mu\text{m}$ (22.01%), $2.6\text{-}5 \mu\text{m}$ (34.25), $5\text{-}10 \mu\text{m}$ (28.69%) and $>10 \mu\text{m}$ (11.77%). Previous investigations using X-ray diffraction (XRD) and scanning electron microscopy (SEM) indicated that small contents of Mn-oxalate hydrate can be present in the AMO as a result of glucose transformation used during the synthesis (Ettler et al., 2014).

An agricultural soil (classified according to US Soil Taxonomy as Inceptisol Typic Dystrudepts) was used as a model soil for chemical stabilization experiments. The soil was polluted by emissions from a Pb smelter located in Pířbram (Czech Republic) and was previously studied by Ettler et al. (2005). The soil properties and main physico-chemical parameters are reported in **Table 4.1**.

Table 4.1

Properties of the studied smelter-polluted agricultural soil.

pH	5.32	
CEC (cmol kg ⁻¹)	6.96	
C _{org} (%)	1.79	
S _{tot} (%)	0.02	
P _{tot} (g kg ⁻¹)	2.42	
Particle size distribution		Total metal concentrations (mg kg ⁻¹)
Clay (%)	10.0	As
Silt (%)	32.7	Cd
Sand (%)	57.3	Sb
Oxalate extractable (g kg ⁻¹)		Pb
Fe	170 ± 9	Zn
Al	396 ± 10	Mn
Mn	4.1 ± 1.0	Fe

Amorphous manganese oxide leaching

The pH-dependent stability of AMO was tested using a pH-static leaching experiment according to the European standard CEN/TS 14,997 (2006). Preliminary determination of steady-state pH and the acid and base consumptions (ANC/BNC) was performed before the pH-static leaching using manual titration and pH measurement every 30 min. The pH-static experiments were carried out at $20 \pm 4^\circ\text{C}$ for 48 h. A mass of 1 g of solid was placed in a 20 mL centrifuge PP bottle and 9.6 ml of MilliQ+ deionised water were added to maintain an L/S ratio of 9.6 with a final ratio of about 10 after addition of the acid/base. Six pH values between 3 and 8 at 1-unit increments were selected to represent the pH range relevant for soil environments. Acid (14 M, 1 M or 0.1 M HNO₃) or base (5 M, 2 M or 1 M NaOH) was added to adjust the pH values. A variant conducted at the natural pH (i.e., without acid/base addition) was included in all cases. The reactors were agitated continuously (except for the time of pH control and titration). After 48 h, the suspended solids were allowed to settle for about 10 min and the physical-chemical parameters (pH, Eh, specific conductivity) were measured immediately using Schott multimeters (Schott Instruments GmbH, Germany) in the leachate before filtration (Millipore®0.45 µm). All the experiments were performed in duplicate and included procedural blanks.

To evaluate the effect of the L/S ratio on AMO dissolution, leaching in deionized water (natural pH) was performed at L/S ratios of 10, 100 and 1000. All the leachates were filtered with 0.45- μm membrane filters (Millipore®) and leachates obtained at L/S of 1000 were also filtered to 0.1 μm (Millipore®) and ultrafiltered to 100 kDa (~10-20 nm) and 5 kDa (~3-5 nm) using a Millipore®Labscale Tangential Flow Filtration (TFF) system equipped with Pellicon XL 50 ultrafiltration cassettes to assess the role of the colloidal-sized fractions on leaching. Leachate samples from each experiment were analyzed for Al, Ba, Ca, Cd, Co, Cr, Cu, Fe, K, Mg, Mn, Na, Ni, P and Zn by inductively coupled plasma optical emission spectrometry (ICP-OES; ThermoScientific iCAP 6500 radial, UK). Residual AMO samples were dried and X-ray diffraction (XRD) patterns were recorded on a PANalytical X'Pert Pro diffractometer with an X'Celerator detector (PANalytical B.V., the Netherlands) (Cu K α radiation, 40 kV and 30 mA, 2 θ range 2-80°, step 0.02, counting time of 150 s). Qualitative analysis of the XRD patterns was performed using PANalytical X'PertHighScore Plus software (version 3) and the ICDDPDF-2 database (2002). The AMO samples were also studied using a TESCAN VEGA scanning electron microscope (SEM; TESCAN Ltd. Czech Republic) equipped with an Oxford Link X-Max 50 energy dispersion spectrometer (EDS; Oxford Instruments, UK). The spectrometer was calibrated against the SPI (SPI supplies, USA) set of standards.

Chemical stabilization experiment

The soil was amended with 2% (w/w) of AMO; 50 g of soil and 1 g of AMO were placed in a 100-ml PE bottle (P-lab, Czech Republic). Every 2 weeks, the soil was homogenized by mixing and rewetted to 30% of the water-holding capacity (WHC) using deionized water. The soils were incubated under these conditions for 2 and 6 months. The experiment was conducted in duplicate with procedural blanks (soil without AMO amendment).

The change in the chemical fractionation of contaminants in the soil after the application of the AMO was examined using the optimized BCR sequential extraction procedure (SEP) (Rauret et al., 1999; Sutherland and Tack, 2002). Although this chemical fractionation scheme was originally designed for metals, its successful application has also been demonstrated for metalloids (Sb, As) (Ettler et al., 2010). The sequential extraction steps should mobilize operatively defined fractions: fraction 1-exchangeable/acid extractable, 2-reducible (targeting Fe and Mn oxides), 3-oxidizable (targeting organic matter and sulphides) and 4-residual.

The pH-dependent leaching according to the European standard CEN/TS 14997 was performed in the pH range of 3-8 on the original soil and the AMO-amended soils after 2 months and 6 months of incubation.

The bulk concentrations of major elements (Ca, K, Na, P, S, Si) in the leachates and SEP extracts were determined using ICP-OES; trace metal(loid)s (Al, As, Cd, Cu, Fe, Mg, Mn, Pb, Sb, Zn) were measured using ICP-MS (ThermoScientific Xseries^{II}, USA). The alkalinity of the samples with pH > 4.5 was measured by back titration (0.05 M HCl) using a Schott TitroLine Easy automatic titrator (SchottInstruments GmbH, Germany). Leachates from pH-static experiment were also analyzed for dissolved organic carbon (DOC) using a Shimadzu TOC-LCPH/CPN analyzer (Shimadzu Co., Japan).

The accuracy of the digestion/measurement procedure was controlled using parallel digestions of standard reference materials SRM NIST 2710 A and 2711 A (Montana soils) and SRM NIST 1643D (Trace elements in water); the accuracy of the SEP was controlled by parallel extraction of CRM 483 certified reference material (Sewage sludge amended soil) and was found to be satisfactory in all cases.

Data treatment

All the data were plotted and statistically treated using SigmaPlot 12 software (Systat Software Inc. USA). The experimental data were evaluated using analysis of variance (ANOVA) at P < 0.05 using the Tukey test.

The PHREEQC-3 speciation solubility code (Parkhurst and Apello, 2013) was used to determine the speciation of elements in the solutions and the possible oversaturation of soil pore waters with respect to the solid phases. The T&H.dat database (downloaded from <http://hydrochemistry.eu>) containing binding constants for dissolved organic matter (DOM) was used for all the calculations. The dissolved organic matter was entered into the code as fulvate (Ettler et al., 2012).

Results

Leaching of AMO

The AMO dissolution in water was highly pH-dependent and exhibited an L-shaped leaching curve in the pH range of 3-8 with natural pH close to 7 (**Fig. 4.1a**). The released Mn concentration was the highest at pH 3 (34.1 g kg^{-1} , 47% dissolved) and decreased to 0.09 g kg^{-1} at pH 8 (0.14% dissolved; **Fig. 4.1a**). The leaching at different L/S ratios indicated a steady-state pH of the suspensions in the range 6.85-7.10. At these natural pH values, 0.2%, 4% and 9.2% of the total amount of Mn was released at L/S 10, 100 and 1000, respectively (**Fig. 4.2**). Although slightly lower Mn release was observed for ultrafiltered suspensions at 100 kDa and 5 kDa, no statistically significant difference was observed, thus indicating no influence of colloidal-sized AMO particles on the Mn concentration in the leachates (**Fig. 4.2**).

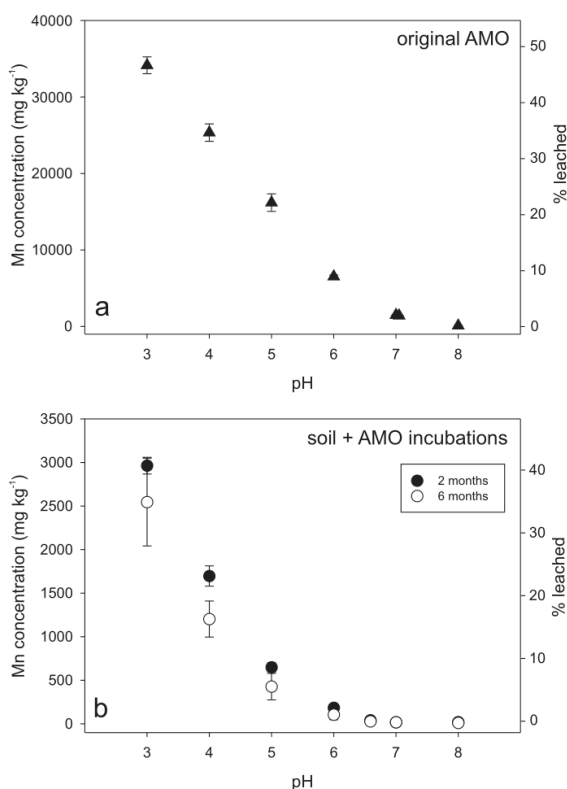


Figure 4.1

The pH-dependent leaching of Mn from the AMO (a) and AMO-amended soil (b). AMO: amorphous manganese oxide.

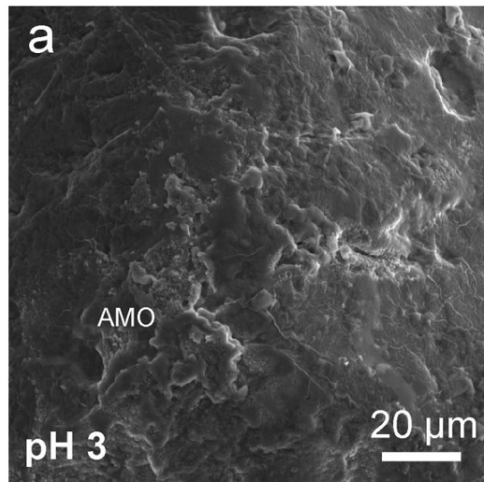
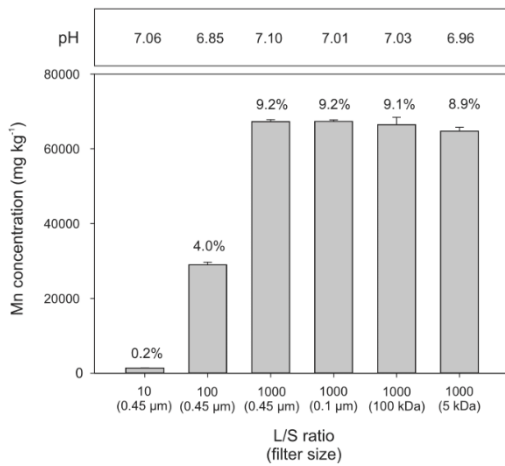


Figure 4.2

Mn leaching from amorphous manganese oxide (AMO) at the natural pH as a function of the liquid-to-solid (L/S) ratio (concentrations in mg/kg and % dissolved). The values obtained at L/S = 1000 for various levels of filtration/ultrafiltration of leachates are statistically identical (ANOVA, $P=0.180$), indicating that there is no influence of colloidal-sized AMO particles on the Mn concentration in the leachate.

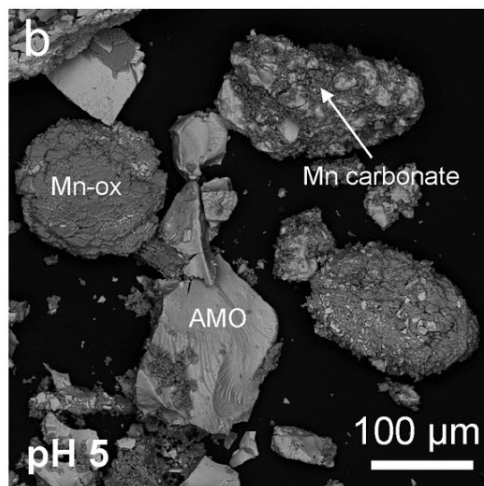
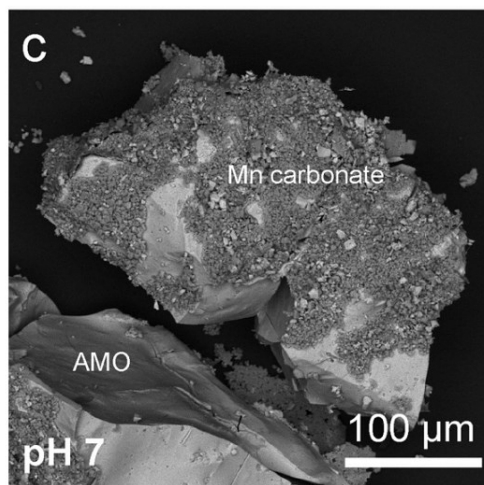


Figure 4.3

Microphotographs of surfaces of amorphous manganese oxide (AMO) after the pH-static leaching experiments. (a) AMO surface after leaching at pH 3 (in secondary electrons, SE); (b) AMO grains in association with residual Mn oxalate (Mn-ox), some of the AMO grains are covered by aggregates of Mn carbonate (rhodochrosite) (leaching at pH 5, in backscattered electrons, BSE); (c) AMO grain covered by secondary rhodochrosite (leaching at pH 7, in BSE).



The XRD analysis indicated that the original AMO was predominantly an amorphous material with traces of hydrated Mn-oxalate ($C_2MnO_4 \cdot 2H_2O$, PDF card 025-0544 with major diffraction line at $18.43^\circ 2\theta$), being a residuum from the AMO synthesis (Ettler et al., 2014). As revealed by XRD and SEM, AMO was highly dissolved at pH 3 with residue consisting of only the X-ray amorphous material (**Fig. 4.3a**; XRD data not shown). Secondary rhodochrosite ($MnCO_3$) appeared in the diffractograms of residues obtained by leaching at pH > 5 (PDF card 044-1472 with major diffraction line at $31.36^\circ 2\theta$) and was also observed on the AMO surface by SEM (**Fig. 4.3b, c**). The PHREEQC-3 calculations indicated that, over the whole pH-range of the leaching test, the leachates were undersaturated with respect to birnessite (MnO_2) and pyrochroite ($Mn(OH)_2$) indicating the general tendency of Mn-oxides and hydroxides to be dissolved (**Table 4.2**). Only under neutral and slightly alkaline conditions, did hausmannite (Mn_3O_4), manganite ($MnOOH$) and pyrolusite (MnO_2) yield positive saturation indices (**Table 4.2**), but XRD and SEM did not document their presence. However, the leachates were oversaturated with respect to rhodochrosite at pH 6 and higher (**Table 4.2**), in relatively good agreement with mineralogical observations.

Chemical fractionation of contaminants in soil treated with AMO

The changes in the chemical fractionation of the metals and metalloids after the treatment with the AMO are reported in **Fig. 4.4**. The most “labile” (exchangeable) fraction of contaminants was especially monitored and statistically evaluated using ANOVA to investigate the effect of chemical stabilization. A simple addition of AMO to soil (denoted in **Fig. 4.4** as Soil + AMO) led to a statistically significant decrease in the amount of As, Pb and Cd bound in the “labile” fraction and the decrease was more pronounced after AMO aging. A decrease in the “labile” fraction of Sb was not recorded immediately after the AMO amendment, but only after the aging. After 6 months of incubation, the decrease in the “labile” fraction of the following contaminants was statistically significant: As (from 5.30 to 2.51 mg kg⁻¹), Pb (from 77.4 to 12.3 mg kg⁻¹), Sb (from 1.17 to 0.42 mg kg⁻¹). In contrast to other contaminants, the decrease in the “labile” fractions of Cu and Zn was not statistically significant and the efficiency of the AMO amendment in their retention was not demonstrated (**Fig. 4.4**). Despite its statistical significance, the decrease in the “labile” fraction of Cd after the AMO treatment was relatively small (from 2.67 to 2.25 mg kg⁻¹); moreover, it is important to note that Cd is predominantly bound in the “labile” fraction even after the AMO treatment and can thus be potentially leached from all the studied soils.

Table 4.2

Mean saturation indices of carbonates and Mn oxides for leachates obtained during pH-static leaching experiments with amorphous manganese oxide (AMO) (calculated by PHREEQC-3).

	pH	<i>Calc</i>	<i>Rhod</i>	<i>Birn</i>	<i>Haus</i>	<i>Man</i>	<i>Pyrol</i>	<i>Pyroch</i>
		CaCO ₃	MnCO ₃	MnO ₂	Mn ₃ O ₄	MnOOH	MnO ₂	Mn(OH) ₂
pH 3	3.02	-11.05	-5.40	-13.1	-20.53	-7.61	-10.92	-10.19
pH 4	4.00	-9.15	-3.52	-9.94	-13.58	-5.07	-7.72	-8.31
pH 5	5.02	-7.13	-1.61	-9.10	-8.92	-3.69	-6.88	-6.40
pH 6	5.99	-5.22	0.05	-4.96	-1.46	-0.79	-2.74	-4.74
pH 7	7.02	-3.11	1.63	-2.45	4.21	1.26	-0.23	-3.16
pH 8	8.01	-1.09	2.39	-0.38	7.81	2.68	1.84	-2.39
Natural pH	7.06	-3.05	1.69	-13.2	-6.37	-4.06	-10.93	-3.10
L/S 100 [0.45 µm] ^a	6.85	nd ^b	0.77	-2.69	2.25	0.71	-0.47	-4.01
L/S 1000 [0.45 µm] ^a	7.10	nd	0.75	-3.68	1.23	0.21	-1.45	-4.03
L/S 1000 [0.1 µm] ^a	7.01	nd	0.55	-4.21	0.30	-0.16	-1.98	-4.23
L/S 1000 [100 kDa] ^a	7.03	nd	0.60	-2.85	1.76	0.55	-0.62	-4.18
L/S 1000 [5 kDa] ^a	6.96	nd	0.46	-1.93	2.39	0.93	0.29	-4.32

Calc: Calcite, **Rhod:** Rhodochrosite, **Birn:** Birnessite, **Haus:** Hausmannite, **Man:** Manganite, **Pyrol:** Pyrolusite, **Pyroch:** Pyrochoite

^a leaching test performed at a given liquid-to-solid (L/S) ratio and pore size of the filters used for filtration/ultrafiltration of the leachates

^b nd: not determined

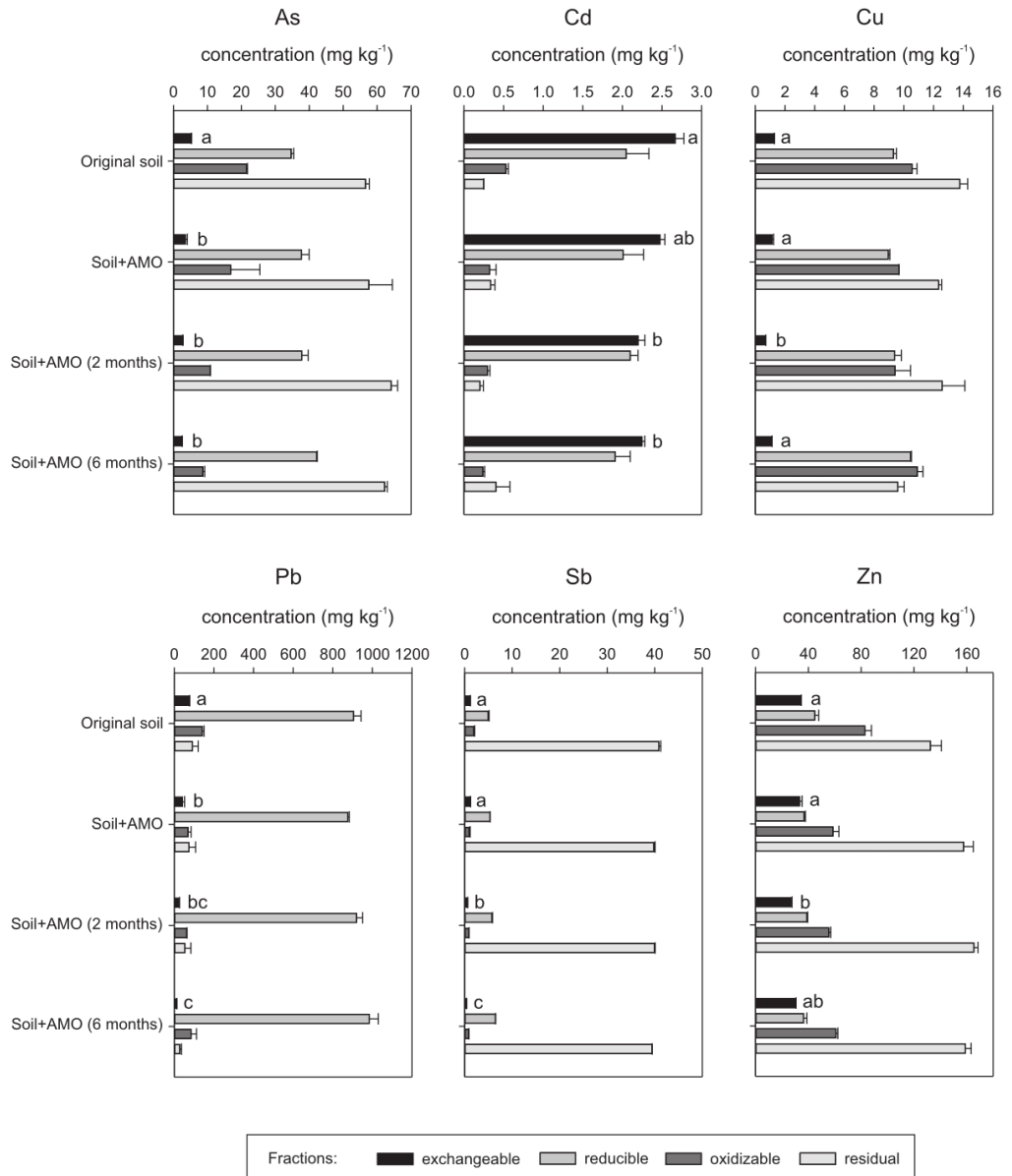


Figure 4.4

Chemical fractionation of metal(oid)s in the original soil and soil amended with amorphous manganese oxide (AMO). Statistically significant differences for the exchangeable fractions are indicated with different letters as obtained by ANOVA ($P < 0.05$) using the Tukey test.

The pH-dependent metal(loid) leaching

Despite the fact that AMO has a tendency to dissolve partially in an aqueous environment (**Fig. 4.1a**), the amendment was significantly less reactive when mixed with the soil. The pH-dependent leaching of Mn in AMO treatments indicated steeper leaching towards acidic conditions in comparison with AMO leaching in water (**Fig. 4.1b**). Moreover, AMO aging led to its stabilization and significantly less Mn was leached from AMO treatments after 6 months of incubation. Despite the fact that a relatively high proportion of AMO from the amended soil still dissolved at pH 3 (41.3% after 2 months, 35.4% after 6 months), the AMO dissolution was significantly lower at pH > 5 (0.2-9.0% after 2 months, 0.1-5.9% after 6 months) (**Fig. 4.1b**).

The ANC/BNC measurements performed prior to pH-static leaching indicated that the natural pH of the original soil was 5.8 and increased after amendment with AMO (pH 6.6 and 6.2 after 2 months and 6 months of incubation, respectively). The pH-dependent releases of contaminants from the amended soils incubated for 2 and 6 months and comparisons with the original soils are reported in **Fig. 4.5**. Up to 62% of the total Cd and up to 20% of the total Zn were leached at pH 3. Whereas practically no effect on the pH-dependent leaching after AMO amendment was observed for Cd and Zn, a decrease in the leaching was observed for the other contaminants. Increased time of incubation generally further decreased the leaching of the metal(loid)s under acidic conditions, but not under neutral and slightly alkaline conditions (**Fig. 4.5**). Copper was a minor contaminant in the studied soil and exhibited U-shaped leaching as a function of the pH, with leached concentration <1.1 mg kg⁻¹ (~3% of total Cu). The AMO amendment decreased the Cu leaching by a factor of up to 2.8. The Pb leaching from the soil exhibited an L-shaped leaching curve as a function of the pH with a maximum leached concentration of 39.9 mg kg⁻¹ at pH 3 (~3.6% of total Pb). The AMO treatment significantly decreased the leaching of Pb, which is a major contaminant, by a factor of 8.3 and 7.0 at pH 3 and 4, respectively. However, the leaching of Pb was not strongly affected by AMO treatment at pH > 5 (**Fig. 4.5**). Arsenic leaching from the soil exhibited a U-shaped leaching curve with the highest leached concentration at pH 8 (3.84 mg kg⁻¹; ~3.3% of total As). The AMO treatment was responsible for a significant decrease in the As leaching by a factor of up to 4.9 after 6 months of incubation (**Fig. 4.5**). Antimony leaching from the soil increased as a function of the pH with the highest leached concentration at pH 8 (1.93 mg kg⁻¹; ~4.0% of total). The AMO treatment significantly decreased the Sb leaching (by a factor up to 9.1) under all the studied

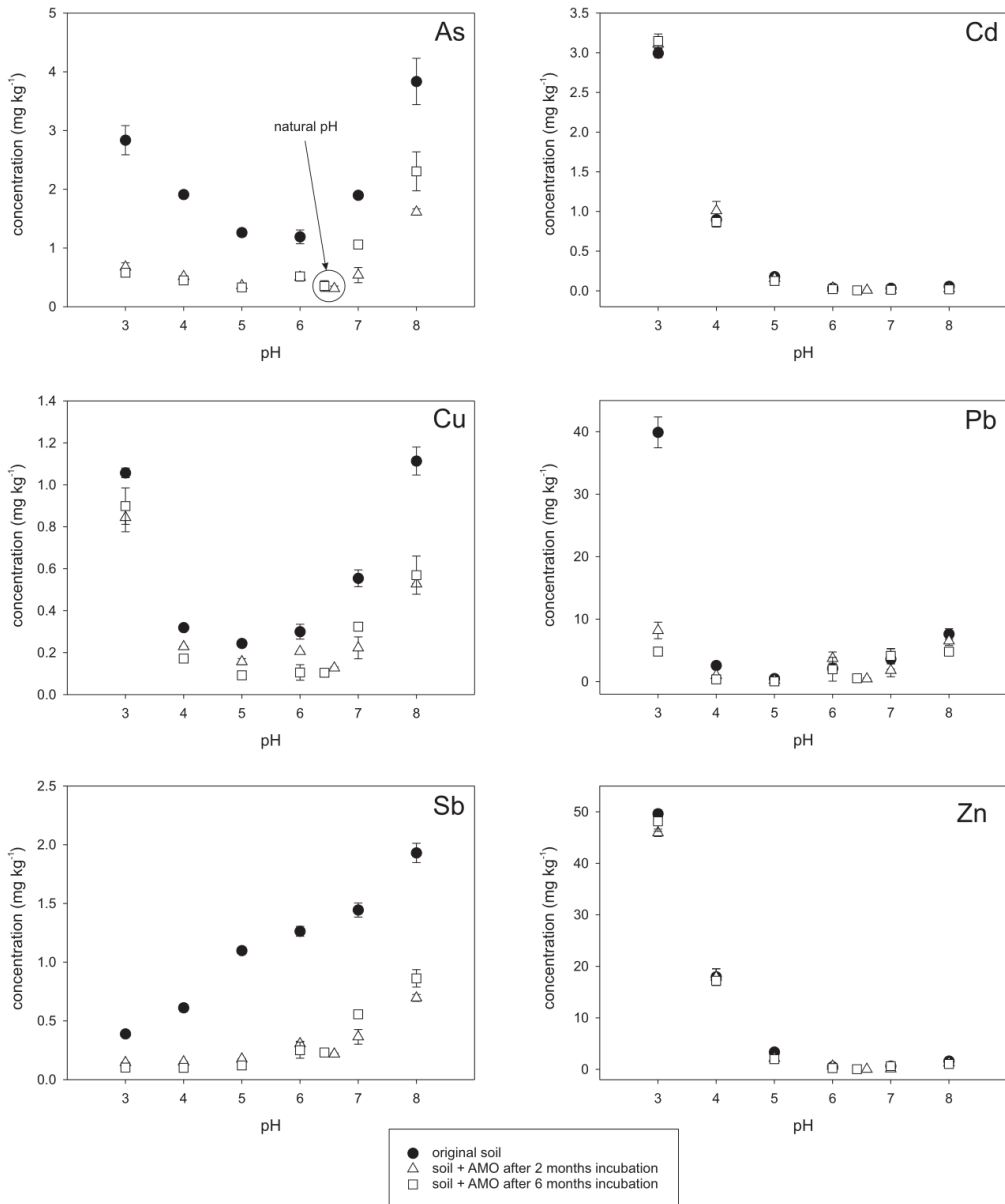


Figure 4.5

The pH-static leaching of metal(loid)s from the original soil and soils amended with amorphous manganese oxide (AMO).

conditions. The overall decrease in the leaching of these four contaminants expressed as % of the control (unamended) soil was as follows: As (20-60%), Cu (35-85%), Pb (7-100% [not efficient for pH values in the range 5-7]) and Sb (11-45%).

Contaminant leaching can also be related to the dissolution of soil organic matter. The pH-dependent DOC leaching exhibited a U-shaped curve for the original soil and both incubations (**Fig. 4.6**). The maximum leached concentrations at pH 8 reached values of 83.6 mg L⁻¹ for the original soil and 66.7 and 51.8 mg L⁻¹ after incubation for 2 and 6 months, respectively. Generally, lower DOC leaching was observed for AMO treatments compared to the original soil (**Fig. 4.6**).

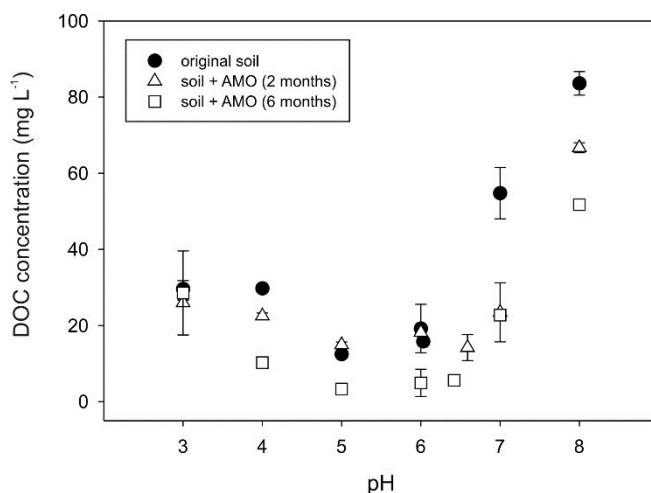


Figure 4.6

Dissolved organic carbon (DOC) leaching as a function of the pH.

The PHREEQC-3 calculations indicated that all the leachates were highly undersaturated with respect to several Mn-oxides and hydroxides, indicating no secondary precipitation. In contrast to the AMO leaching in aqueous environments, only soil leachates at pH > 6 were potentially oversaturated with secondary rhodochrosite. Other secondary phases which could be also responsible for retention of contaminants by sorption (Al- and Fe-oxides) were predicted by the PHREEQC-3 calculations to be oversaturated in leachates especially at circumneutral pH values.

Discussion

Effect of L/S ratio and pH on the leaching of AMO

Leaching of solids at high L/S ratios indicates long-term stability of a given material (Ettler et al., 2008) and consequently much higher dissolution of AMO can be expected in a longer-term perspective when exposed to soil solutions. Our results on leaching at various L/S ratios (**Fig. 4.2**) are in agreement with Della Puppa et al. (2013), who observed that 0.24% and 5.7% of the AMO dissolved at L/S of 10 and 500, respectively. Despite the small amount of colloidal-sized particles in the original AMO (3.28% of particles <1 μm), our leaching results on filtered/ultrafiltered suspensions indicate that they do not affect the Mn leaching from AMO (**Fig. 4.2**), probably due to its aggregation in soils (Ettler et al., 2014).

The pH-static experiments in an aqueous environment clearly indicate that the AMO dissolution is pH-dependent, as was previously demonstrated in a long-term weathering study in contrasting soils with various pH values (Ettler et al., 2014). However, when used as an amendment in soil, its dissolution is significantly less pronounced and supports the hypothesis about AMO “stabilization” in soil (**Fig. 4.1**). The addition of AMO to the soil led to an increase in the natural pH of the soil due to its partial dissolution connected with the release of OH^- ions (Micháľková et al., 2014).

Effect of time and pH on metal(loid) stabilization by AMO

The efficiency of metal(loid) retention after application of a stabilizing agent is a key parameter determining the chemical stabilization process in contaminated soils (Bolan et al., 2014; Komárek et al., 2013). Previous investigations indicated that a novel amorphous manganese oxide (AMO) has a high potential for adsorption of metals (Della Puppa et al., 2013) and it was found to have highly promising applications for remediation of polluted soils (Micháľková et al., 2014). The remediation potential of a given amendment is often evaluated by various extraction methods (e.g., deionized water, CaCl_2 , EDTA, acetic acid) and comparisons with untreated soil (Cheng and Hseu, 2002; Mech et al., 1994; Micháľková et al., 2014; Tsang et al., 2013; 2014). For example, Micháľková et al. (2014) recently demonstrated that soil amendment with AMO led to a decrease in CaCl_2 -extractable Cu to 8% of the value in the control

(untreated) soil and Pb concentrations decreased to values below the detection limit. Although they are often criticized, sequential extraction procedures are also suitable tools for assessment of the amendment efficiency in soils. Changes in the chemical fractionation of contaminants after the addition of an amendment are commonly evaluated, especially the most “labile” exchangeable fraction. Recently, Kumpiene et al. (2012) demonstrated that the amount of As bound in the exchangeable fraction of the sequential extraction significantly decreased in amine spoil treated with compost, zerovalent iron and coal fly ash in comparison with the original spoil material; moreover, the transfer of As to less available fractions and binding to Fe-oxides was documented by X-ray absorption spectroscopy and microbeam X-ray fluorescence. A statistically significant decrease in exchangeable fraction of metal(loid)s was observed after amendment with Mn-oxide in numerous studies (e.g. Michálková et al., 2014; Tsang et al., 2013) and was in agreement with our results for all the studied contaminants except Zn (**Fig. 4.4**). Along with this trend, an increase of binding to less available reducible fraction (Fe-oxides) was observed for Pb and mainly for redox sensitive species such as As and Sb (**Fig. 4.4**), which is in agreement with other soil remediation studies (Kumpiene et al., 2012; Michálková et al., 2014).

Nevertheless, it is important to stress that the extraction efficiency of simple leaching tests used for these evaluations is often dictated by the nature of the extracting solution (pH, presence of ligands etc.) and potential pH changes in the environment are not taken into account. The stability of the amended soil under a wider range of pH conditions thus provides additional insights needed for assessment of the treatment efficiency.

The pH-dependent leaching experiments performed on the original and stabilized soils indicated that the AMO treatments were not efficient for Cd and Zn, where up to 62% and 20% of the total concentrations were leached, respectively (**Fig. 4.5**). This phenomenon can be explained differently. It can be related to the fact that these metals as usually found in smelter-polluted soils are often present in “labile” forms, as revealed by sequential extraction data (**Fig. 4.4**; Chrastný et al., 2012; Ettler et al., 2012). Moreover, the speciation of these contaminants in the soil pore water solution can affect their binding to soil constituent by adsorption (Ettler et al., 2009; 2012). Another explanation can be related to their direct sorption on AMO. Della Puppa et al. (2013) reported that AMO is a more efficient sorbent for Pb and Cu than for Cd and Zn. Moreover, the Cd and Zn sorption onto AMO was found to be highly pH-dependent with the lowest sorption at pH 4 (~50%) in comparison with Cu (~65%) and Pb (~95%) (Della Puppa et al., 2013).

In contrast, relatively efficient chemical stabilization was found for Pb, As, Cu and Sb despite the fact that only <4% of their total concentration was leached from the soil. For all these contaminants, the efficiency was more pronounced under acidic conditions with generally the highest decrease in leached concentrations in longer-term incubations (6 months) (**Fig. 4.5**). Particularly high retention compared to the untreated soil was observed for Pb under acidic conditions (pH 3-4) and can be attributed to its strong binding to AMO (**Fig. 4.5**). Efficient sorption of Pb to Mn-oxides (birnessite, todorokite, cryptomelane) originates from their low pH_{zpc} values ranging between 1.75 and 3.50 (Della Puppa et al., 2013; Feng et al., 2007), which is, however, not the case for AMO. It is also known that the sorption capacity of birnessite for Pb is much higher than that for other metals (Cd, Cu, Zn), which is generally explained by Pb occupancy in both the interlayer and surface edge sites of Mn-oxides, while other metals occupy mostly interlayer sites (Wang et al., 2012a). Nevertheless, contradictory data are available in the literature on the pH-dependent adsorption edges of Pb on Mn-oxides. Whereas Della Puppa et al. (2013) reported that Pb adsorption on AMO was almost pH-independent and was similar to that of birnessite, Zaman et al. (2009) reported that Pb adsorption edges on MnO₂ (unspecified from the mineralogical point of view) were between pH 5 and 6. In addition, Villalobos et al. (2005a) also demonstrated a significant increase in the Pb sorption capacity for δ -MnO₂ as a function of the pH (range 4-6.5).

When compared to Pb, Cu is much less efficiently sorbed onto Mn-oxides (e.g. Della Puppa et al., 2013; Feng et al., 2007; Wang et al., 2012a). However, AMO application to soils led to a decrease in the Cu leaching (35-85% of the control) (**Fig. 4.5**). The leaching of As also decreased after AMO application to soils (20-60% of the control) (**Fig. 4.5**); similarly, Bagherifam et al. (2014) demonstrated that, after the addition of 2% Mn-oxide to a polluted soil, the DTPA-extractable As decreased to 80% of the control. Numerous studies demonstrated that As can be efficiently sorbed by Mn-oxides, which also help to oxidize As(III) to As(V) (Chen et al., 2006 Ying et al., 2012). Nevertheless, it can be extremely difficult to describe As sorption onto Mn-oxides in the presence of other contaminants (metals). Villalobos et al. (2014) recently demonstrated that As(III) oxidation increases with decreasing pH, but As(V) sorption was higher at pH 6 than at pH 4.5. Other contaminants (Pb, Zn) decreased As(III) oxidation due to site blockage, but in turn their presence increased As(V) sorption (Villalobos et al., 2014). Higher Cu and As leaching from the original soil and both treatments at pH > 7 are probably due to NaOH addition during the pH-static leaching test, which promotes partial dissolution of soil organic matter (**Fig. 4.6**). Our SEP data (**Fig. 4.4**) and other studies (Ettler et al., 2010; Michálková et al., 2014)

indicated that particularly Cu and As can occur insignificant proportions in the oxidizable fraction of the sequential extraction (targeting soil organic matter). Moreover, As is known to be generally more mobile at higher pH (Komárek et al. (2013) and references therein). In comparison with other contaminants, contrasting leaching patterns were observed for Sb with an increase in leaching as a function of time. The AMO application led to a decrease in the Sb leaching in the range of 11-45% of the control (**Fig. 4.5**). Relatively little information is available on the efficiency of soil amendments in Sb retention; a recent study by Bagherifam et al. (2014) reported that, after soil treatment with 2% Mn-oxide, the DTPA- extractable Sb concentration decreased by 50%, which is in agreement with our results. An increase in leaching at $\text{pH} > 7$ can be partly related to dissolution of soil organic matter, but may also be connected with the dissolution of soil Fe-oxides, which can be highly responsible for Sb binding in smelter-affected soils (Ettler et al., 2010) (an increase in Fe leaching as a function of the pH was documented, data not shown). In addition, Wang et al. (2012b) recently demonstrated that Sb(V) sorption onto manganite ($\gamma\text{-MnOOH}$) is efficient under acidic conditions, but Sb can be desorbed at $\text{pH} > 6$, which can also be partly responsible for increased Sb leaching after AMO treatments at higher pH (**Fig. 4.5**).

Conclusions

Amorphous manganese oxide (AMO) was used as an amendment for a Pb smelter polluted agricultural soil and the pH-dependent stability of the treatments was evaluated after 2 and 6 months of incubation in the pH range 3-8. Sequential extraction indicated that AMO treatments lead to a statistically significant decrease in the “labile” fraction of As and Sb in the soil. The pH-static experiments indicated that no effect of the AMO treatment was observed for Cd and Zn, whereas the leaching of other contaminants decreased significantly compared to the original soil: As (down to 20% of the control), Cu (35%), Pb (7%), Sb (11%). The remediation efficiency was more pronounced under acidic conditions and the time of incubation generally led to increased retention of the studied contaminants. The AMO thus proved to be a promising agent for chemical stabilization of multiple metal(loid)s in contaminated soils. Its effects on the bioavailable concentrations of metal(loid)s and its applications in field experiments are currently under investigation.

Chapter V

Stability, transformations and stabilizing potential of an amorphous Mn oxide and its surface-modified form in contaminated soils

Z. Michálková, M. Komárek, M. Vítková, M. Řečínská, V. Ettler

Manuscript submitted to Applied Geochemistry.

Content

Abstract	109
Introduction	110
Materials and methods	111
Adsorbent synthesis and characterization	111
Properties of the studied soil samples	112
Stability in pure water	113
Adsorption kinetics study	113
Incubation batch experiments	113
pH-static leaching experiments	115
Statistical analysis	115
Results and discussion	115
Adsorbent synthesis and characterization	115
Characterization of model contaminated soils	117
Stability in pure water	119
Adsorption kinetics study	121
Incubation batch experiments	123
pH-static leaching experiment	132
Conclusions	134

Abstract

A surface-modified amorphous manganese oxide (SM-AMO) was prepared to increase the stability of a previously studied promising stabilizing agent and to compare its immobilizing efficiency with respect to contaminating metals with the original material. To synthesize the SM-AMO, the AMO surface was synthetically covered with a coating of MnCO_3 because newly formed rhodochrosite precipitates were previously found to increase the stability of AMO particles in soils. A preliminary experiment evaluating the long-term stability of both materials in pure water suggested higher stability for the SM-AMO particles, showing a smaller release of Mn compared to the original AMO. An adsorption kinetics study focused on As, Cd, Pb and Zn showed lower adsorption rates and adsorption capacity for Zn, probably as a result of partial surface passivation. In comparison to these results for simple controlled systems, different effects were recorded when the two materials were applied to contaminated soils. When incubated in soil, a constantly lower mass loss was recorded in the case of SM-AMO. There were no significant differences in the release of Mn and DOC into the soil solution or in the stabilizing efficiency with regard to contaminating metal(loid)s between the original and surface-modified materials. Concerning the potential solid phase transformations in soil conditions, we observed a gradual equilibration between both materials. While the newly formed rhodochrosite precipitated on the AMO surface, the MnCO_3 coatings on SM-AMO gradually dissolved, equilibrating the surface composition of the two materials. Both amendments also effectively supported microbial activity, especially in the more contaminated soil sample. Thus, despite the smaller mass loss, the effectiveness of both materials is comparable in the long term.

Introduction

Manganese oxides/hydroxides (generally referred as Mn oxides) are ubiquitous minerals present in virtually all types of soils and sediments worldwide. They usually occur as coatings or fine-grained aggregates with large surface areas, and, although they are present in only small amounts, they are considered one of the main driving factors controlling the partitioning of metals/metalloids between the solid and liquid phases in soil (Post, 1999). Manganese oxides form strong inner-sphere complexes with metals (e. g., Cd, Pb, Zn) (Lefkowitz and Elzinga, 2015; Qin et al., 2011) and are thus able to reduce their bioavailability and bioaccessibility very effectively (Beak et al., 2008; Hettiarachchi et al., 2000; Sapin-Didier et al., 1997). The ability of manganese oxides to take part in various redox reactions is used to oxidize more mobile and toxic As(III) to As(V) in remediation processes (Chiu and Hering, 2000; Manning et al., 2002). In contrast, these materials are not considered to be suitable for the remediation of Cr in the environment due to the risk of Cr(III) oxidation to Cr(IV) (Landrot et al., 2012). The ability of Mn oxides to effectively scavenge metals/metalloids has been used in many environmental applications, including contaminated water treatment (Chang et al., 2008; Han et al., 2006; Liu et al., 2009; Liu et al., 2016; Ociński et al., 2016) and chemical stabilization of metals/metalloids in contaminated soils (Ettler et al., 2015; Chen et al., 2000a, b; Komárek et al., 2013; McCann et al., 2015; Michálková et al., 2014; 2016).

In the last two decades, intensive research has been conducted in the field of chemical immobilization of metals/metalloids in contaminated soils because this remediation technique has the potential to be cheaper and less disturbing than conventional remediation methods, e.g., soil excavation and landfilling (Kumpiene et al., 2008). In this case, various stabilizing agents, including alkaline materials (Gray et al., 2006), organic matter (Soares et al., 2015), phosphates (Sun et al., 2016), clays (Yin and Zhu, 2016), zeolites (Shi et al., 2009), industrial waste and byproducts (Garau et al., 2011), elemental Fe (Tiberg et al., 2016) or Fe (Kim et al., 2012), Mn (McCann et al., 2015) and Al (García-Sánchez et al., 2002) oxides are applied to soil to decrease the mobility and bioavailability of contaminating metals/metalloids. The main mechanisms involved in this process are considered to be adsorption, complexation with organic ligands, (co-)precipitation or ion exchange (Kumpiene et al., 2008). To date, most of the studies have focused on the stabilization efficiency of applied amendments and information on the stability and potential transformations of the applied materials in soil conditions remain scarce.

In this study, a surface-modified amorphous manganese oxide (SM-AMO) was prepared as a potentially more stable alternative to the original amorphous manganese oxide (AMO), which has proven in our previous studies to be a highly efficient stabilizing agent usable both for metal(loid)-contaminated soils (Ettler et al., 2015; Micháľková et al., 2014; 2016). The affinity towards both cationic and anionic contaminants was also confirmed by adsorption experiments when the recorded adsorption capacities reached 2.24, 0.52, 4.02 and 0.46 mmol g⁻¹ for Cd, Cu, Pb and Zn, respectively (Della Puppa et al., 2013; Micháľková et al., 2014). The recorded adsorption maximum for As was 1.79 mmol g⁻¹, which represents one of the highest adsorption capacities reported for As from the Mn oxide-based materials to date (Micháľková et al., 2016). Although highly efficient, the drawback of this agent lies in its relatively lower stability, especially at lower pH values, which may be followed by increased dissolution of soil organic matter (SOM) (Ettler et al., 2014; Micháľková et al., 2014). To minimize these unwanted effects, surface pretreatment with MnCO₃ coating prior to the direct application of AMO particles to soil was proposed, as this phase was found as the main alteration product on the surface of raw AMO particles incubated in contaminated soils. It was observed that the formation of this layer was connected with higher stability of AMO particles and decreased their oxidative effects towards SOM as well (Ettler et al., 2014). Surface modification of the AMO particles before their application could thus help to optimize the properties of this novel promising stabilizing agent.

Materials and methods

Adsorbent synthesis and characterization

The amorphous manganese oxide (AMO) was synthesized according to Della Puppa et al. (2013) using the modified sol-gel method for the preparation of birnessite (Ching et al., 1997). The gel was then air-dried, finely milled and washed three times with deionized water to obviate the synthesis residue on the AMO surface. The surface-modified AMO (SM-AMO) was subsequently prepared by incubating the material in deionized water saturated with CO₂. For each batch, 3 g of AMO were mixed with 30 mL of deionized water at 10:1 L/S and placed in a 50-mL burette. The CO₂ was formed by dropping diluted HCl into NaHCO₃ (30 g of NaHCO₃ per each batch), being captured and conducted into the AMO suspension. After the end of

the reaction, the burettes were closed tightly. This procedure was repeated over another three consecutive days and on the fifth day, the modified AMO particles were filtrated and air dried. For comparison purposes, another set of AMO samples was incubated in deionized water in an open system (one batch consisted again of 3 g of AMO and 30 mL of deionized water) for the same amount of time as the samples actively saturated with CO₂.

The solid phases were identified using X-ray diffraction spectrometry (XRD; PANalytical B.V., the Netherlands) (CuK α radiation, 40 kV and 30 mA, range 10-80° 2 θ , step 0.02, counting time of 300 s), together with scanning electron microscopy/energy dispersive X-ray spectroscopy (SEM/EDX; TESCAN Ltd., Czech Republic) equipped with an EDX detector Bruker Quantax 125 eV. The accelerating voltage was set to 15 kV, and element quantification was carried out using a Quantax Esprit 1.9 software. Qualitative XRD analysis was performed using PANalytical X'Pert HighScore Plus software (version 3) and the ICDD PDF-2 database (2003). The pH of the studied oxides was determined in deionized water at 1:10 w/v, and pH_{zpc} was assessed using the immersion technique (Fiol and Villaescusa, 2009). The specific surface was determined using the Brunauer-Emmett-Teller (BET) method (Nova e-Series analyzer, Quantachrome Instruments, USA).

Characterization of model contaminated soils

For the purpose of this study, two models of soils contaminated with metals and As were used. The first soil (Fluvisol) was collected from Litavka river alluvium heavily polluted with As, Cd, Pb and Zn as a result of historical activity of a nearby Pb-processing smelter in Příbram (Czech Republic). The second soil (Leptosol) was sampled at Smolotely village (Czech Republic), where As occurs naturally in extremely high concentrations due to the presence of As-bearing minerals.

Soil samples were collected from the superficial layer (0–20 cm), air dried, homogenized and sieved through a 2-mm stainless sieve. The particle size distribution was determined using the hydrometric method (Gee and Or, 2002). Soil pH was measured in suspension using a 1:2.5 (w/v) ratio of soil/deionized water or 1 M KCl (ISO 10390:1994). The total organic carbon content (TOC) was determined using the carbon analyzer TOC-L CPH (Shimadzu, Japan). The cation exchange capacity was determined using the 0.1 M BaCl₂ extraction method (Carter and Gregorich, 2008). The pseudo total concentrations of elements were determined using the US EPA *aqua regia* extraction method (US EPA method 3051a) with microwave digestion

(SPD-Discover, CEM, USA) and ICP-OES analysis (Agilent 730, Agilent Technologies, USA). The fractionation of metals was determined using the BCR sequential extraction procedure by Rauret et al. (2000) and the fractionation of As was determined according to Wenzel et al. (2001a). The standard reference materials 2710a Montana Soil I (NIST, USA) and CRM 483 (Institute for Reference Materials and Measurements, EU) were used for QA/QC. All chemicals used in the experiments were of analytical grade.

Stability in pure water

Preliminary stability experiments were performed by agitating the AMO or SM-AMO particles (w/v ratio of 1/50 and 1/500) in deionized water up to 4 weeks. The solution was collected in periodic intervals, pH and Eh were measured and the contents of elements were determined using ICP-OES. The experiment was performed in duplicates.

Adsorption kinetics study

Adsorption experiments were used to evaluate the adsorption kinetics of the metal(loid)s (As, Cd, Pb and Zn) present in the model soils in the tested materials. All adsorption experiments were performed using 0.01 M NaNO₃ as the background electrolyte. The kinetic study was performed in a suspension of 1 g L⁻¹ of the AMO/SM-AMO and 0.1 mM L⁻¹ of As, Cd, Pb and Zn, which were added as Na₂HAsO₄•7H₂O, Cd(NO₃)₂•4H₂O, Pb(NO₃)₂ and Zn(NO₃)₂•6H₂O, respectively. The experiment was conducted separately for each metal(loid) and adsorbent. The suspension was then agitated for up to 2 hours in the case of Cd, Pb and Zn and 24 hours in the case of As. The pH was adjusted continuously at pH 5 (Cd, Pb and Zn) and 7 (As) using NaOH/HNO₃ and an automatic titration device (TitroLine alpha plus, SI Analytics, Germany). Five mL of the suspensions were collected after each time step in duplicates and filtered immediately through a 0.45-µm nylon syringe filter. Metal(loid) concentrations in the solutions were determined using ICP-OES. The obtained kinetic data were modeled using the pseudo-second-order equation (Micháľková et al., 2016).

Incubation batch experiments

Incubation batch experiments were performed to investigate the stability and transformations of the AMO and SM-AMO particles in model contaminated soils,

their influence on soil solution characteristics and the mobility of metals/metalloids. The experiment was conducted in two variants in duplicates using the Fluvisol and Leptosol soils. Firstly, to examine the possible transformations and stability of AMO/SM-AMO particles, 1-g aliquots of AMO/SM-AMO were placed into two-layered sealed polypropylene poaches. These poaches were then placed into plastic pots together with 150 g of Fluvisol or Leptosol soil. The poaches were situated approximately 3 cm from the bottom of the pot and rhizon samplers (mean pore volume size 0.15 μm ; Rhizosphere Research Products, Netherlands), enabling the collection of the soil solution below the poaches.

The second variant of the experiment focused mainly on the changes in metal/metalloid mobility and other characteristics of soil solutions in AMO/SM-AMO-amended soils. 200 g of soil samples were mixed with AMO/SM-AMO at a concentration of 1% (w/w) and placed into plastic pot with a rhizon sampler as above. A control variant without any AMO was included. Pots with and without poaches were watered with deionized water to maintain ~60-70% of the water holding capacity. The experiment was performed in separate pots for time intervals of 1, 2, 4 and 10 weeks. After these periods, the soil solution was collected. The content of metals/metalloids and DOC (dissolved organic carbon) was determined using ICP-OES and a TOC/DOC analyzer, respectively. The pH and Eh of the soil solutions were monitored as well. In addition, the PHREEQC-3 speciation solubility code (Parkhurst and Appelo, 2013) was used to determine the speciation of selected elements in the solutions and the possible oversaturation of soil pore water with respect to solid phases (saturation indices, SI). For this purpose, all the measured parameters and concentrations of cations as well as anions were included. The T&H.dat database was used for all the calculations, which enables the use of DOC in the simulations as documented by Ettler et al. (2012). With reference to Borůvka et Vácha (2006), who studied fractionation into fulvic acids (FA) and humic acids (HA), and the fact that HA/FA ratio changes with pH and soil type, the dissolved organic carbon was entered into the code as fulvate and humate in a model ratio of 1:1. The content of inorganic carbon was calculated based on the partial pressure of CO_2 ($p\text{CO}_2$) in soils and on the assumption that $p\text{CO}_2$ affects the final pH (i.e., the actual changes in pH during the incubation experiments were taken into account for each simulation). The poaches with AMO/SM-AMO were extracted from the soil at chosen time intervals and air dried, and the change in AMO/SM-AMO weight was determined. The AMO/SM-AMO particles were subsequently examined using XRD and SEM/EDX under the same conditions as described in chapter “Adsorbent synthesis and characterization.”

Additionally, the activity of soil microorganisms in the control soils and soils amended with AMO/SM-AMO (1%, w/v) was determined. Soil samples were collected at the same time as when the soil solution was collected and the microbial activity was determined using a simple dehydrogenase assay (Rogers and Li, 1985).

pH-static leaching experiments

The pH-static leaching experiments were performed to determine the influence of pH changes on the leachability of metals/metalloids and stability of AMO/SM-AMO in amended soils. Soil samples were mixed with AMO/SM-AMO at a concentration of 1% (w/w) and maintained at ~60-70% of the water holding capacity for 4 weeks. A control variant without AMO/SM-AMO addition was included. An amount of 1.5 g of dry soil was then watered with 15 mL of deionized water and leached for 48 hours (CEN/TS 14997, 2006; Van Herreweghe et al. 2002) at pH 4, 5, 6, 7 and 8. The pH was continuously controlled and adjusted using NaOH/HNO₃. A variant with natural soil pH (i.e., without pH adjusting) was also included. All experiments were performed in triplicates. After the end of the experiment, the pH of samples without pH adjustments was determined. All samples were then centrifuged (5000 rpm, 10 min) and filtered through 0.45- μ m nylon syringe filters. The Eh value was measured in filtrates using a digital multimeter (Multi 3420, WTW, Germany). Metals/metalloids and DOC concentrations in leachates were measured using ICP-OES and a TOC/DOC analyzer, respectively.

Statistical analysis

All statistical analyses were performed using SigmaPlot 12.5 (StatSoft Inc., USA). The experimental data were evaluated using analysis of variance (ANOVA) at $P < 0.05$ using the Tukey test.

Results and discussion

Adsorbent synthesis and characterization

For the XRD spectra obtained for the original AMO, the samples incubated in water saturated with CO₂ and water equilibrated with atmospheric CO₂ are depicted in **Fig. 5.1**. The AMO particles incubated in water equilibrated solely with atmospheric CO₂ showed almost the same pattern as the original ones, with no significant changes.

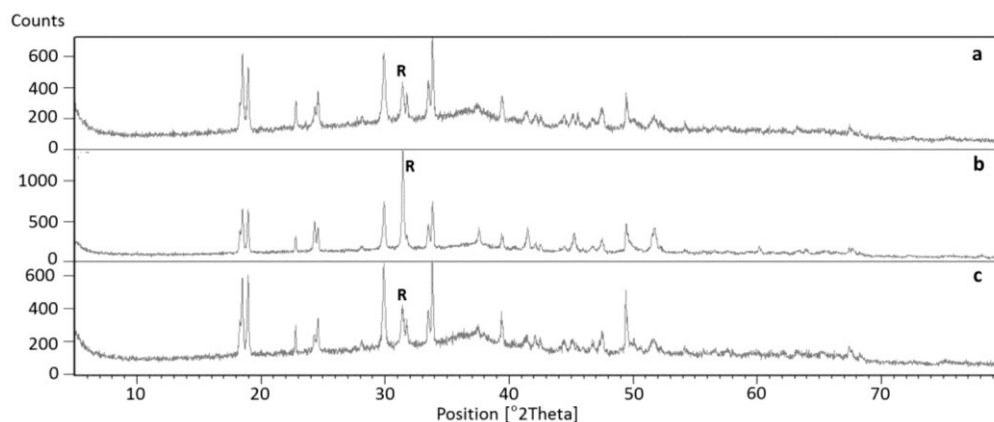


Figure 5.1

Comparison of XRD spectra obtained for the original amorphous manganese oxide (AMO) (a), AMO incubated in deionized water saturated with CO_2 (b) and AMO incubated in water equilibrated with atmospheric CO_2 (c).

In contrast, the spectra received for particles incubated in CO_2 -saturated water showed a significant increase in the intensity of the MnCO_3 peak, indicating the presence of a newly formed carbonate phase. The Mn-oxalate was another phase identified in all the examined samples, in agreement with previous observations of Ettler et al. (2014). These results were further confirmed by SEM/EDX (**Fig. 5.2**), where MnCO_3 was found to form a coating on the original AMO particles. For that reason, further experimental work addressed only original AMO particles and surface-modified particles incubated in water saturated with CO_2 (SM-AMO). The physico-chemical properties of the AMO/SM-AMO are summarized in **Table 5.1**. The pH of SM-AMO was higher than that of the original AMO, but a higher pH_{zpc} was recorded in the case of the AMO. These values are lower than those reported for the AMO by Della Puppa et al. (2013), probably due to the purification washing step after the milling of the dry material that was added to the original synthesis protocol.

Table 5.1

Physico-chemical properties of the amorphous manganese oxide (AMO) and its surface-modified variant (SM-AMO).

	pH	pH_{zpc}	BET ($\text{m}^2 \text{g}^{-1}$)
AMO	6.03	6.97	135
SM-AMO	6.43	6.29	189

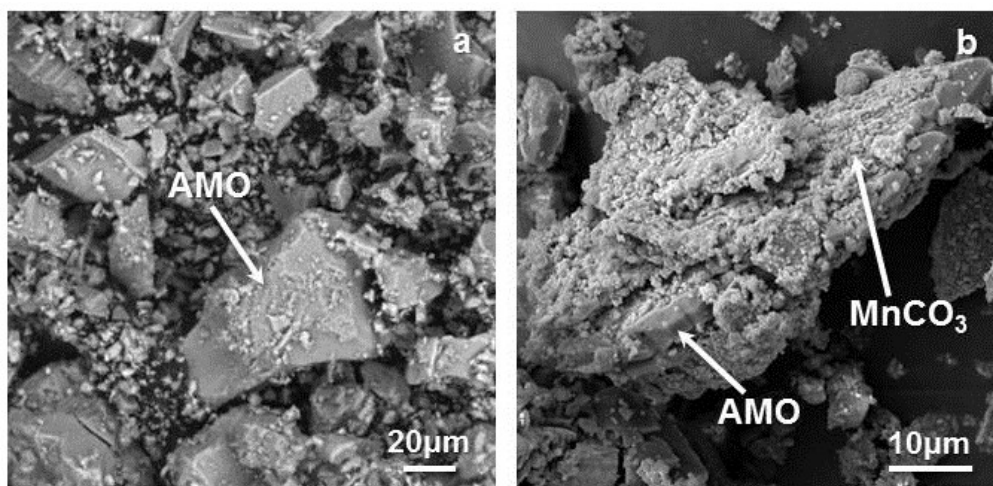


Figure 5.2

SEM images of original AMO particles (a) and AMO particles incubated in deionized water saturated with CO₂ (b). AMO: amorphous manganese oxide.

Characterization of model contaminated soils

The basic physico-chemical properties of the studied soils are summarized in **Table 5.2**. Both soils were slightly acidic. The Leptosol, as an insufficiently developed soil, had a coarser texture and lower content of soil organic matter (SOM) than the Fluvisol. In contrast, the Leptosol showed a higher cation exchange capacity, mainly due to the significantly higher content of Fe oxides. The limit values set for metals/metalloids in agricultural soils by the Ministry of the Environment of the Czech Republic (Act No. 13/1994) were exceeded for As, Cd, Pb and Zn in the Fluvisol and As in the Leptosol. Both soils differ in the origin of contamination. Whereas the multi-metallic contamination of the Fluvisol originates from the historical smelting activities and leachates from surrounding slag heaps, the high As concentration in the Leptosol has its origin in the bedrock rich in As-bearing minerals. Metal(loid) fractionation in the studied soils was evaluated using sequential extraction procedures (**Table 5.3**). In the Leptosol, the largest portion of As (~67%) was present in the fraction bound to amorphous and poorly crystalline hydrous oxides of Fe, Al and Mn. Although the amount of As in the two most labile fractions, usually related to non-specifically and specifically bound As, was relatively low (0.36 and 8.63%, respectively), the absolute amount of As bound in these fractions was still very high due to the extreme As concentrations in the original soil. In the case of the

Fluvisol, the largest fraction of As (72%) was present in the fraction associated with amorphous and the poor crystalline hydrous oxides of Fe, Mn and Al, similarly to the case of Leptosol. The major part of Cd and Zn in Fluvisol was present in the most mobile exchangeable fraction (61% and 46%, respectively), whereas Pb was found mainly in the reducible fraction (61%), usually associated with metals bound to Fe, Mn and Al oxides.

Table 5.2

Basic physico-chemical characteristics of the studied soils. Limit concentrations of metals/metalloids in agricultural soils are set according to the Ministry of the Environment of the Czech Republic (Act No. 13/1994). <DL: below detection limit.

	Fluvisol	Leptosol	
pH _{H2O}	5.95	6.09	
pH _{KCl}	5.14	4.87	
CEC (cmol kg ⁻¹)	9.08 ± 0.52	15.85 ± 0.53	
TOC (%)	2.15	1.16	
Particle size distribution (%)			
Clay (%)	7	6	
Silt (%)	31	7	
Sand (%)	62	87	
Texture	sandy loam	loamy sand	
	Pseudo total metal concentrations (mg kg⁻¹) (n = 3)		Limit concentrations (mg kg⁻¹)
As	296 ± 6	17 563 ± 2798	30
Pb	3539 ± 375	73 ± 12	140
Cd	39 ± 1	<DL	1
Zn	4002 ± 68	193 ± 12	200
Cu	68 ± 3	51 ± 5	100
Fe	37 408 ± 195	68 910 ± 4274	no limit
Mn	4276 ± 34	1096 ± 124	no limit

Table 5.3

Fractionation of As, Cd, Pb and Zn in the studied soils.

Fractionation of As (sequential extraction by Wenzel et al. 2001) (mg kg⁻¹) (n=3)					
	FA: non- specifically sorbed	FB: specifically adsorbed	FC: bound to amorphous and poorly crystalline hydrous oxides of Fe, Al and Mn	FD: bound to well- crystallized hydrous oxides of Fe, Al and Mn	FE: residual phase
Fluvisol	0.16 ± 0.02	20.2 ± 0.1	214 ± 4	45.9 ± 8.4	16
Leptosol	64 ± 3	1516 ± 96	11 777 ± 1968	5753 ± 537	-
Fractionation of metals in the Fluvisol (sequential extraction by Rauret et al. 2000) (mg kg⁻¹) (n=3)					
	FA: exchangeable	FB: reducible	FC: oxidizable	FD: residual phase	
Cd	24.0 ± 0.3	8.0 ± 1.1	1.3 ± 0.2	6	
Pb	281 ± 11	2165 ± 176	705 ± 93	388	
Zn	1822 ± 50	816 ± 45	298 ± 32	1066	

Stability in pure water

The stability of the original and surface-modified AMO was preliminarily compared in a simple system with deionized water based on the amount of Mn released into the solution (**Fig. 5.3**). Generally, more Mn was released from both materials at the ratio of 1/500 (w/v). In the case of both ratios used (i.e., 1/50 and 1/500), the release of Mn was lower in the case of SM-AMO. Maximal recorded amounts of released Mn corresponded to 7.6 and 5.7% of the total Mn contained in AMO and SM-AMO at the ratio of 1/50, and 21.8 and 17.5% at the ratio of 1/500. The Eh measurements confirmed oxidative conditions during the whole experiment with pH values ranging from 6.6 to 7.1 (**Fig. 5.4**). Della Puppa et al. (2013) also examined the stability of AMO particles in pure water over a period of 400 hours and observed two dissolution steps for the ratio of 1/500 (w/v). The first one was reached within 20 hours and was assigned to the release of weakly sorbed Mn. The second step was reached after 200 hours and could correspond to the dissolution of AMO particles. In our case,

a slow gradual dissolution (i.e., release of Mn) of AMO/SM-AMO was observed throughout the experiment. In contrast to Mn, the amount of released K (**Fig. 5.5**) remained stable, in agreement with the observations of Della Puppa et al. (2013). This was explained by the release of weakly sorbed K and KMnO_4 residue on the particles' surface; no K was found inside the birnessite structure synthesized according to Ching et al. (1997).

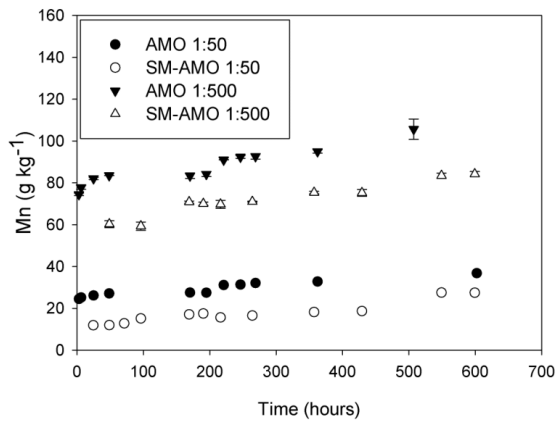


Figure 5.3

The amount of released Mn in time and at a w/v ratio ($n=2$). AMO: amorphous manganese oxide, SM-AMO: surface-modified amorphous manganese oxide.

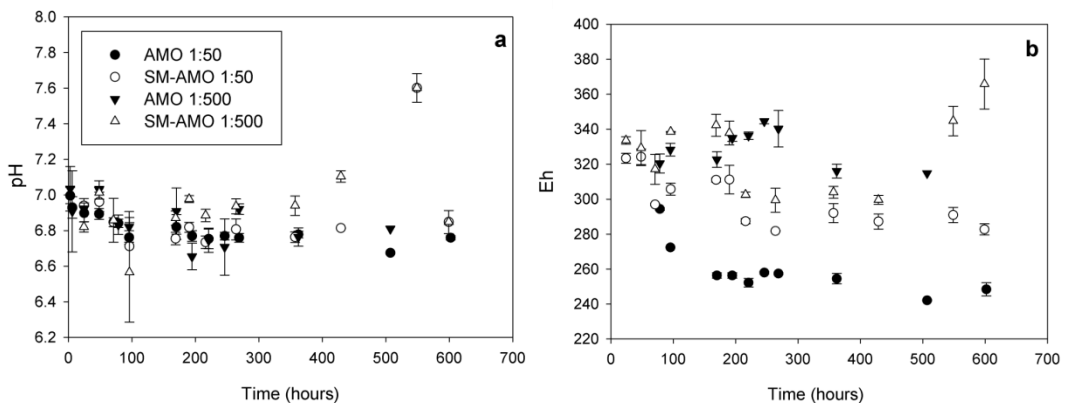


Figure 5.4

pH (a) and Eh (b) values determined in solution after long-term agitation of the amorphous manganese oxide (AMO; 1/50 and 1/500 w/v) and its surface-modified variant (SM-AMO; 1/50 and 1/500 w/v) ($n=2$).

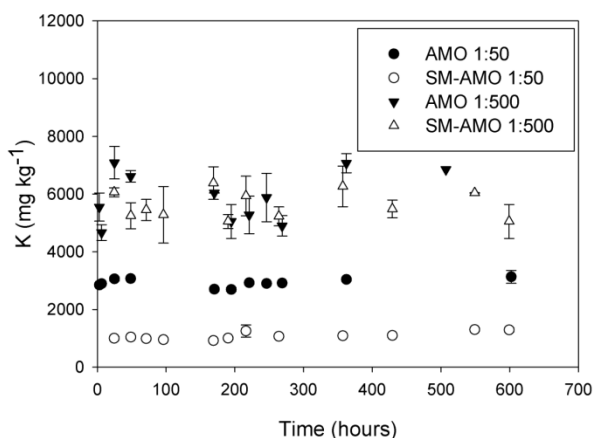


Figure 5.5

Potassium content in solution after the long-term agitation of the amorphous manganese oxide (AMO; 1/50 and 1/500 w/v) and its surface-modified variant (SM-AMO; 1/50 and 1/500 w/v) ($n=2$).

Adsorption kinetics study

The adsorption kinetics of the studied metal(loid)s onto AMO/SM-AMO and the corresponding amounts of released Mn are depicted in **Fig. 5.6**, and the modeled pseudo-second order kinetic parameters are summarized in **Table 5.4**. When recalculated to molar concentrations, the highest adsorption rate was generally recorded in the case of Pb, being ~6, 9 and 21 times higher than in the case of Zn, Cd and As, respectively (data for the AMO). These results correlate well with those obtained in previous studies, where Pb had the highest affinity and adsorption capacity towards AMO (Della Puppa et al., 2013; Micháľková et al., 2014; 2016). These findings are in accordance with the strong potential of Mn oxides to bind Pb (Beak et al., 2008; Feng et al., 2007; Villalobos et al., 2005). Comparing the original and surface-modified AMO, a higher adsorption rate was observed in all cases for the original AMO. However, the recorded equilibria times were similar for the two materials. Although the adsorption rates differed between AMO and SM-AMO, both materials reached almost the same equilibrium concentration of adsorbed metals/metalloids in the case of Cd, Pb and As, yielding nearly 100% sorption of Pb and As under given conditions. The only exception was Zn, for which SM-AMO was able to adsorb 10% less than AMO. Decreased SM-AMO adsorption rate/capacity compared to the AMO can be explained by the partial surface passivation with MnCO_3 . Similarly, rhodochrosite formed on the birnessite surface and microbial

activity passivated its surface, inhibiting further As(III) oxidation (Ying et al., 2011). Regarding the amount of released Mn, there were almost no differences between the original and surface-modified AMO at pH 5 (Figs. 5.6a2, b2 and c2), but the amount of dissolved Mn was visibly reduced at pH 7 (Fig. 5.6d2) in the case of SM-AMO, suggesting the possible dissolution of the MnCO_3 layer at lower pH values.

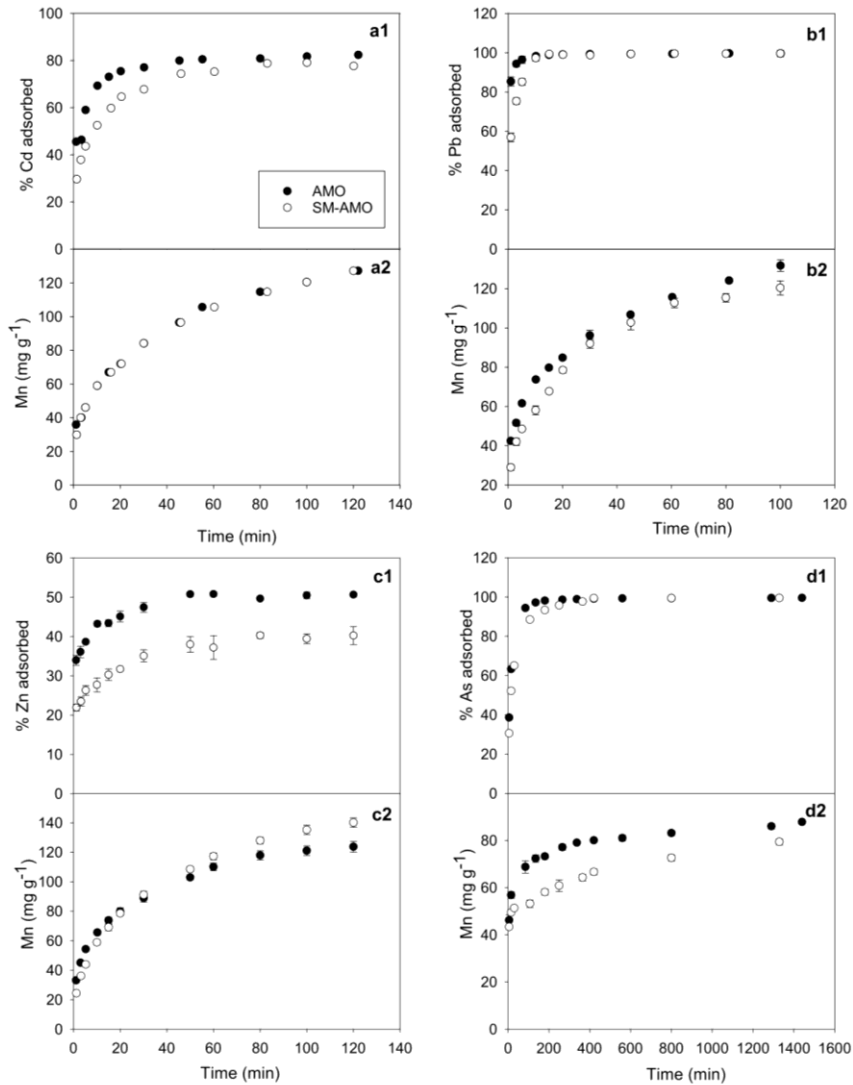


Figure 5.6

Kinetics of Cd (a1), Pb (b1), Zn (c1) and As (d1) adsorption onto the tested materials with corresponding amounts of released Mn (a2, b2, c2 and d2), initial metal(loid)s concentrations of 0.1 mM (n=2). AMO: amorphous manganese oxide, SM-AMO: surface-modified amorphous manganese oxide.

Table 5.4

Pseudo-second-order kinetic parameters obtained for the adsorption of Cd, Pb and Zn and pH 5 and As(V) at pH 7 onto the amorphous Mn oxide (AMO) and the surface-modified amorphous Mn oxide (SM-AMO).

		k_2 (g mmol ⁻¹ min ⁻¹)	q_e (mmol g ⁻¹)	R ²
Cd	AMO	6.972	0.079	1.00
	SM-AMO	2.813	0.078	0.99
Pb	AMO	63.657	0.098	1.00
	SM-AMO	18.063	0.098	1.00
Zn	AMO	11.453	0.051	1.00
	SM-AMO	5.130	0.041	1.00
As	AMO	3.095	0.095	1.00
	SM-AMO	0.820	0.095	1.00

Incubation batch experiments

The aim of the incubation experiments was to compare the stability and potential transformations of AMO and SM-AMO directly in soil conditions and their possible influence on the mobility of soil contaminants. The application of both materials resulted in a significant increase in soil pH compared to the control (**Table 5.5**). As the incubation time increased, the pH naturally decreased in all variants, including control soils, yet the influence of AMO/SM-AMO application was still visible after 10 weeks, with the Fluvisol increasing in pH from 5.1 (Control) to 6 and 5.9. Another situation occurred in the Leptosol, where, apart from an initial rapid increase, the pH of the AMO/SM-AMO-amended variants decreased below the control after 10 weeks. However, the results of the adsorption experiment might suggest a lower efficiency of SM-AMO with regard to the immobilization of metals/metalloids in soils; the effectiveness of both materials was in general very similar, yielding just few differences between the original and surface-modified AMO particles. Both materials (application of 1% w/w) were able to decrease the amount of Cd and Zn in the Fluvisol solution by 64% and 77% of the control (**Figs. 5.7a, c**), whereas the Pb concentrations decreased below the limit of detection (**Fig. 5.7b**) after 10 weeks. The behavior of the target metals may be related to the potential precipitation of carbonates. Although most of the solutions were undersaturated (SI < 0) with respect to metal carbonates, otavite (CdCO₃), smithsonite (ZnCO₃) and cerussite (PbCO₃)

were predicted to be the main solubility-controlling phases, yielding SI close to zero (**Table 5.6**). Moreover, the precipitation of Al/Fe oxyhydroxides might be responsible for further sorption of metals. Rhodochrosite (MnCO_3) was the only Mn-phase predicted to have positive saturation indices in all of the Fluvisol solutions (**Table 5.6**). The amount of As in the Leptosol solution (**Fig. 5.7d**) in amended variants decreased significantly at the beginning of the experiment but subsequently increased gradually with the incubation time towards control values. This progression was probably connected with the drop in pH observed in the AMO/SM-AMO-amended variants (**Table 5.6**) because we have recently shown that the adsorption of As onto AMO generally decreases with decreasing pH (Michálková et al., 2016), which is in contrast to other studies (Dixit and Hering, 2003; Zhang et al., 2016). In addition, the behavior of As is related to important speciation changes as predicted using the PHREEQC-3 code. In particular, different As speciation clearly reflected the decrease in pH (Bowell et al., 2014 and references therein); i.e., the form of HAsO_4^{2-} prevailed at the beginning (>70%), while an increasing trend was observed for H_2AsO_4^- , reaching nearly 100% after 10 weeks for both AMO/SM-AMO (**Table 5.7**). A different charge of the species is probably responsible for their different sorption affinities. Further, negative SI for Al/Fe oxyhydroxides calculated with increased time (**Table 5.6**) indicated the potential dissolution of such phases, which can subsequently enhance the release of As (Davranche et al., 2013).

Table 5.5

The pH of the soil solution from the Fluvisol and the Leptosol. AMO: amorphous manganese oxide (1%, w/w), SM-AMO: surface-modified amorphous manganese oxide (1%, w/w), w: week(s) (n=2).

	Fluvisol				Leptosol			
	1 w	2 w	4 w	10 w	1 w	2 w	4 w	10 w
Control	5.73 ± 0.09	5.68 ± 0.09	5.19 ± 0.07	5.11 ± 0.07	5.97 ± 0.04	5.80 ± 0.11	5.48 ± 0.02	5.31 ± 0.05
AMO	7.31 ± 0.05	6.83 ± 0.04	6.57 ± 0.07	6.00 ± 0.21	7.80 ± 0.07	6.54 ± 0.39	5.81 ± 0.06	5.00 ± 0.09
SM-AMO	7.16 ± 0.06	6.64 ± 0.13	6.49 ± 0.08	5.90 ± 0.12	7.49 ± 0.80	6.83 ± 0.26	5.76 ± 0.02	4.91 ± 0.02

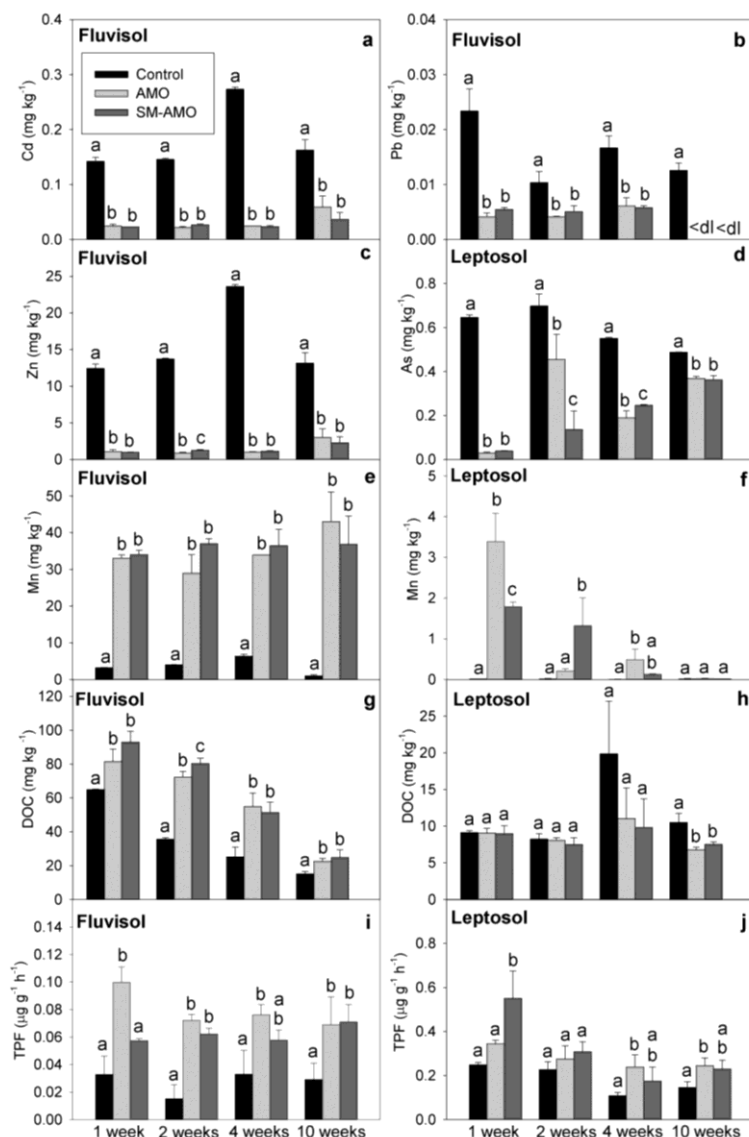


Figure 5.7

Characteristics of the soil solutions obtained from soils homogeneously mixed with the stabilizing amendments: concentrations of Cd (a), Pb (b), Zn (c) and DOC (e) in solutions from the Fluvisol concentration of As (d), DOC (f) in solutions from the Leptosol (n=2) and activity of soil dehydrogenase in Fluvisol (i) and Leptosol (j) (n=3). C: control, AMO: amorphous manganese oxide (1%, w/w), SM-AMO: surface-modified amorphous manganese oxide (1%, w/w), <dl: values below the limit of detection. Statistical evaluation is performed separately for every single time interval, data with the same letter represent statistically identical values (P<0.05).

Table 5.6

Saturation indices of selected solubility-controlling phases calculated by PHREEQC-3 in solutions from mixed soil samples. AMO: amorphous manganese oxide (1%, w/w), SM-AMO: surface-modified amorphous manganese oxide (1%, w/w).

	<i>Cerussite (PbCO₃)</i>		<i>Otavite (CdCO₃)</i>		<i>Smithsonite (ZnCO₃)</i>		<i>Boehmite (AlOOH)</i>		<i>Fe(OH)₃</i>		<i>Rhodochrosite (MnCO₃)</i>	
	AMO	SM-AMO	AMO	SM-AMO	AMO	SM-AMO	AMO	SM-AMO	AMO	SM-AMO	AMO	SM-AMO
<i>Fluvisol</i>												
1 week	-1.47	-1.18	0.31^a	-0.08	-0.13	-0.38	- ^b	0.41	1.35	1.40	2.73	2.47
weeks	-1.51	-1.09	-0.29	-0.51	-0.58	-0.71	-	0.60	1.03	0.90	2.20	2.03
4 weeks	-1.26	-1.31	-0.38	-0.68	-0.71	-0.88	0.66	0.38	0.59	0.52	2.08	1.89
10 weeks	-1.01	-1.40	-0.37	-0.88	-0.69	-1.03	-	-	-0.61	-0.34	1.75	1.44
							<i>Boehmite (AlOOH)</i>		<i>Fe(OH)₃</i>		<i>Rhodochrosite (MnCO₃)</i>	
							AMO	SM-AMO	AMO	SM-AMO	AMO	SM-AMO
<i>Leptosol</i>												
1 week							-	0.12	-	1.85	1.48	0.87
2 weeks							-	-	-	-	-1.55	0.57
4 weeks							-	-1.16	-	-1.73	-0.78	-1.33
10 weeks							-	-	-	-	-2.46	-2.67

^a Oversaturation of the solutions with respect to the solid phases is indicated in bold.

^b -; not calculated

Table 5.7

The effect of AMO/SM-AMO treatment on the distribution of selected species calculated by PHREEQC-3. AMO: amorphous manganese oxide, SM-AMO: surface-modified amorphous manganese oxide.

	Mn^{2+}		$MnHCO_3^+$		$MnCO_3$		Zn^{2+}		$ZnHCO_3^+$		$ZnCO_3$	
<i>Fluvisol - pouches</i>	AMO	SM-AMO	AMO	SM-AMO	AMO	SM-AMO	AMO	SM-AMO	AMO	SM-AMO	AMO	SM-AMO
1 week	63.6%	51.2%	35.2%	46.7%	1.18%	2.16%	54.6%	41.7%	42.9%	53.9%	2.54%	4.42%
2 weeks	73.0%	71.5%	26.5%	28.2%	0.47%	0.25%	65.4%	63.8%	33.6%	35.7%	1.05%	0.57%
4 weeks	66.4%	76.5%	33.2%	23.3%	0.34%	0.18%	58.1%	69.6%	41.2%	30.0%	0.74%	0.42%
10 weeks	66.4%	75.3%	33.5%	24.5%	0.16%	0.13%	58.1%	68.2%	41.6%	31.5%	0.35%	0.31%
<i>Fluvisol - mix</i>	AMO	SM-AMO	AMO	SM-AMO	AMO	SM-AMO	AMO	SM-AMO	AMO	SM-AMO	AMO	SM-AMO
1 week	58.1%	71.4%	23.8%	18.6%	18.1%	9.99%	42.3%	58.1%	24.6%	21.5%	33.1%	20.4%
2 weeks	69.5%	76.0%	24.4%	20.7%	6.17%	3.34%	58.2%	66.9%	28.9%	25.7%	13.0%	7.39%
4 weeks	67.1%	76.3%	28.9%	21.3%	4.00%	2.44%	56.8%	67.8%	34.7%	26.8%	8.51%	5.44%
10 weeks	59.7%	69.6%	38.9%	29.5%	1.45%	0.86%	50.4%	61.3%	46.5%	36.8%	3.07%	1.90%
	Mn^{2+}		$MnHCO_3^+$		$MnCO_3$		$H_2AsO_4^-$		$HAsO_4^{2-}$			
<i>Leptosol - pouches</i>	AMO	SM-AMO	AMO	SM-AMO	AMO	SM-AMO	AMO	SM-AMO	AMO	SM-AMO		
1 week	83.6%	76.1%	15.2%	23.1%	1.20%	0.79%	83.5%	91.9%	16.5%	8.13%		
2 weeks	74.5%	68.8%	25.1%	30.8%	0.38%	0.38%	96.1%	96.7%	3.89%	3.32%		
4 weeks	69.1%	67.2%	30.2%	32.5%	0.71%	0.29%	93.8%	97.6%	6.20%	2.40%		
10 weeks	63.9%	65.1%	35.9%	34.6%	0.23%	0.26%	98.2%	97.9%	1.81%	2.07%		
<i>Leptosol - mix</i>	AMO	SM-AMO	AMO	SM-AMO	AMO	SM-AMO	AMO	SM-AMO	AMO	SM-AMO		
1 week	91.6%	94.8%	2.46%	2.36%	5.96%	2.82%	15.0%	27.0%	85.0%	73.0%		
2 weeks	99.2%	90.8%	0.68%	7.27%	0.09%	1.89%	77.1%	62.3%	22.9%	37.7%		
4 weeks	90.5%	88.9%	9.24%	10.8%	0.23%	0.24%	94.4%	95.0%	5.60%	4.97%		
10 weeks	72.0%	67.0%	27.9%	33.0%	0.10%	0.10%	99.0%	99.2%	1.02%	0.84%		

Furthermore, AMO/SM-AMO particles were analyzed to examine the stability and transformations of both materials. A higher mass loss was recorded consistently for AMO at all time intervals (**Fig. 5.8**), showing an increasing tendency in time. After 10 weeks of incubation in both soils, the mass loss recorded for the SM-AMO was ~40% lower than that of the AMO. Interestingly, this weight loss did not correlate with Mn concentrations found in corresponding soil solutions. While the recorded weight losses were almost identical for the two soils (**Figs. 5.8a1, b1**), the amount of released Mn was 2 orders of magnitude lower in the case of the Leptosol (**Fig. 5.8b2**) compared to Fluvisol (**Fig. 5.8a2**). Additionally, there were no significant differences in Mn concentrations in the soil solution from AMO and SM-AMO-amended variants, which was probably caused by the possible readsorption/precipitation of released free Mn species in soil. Although the total Mn concentrations were similar, PHREEQC-3 calculations showed differences in Mn speciation (**Table 5.7**). Whereas a higher portion of free Mn^{2+} was present in the SM-AMO-amended Fluvisol, the opposite trend was recorded in the case of the Leptosol. Based on XRD and SEM/EDX analyses, we observed equilibration between both materials with time, which was further confirmed by PHREEQC-3 calculations showing no significant differences in rhodochrosite precipitation in the long term between AMO and SM-AMO (**Table 5.7**). According to XRD, an increased intensity of MnCO_3 peaks was recorded after 1 week of incubation of the AMO in both soils, which subsequently remained relatively stable over the experiment. These results were in accordance with those obtained from SEM/EDX analysis (**Fig. 5.9** and **Table 5.8**). Based on percentual atomic surface concentrations (**Table 5.8**), the formation of carbonates is suggested after AMO application even after the 1-week incubation in soil. In the case of SM-AMO, the intensity of MnCO_3 peaks decreased gradually, suggesting the dissolution of the MnCO_3 layer, which was reflected also by the decreasing C content on the SM-AMO surface (**Table 5.8**) and visual reduction of the rhodochrosite cover (**Fig. 5.9**). This decrease was more pronounced in the case of Leptosol probably due to the lower pH.

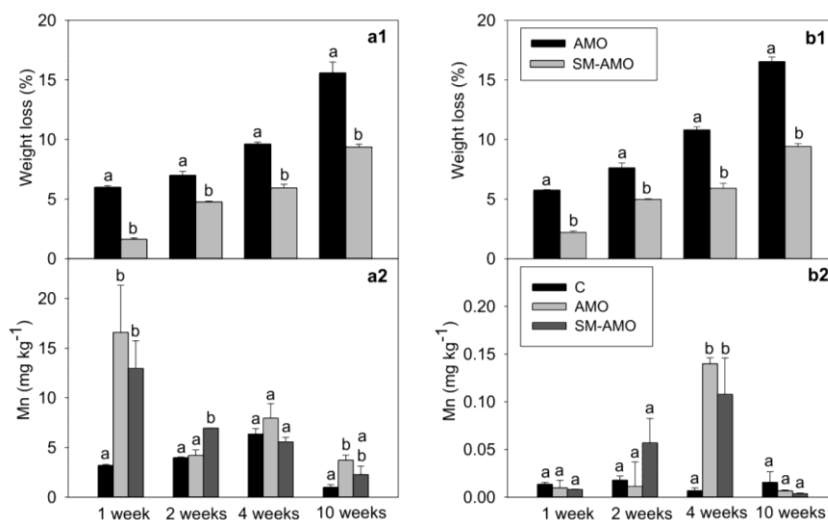


Fig. 5.8

Weight loss of the materials incubated in the Fluvisol (a1) and Leptosol (b1) with corresponding Mn concentrations detected in soil solutions (n=2).

C: control, AMO: amorphous manganese oxide, SM-AMO: surface-modified amorphous manganese oxide. Statistical evaluation is performed separately for every single time interval, data with the same letter represent statistically identical values (P<0.05).

Table 5.8

Atomic concentrations on surfaces determined by EDX for original materials and particles incubated in soil for 1 and 10 weeks.

AMO: amorphous manganese oxide, SM-AMO: surface-modified amorphous manganese oxide, (n=2).

	C (at. %)	O (at. %)	Mn (at. %)	K (at. %)
AMO	6.76 ± 1.93	70.01 ± 2.40	22.87 ± 0.55	0.57 ± 0.12
SM-AMO	31.70 ± 4.76	59.29 ± 3.42	8.91 ± 1.50	0.02 ± 0.00
<i>Fluvisol</i>				
AMO 1 w	15.71 ± 0.20	59.41 ± 0.13	24.53 ± 0.17	0.23 ± 0.10
AMO 10 w	15.84 ± 3.59	63.36 ± 1.49	20.56 ± 2.04	0.13 ± 0.06
SM-AMO 1 w	25.72 ± 7.29	56.26 ± 0.10	17.77 ± 7.07	0.09 ± 0.08
SM-AMO 10 w	25.12 ± 4.74	56.01 ± 1.50	18.62 ± 3.18	0.06 ± 0.03
<i>Leptosol</i>				
AMO 1 w	15.99 ± 1.18	58.25 ± 5.67	25.01 ± 4.16	0.38 ± 0.04
AMO 10 w	12.84 ± 0.40	62.87 ± 0.34	24.01 ± 0.71	0.13 ± 0.03
SM-AMO 1 w	22.46 ± 1.32	54.22 ± 0.89	23.07 ± 1.54	0.13 ± 0.02
SM-AMO 10 w	13.96 ± 0.15	63.58 ± 0.07	22.29 ± 0.23	0.07 ± 0.04

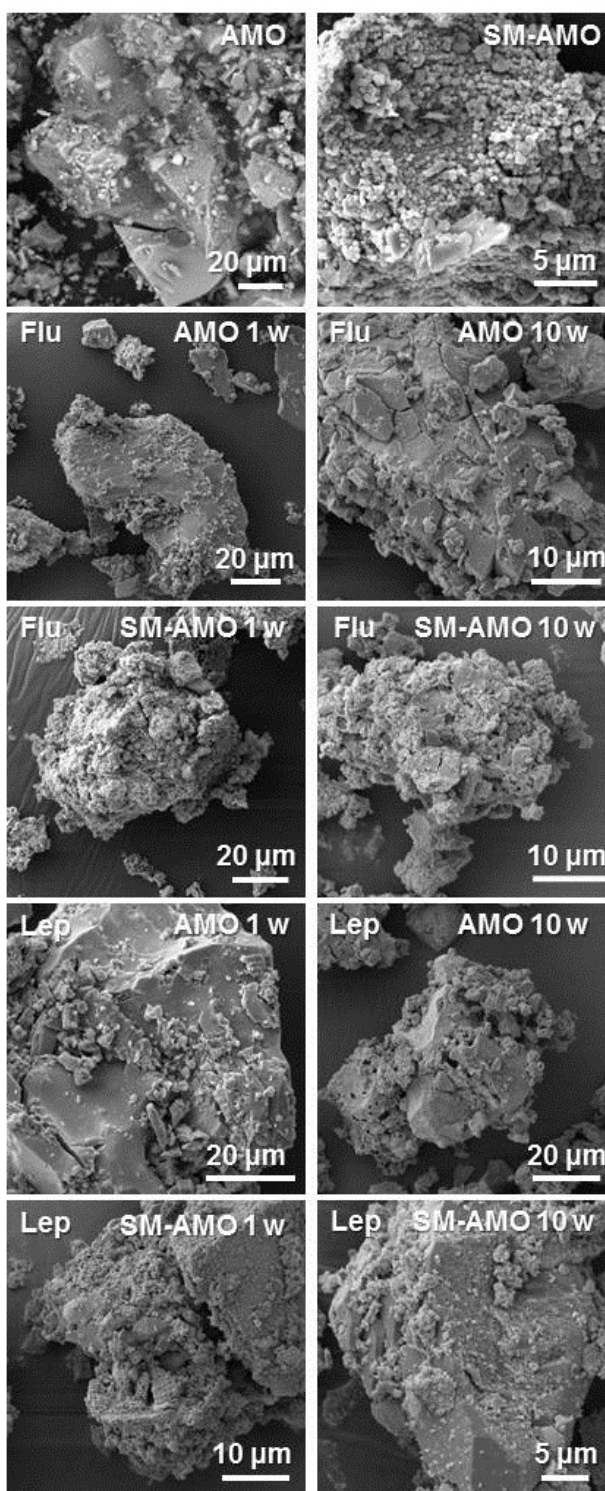


Fig. 5.8

SEM images of the original amorphous manganese oxide (AMO) and its surface-modified variant (SM-AMO) and the same materials incubated in the Fluvisol (Flu) and the Leptosol (Lep) for 1 and 10 weeks.

Microbially induced rhodochrosite formation on birnessite surfaces has been repeatedly demonstrated as a consequence of both bioreduction of Mn(IV) present in the birnessite structure and CO₂ generated by microbial respiration (Fisher et al., 2008; Johnson et al., 2016; Lovley and Phillips, 1988; Ying et al., 2011). In contrast to the mentioned studies operating with simple systems (one mineral phase, one microbial species, one source of organic C), Ettler et al. (2014) observed rhodochrosite formation at the AMO surface after 30 days of incubation and emphasized the extent complexity of the soil system and resulting difficulties connected with the interpretation of complex reactions involving both physico-chemical and biological (i.e., microbial in this case) mediators.

To evaluate the influence of the tested materials on microbial activity in contaminated soils, a widely used and simple soil dehydrogenase assay (**Fig. 5.7i, j**) was chosen due to its non-specific nature, making it possible to involve the performance of the whole microbial community (Carbonell et al., 2000). In this test, the microbial activity is quantified indirectly based on TPF (1,3,5-triphenylformazan) production. In most cases, AMO/SM-AMO addition increased microbial activity, and these changes were more pronounced in the Fluvisol. The reason could be the generally higher toxicity of the Fluvisol because the obtained TPF concentrations were an order of magnitude lower than in the case of the Leptosol (the TPF production is supposed to be directly proportional to microbial activity). Zinc is supposed to be the main toxic species in the Fluvisol because a significant amount is present in the exchangeable fraction (~1800 mg kg⁻¹; **Table 5.3**). Additionally, we recently observed extremely high (i.e., in orders of g kg⁻¹ dry weight) concentrations of Zn in sunflower (*Helianthus annuus* L.) tissues grown on this Fluvisol that were connected with leaves chlorosis and growth inhibition (unpublished results). Thus, the reason for the increased microbial activity after AMO/SM-AMO addition may be the lowered bioavailability of contaminating metals/metalloids together with an increased amount of dissolved organic matter (**Fig. 5.7g**) in soil solution, which can be used as an additional substrate and promote microbial growth (Michálková et al., 2014). Additionally, some microorganisms may mediate the bioreduction of Mn(IV) present in AMO/SM-AMO to Mn(II). Increased microbial activity (and resulting increased microbial respiration) recorded after the AMO/SM-AMO addition might elevate the partial CO₂ pressure in soil, which may enhance rhodochrosite precipitation (Fisher et al., 2008; Johnson et al., 2016; Lovley and Phillips, 1988; Ying et al., 2011). In contrast, dissolution of AMO/SM-AMO may further promote SOM dissolution and microbial growth.

pH-static leaching experiment

The aim of the pH-static leaching experiment was to observe the influence of pH on the stability and stabilizing efficiency of the unmodified and surface-modified materials. The application of both agents proved to increase the pH of the Fluvisol, whereas the Leptosol with a higher natural pH was affected only by the SM-AMO (**Table 5.9**). Concerning the changes in the leachability of the studied metals/metalloids (**Figs. 5.10a, b, c, d, e**), the application of both materials yielded generally very similar results with few exceptions in the natural (non-adjusted) samples; the SM-AMO was more efficient in stabilizing Pb and As in the Fluvisol (**Figs. 5.10b and d**) and As in the Leptosol (**Fig. 5.10e**). In contrast to static batch incubations (**Fig. 5.7**), the concentration of released metals/metalloids was in this case up to two orders of magnitude higher due to the more invasive experimental conditions consisting of 48-hours constant agitating. For that reason, the decrease in contaminant mobility after the addition of AMO/SM-AMO was not as pronounced as in the case of static batches, as observed previously in our previous study (Micháľková et al., 2016). The leachability of Cd and Zn in the Fluvisol (**Figs. 5.10a, c**) decreased similarly with increasing pH and reached the highest values at a lower pH (pH 4 and 5). At these pH values, the effect of the applied amendments was also insignificant, becoming apparent at pH 6 (Zn) and 6.4 (Cd). Lead had the lowest extractability at pH 5 and increased sharply towards neutral/basic pH values (**Fig. 5.10b**). As Pb extractability usually decreases with increasing pH (Steinnes, 2013), this unusual behavior was probably connected with increased dissolution of SOM at higher pH values (**Fig. 5.10h**) associated with the release of organically bound Pb ($\sim 705 \text{ mg kg}^{-1}$ according to sequential extraction; **Table 5.3**). The highest leachability of As from the Leptosol was recorded at pH 7, where SM-AMO was found to be more effective than AMO. Manganese leaching (**Figs. 5.10f, g**) was strongly pH dependent, decreasing with increasing pH, which is the same trend as observed in our previous studies (Ettler et al., 2015; Micháľková et al., 2016). In this case, almost no differences in the release of Mn between AMO and SM-AMO were recorded, similarly to static batches.

Table 5.9

The pH of the natural (non-adjusted) soil samples from the pH-static leaching experiments. *AMO*: amorphous manganese oxide (1%, w/w), *SM-AMO*: surface-modified amorphous manganese oxide (1%, w/w), (n=3).

	Control	AMO	SM-AMO
Fluvisol	6.03 ± 0.01	6.58 ± 0.03	6.40 ± 0.05
Leptosol	6.43 ± 0.06	6.39 ± 0.04	6.65 ± 0.09

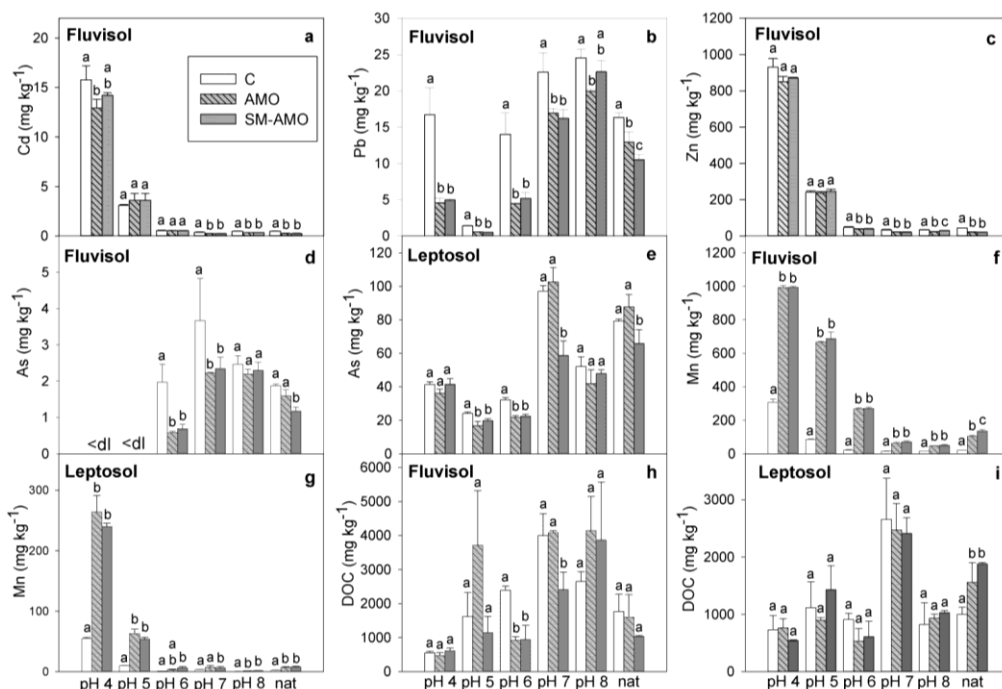


Figure 5.10

The results of pH-static leaching experiment: Cd (a), Pb (b), Zn (c), As (d), Mn (f) and DOC (h) concentrations in the Fluvisol extracts, and As (e), Mn (g) and DOC (i) concentrations in the Leptosol extract (n=3). C: control, AMO: amorphous manganese oxide (1%, w/w), SM-AMO: surface-modified amorphous manganese oxide (1%, w/w), nat – variants with natural (non-adjusted) pH, <dl: values below the limit of detection. Statistical evaluation is performed separately for every single pH value, data with the same letter represent statistically identical values (P<0.05).

Conclusions

To increase its stability, amorphous manganese oxide was synthetically covered with MnCO_3 coatings (SM-AMO) because the newly formed rhodochrosite phase was previously found to form on particles' surfaces in soils, increasing their stability (Ettler et al., 2014). A preliminary experiment was performed to evaluate the long-term stability of both materials in pure water. The SM-AMO particles showed a lower Mn release compared to the original AMO. A study of the adsorption kinetics of As, Cd, Pb and Zn showed lower adsorption rates and adsorption capacity for Zn, probably due to partial surface passivation of the SM-AMO. However, the effects recorded in soil systems were different from those obtained in simple controlled systems (i.e., stability in pure water and adsorption kinetics). When applied to soil, a lower mass loss was recorded in the case of SM-AMO. In addition, neither significant differences in the Mn and DOC release into soil solution nor differences in the stabilizing efficiency towards contaminating metal(loid)s between the original and surface-modified materials were observed. Concerning the potential AMO/SM-AMO alterations in soil conditions, differences in the surface composition (i.e., amount of precipitated rhodochrosite) gradually disappeared with increasing incubation time. While the newly formed rhodochrosite precipitated on the AMO surface, the MnCO_3 coating on the SM-AMO gradually dissolved and reached a new equilibrium between the AMO and rhodochrosite. Both amendments also positively influenced microbial activity, especially in the soil with higher available metal concentrations. It can thus be concluded that despite the lower mass loss, both materials are comparably efficient in the long term and the preliminary modification of the AMO surface is not necessary. However, the amendment should be applied only to alkaline, neutral or slightly acidic soils to prevent its dissolution.

Chapter VI

The application of an amorphous manganese oxide effectively reduces metal(loid) uptake by sunflower (*Helianthus annuus* L.)

Z. Michálková, D. Martínez-Fernández, M. Komárek

Manuscript in preparation.

Content

Abstract	137
Introduction	138
Materials and methods	139
Material synthesis and characterization	139
Soil characteristics	139
Rhizobox experiment	140
Statistical treatment	141
Results and discussion	141
Soil and stabilizing agent properties	141
Availability of metal(loid)s	143
Plant growth and metal uptake	145
Conclusions	151

Abstract

An amorphous manganese oxide (AMO) synthesized in our previous studies showed an important stabilizing potential for metals and As in contaminated soils, but its influence on green plants has not been investigated yet. For this reason, experiments with rhizoboxes were performed in order to evaluate the AMO influence on mobility of metal(loid)s in rhizosphere and bulk soil of sunflower (*Helianthus annuus* L.) plants. Concerning the fractionation of metal(loid)s in soil, the AMO was able to effectively reduce water- and 0.01 M CaCl₂-extractable fractions of Cd, Pb and Zn. The decreased bioavailability of contaminating metal(loid)s resulted in significant increase of microbial activity in AMO-amended soil being ~3.5 fold higher in the rhizosphere and ~9-fold higher in bulk soils compared to the control. Together with metal(loid) extractability, the AMO was also able to significantly reduce the uptake of metals and ameliorate plant growth. The former was important especially in the case of Zn as this metal was taken up in excessive amounts from the control soil causing strong phytotoxicity and even death of young seedlings. On the other hand, AMO application led to significant release of Mn that was readily taken up by plants. Resulting biomass concentrations exceeded Mn toxicity thresholds while plants were showing emergent Mn phytotoxicity symptoms. Therefore, AMO should be applied only to neutral or alkaline soils.

Introduction

Chemical stabilization of metals/metalloids in contaminated soils using various types of amendments is a perspective method of soil remediation. In this technique, different organic and inorganic materials are applied to soil in order to decrease the mobility and also the bioavailability and bioaccessibility of contaminating metals/metalloids. This can be reached by the adsorption, complexation with organic ligands, ion exchange or surface precipitation (Kumpiene et al., 2008). Besides chemical stabilization, living plants (together with associated microorganisms) can take part in contaminants immobilization in soil and may therefore prevent potential additional contamination spreading (Pulford and Watson, 2003). In fact, combination of chemical and phyto-stabilization is often used in projects focused on restoration and revegetation of contaminated sites. In this case, stabilizing amendments are applied prior to phytostabilization in order to decrease the phytotoxicity and bioavailability of contaminants and promote subsequent plant growth (Yang et al., 2016). Potential stabilizing agents thus should be tested first at laboratory level not just with regard to their adsorption properties or potential to immobilize metals/metalloids in “pure” soil, but attention should be paid also to their effects and behavior when applied in combination with living plants.

As previously shown in some stabilization studies (Friesl et al., 2006; Torri and Lavado, 2009), results obtained from simple “soil+amendment” systems do not necessarily correlate with those from systems with plants. Even when plants are used in the experimental design, changes of metal mobility in soil do not always correspond to changes in metal uptake. For example, McBride and Martínez (2000) performed a pot experiment testing the efficiency of various stabilizing amendments on immobilization of metals in a contaminated soil together with the influence on maize (*Zea mays* L.) growth. In this case, ferrihydrite was able to reduce the amount of 0.01 M CaCl₂-extractable Cu in soil by 93%. Yet, no effect of this amendment on reduction of Cu uptake by maize was recorded. The potential phytotoxicity of applied amendments has to be taken into account as well, as the amendment itself may harm the plant growth. Oustriere et al. (2016) tested poultry manure derived biochar alone and in combination with iron grit for stabilization of Cu in contaminated soil. Application of this material resulted in 4- to 10-fold increase of Cu in pore water together with significant reduction of biomass yield of roots and shoots of dwarf bean (*Phaseolus vulgaris* L.).

In our previous studies (Michálková et al., 2014; 2016), the synthesized amorphous manganese oxide (AMO) proved to be a highly effective amendment in decreasing the mobility of Cd, Cu, Pb, Zn and As in contaminated soils. Despite these promising results, all experiments to date were conducted using only soil - the influence of AMO on living plants has not been examined yet. Additionally, Ettler et al. (2014) pointed out the potential phytotoxicity of free Mn^{2+} ions released at increased levels to soil solution after AMO application. The aim of this study was therefore to determine the influence of AMO application on mobility of metals in bulk soil and sunflower (*Helianthus annuus* L.) rhizosphere together with its effects on plant growth and metal uptake.

Materials and methods

Material synthesis and characterization

The amorphous manganese oxide (AMO) was synthesized according to Della Puppa et al. (2013) using the modified sol-gel method for preparation of birnessite (Ching et al., 1997). The pH of the studied oxides was measured in deionized water at 1:10 w/v, pH_{zpc} was determined using the immersion technique (Fiol and Villaescusa, 2009) at 1.25:100 w/v. The specific surface was determined using the Brunauer-Emmett-Teller (BET) method and a Nova e-Series analyzer (Quantachrome Instruments, USA).

Soil characteristics

For the purpose of the study, a model multi-metal contaminated soil was used. The soil (Fluvisol) was collected in the Litavka river alluvium heavily polluted with As, Cd, Pb and Zn as a result of historical activity of a nearby Pb-processing smelter in Příbram (Czech Republic). Soil samples were collected from the superficial layer (0–20 cm), air dried, homogenized and sieved through a 2-mm stainless sieve. Particle size distribution was determined using the hydrometric method (Gee and Or, 2002). Soil pH was measured in suspension using a 1:2.5 (w/v) ratio of soil/deionized water or 1 M KCl (ISO 10390:1994). Total organic carbon content (TOC) was determined using the carbon analyzer TOC-L CPH (Shimadzu, Japan). Cation exchange capacity was analyzed using the 0.1 $BaCl_2$ extraction (Carter and Gregorich, 2008). Total concentrations of elements in soil were determined using the digestion in HNO_3/HF under microwave conditions (SPD-Discover, CEM, USA) and

inductively-coupled plasma optical emission spectrometer (ICP-OES, Agilent 730, Agilent Technologies, USA). Fractionation of metals in soil was determined using the modified BCR extraction by Rauret et al. (1998) and As fractionation was determined according to Wenzel et al. (2001a). The standard reference materials 2710a Montana Soil I (NIST, USA) and CRM 483 (Institute for Reference Materials and Measurements, EU) were used for QA/QC. All chemicals used were of analytical grade.

Rhizobox experiment

Rhizoboxes are special devices designed to enable easy separation of rhizosphere soil from plant roots using a nylon nano-membrane (Wenzel et al., 2001b). Experiments in rhizoboxes were performed in order to evaluate the influence of applied stabilizing amendment (AMO) on the mobility of metals in soil together with its interactions in the sunflower (*Helianthus annuus* L.) rhizosphere. Firstly, soil was mixed with the AMO (1%, w/w) and watered with deionized water for 4 weeks in order to maintain 60-70% of the water holding capacity. After that, soil compartments of the rhizoboxes were filled with the soil and 10 sunflower seeds were planted in each rhizobox. Rhizoboxes were randomly distributed on a bench in a glasshouse (20-25°C, 13 h daylight/11 h darkness, photosynthetically active radiation $225 \mu\text{E m}^{-2} \text{s}^{-1}$, and humidity of 60-80%) and watered with deionized water. After 30 days of growth, the whole plants were harvested and stems and roots were separated. Rhizosphere soil samples were collected as a 0.5 mm thin layer below the membrane impacted by the roots. Samples of bulk soil were collected from the opposite part of the rhizobox and were regarded as not influenced by root exudates. Immediately after the collection, microbial activity in fresh soil samples was determined using the soil dehydrogenase test (Rogers and Li, 1985).

Plant samples were washed with deionized water, dried at 60°C to constant weight and weighed. The amount of 150 mg of each sample was then digested overnight at 150°C using 2 mL H_2O_2 and 8 mL of concentrated HNO_3 . The content of metals/metalloids in digestate was determined using ICP-OES. Soil samples were air-dried and subsequently analyzed. The pH of the samples was determined in the suspension with deionized water (1:2.5, w/v). Soil samples were then extracted with deionized water (1:10, w/v) for 2 hours, centrifuged and filtered through 0.45 μm nylon syringe filter. The Eh value was measured in the filtrate and contents of metals and dissolved organic carbon (DOC) were determined using ICP-OES and TOC/DOC analyzer, respectively.

Statistical treatment

All statistical analyses were performed using SigmaPlot 12.5 (StatSoft Inc., USA). The experimental data were evaluated using analysis of variance (ANOVA) at $P < 0.05$ using the Tukey test.

Results and discussion

Soil and stabilizing agent properties

The amorphous manganese oxide (AMO) originally synthesized by Della Puppa et al. (2013) was used in this rhizobox study as it proved to be highly efficient in decreasing the mobile fraction of metals/metalloids in contaminated soils in our previous studies (Michálková et al., 2014; 2016). According to Della Puppa et al. (2013), the pH and pH_{zpc} of this material is 8.1 and 8.3, respectively, while the BET surface was determined to be $135 \text{ m}^2 \text{ g}^{-1}$ (Michálková et al., 2016). A contaminated Fluvisol was used as a model contaminated soil (**Table 6.1**). This soil is heavily contaminated with Cd, Pb, Zn and As due to occasional floods bringing the contamination from historical Pb-smelter slag heaps in river surroundings. On the basis of sequential extractions (**Table 6.2**), Zn is the most mobile contaminating metal yielding more than 1800 mg kg^{-1} in the exchangeable fraction. Although the total amount of Pb is comparable with that of the Zn, this metal is much less available yielding $\sim 280 \text{ mg kg}^{-1}$ in the exchangeable fraction. The relatively highest mobile metal was Cd as $\sim 62\%$ (i.e., 24 mg kg^{-1}) of the total amount was present in the exchangeable pool. In contrast, As showed quite low mobility being bound predominantly to the reducible fraction (roughly corresponding to amorphous and poorly crystalline oxides of Fe, Al and Mn).

Table 6.1

Basic physico-chemical characteristics of the model contaminated soil. Limit concentrations of metals/metalloids in agricultural soils are set according to the Ministry of the Environment of the Czech Republic (Act No. 13/1994).

Fluvisol		
pH _{H2O}	5.95	
pH _{KCl}	5.14	
CEC (cmol kg ⁻¹)	9.08 ± 0.52	
TOC (%)	2.15	
Particle size distribution (%)		
Clay (%)	7	
Silt (%)	31	
Sand (%)	62	
Texture	sandy loam	
Total metal concentrations (mg kg⁻¹) (n = 3)	Limit concentrations (mg kg⁻¹)	
As	296 ± 6	30
Pb	3539 ± 375	140
Cd	39 ± 1	1
Zn	4002 ± 68	200
Cu	68 ± 3	100
Fe	37,408 ± 195	no limit
Mn	4276 ± 34	no limit

Table 6.2

Fractionation of As, Cd, Pb and Zn in the contaminated soil.

Fractionation of As (sequential extraction by Wenzel et al. 2001a) (mg kg⁻¹) (n=3).					
	FA: non- specifically sorbed	FB: specifically adsorbed	FC: bound to amorphous and poorly crystalline hydrated oxides of Fe, Al and Mn	FD: bound to well- crystallized hydrated oxides of Fe, Al and Mn	FE: residual phase
As	0.16 ± 0.02	20.2 ± 0.1	214 ± 4	45.9 ± 8.4	16

Fractionation of metals in the Fluvisol (sequential extraction by Rauret et al., 2000) (mg kg⁻¹) (n=3)				
	FA: exchangeable	FB: reducible	FC: oxidizable	FD: residual phase
Cd	24.0 ± 0.3	8.0 ± 1.1	1.3 ± 0.2	6
Pb	281 ± 11	2165 ± 176	705 ± 93	388
Zn	1822 ± 50	816 ± 45	298 ± 32	1066
Fe	14.8 ± 1.4	4243 ± 76	3481 ± 373	29 669
Mn	189 ± 5	2214 ± 240	760 ± 83	1113

Availability of metal(loid)s

The aim of the short study was to investigate the effect of AMO on plant growth and metal(loid) uptake together with microbial activity and fractionation of metal(loid)s in a contaminated soil as the potential (phyto)toxic effects are closely related to the bioavailable metal(loid) pool in soil. As mentioned in the previous studies dealing with AMO (Ettler et al., 2014; Michálková et al., 2014; 2016), its application resulted in significant increase of soil pH (**Table 6.3**), from ~6 to ~7 in water extract, yet there were no observed significant differences between rhizosphere and bulk soil. The availability of metal(loid)s in soil was determined using deionized water (DI) and 0.01 M CaCl₂ extractions similarly to other studies (Houba et al., 2000; Pueyo et al., 2004; Sharmasankar and Vance, 1997; Xenidis et al., 2010) (**Table 6.3**). However, it is needed to mention that the interpretation of the extractions results is more difficult when dealing with rhizosphere soil than with soil samples not affected by plants. In

the case of rhizosphere, the potentially extractable metal(loid) pool may be reduced by plant and microbial uptake and differences in metal(loid) extractability between rhizosphere and bulk soil are thus more complicated to explain. Extractability (by DI and CaCl₂ as well) of all contaminating metals (Cd, Pb, Zn) decreased significantly in AMO-amended soils compared to control. The stabilization effectiveness of AMO was previously explained as a combined effect of pH increase favoring the sorption of cationic metals and significant sorption capacities of AMO towards targeted metals (Della Puppa et al., 2013; Michálková et al., 2014). The only contaminant showing no decrease after AMO addition was As in the case of DI extraction as the As contents in CaCl₂ extracts were below the limit of detection. Here, AMO influence on As mobility might be misrepresented by inappropriate experimental technique (i.e., shaking with DI) as in our recent study (Michálková et al., 2016) dealing with the same soil, As contents in directly sampled soil solutions were below the limit of detection just as in the case of the CaCl₂ extraction. On the other hand, AMO application to acidic soils led to significantly increased concentrations of extractable Mn which is an already known drawback of this agent (Ettler et al., 2014; Michálková et al., 2014). For that reason, its possible phytotoxic effects should be investigated in this study.

Microbial activity in soil was evaluated using the soil dehydrogenase (DH) assay (**Fig. 6.1**). This simple test is the most widely used soil enzymatic test enabling to quantify the activity of the whole microbial community (Kumar et al., 2013). Despite some criticism pointing at the dependence of DH activity on actual soil and site conditions (Beyer et al., 1993), it remains a useful tool for comparing various soil managements, remediation techniques etc. for one specific soil under the same conditions. In our case, AMO application resulted in significant increase of DH activity, which was ~3.5-fold higher in the rhizosphere and ~9-fold higher in bulk soils. Concerning differences between rhizosphere and bulk soil, higher activity was recorded in both cases (i.e., control and AMO-amended soil) in rhizosphere soil. This is in accordance with the known ability of root exudation together with root respiration to promote microbial growth and activity by supplying easily available C sources while increasing at the same time the rate of soil organic matter (SOM) decomposition (the so-called rhizosphere priming effect) (Kuzyakov, 2002; Kuzyakov and Cheng, 2001).

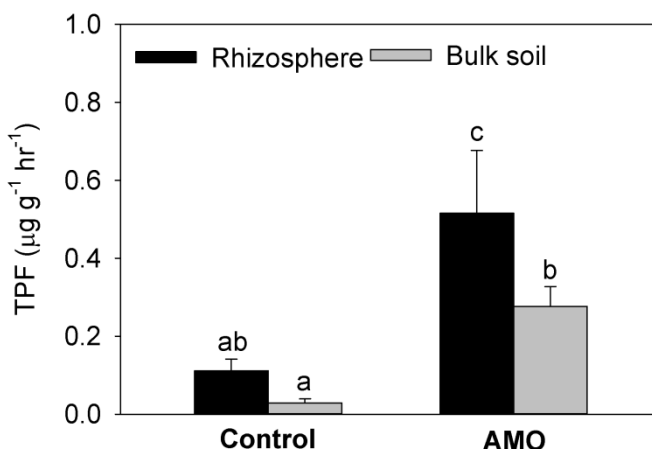


Figure 6.1

Soil dehydrogenase activity in control soil and soil amended with the amorphous manganese oxide (AMO, 1% w/w). Data with the same letter represent statistically identical values ($P < 0.05$) ($n = 4$).

Plant growth and metal uptake

Besides AMO influence on the fractionation of metal(loid)s in soil, its impact on sunflower growth and metal uptake was investigated as well. Firstly, it is needed to mention that the control soil itself proved as highly phytotoxic. After 30 days of growth, plants were harvested as those in control variants virtually started to die. Zinc is supposed to be the main contaminant responsible for the mentioned phytotoxicity. Its high availability in soil was firstly suggested by the results of sequential extraction (**Table 6.2**) where more than 1800 mg Zn kg⁻¹ was present in the most labile exchangeable fraction. Additionally, Zn had the highest extractability from the studied elements (**Table 6.3**). According to Chaney (1993), monocots are generally much more tolerant to increased Zn concentrations than dicots, and in fact, grasses species were the only plants growing on the sampling site. Finally, Zn was found to be present in extremely high concentrations also in sunflower tissues (**Table 6.4**) yielding ~1470 mg g⁻¹ dry weight (DW) in shoots and ~17,700 mg g⁻¹ DW in roots in control soil. Sunflower is generally treated as a relatively metal-tolerant plant species tested repeatedly for phytoextraction purposes (Hattab-Hambli et al., 2016; Lin et al., 2009; Zalewska and Nogalska, 2004). Although Chaney (1993) refers to 300 mg Zn kg⁻¹ DW in leaves as a toxicity threshold for most of dicots, Zalewska and

Nogalska (2004) did not observed toxic effects on sunflower even at concentrations of 515 mg Zn kg⁻¹ DW. At a concentration of 898 mg Zn kg⁻¹ DW, the biomass yield was significantly reduced. Concentrations reached in our experiment far exceeded those reported as phytotoxic. By contrast, AMO application resulted in significant reduction of Zn uptake decreasing the Zn concentrations in shoots and roots down to ~250 and ~2190 mg kg⁻¹ DW, respectively.

Concerning the effects on sunflower growth, biomass yield in AMO-amended variants increased 1.7 and 3.4-times for shoots and roots compared to the control. Root growth and development was significantly inhibited in the control soil (**Fig. 6.2**), most probably as a result of Zn phytotoxicity. Li et al. (2012) investigated Zn-induced phytotoxicity mechanisms involved in root growth inhibition of wheat (*Triticum aestivum* L.). In their study, wheat seeds (and subsequently seedlings) were exposed to solutions containing from 2 (control) to 197 mg Zn L⁻¹. In their case, no significant influence on seed germination was observed, yet all Zn doses (the lowest of 34 mg L⁻¹) significantly reduced root length and development. This inhibition effect was more pronounced in the case of roots than shoots which is in accordance with trend observed in our study (**Table 6.4**). The highest dose of Zn induced the loss of viability of cells in the root tips and caused their increased lignification.

The other soil contaminants (Cd, Pb) were taken up just in limited extent, the contents of As in sunflower tissues were below the limit of detection in all cases. All targeted metallic contaminants were stored preferentially in the roots as compartmentalization of potentially toxic elements in physiologically less active parts in order to protect younger tissues (Rivelli et al., 2012). The extent of root to shoot translocation depended on the particular metal. While the concentrations of Zn and Cd in shoots was an order of magnitude lower than in roots, Pb was bound in roots more strongly showing almost no translocation to shoot. These results are in accordance with general abilities of mentioned metals to be transported within plants (Kabata-Pendias, 2011). As in the case of Zn, AMO proved efficient in decreasing Cd and Pb uptake.

Besides reduced root growth, chlorosis/necrosis developed on young sunflower leaves grown in control soil as a symptom of Zn toxicity (Kabata-Pendias, 2011; Rout and Das, 2003). Although visibly in better condition, leaves of sunflowers cultivated in the AMO-amended soil showed before the end of experiment marks of emergent necrotic brown spots as well. While the sunflowers from the control soil contained excess of Zn, plants grown on AMO-amended soil taken up significant amount of Mn released due to AMO dissolution resulting in concentrations about 4420 and

7320 mg Mn kg⁻¹ DW in shoots and roots, respectively. Toxicity thresholds for Mn differ significantly amongst plant species, yet most plants are affected at concentrations above 500 mg Mn kg⁻¹ DW. In the case of resistant plant species or genotypes, concentrations above 1000 mg Mn kg⁻¹ DW are possible while hyperaccumulators may take up more than 10 000 mg Mn kg⁻¹ DW (Greger, 1999). According to Kabata-Pendias (2011), appropriate Fe:Mn ratio (ideally between 1.5 and 2.5) is necessary for a healthy plant metabolism, while below this range, Mn toxicity (and Fe deficiency) symptoms may occur. The calculated ratio of 0.013 for sunflowers cultivated in AMO-amended soil thus strongly suggests Mn phytotoxicity that probably started to manifest before the end of experiment. As in the case of Mn, excess Zn concentrations also interfere with Fe uptake and translocation and may result in Fe deficiency (Chaney, 1993; Fernando and Lynch; 2015; Rivelli et al., 2012). The other elements impacted by AMO application were Mg and P, whose concentrations in shoots were significantly lower in AMO-amended variants. But, although Mg and P contents were reduced compared to control, their concentrations remained within the range recorded for healthy sunflowers (Gunes and Inal, 2009; Kötschau et al., 2014).

Although AMO application effectively reduced metal uptake and significantly ameliorate sunflower growth compared to the control, toxicity symptoms related with excess of Mn in plant tissues were recorded. Drawbacks concerning potential phytotoxicity of Mn released from AMO in acidic soils (Ettler et al., 2014) were thus confirmed in this case. AMO solubility was found to depend on factors like soil pH, cation exchange capacity (CEC) or SOM content. In our recent studies (Micháľková et al., 2016; Micháľková et al., submitted manuscript – Chapter V), we measured the concentrations of Mn in soil solutions from Fluvisol (the same soil as used in this rhizobox study), Chernozem (alkaline pH, high CEC) and Leptosol (high CEC, low SOM content) amended with AMO (1%, w/w). Here, the recorded concentrations of Mn in Chernozem and Leptosol solution were 1 to 2 orders of magnitude lower than in the Fluvisol. As Mn uptake is fundamentally dependent on its availability in soil, suitable soil conditions (neutral or slightly alkaline pH, lower content of SOM, higher cation exchange capacity) may thus eliminate the risk of increased AMO dissolution and subsequent excessive plant uptake.

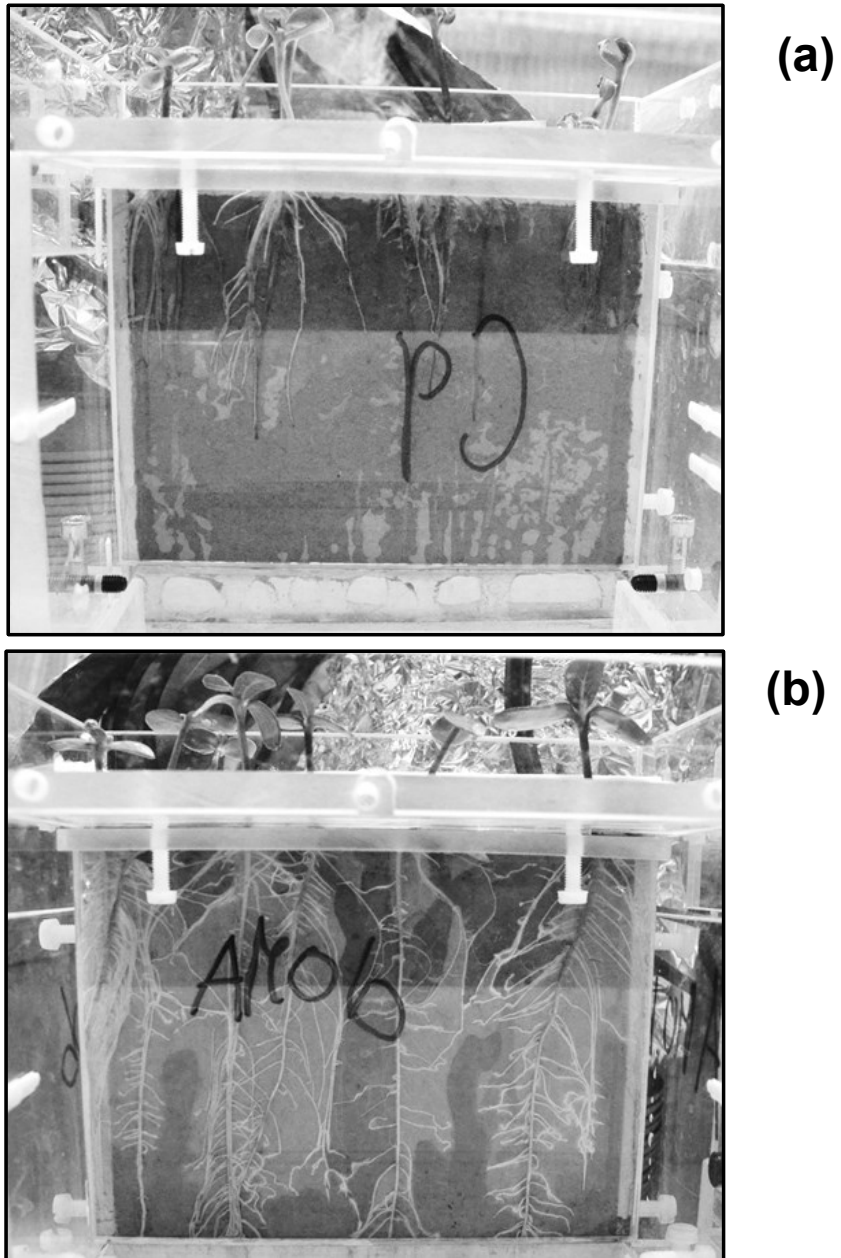


Figure 6.2
Roots of sunflower grown in control (a) and AMO-amended soil (b) after 25 days of growth.

Table 6.3

pH, Eh (mV) and concentrations of elements (mg kg⁻¹) in soil solutions extracted with deionized water and 0.01 M CaCl₂. Data with the same letter represent statistically identical values (P<0.05) (n=4).

	pH	Eh	Mn	Fe	Zn	Pb	As	Cd	Cu	Ni	Mg	Ca	K	Na	Ti	Al
<i>Extraction with deionized water</i>																
C_{rh}	5.99a (0.10)	481a (14)	13.2a (11.2)	19.5a (15.1)	51.2a (14.7)	1.6a (0.6)	0.18a (0.15)	0.62a (0.21)	0.74a (0.22)	0.12a (0.02)	12.7a (3.3)	128a (67)	101 (49)	6.3a (1.9)	0.44a (0.34)	23a (20)
AMO_{rh}	7.23b (0.16)	475a (7)	37.4b (6.5)	3.4a (1.0)	3.8b (1.2)	0.3b (0.1)	0.11a (0.01)	0.08b (0.02)	0.39b (0.04)	0.03b (0.01)	5.8b (0.7)	31b (2)	81 (40)	3.3b (0.4)	0.07a (0.02)	2.5a (0.7)
C_{bu}	5.83a (0.14)	515b (9)	8.1a (4.5)	53.5b (6.9)	30.2c (2.7)	4.2c (0.5)	0.55b (0.10)	0.32c (0.03)	0.59ab (0.04)	0.10ac (0.00)	9.4ab (0.7)	48b (22)	40 (4)	3.6b (0.8)	1.09b (0.11)	61b (9)
AMO_{bu}	7.09b (0.24)	506b (7)	43.2b (8.9)	52.0b (5.9)	12.0d (1.5)	3.5c (0.5)	0.56b (0.05)	0.14bc (0.01)	0.57ab (0.02)	0.09a (0.02)	9.2ab (0.5)	38b (7)	73 (15)	3.1b (0.5)	1.20b (0.11)	61b (6)
ANOVA	***	***	***	***	***	***	***	***	**	***	***	**	ns	**	***	***
<i>Extraction with 0.01 M CaCl₂</i>																
C_{rh}	n.a.	n.a.	40a (9)	0.47a (0.05)	480a (23)	1.6a (0.2)	bdl	10.4a (0.2)	0.27a (0.01)	0.51a (0.03)	74a (2)	n.a.	110a (10)	17.6a (10.2)	bdl	0.90a (0.06)
AMO_{rh}	n.a.	n.a.	585b (42)	0.22b (0.05)	48b (26)	0.1b (0.0)	bdl	2.2b (0.7)	0.13bc (0.03)	0.10b (0.02)	65b (4)	n.a.	158b (20)	7.3ab (1.0)	bdl	0.30bc (0.07)
C_{bu}	n.a.	n.a.	53a (31)	0.19b (0.08)	363c (17)	1.5a (0.0)	bdl	9.1c (0.2)	0.17b (0.02)	0.45c (0.02)	62b (1)	n.a.	95a (6)	7.4ab (1.0)	bdl	0.39c (0.11)
AMO_{bu}	n.a.	n.a.	612b (95)	0.13b (0.06)	61b (29)	0.1b (0.0)	bdl	2.6b (0.6)	0.11c (0.01)	0.10b (0.03)	58b (5)	n.a.	169b (33)	6.2b (0.3)	bdl	0.22b (0.07)
ANOVA	-	-	***	***	***	***	-	***	***	***	***	-	***	*	-	***

C_{rh}: Rhizosphere control soil, AMO_{rh}: AMO-amended rhizosphere soil, C_{bu}: Control bulk soil, AMO_{bu}: AMO-amended bulk soil

n.a.: not analyzed, bdl: below limit of detection, ns: not significant, * P<0.05, ** P<0.01, ***P<0.001

Table 6.4

Biomass production (g/10 plants) and content of elements (mg/g DW) in shoots and roots of sunflower (*Helianthus annuus* L.) grown in control soil and soil amended with amorphous manganese oxide (AMO, 1% w/w). Data with the same letter represent statistically identical values ($P < 0.05$) ($n=4$).

	FW	DW	Mn	Fe	Zn	Pb	Cd	Cu	P	Mg	Ca	K	Na	Se	Al
<i>Shoot</i>															
Control	0.55a	0.18a	0.20a (0.03)	0.083 (0.031)	1.47a (0.46)	0.003 (0.001)	0.014 (0.004)	0.022 (0.004)	8.50a (1.04)	6.36a (0.61)	6.92 (1.52)	9.11 (1.38)	0.45a (0.06)	0.004a (0.000)	0.011 (0.006)
AMO	2.27b	0.30b	4.42b (3.58)	0.055 (0.013)	0.25b (0.17)	bdl	0.009 (0.003)	0.020 (0.04)	2.62b (1.35)	2.87b (1.50)	4.26 (3.19)	22.9 (17.6)	0.23b (0.02)	0.006b (0.002)	0.009 (0.002)
ANOVA	**	**	*	ns	**	-	ns	ns	***	**	ns	ns	***	**	ns
<i>Root</i>															
Control	0.16a	0.026a	0.70a (0.41)	0.859 (0.510)	17.4a (7.74)	0.35 (0.19)	0.196a (0.109)	0.070 (0.023)	5.76 (2.36)	3.19 (1.24)	11.96 (8.03)	16.3a (26.9)	0.83a (0.46)	0.013 (0.014)	0.77 (0.54)
AMO	1.15b	0.088b	7.32b (1.58)	0.168 (0.124)	2.19b (0.36)	0.14 (0.08)	0.034b (0.019)	0.039 (0.019)	4.15 (0.68)	2.58 (0.53)	5.23 (0.65)	37.7b (10.2)	1.73a (0.67)	0.006 (0.003)	0.12 (0.05)
ANOVA	**	**	***	ns	***	ns	***	ns	ns	ns	ns	**	*	ns	ns

bdl: below limit of detection, *ns*: not significant, * $P < 0.05$, ** $P < 0.01$, *** $P < 0.001$

Conclusions

Most studies evaluating the potential of new stabilizing amendments focus predominantly on their direct influence on contaminants mobility. However, their use for the remediation of contaminated sites and subsequent revegetation is also affected by the local plants and soil microorganisms and needs to be investigated. For this reason, the effect of AMO application on sunflower (*Helianthus annuus* L.) growth and metal(loid) uptake was investigated. Based on the performed soil extractions, microbial activity assay and rhizobox experiment with, the AMO appears to be an effective stabilizing agent being able to significantly decrease bioavailability of the studied contaminants and promote plant growth. Nevertheless, the known drawback of this agent, reductive dissolution of AMO in acidic soil connected with release of Mn, resulted in excessive Mn concentrations in sunflower plants that were manifested by symptoms of Mn phytotoxicity. As Mn uptake is fundamentally dependent on its bioavailable fraction, AMO application is recommended for soils where lower solubility of this phase is expected (higher pH, higher cation exchange capacity). These results stress the importance of studies performed in the soil-plant continuum in order to provide information needed for field application.

Chapter VII

Biochar coated by amorphous manganese oxide efficiently removes various metal(loid)s from aqueous solution

L. Trakal, Z. Michálková, A. Piqueras Barceló, M. Vítková, P. Ouředníček, S. Číhalová, M. Komárek

Manuscript in preparation, with permission of the corresponding author (L. Trakal).

Content

Abstract	155
Introduction	156
Materials and methods	157
Sorbents preparation	157
Sorbents characterization	158
Sorption experiments	159
Results and discussion	159
Properties of newly synthesized AMO-biochar composites	159
Chemical characterization of all tested sorbents	166
Removal of various metal(loid)s from aqueous solution	167
Conclusions	173

Abstract

A newly synthesized AMOchar and biochar stirred with pure AMO under given pH value (BC+AMO) were tested to remove various metal(loid)s from aqueous solution. The AMOchar was formed mainly by Mn-oxalates which had coated surface of the pristine biochar. In contrast, the formation of rhodochrosite (MnCO_3) was determined in the AMO+BC complex. In comparison with the pristine biochar (BC) both AMO-biochar composites were able to remove significantly higher amounts of various metal(loid)s from the solution. Despite the rather high pH of the AMOchar, such modified biochar was able to sorb efficiently not only Pb(II), almost 99%, and Cd(II), 51.2%, but also a very high amount of As(V), 91.4%. Additionally, both AMO-biochar composites were able to reduce Mn leaching. This can avoid potential post-contamination caused by the dissolution of less stable Mn-oxalates as observed in the pure AMO.

Introduction

As reviewed by Mohan et al. (2014), the biochar removal efficiency usually results in a few milligrams of remediated metal(loid) per gram of activated carbon. Because of that and due to its porous structure (represented by large active surface), biochar has recently also been modified using various secondary oxides in order to improve its sorption efficiency.

Often, biochar has been modified using Fe-oxides (e.g. magnetite). Trakal et al. (2016) showed that metal sorption of the biochars with well-developed structure was significantly improved after the modification, however, the biochars represented by lower BET surface ($< 100 \text{ m}^2 \text{ g}^{-1}$) showed negligible and/or negative effect. The same effect has also been confirmed by Mohan et al. (2015); Han et al. (2015); and Yan et al. (2015).

Next, biochar could also be modified by Mn-oxides having usually very high immobilization potential for metal(loid)s as reviewed by Komárek et al. (2013). Specifically, the Mn-oxides can be used not only for the more common divalent metals (e.g. Pb(II), Cd(II), Cu(II), etc.) through the adsorption process onto amphoteric surface groups of the Mn-oxides (Komárek et al., 2013), but also for As(V) and/or Cr(VI) due to the initial oxidation/reduction process and consequent sorption, surface complexation and/or co-precipitation with birnessite and hydrous manganese oxide (Lenoble et al., 2004; Komárek et al., 2013). Despite the high potential of various metal(loid)s to improve the biochar removal rate for metal(loid)s such as As(V) (Wang et al., 2015a; 2015d), Cd(II) (Wang et al., 2015b) and Pb(II) (Wang et al., 2015b; 2015c), only a few studies have been published. With respect to these papers, amorphous manganese oxide (AMO) was utilized in this study for the biochar modification, because of its very high efficiency to immobilize various metal(loid)s as shown in the recent studies of Della Puppa et al. (2013), Michálková et al. (2014; 2016) and Ettler et al. (2015). Furthermore, stability of the pure AMO was found to be rather low (represented by intensive Mn leaching) and strongly pH-dependent (Della Puppa et al., 2013; Ettler et al., 2014; 2015). Therefore, the AMO stability needs to be improved.

In this study, concerning the improvement of the AMO stability together with the biochar sorption enhancement, pristine biochar was modified by the AMO using two different approaches. The specific objectives of this research were to: (i)

synthesize a new AMO-biochar composites; (ii) characterize resulting biosorbents; (iii) compare the As(V), Cd(II), and Pb(II) depletion from aqueous solution using AMO, pristine biochar and both biochar-AMO composites under given pH value; and (iv) monitor the stability of newly synthesized biosorbents.

Materials and methods

Sorbents preparation

The same grape stalks biochar as selected previously by Trakal et al. (2014) for its highest metal sorption was utilized as a pristine biochar (BC). Next, two AMO-modified biochars were prepared in two different ways at three AMO/BC ratios (**Table 7.1**): 1/2, 1/1, 2/1 (w/w). In the first approach, biochar was added directly into the reaction mixture for the synthesis of AMO (AMOchar). Specifically, biochar was mixed with 0.4 M KMnO_4 solution and subsequently 1.4 M glucose solution was added (Della Puppa et al., 2013). The resulting gel was then washed several times with deionized water, dried at laboratory temperature and milled in agar mortar. In the second approach, the already prepared AMO and biochar were mixed together at three AMO/BC ratios (**Table 7.1**): 1/2, 1/1, 2/1 (w/w) and agitated together in deionized water (20/1; L/S) for 24 hours at pH 9.00 (mean pH value between pH_{zpc} of pristine BC and pure AMO, respectively; AMO+BC composite). The desired pH value was maintained using 0.1 M KOH. The pure amorphous Mn-oxide (AMO) was also prepared according to Della Puppa et al. (2013). Additionally, biochar-birnessite complex (synthesized according to Wang et al., 2015a) was prepared in order to compare its removal efficiency with that of both AMO-biochar modifications.

Table 7.1

Overview of used sorbents.

Symbol	Component (%)		Comment/Reference
	Biochar	Mn-oxide	
AMO	100	0	Synthesis according to Della Puppa et al. (2013)
BC	0	100	Pyrolysis of grape stalks Trakal et al. (2014)
AMO+BC 1:2	67	33	Agitation under pH = 9.00 (mean pH value between pH_{ZPC} of the BC and AMO, respectively)
AMO+BC 1:1	50	50	
AMO+BC 2:1	33	67	
AMOchar 1:2	67	33	Application of the BC during the actual synthesis of the AMO
AMOchar 1:1	50	50	
AMOchar 2:1	33	67	
BCB	Biochar modification by birnessite according to Wang et al. (2015a)		

AMO: amorphous manganese oxide, BC: pristine biochar

Sorbents characterization

Firstly, all newly synthesized biochars were analysed for the following characteristics: (i) pH value using an inoLab® pH meter (pH 7310, WTW, Germany); (ii) pH of the point of zero charge (pH_{ZPC}) determined using the immersion technique (IT) described in the study of Fiol and Villaescusa (2009); and (iii) cation exchange capacity (CEC) determined using the 0.1 M BaCl₂ (1:50 w/V) protocol (Trakal et al., 2012). These data were then compared with those of the pristine biochar and the AMO, presented elsewhere in papers of Della Puppa et al. (2013) and Trakal et al. (2014), respectively. Next, presence of Mn-oxides has also been verified using X-ray diffraction analyses (XRD; PANalytical X'Pert Pro diffractometer with X'Celerator detector). The exact Mn-oxides-biochar structure binding energies were then studied through X-ray photoelectron spectroscopy (XPS; Omicron Nanotechnology, Ltd.) and the Casa XPS program (for spectra evaluation). The SEM images of Mn-oxides-biochar composites were provided using high-resolution scanning electron microscope JEOL JSM-7401F Fesem (USA) and the SEM TESCAN VEGA3XMU (TESCAN Ltd., Czech Republic) equipped with a Bruker QUANTAX200 energy dispersive X-ray spectrometer (EDS).

Sorption experiments

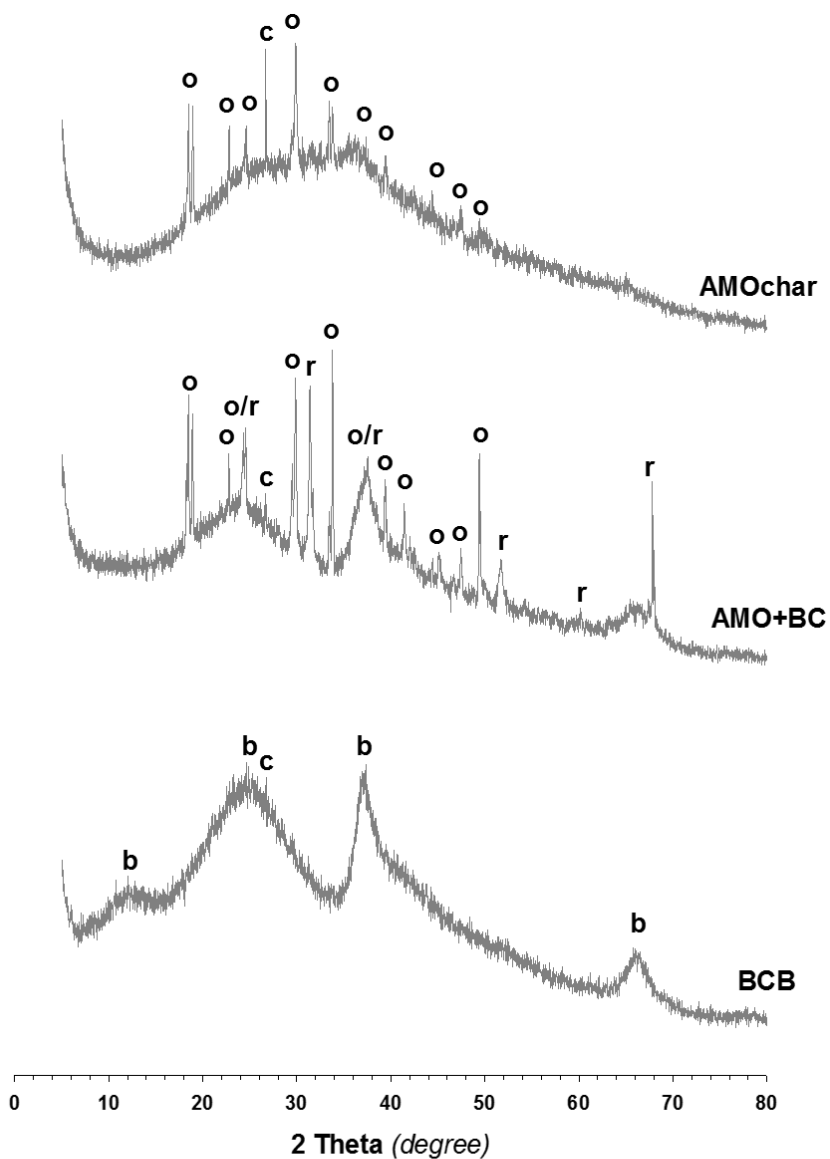
For the aim of this study the sorption kinetics of As(V), Cd(II) and Pb(II) in respect of all sorbents, a set of batch sorption experiments was performed. All studied materials were agitated in 1 mM solution of As(V), Cd(II) and Pb(II) (supplied as $\text{Na}_2\text{HAsO}_4 \cdot 7\text{H}_2\text{O}$, $\text{Cd}(\text{NO}_3)_2 \cdot 4\text{H}_2\text{O}$ and $\text{Pb}(\text{NO}_3)_2$, respectively; analytical grade; Lach-Ner, Czech Republic) in the ratio of 500/1 (L/S). The 0.01 M NaNO_3 was used as a background electrolyte. The pH was continuously adjusted to the value of 5.00 (Cd(II) and Pb(II)) or the value of 7.00 (As(V)) to avoid precipitation of the studied metal(loid)s. The suspension was collected at given time intervals (3 – 450 minutes) and filtered immediately through 0.45- μm nylon filter (VWR, Germany). The content of the studied metal(loid)s (including also Mn and K) in solution was then determined using inductively coupled plasma optical emission spectrometry (ICP-OES, Agilent 730, Agilent Technologies, USA). Additionally, concentration of dissolved organic carbon (DOC) in solution was determined using the carbon analyser TOC-L CPH (Shimadzu, Japan).

Results and discussion

Properties of newly synthesized AMO-biochar composites

Firstly, the presence of birnessite in the structure of the biochar was verified. The X-ray diffraction (XRD) patterns (**Fig. 7.1**) as well as the SEM-EDS (**Fig. 7.3**) of biochar-birnessite (BCB) confirmed the same composition as in the study of Wang et al. (2015a). Partly crystalline K-exchanged birnessite ($\text{K}_{0.5}\text{Mn}_2\text{O}_{4.3}(\text{H}_2\text{O})_{0.5}$; PDF-2 card 01-087-1497) was detected in the BCB composite. Additionally, the XPS wide scan (Figure A2) showed that the amount of Mn2p on the BCB surface was 14.0% (atomic), which was a higher quantity than in the study of Wang et al. (2015a); (9.40%). More specifically, deconvolution of Mn2p band of BCB showed three bands binding energies (641.47, 643.03, and 645.11 eV), which corresponds to the presence of Mn_xO_y or birnessite (Mn(III), Mn(IV)), and residual KMnO_4 (Mn(VII)).

Next, two newly synthesized AMO-biochar composites were analysed. The XRD pattern (**Fig. 7.1**) of the AMOchar confirmed its amorphous character (obvious from the wide shape of the pattern), where all peaks were represented by Mn-oxalate hydrate ($\text{C}_2\text{MnO}_4 \cdot \text{H}_2\text{O}$; PDF-2 card 00-025-0544; as the best reflection of the AMO



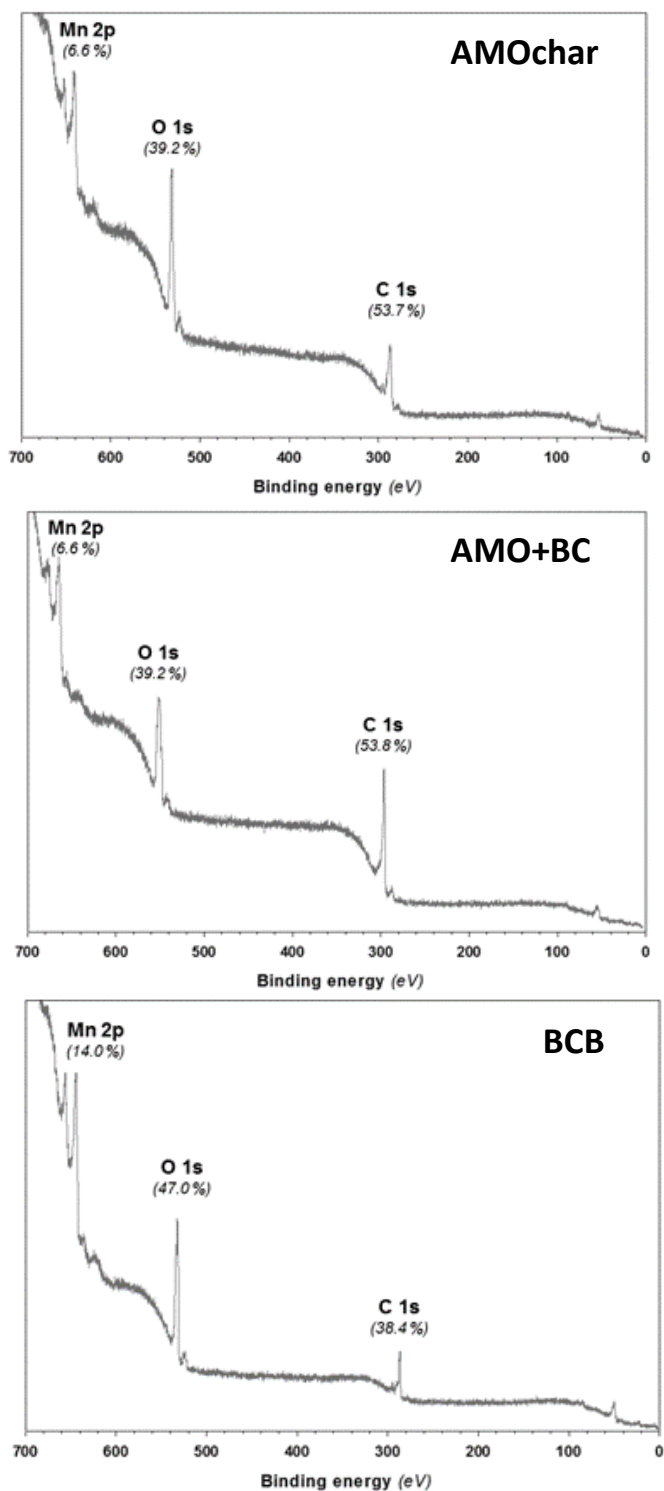
o – Mn-oxalate hydrate ($C_2MnO_4 \cdot 2H_2O$); PDF-2 card: 00-025-0544
 r – rhodochrosite ($MnCO_3$); PDF-2 card: 01-086-0172
 b – birnessite K-exchanged ($K_{0.5}Mn_2O_{4.3}(H_2O)_{0.5}$); PDF-2 card: 01-087-1497
 c – carbon; PDF-2 card: 00-026-1080

Figure 7.1

Comparison of X-ray diffraction (XRD) patterns of the AMOchar, AMO+BC, and BCB composites before sorption.

according to Ettler et al., 2014) and by carbon (PDF-2 card 00-026-1080), shows the presence of the biochar. Second, apart from the presence of Mn-oxalate hydrate and carbon, the presence of rhodochrosite (MnCO_3 ; PDF-2 card 01-086-0172) was also confirmed by the XRD investigation of the BC+AMO composite. The formation of the rhodochrosite was previously explained by Ettler et al. (2014) as a reaction of the removed Mn from oxalates of the AMO with atmospheric CO_2 . Additionally, such leached Mn could react with the biochar, which contains CO_3^{2-} groups (presented by Trakal et al., 2014). The alkaline pH conditions during the actual synthesis/reaction (pH = 9.00) can also increase the rhodochrosite precipitation. Furthermore, the XPS spectra of both AMO-biochar composites (**Fig. 7.2**) show the presence of Mn2p in the amount of 6.60% (atomic). The deconvolution of Mn2p band of both modified biochars shows three bands of binding energies (between 641.47 – 646.30 eV). This corresponds to the presence of Mn_xO_y /Mn-oxalate (Mn(III), Mn(IV)), MnCO_3 (Mn(II)) and residual KMnO_4 (Mn(VII)). Additionally, a detailed scan of C1s (**Fig. 7.2b**) shows three peaks corresponding to: (i) π -bond on graphite C (284.55 ± 0.32 eV); (ii) C–O bond represented mainly by CO_3^{2-} (286.06 ± 0.05 eV); and (iii) O=C–O bond represents carboxylic group (288.60 ± 0.10 eV). This is in agreement with the study of Wang et al. (2015b). Each Mn-biochar composite has its individual proportion of the three peaks, where AMO+BC has the highest peak of graphite C whereas the highest peak of C–O bond has the AMOchar. This fact, therefore, reflects different synthesis of both composites, where BC+AMO shows a similar C1s band as the pristine biochar (Trakal et al., 2014). Moreover, such difference between both AMO-biochar composites was more obvious from the deconvolution of O1s, where the peak ($531.08/529.75$ eV) represents O(II) in oxides (eventually in carbonates) for AMOchar and AMO+BC composite, respectively. The peaks at (532.65 and 534.03 eV) represent oxygen bound in carboxylic group and the peaks at (533.99 and 534.03 eV) then reflect absorbed H_2O .

Concerning the structure and surface morphology of a new AMOchar, the SEM images were obtained and coupled with EDS analysis in order to determine the Mn-oxides loading onto the surface of the biochar. **Figure 7.3** shows Mn-oxalates coatings on the surface of the pristine biochar originated during the actual synthesis. On the other hand, the AMO+BC composite shows individual particles of the AMO and biochar (**Fig. 7.3**), where the surface of biochar is partly occupied by clusters of the Mn-oxalate and/or rhodochrosite (**Fig. 7.3**). The presence of the rhodochrosite (confirmed by the XRD pattern) was detectable only by the high-resolution SEM, which could be due to its very small crystal size (≈ 100 nm) caused by the short time of stirring during the preparation.



(a)

Figure 7.2a
XPS analyses of newly synthesized Mn oxide-biochar composites, (a) wide scan of the AMOchar, AMO+BC, and BCB.

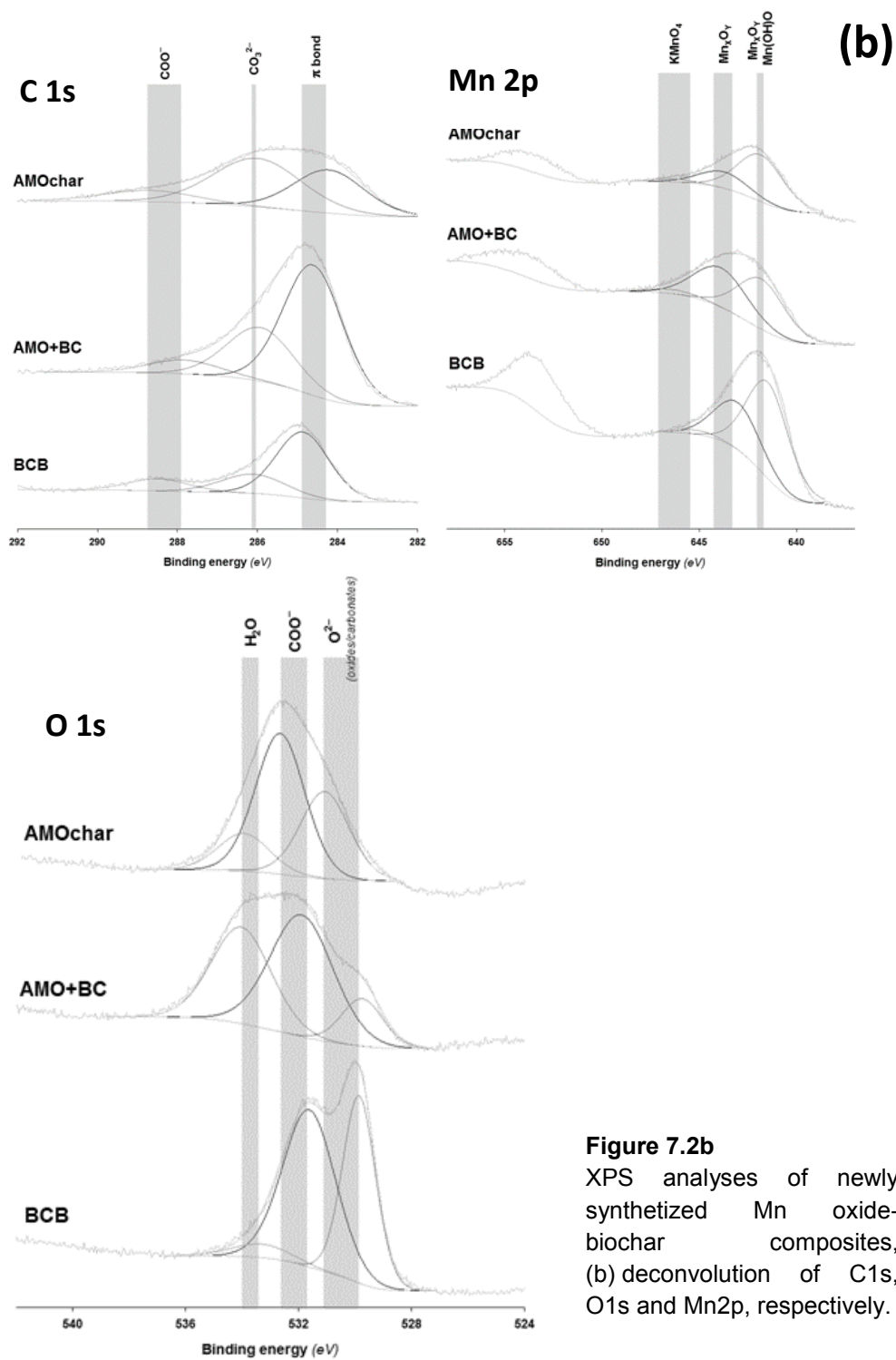
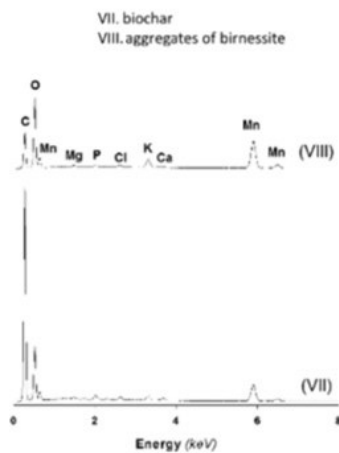
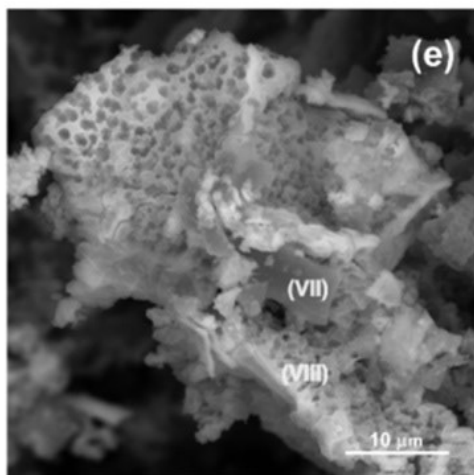
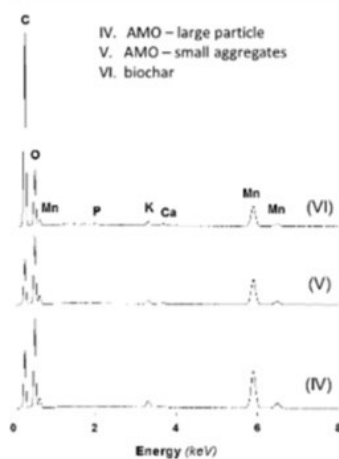
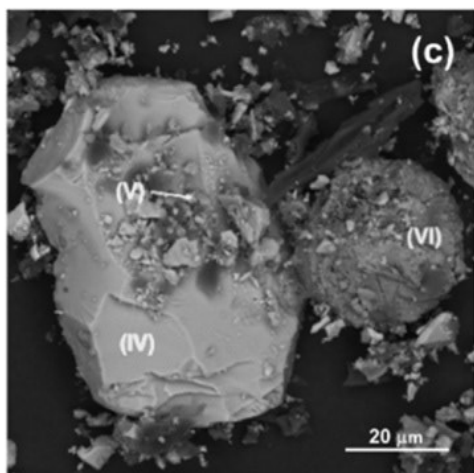
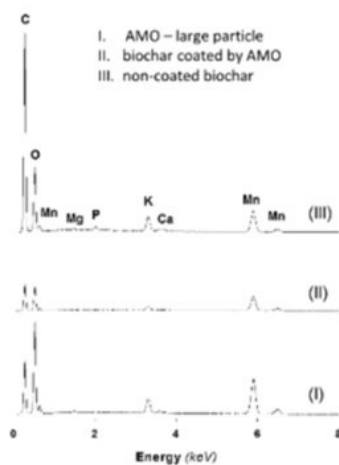
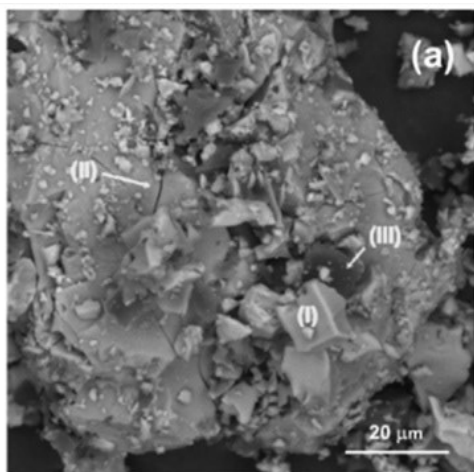


Figure 7.2b
XPS analyses of newly synthesized Mn oxide-biochar composites, (b) deconvolution of C1s, O1s and Mn2p, respectively.



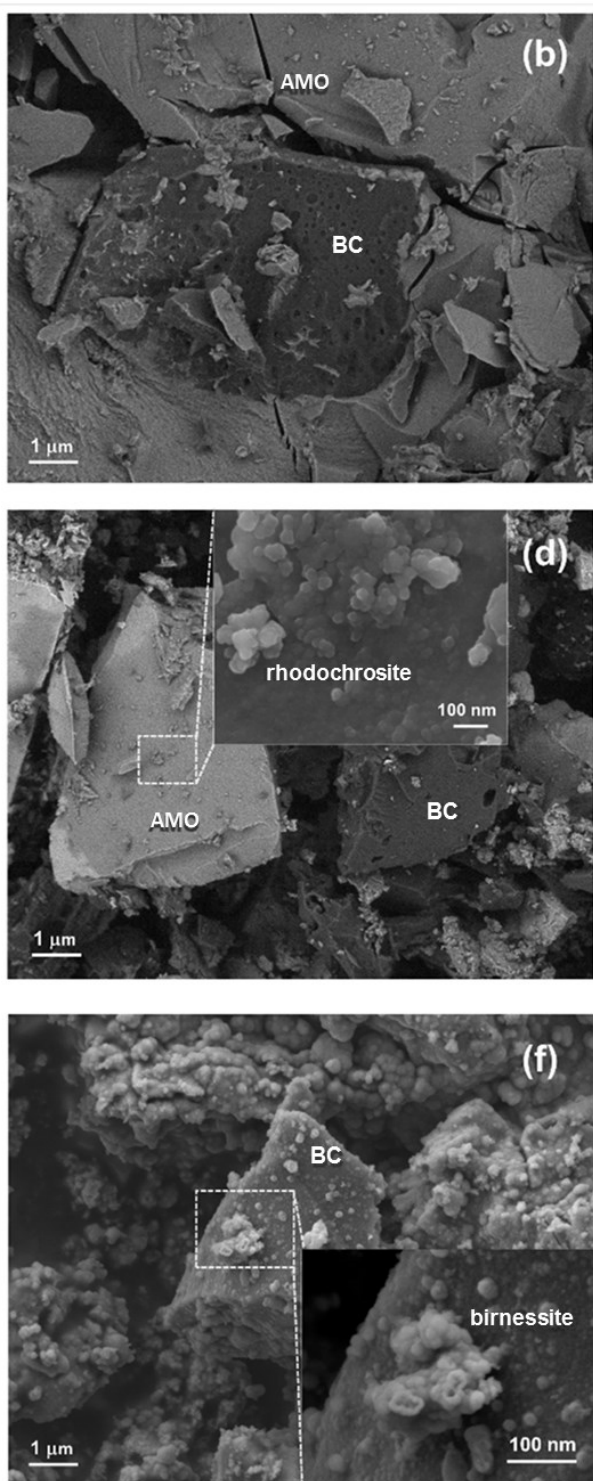


Figure 7.3

The SEM-EDS images in back-scattered electrons (BSE) (a, c, e) with corresponding EDS spectra and the high-resolution SEM (b, d, f), respectively, of the AMOchar (a, b), AMO+BC composite (c, d) and biochar-birnessite (BCB) complex (e, f).

Chemical characterization of all tested sorbents

Table 7.2 presents selected chemical characteristics of all sorbents. The pH value of all sorbents (except birnessite and biochar-birnessite complex) was alkaline. When the biochar was modified directly by the AMO during its synthesis (AMOchar), the resulting pH of all three ratios was significantly reduced to an equal pH value (approx. 8.4) in comparison to the pristine biochar (10.0). In the case of AMO+BC composite, the resulting pH values vary between 9.02 (for AMO+BC 2:1) and 9.52 (for AMO+BC 1:2). This low reduction in pH (compared to AMOchar) was caused by maintaining the pH value around 9.00 during the reaction. Concerning the biochar modification by birnessite, the resulting BCB composite has dropped to a neutral pH (6.98), which reflects the acidic conditions during the actual synthesis. Next, as discussed in the paper of Della Puppa et al. (2013), the pure AMO shows a theoretically positively charged surface as the pH of aqueous solution was 5.00/7.00 and the pH of the point of zero charge (pH_{ZPC}) was 8.30. Moreover, all prepared AMO-biochar composites also showed a theoretically positively charged surface, whereas the surface of BCB was theoretically negatively charged during the As(V) sorption. The cation exchange capacity (CEC) of the pristine biochar (BC) was $40.2 \text{ cmol kg}^{-1}$ (Trakal et al., 2014), which was similar to that of the pure AMO ($34.0 \text{ cmol kg}^{-1}$; Della Puppa et al., 2013) but the CEC of pure birnessite was more than 6-times higher compared to the BC. The CEC value of the biochar-birnessite composite was equal to that of the pristine biochar. Concerning the AMO+BC, all three ratios showed values within the range of $28.1 - 31.2 \text{ cmol kg}^{-1}$. Finally, the CEC values of all AMOchars significantly increased compared to the pristine biochar and pure AMO, respectively. This could be caused by a mutual interaction of Mn-oxides with the surface of pure biochar. As the CEC value is represented as a driving factor for metal(loid)s removal (Trakal et al., 2014), such a modified biochar could, therefore, be a very efficient sorbent.

Table 7.2

Selected characteristics of all sorbents.

Sorbent	BET (m² g⁻¹)	pH	pH_{ZPC}	CEC (cmol kg⁻¹)	Reference
AMO	14.8	8.10 ± 0.30	8.30 ± 0.10	34.0 ± 1.0	Della Puppa et al. (2013)
Biressite	76.5	3.30 ± 0.10	2.70 ± 0.30	247 ± 29	Della Puppa et al. (2013)
BC	72.0	10.0 ± 0.10	9.92 ± 0.10	40.2 ± 0.3	Trakal et al. (2014)
AMO+BC 1:2	/	9.52 ± 0.02	8.89 ± 0.10	28.1 ± 0.6	This study
AMO+BC 1:1	/	9.36 ± 0.04	8.49 ± 0.10	24.5 ± 0.1	This study
AMO+BC 2:1	/	9.02 ± 0.06	8.09 ± 0.10	31.2 ± 0.3	This study
AMOchar 1:2	/	8.40 ± 0.02	7.94 ± 0.10	65.3 ± 2.4	This study
AMOchar 1:1	/	8.35 ± 0.03	8.00 ± 0.10	77.1 ± 1.6	This study
AMOchar 2:1	/	8.47 ± 0.03	7.88 ± 0.10	78.9 ± 1.0	This study
BCB	/	6.98 ± 0.03	6.39 ± 0.10	40.8 ± 0.2	This study ^a

^abiochar-biressite composite was synthesized according to Wang et al. (2015a)

Removal of various metal(loid)s from aqueous solution

Compared to the modified sorbents and pure AMO, the pristine biochar (BC) proved a lower sorption of the As(V), Cd(II), and Pb(II) from aqueous solution (**Fig. 7.4**). The As(V) removal was negligible due to a very high pH of the aqueous solution. The amount of sorbed Cd(II) and Pb(II) was approximately 15.0% and 60.0%, respectively, where the removal rate of Cd(II) and Pb(II) continuously decreased in time (**Fig. 7.5**). This unexpected trend was caused by the initial precipitation of both metals when, at the start of the experiment, it was not possible to maintain the set-up pH value (5.00) due to the alkaline pH of the BC.

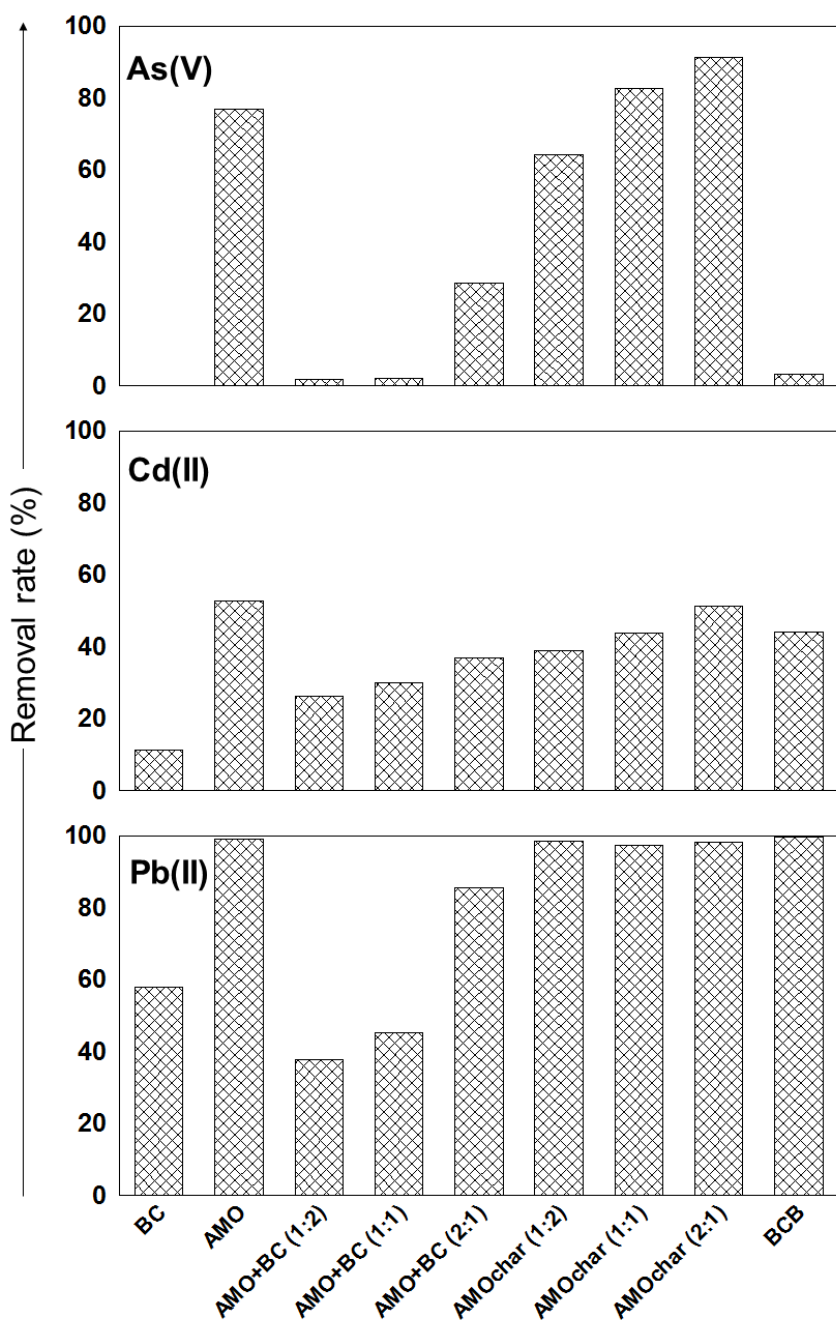


Figure 7.4

Maximum removal efficiency of metal(loid)s onto studied sorbents (obtained from kinetic experiment at equilibrium state).

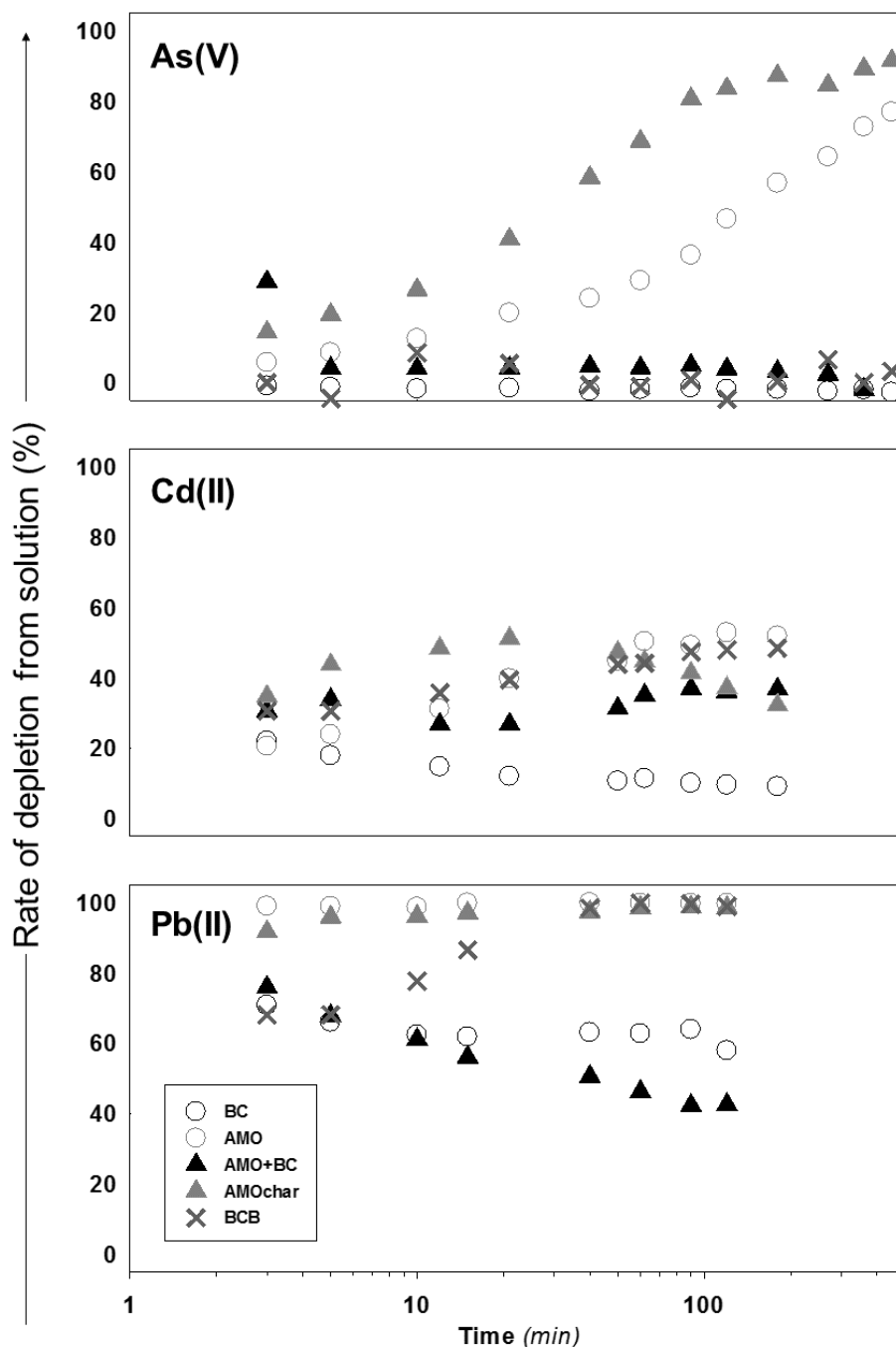


Figure 7.5
 Kinetics of metal(loid)s onto selected sorbents under constant pH value.

The pure AMO was very efficient in removing both metals and metalloids (**Fig. 7.4**) from solution which has also been confirmed by Della Puppa et al. (2013); Ettler et al. (2015); and Michálková et al. (2016). The removal rates of the studied metal(loid)s were 76.9% of As(V), 52.8% of Cd(II), and 99.9% of Pb(II). Additionally, the equilibrium was reached after several minutes for Pb(II), after one hour for Cd(II), and after 7 hours for As(V) (**Fig. 7.5**). Such a fast sorption (especially for Pb) was also previously confirmed by Della Puppa et al. (2013).

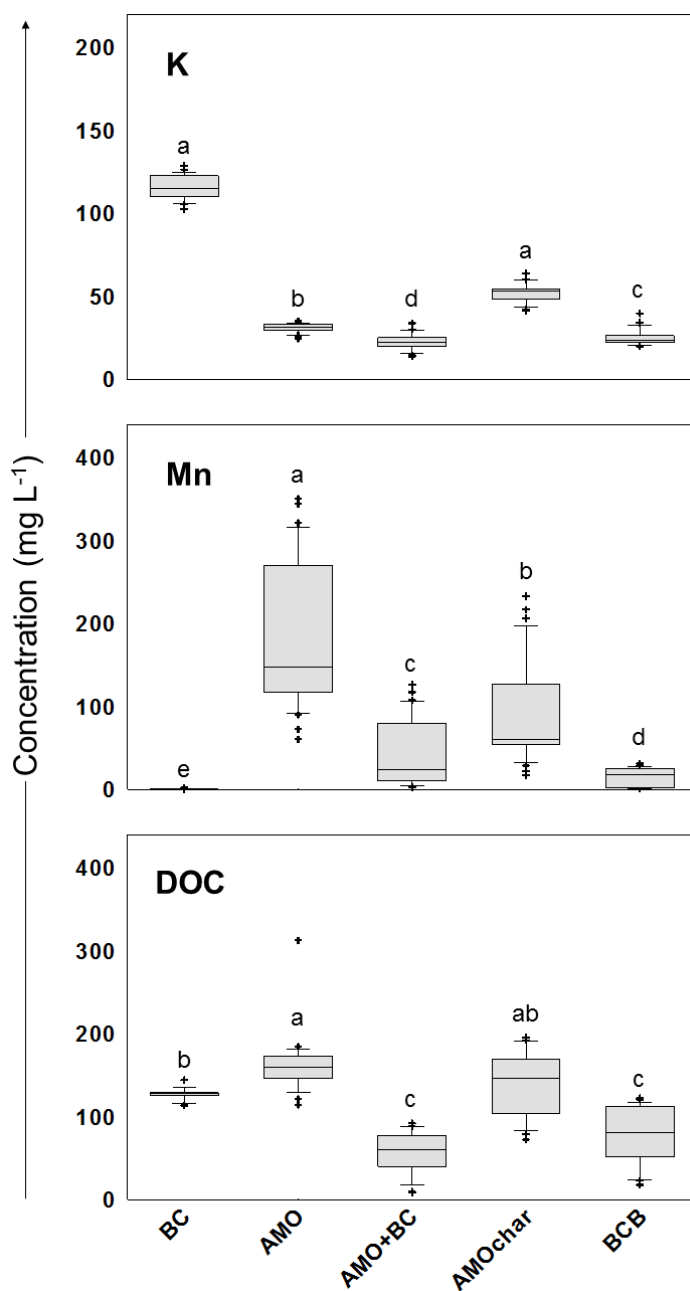
The removal efficiency of the BCB presented previously by Wang et al. (2015a) was very high (> 99.0%) for Pb(II), rather high (\approx 48.0%) for Cd(II) but very limited (< 9.0%) for As(V). Maximum sorption of BCB was 3.42 g kg^{-1} for As(V) and 105 g kg^{-1} for Pb(II) which was 3- and 2-times more, respectively, as reported for birnessite-pine biochar (BPB) by Wang et al. (2015a). Such difference (in case of the BCB) could be explained by different origins of the two biochars. As reported in paper of Trakal et al. (2014), woody-biochars with well-developed structure were less efficient for Pb(II) and Cd(II) sorption than those with a poorly developed structure (e.g. from grape stalks).

The AMOchar has proved to be a very complex sorbent suitable not only for removing both tested metals but also for the sorption of As(V). In particular, the AMOchar was able to remove > 98.5% of dissolved Pb(II), 34.5 - 51.2% of dissolved Cd(II), and 64.3 - 91.4% of dissolved As(V) (**Fig. 7.4**). Generally, the samples with higher doses of AMO were able to remove greater amounts of metal(loid)s, which reflects a high affinity of all tested metal(loid)s to sorb on the Mn-oxides surface (Komárek et al., 2013). Furthermore, the biochar stirred with AMO under given pH conditions (AMO+BC) also showed significant enhancement in metal(loid)s sorption compared with the BC (**Fig. 7.4**). The improvement was more obvious for the ratio of 2:1 (AMO:BC), where the surface of the biochar was intensively occupied by Mn-oxalate as well as by rhodochrosite (as discussed earlier).

The reaction speed of metal(loid)s sorption on selected biochars is presented in **Fig. 7.4**. In general, the equilibrium state was reached within 1 hour or less for Pb(II) and Cd(II), respectively, but within 8 hours for As(V). This is in agreement with other studies (e.g. Trakal et al., 2014; Wang et al., 2015a; 2015d). The fastest metal(loid)s sorption (except the pure AMO) was detected on the AMOchar, especially that where higher amount of AMO was present (data not shown). The second fastest sorption occurred in the case of the biochar-birnessite composite (the greatest contrast was recorded for Pb; see **Fig. 7.5**). The kinetics of the AMO+BC composite shows similar

behaviour as the BC, as the removal rate continuously decreased in the case of Cd(II) and Pb(II), respectively. As already explained above for the BC, the initial precipitation of both metals was caused by the very alkaline pH of the sorbent.

Finally, **Fig. 7.6** shows the leaching of selected elements during metal(loid)s sorption in all the chosen sorbents that were tested. The standard deviation reflects the concentration changes in K, Mn and DOC that had occurred during the experiment which tested sorption of individual metal(loid)s. Potassium leaching had not changed significantly in time and the leaching proceeded in the following order ($BC \approx AMOchar > AMO > BCB > AMO+BC$). The high content of K in the BC was described previously by Trakal et al. (2014). Manganese leaching was negligible from the pristine biochar but a very high quantity of Mn was leached from the pure AMO (60.0 - 351 mg L⁻¹). Additionally, Mn leaching had continuously increased in time during metal(loid)s sorption, which could be caused by the gradual dissolution of low-stability Mn-oxalates (Ettler et al., 2014). Nevertheless, both AMO-biochar composites show the reduction in Mn leaching (more intensive for the AMO+BC). This demonstrates that: (i) stabilization had occurred in the Mn-oxalates on the structure of AMOchar; and (ii) some Mn was pre-leached during the stirring of the AMO+BC composite. Additionally, the BCB complex shows an even higher reduction in Mn-leaching, probably caused by higher stability of birnessite compared with Mn-oxalates. The DOC (dissolved organic carbon) leaching was also measured during the metal(loid)s sorption. In the test, the pristine biochar showed very similar DOC concentrations over the period of the experiment duration (as indicated by minimum SD; **Fig. 7.6**). By contrast, more variable and significantly higher DOC concentration was observed in the pure AMO (described also by Michálková et al., 2014). The mean value of leaching of DOC from the AMOchar had varied in time but, otherwise, it was similar to that of the pristine biochar. The DOC leaching was significantly reduced in the AMO+BC and the BCB composites. This could be due to: (i) pre-leaching during the preparation of AMO+BC and (ii) higher stability resulting from acidic conditions during the BCB synthesis.

**Figure 7.6**

Mean concentration \pm SD of potassium (K), manganese (Mn) and dissolved organic carbon (DOC) in the solution during the sorption experiment of the studied metal(loid)s. Data shown are statistically significant (using one-way ANOVA). Differences between the means were determined using Tukey's test at ($p < 0.05$).

Conclusions

A newly synthesized AMOchar, i.e., biochar coated by the AMO, was formed mainly by Mn-oxalates, whereas in the case of AMO+BC composite, crystals of rhodochrosite were also detected in addition to Mn-oxalates. Despite the rather high pH of AMOchar, this composite was able to sorb not only Pb(II) and Cd(II) but also a high quantity of As(V). In comparison with the pristine biochar and the biochar-birnessite modification, the AMOchar was the most suitable biosorbent for removing various metal(loid)s from aqueous solution. Additionally, the AMOchar was able to reduce Mn leaching in comparison with the pure AMO.

Chapter VIII

Summary

The thesis evaluated the use of selected (nano)oxides for the stabilization of metals and metalloids in contaminated soils. We dealt basically with two Fe nanooxides and one partially nanoscale amorphous Mn oxide. Both Fe oxides, commercial nanomaghemite (Fe III) and nanomagnetite (Fe II,III), were chosen as promising materials for chemical stabilization that have not been yet widely tested for soil applications. The amorphous Mn oxide (AMO) was a newly synthesized phase in our laboratory (Della Puppa et al., 2013) and was tested to evaluate its potential to stabilize metals/metalloids in contaminated soils.

In general, the experimental work can be divided into 5 main sections: i) basic characterization of the (nano)oxides and contaminated soils, ii) adsorption properties of the tested oxides, iii) stabilizing potential of the oxides in a simple soil-amendment system, iv) oxides transformations in soils, and v) their interactions with living plants and microorganisms. The aim was thus to provide a complex view on chosen stabilizing amendments regarding not just their direct influence on contaminants mobility, but also their stability and transformations in soil conditions together with their influence on soil microorganisms and higher plants. Several soil samples contaminated with metals and metalloids were chosen for our experiments. These soils differed in basic physico-chemical characteristics, content and type of contaminating metals/metalloids (e.g., Cd, Cu, Pb, Zn, As) or origin of contamination (i.e., anthropogenic, geogenic or artificial spiking). Such approach enabled us to study the behavior of tested materials in various soil conditions with respect to various contaminants.

As adsorption is the key process playing role in stabilization of metals/metalloids in contaminated soils, adsorption kinetics together with adsorption capacities of the tested materials towards Cd, Cu, Pb and As were studied. In this context, the most effective material showed to be the AMO (one to two orders of magnitude higher adsorption capacities than Fe III and Fe II,III) (**Table 8.1**). As expected, while the adsorption capacity for metallic elements (i.e., Cd, Cu and Pb) generally increased with increasing pH for all tested materials, the adsorption of As(V) showed a different trend. In this case, the adsorption capacity of Fe III and Fe II,III increased with decreasing pH, which is in accordance with a general trend observed for adsorption of this compound. In contrast, adsorption of As(V) onto the AMO increased with increasing pH. This uncommon trend could be explain by the unusually high pH_{zpc} of the AMO (8.1) favoring the adsorption of anionic species together with significant dissolution of this phase at decreasing pH. The adsorption of As(V) was further

studied using XPS analysis that confirmed the chemical sorption as the main process involved in As(V) sorption on the AMO surface.

Table 8.1

Maximal adsorption capacities observed for the studied amendments under given experimental conditions. Adsorption of Pb onto Fe III and Fe II,III did not fit the Langmuir model.

Material	Metal/metalloid	Experimental pH	S_{max} (mmol g⁻¹)
AMO	Cd	4.25	2.243
	Cu	4.25	0.522
	Pb	5.85	4.019
	As(V)	8.00	1.79
Fe III	Cd	4.25	0.088
	Cu	4.25	0.156
	Pb	5.85	n.a.
	As(V)	4.00	0.151
Fe II,III	Cd	4.25	0.100
	Cu	4.25	0.066
	Pb	5.85	n.a.
	As(V)	4.00	0.139

AMO: amorphous manganese oxide; Fe III: nanomaghemite; Fe II,III: nanomagnetite; S_{max}: maximal adsorption capacity

While the adsorption tests provided some general information on metal(loid) adsorption onto the (nano)oxides, the behavior of these materials directly in soil conditions needed to be investigated as well. For this reason, several sets of experiments including static batch, column or pH-static leaching experiments were performed. Generally, the influence of (nano)oxides addition on contaminants mobility together with other physico-chemical soil characteristics was observed. Again, the most efficient stabilizing agent proved to be the AMO, being the most effective in reducing the labile pools of Cd, Cu, Pb, Zn and As in model contaminated soils. On the other hand, Fe III and Fe II,III addition generally showed a minimal effect on contaminants mobility. Application of the AMO was further connected with the increase of soil pH that was more pronounced in more acidic conditions. This buffering effect was also associated with AMO dissolution and unwanted oxidation of

soil organic matter (SOM). For these reasons, AMO application can be recommended for neutral or slightly alkaline contaminated soils.

Besides the stabilizing efficiency, the stability and potential alterations of the amendments in soil conditions are another important factor for their long-term performance. Possible transformations of the tested materials were examined both by long-term agitation in soil solution and direct incubation in soil conditions. The SEM/EDS analysis performed after one-month agitating in soil solution showed MnCO_3 (rhodochrosite) coatings on the AMO surface, while no significant changes were recorded in the case of Fe III and Fe II,III. In our previous study focused on AMO alterations in contaminated soils (Ettler et al., 2014), rhodochrosite precipitates were identified as the main newly-formed phase. As the observed rhodochrosite formation was connected with increased stability of the AMO and decreased SOM dissolution, synthetic surface coverage with MnCO_3 coatings (SM-AMO) prior to its application was proposed. The stability, alterations and stabilizing efficiency towards targeted contaminants was further examined for the original and surface-modified materials. SM-AMO had a constantly lower mass loss than AMO. On the other hand, the the stabilizing efficiency together with the amount of manganese and DOC released to soil solution were similar for both materials. The differences in surface composition of both materials decreased with time as rhodochrosite precipitated on the AMO surface while the SM-AMO coating was gradually dissolving.

As the soil represents a living system inhabited by numerous micro- and macroorganisms, the use of stabilizing agents should always take into account this factor. In order to investigate their effects on soil microbial activity, simple respiration and soil dehydrogenase assays were performed using various soils and amendments. Generally, AMO application promoted soil microbial activity in all cases while no significant changes were observed in the case of Fe III and Fe II,III. This effect is supposed to be the consequence of both decreased bioavailability/toxicity of contaminating metals and increased SOM dissolution that can provide additional substrate for microbes. Yet, increased microbial activity was recorded even in cases when DOC concentrations remained at control level confirming thus the ability of AMO to lower the toxicity of the contaminating metal(loid)s. Furthermore, the effect of AMO on sunflower (*Helianthus annuus* L.) growth and metal uptake was examined. The AMO proved efficient in decreasing uptake of Cd, Pb and Zn, eliminating Zn toxicity symptoms and promoting plant growth. On the other hand, Mn released from AMO was readily taken up by plants in

excessive amounts showing emerging symptoms of Mn phytotoxicity especially in acidic soils.

Due to the ability of AMO to efficiently adsorb metals (Cd, Cu, Pb, Zn) and As, we also recently tried to synthesize various types of composite AMO-biochar sorbents in order to ameliorate biochar sorption capacity and reduce content of Mn released from the AMO. From all the tested variants, 2:1 (w/w) AMO-biochar composite (denoted as AMOchar) was the most efficient in adsorbing Cd(II), Pb(II) and As(V) from aqueous solution with reduced Mn leaching compared to the AMO. A field experiment focused on metal(loid) stabilization is currently under preparation.

The use of Fe and Mn oxides generally represents a viable solution for stabilization of metal(loid)s in contaminated soils. Particular stabilizing amendment suitable for given locality has to be always selected with respect to contaminating metal(loid)s, site conditions, vegetation cover and costs associated with their application. From the three (nano)oxides studied in this PhD thesis, the AMO proved to be the most efficient stabilizing amendment applicable both for the immobilization of metals and As. Moreover, it is able to efficiently promote microbial activity and plant growth, but its application is recommended only in soils with neutral or slightly alkaline pH where the risk of unwanted Mn release is minimized. Results of this PhD thesis thus highlight the need for a complex approach in stabilizing agents testing including interactions both with biotic and abiotic parts of soil environment in order to obtain complete information about its efficiency and applicability.

References

- Adriano DC (2001) Trace elements in the terrestrial environments: Biogeochemistry, bioavailability, and risks of metals. Springer-Verlag. New York. Berlin. Heidelberg
- Ajith N, Dalvi AA, Swain KK, Devi PSR, Kalekar BB, Verma R, Reddy AVR (2013) Sorption of As(III) and As(V) on chemically synthesized manganese dioxide. J Environ Sci Health 48, 422-428
- Ali NA, Ater M, Sunahara GI, Robidoux PY (2004) Phytotoxicity and bioaccumulation of copper and chromium using barley (*Hordeum vulgare* L.) in spiked artificial and natural forest soils. Ecotoxicol Environ Saf 57, 363-374
- Alloway BJ (ed.) (1995) Heavy metals in soils. Trace metals and metalloids in soils and their bioavailability, Second edition. Blackie Academic & Professional. London
- Alloway BJ (ed.) (2013) Heavy metals in soils: Trace metals and metalloids in soils and their bioavailability, Third edition. Springer Dordrecht Heidelberg New York London
- An B, Zhao D (2012) Immobilization of As(III) in soil and groundwater using a new class of polysaccharide stabilized Fe-Mn oxide nanoparticles. J Hazard Mater 211-212, 332-341
- Anawar HM (2012) Arsenic speciation in environmental samples by hydride generation and electrothermal atomic absorption spectrometry. Talanta 88, 30-42
- Auffan M, Achouak W, Rose J, Chanec C, Waite DT, Masion A, Woicik J, Wiesner MR, Bottero JY (2008) Relation between the redox state of iron based nanoparticles and their cytotoxicity towards *Escherichia coli*. Environ Sci Technol 42 (17), 6730-6735
- Auffan M, Shipley HJ, Yean S, Kan AT, Tomson M, Rose J, Bottero JY (2007) Nanomaterials as adsorbants. In: Wiesner MR, Bottero JY (eds) Environmental nanotechnology: applications and impacts of nanomaterials. McGraw Hill, New York
- Bagherifam S, Lakzian A, Fotovat A, Khorasani R, Komarneni S (2014) In situ stabilization of As and Sb with naturally occurring Mn, Al and Fe oxides in calcareous soil: Bioaccessibility, bioavailability and speciation studies. J Hazard Mater 273, 247-252
- Beak DG, Basta NT, Scheckel KG, Traina SJ (2008) Linking solid phase speciation of Pb sequestered to birnessite to oral Pb bioaccessibility: Implications for soil remediation. Environ Sci Technol 42, 779-785
- Beyer L, Wachendorf C, Elsner DC, Knabe R (1993) Suitability of dehydrogenase activity assay as an index of soil biological activity. Biol Fertil Soil 16, 52-56
- Bhargava A, Carmona FF, Bhargava M, Srivastava S (2012) Approaches for enhanced phytoextraction of heavy metals. J Environ Manag 105, 103-120
- Bolan N, Adriano DC, Curtin D (2003) Soil acidification and liming interactions with nutrient and heavy metal transformation and bioavailability. Adv Agron 78, 215-272

- Bolan N, Kunhikrishnan A, Thangarajan R, Kumpiene J, Park J, Makino T, Kirkham MB, Scheckel K (2014) Remediation of heavy metal(loid)s contaminated soils - to mobilize or to immobilize? *J Hazard Mater* 266, 141-166
- Bolster CH, Hornberger GM (2007) On the use of linearized Langmuir equations. *Soil Sci Soc Am J* 71, 1796-1806
- Borůvka L, Vácha R (2006) Litavka river alluvium as a model area heavily polluted with potentially risk elements. *Phytoremediation of Metal-Contaminated Soils*, J.-L. Morel et al. (eds.). Springer, Netherland. pp. 267-298.
- Bowell RJ, Alpers CN, Jamieson HE, Nordstrom DK, Majzlan J (2014) The environmental geochemistry of arsenic: an overview. *Rev Mineral Geochem* 79, 1-16.
- Breemen N, Buurman P (2002) *Soil Formation*. Second edition. Kluwer Academic Publishers. New York, Boston, Dordrecht, London, Moscow.
- Brown GE (1990) Spectroscopic studies of chemisorption reaction mechanisms at oxide - water interfaces. *Rev Mineral* 23, 309-363
- Bujňáková Z, Baláž P, Zorkovská A, Sayagués MJ, Kováč J, Timko M (2013) Arsenic sorption by nanocrystalline magnetite: an example of environmentally promising interface with geosphere. *J Hazard Mater* 262, 1204-1212
- Cancès B, Juillot F, Morin G, Laperche V, Polya D, Vaughan DJ, Hazemann J-L, Proux O, Brown GE Jr, Calas G (2008) Changes in arsenic speciation through a contaminated soil profile: A XAS based study. *Sci Total Environ* 397, 178-189
- Cappuyns V, Van Herreweghe S, Swennen R, Ottenburgs R, Deckers J (2002) Arsenic pollution at the industrial site of Reppel-Bocholt (north Belgium). *Sci Total Environ* 295, 217-240
- Carbonell G, Pablos MV, García P, Ramos C, Sánchez P, Fernández C, Tarazona JV (2000) Rapid and cost-effective multiparameter toxicity tests for soil microorganisms. *Sci Total Environ* 247, 143-150
- Carter MR, Gregorich EG (2008) *Soil sampling and methods of analysis*, 2nd edn. Canadian Society of Soil Science, CRC Press, Boca Raton
- CEN/TS 14,997 (2006) *Characterization of waste - Leaching behaviour tests -Influence of pH on leaching with continuous pH-control*, CEN, Brussels
- Cerqueira B, Covelo EF, Andrade ML, Vega FA (2011) Retention and mobility of copper and lead in soils as influenced by soil horizon properties. *Pedosphere* 21, 603-614
- Chander K, Brookes PC (1991) Is the dehydrogenase assay invalid as a method to estimate microbial activity in copper-contaminated soils? *Soil Biol Biochem* 23, 909-915
- Chang AC, Crowley DE, Page AL (2004) *Assessing bioavailability of metals in biosolids treated soils: Biosolids and residuals*. Water Environment Research Foundation. 208 p. ISBN: 1-84339-679-3.

- Chang YY, Song KH, Yang JK (2008) Removal of As(III) in a column reactor packed with iron-coated sand and manganese-coated sand. *J Hazard Mater* 150, 565-572
- Charlet L, Morin G, Rose J, Wang Y, Auffan M, Burnol A, Fernandez- Martinez A (2011) Reactivity at (nano)particle-water interfaces, redox processes, and arsenic transport in the environment. *Comptes Rendus Geosci* 343, 123-139
- Chen Z, Kim KW, Zhu YG, McLaren R, Lui F, He JZ (2006) Adsorption ($\text{As}^{\text{III,V}}$) and oxidation (As^{III}) of arsenic by pedogenic Fe-Mn nodules. *Geoderma* 136, 566-572
- Chen ZS, Lee GJ, Liu JC (2000a) The effects of chemical remediation treatments on the extractability and speciation of cadmium and lead in contaminated soils. *Chemosphere* 41, 235-242
- Chen M, Xu P, Zeng G, Yang C, Huang D, Zhang J (2015) Bioremediation of soils contaminated with polycyclic aromatic hydrocarbons, petroleum, pesticides, chlorophenols and heavy metals by composting: Applications, microbes and future research needs. *Biotechnol Adv* 33, 745-755
- Chen HM, Zheng CR, Tu C, Shen ZG (2000b) Chemical methods and phytoremediation of soil contaminated with heavy metals. *Chemosphere* 41, 229-234
- Cheng SF, Hseu ZY (2002) In-situ immobilization of cadmium and lead by different amendments in two contaminated soils. *Water Air Soil Pollut* 140, 73-84
- Ching S, Petrovay DJ, Jorgensen ML, Suib SL (1997) Sol-gel synthesis of layered birnessite-type manganese oxides. *Inorg Chem* 36, 883-890
- Chiu V, Hering J (2000) Arsenic adsorption and oxidation at manganite surfaces. 1. Method for simultaneous determination of adsorbed and dissolved arsenic species. *Environ Sci Technol* 34, 2029-2034
- Chrastný V, Vaněk A, Teper L, Cabala J, Procházka J, Pechar L, Drahotka P, Penížek V, Komárek M, Novák M (2012) Geochemical position of Pb, Zn and Cd in soils near the Olkusz mine/smelter, South Poland: effects of land use, type of contamination and distance from pollution source. *Environ Monit Assess* 184, 2517-2536
- Contin M, Mondini C, Leita L, De Nobili M (2007) Enhanced soil toxic metal fixation in iron (hydr)oxides by redox cycles. *Geoderma* 140, 164-175
- Contin M, Mondini C, Leita L, Zacheo P, Crippa L, De Nobili M (2008) Immobilisation of soil toxic metals by repeated additions of Fe(II) sulphate solution. *Geoderma* 147, 133-140
- Cornell RM, Schwertmann U (2003) *The Iron Oxides. Structures, properties, reactions, occurrences and uses*. Second edition. Wiley Verlag.
- Dai R, Liu J, Yu C, Sun R, Lan Y, Mao JD (2009) A comparative study of oxidation of Cr(III) in aqueous ions, complex ions and insoluble compounds by manganese-bearing mineral (birnessite). *Chemosphere* 76, 536-541

- Dalvi AA, Ajith N, Swain KK, Verma R (2015) Sorption of arsenic on manganese dioxide synthesized by solid state reaction. *J Environ Sci Health* 50, 866-873
- Davranche M, Dia A, Fakhri M, Nowack B, Gruau G, Ona-anguema G, Petitjean P, Martin S, Hochreutener R (2013) Organic matter control on the reactivity of Fe(III)-oxyhydroxides and associated As in wetland soils: A kinetic modeling study. *Chem Geol* 335, 24-35
- Della Puppa L, Komárek M, Bordas F, Bollinger JC, Joussein E (2013). Adsorption of copper, cadmium, lead and zinc onto a synthetic manganese oxide. *J Colloid Interface Sci* 399, 99-106
- Dermont G, Bergeron M, Mercier G, Richer-Lafleche M (2008) Soil washing for metal removal: A review of physical/chemical technologies and field applications. *J Hazard Mater* 152, 1-31
- Di Palma L, Gueye MT, Petrucci E (2015) Hexavalent chromium reduction in contaminated soil: A comparison between ferrous sulphate and nanoscale zero-valent iron. *J Hazard Mater* 281, 70-76
- Dixit S, Hering JG (2003) Comparison of arsenic(V) and arsenic(III) sorption onto iron oxide minerals: Implications for arsenic mobility. *Environ Sci Technol* 37, 4182-4189
- Dong DM, Nelson YM, Lion LW, Shuler ML, Ghiorse WC (2000) Adsorption of Pb and Cd onto metal oxides and organic material in natural surface coatings as determined by selective extractions: new evidence for the importance of Mn and Fe oxides. *Water Res* 34, 427-436
- Drahota P, Rohovec J, Filippi M, Mihaljevič M, Rychlovský P, Červený V, Pertold Z (2009) Mineralogical and geochemical controls of arsenic speciation and mobility under different redox conditions in soil, sediment and water at the Mokrosko-West gold deposit, Czech Republic. *Sci Total Environ* 407, 3372-3384
- Driehaus W, Seith R, Jekel M (1995) Oxidation of arsenate(III) with manganese oxides in water treatment. *Water Res* 29, 297-305
- Droz B, Dumas N, Duckworth OW, Peña J (2015) A comparison of the sorption reactivity of bacteriogenic and mycogenic Mn oxide nanoparticles. *Environ Sci Technol* 49, 4200-4208
- Duker AA, Carranza EJM, Hale M (2005) Arsenic geochemistry and health. *Environ Int* 31, 631-641
- Ettler V, Knytl V, Komárek M, Della Puppa L, Bordas F, Mihaljevič M, Klementová M, Šebek O (2014) Stability of a novel synthetic amorphous manganese oxide in contrasting soils. *Geoderma* 214-215, 2-9
- Ettler V, Mihaljevič M, Šebek O, Matys Grygar T, Klementová M (2012) Experimental in situ transformation of Pb smelter fly ash in acidic soils. *Environ Sci Technol* 46, 10539-10548

- Ettler V, Šebek O, Grygar T, Klementová M, Bezdička P, Slavíková H (2008) Controls on metal leaching from secondary Pb smelter air-pollution-control residues. *Environ Sci Technol* 42, 7878-7884
- Ettler V, Tejnecký V, Mihaljevič M, Šebek O, Zuna M, Vaněk A (2010) Antimony mobility in lead-smelter polluted soils. *Geoderma* 155, 409-418
- Ettler V, Tomášová Z, Komárek M, Mihaljevič M, Šebek O, Michálková Z (2015) The pH-dependent long-term stability of an amorphous manganese oxide in smelter-polluted soils: Implication for chemical stabilization of metals and metalloids. *J Hazard Mater* 286, 386-394
- Ettler V, Vaněk A, Mihaljevič M, Bezdička P (2005) Contrasting lead speciation in forest and tilled soils heavily polluted by lead metalurgy. *Chemosphere* 58, 1449-1459
- Ettler V, Vrtišková R, Mihaljevič M, Šebek O, Grygar T, Drahotka P (2009) Cadmium, lead and zinc leaching from smelter fly ash in simple organic acids-simulators of rhizospheric soil solutions. *J Hazard Mater* 170, 1264-1268
- Essington ME (2004) *Soil and Water Chemistry: An Integrative Approach*. CRC Press. Boca Ranton
- Fandeur D, Juillot F, Morin G, Olivi L, Cognigni A, Webb SM, Ambrosi JP, Fritsch E, Guyot F, Brown GE Jr. (2009) XANES evidence for oxidation of Cr(III) to Cr(VI) by Mn oxides in a lateritic regolith developed on serpentinized ultramafic rocks of New Caledonia. *Environ Sci Technol* 43, 7384-7390
- Farrow EM, Wang J, Burken JG, Shi H, Yan W, Yang J, Hua B, Deng B (2015) Reducing arsenic accumulation in rice grain through iron oxide amendment. *Ecotoxicol Environ Saf* 118, 55-61
- Febrianto J, Kosasih AN, Sunarso J, Ju YH, Indraswati N, Ismadji S (2009) Equilibrium and kinetic studies in adsorption of heavy metals using biosorbent: A summary of recent studies. *J Hazard Mater* 162, 616-645
- Feng XH, Zhai LM, Tan WF, Liu F, He JZ (2006) The controlling effect of pH on oxidation of Cr(III) by manganese oxide minerals. *J Colloid Interface Sci* 298, 258-66
- Feng XH, Zhai LM, Tan WF, Lui F, He JZ (2007) Adsorption and redox reactions of heavy metals on synthesized Mn oxide minerals. *Environ Pollut* 147, 366-373
- Fernando DR, Lynch JP (2015) Manganese phytotoxicity: new light on an old problem. *Ann Bot* 116, 313-319
- Fiol N, Villaescusa I (2009) Determination of sorbent zero charge: usefulness in sorption studies. *Environ Chem Lett* 7, 79-84
- Fisher TB, Heaney PJ, Jang JH, Ross DE, Brantley SL, Post JE, Tien M (2008) Continuous time-resolved X-ray diffraction of the biocatalyzed reduction of Mn oxide. *Am Miner* 93, 1929-1932

- Foster AL, Brown GE Jr, Parks GA (2003) X-ray absorption fine structure study of As(V) and Se(IV) sorption complexes on hydrous Mn oxides. *Geochim Cosmochim Acta* 67, 1937-1953
- Freundlich H (1909) H. Kapillarchemie. Akademische Verlagsgesellschaft, Leipzig, Germany.
- Friák M, Schindlmayr A, Scheffler M (2007) Ab initio study of the half-metal to metal transition in strained magnetite. *New J Phys* 9, 5
- Friesl W, Friedl J, Platzer K, Horak O, Gerzabek MH (2006) Remediation of contaminated agricultural soils near a former Pb/Zn smelter in Austria: Batch, pot and field experiments. *Environ Pollut* 144, 40-50
- Fu F, Dionysiou DD, Liu H (2014) The use of zero-valent iron for groundwater remediation and wastewater treatment: A review. *J Hazard Mater* 267, 194-205
- García-Sánchez A, Alvarez-Ayuso E, Rodríguez-Martin F (2002) Sorption of As(V) by some oxyhydroxides and clay minerals. Application to its immobilization in two polluted mining soils. *Clay Miner* 37, 187-194
- Garau G, Silvetti M, Castaldi P, Mele E, Deiana P, Deina S (2014) Stabilising metal(loid)s in soil with iron and aluminium-based products: Microbial, biochemical and plant growth impact. *J Environ Manag* 139, 146-153
- Gee GW, Bauder JW (1986) Particle-size analysis. In: Klute, A. (Ed.), *Methods of Soil Analysis. Part I: Physical and Mineralogical Methods*. American Society of Agronomy - Soil Science Society of America, Madison, pp. 383-411
- Gee GW, Or D (2002) Particle size analysis. In: Dane JH, Topp GG (eds.) *Methods of soil analysis, Part 4, physical methods*, Madison, WI. Soil Science Society of America.
- Geebelen W, Sappin-Didier V, Ruttens A, Carleer R, Yperman J, Bongue- Boma K, Mench M, van der Lelie N, Vangronsveld J (2006) Evaluation of cyclonic ash, commercial Na-silicates, lime and phosphoric acid for metal immobilisation purposes in contaminated soils in Flanders (Belgium). *Environ Pollut* 144, 32-39
- Giménez J, Martínez M, de Pablo J, Rovira M, Duro L (2007) Arsenic adsorption onto natural hematite, magnetite and goethite. *J Hazard Mater* 141, 575-580
- Giral M, Zagury GJ, Deschênes L, Blouin J-P (2010) Comparison of four extraction procedures to assess arsenate and arsenite species in contaminated soils. *Environ Pollut* 158, 1890-1898
- Gleyzes C, Tellier S, Astruc M (2002) Fractionation studies of trace elements in contaminated soils and sediments: a review of sequential extraction procedures. *Trends Anal Chem* 21, 451-467
- Goldberg S (2013) *Surface Complexation Modeling. Reference Module in Earth Systems and Environmental Sciences*. Elsevier.
- González JC, Lavilla I, Bendicho C (2003) Evaluation of non-chromatographic approaches for speciation of extractable As(III) and As(V) in environmental solid samples by FI-HGAAS. *Talanta* 59, 525-534

- Gray CW, Dunham SJ, Dennis PG, Zhao FJ, McGrath SP (2006) Field evaluation of in situ remediation of a heavy metal contaminated soil using lime and red mud. *Environ Pollut* 142, 530-539
- Greger M (1999) Metal availability and bioconcentration in plants. In: Prasad MN, Hagemeyer J. (eds.) *Heavy Metal Stress in Plants*, 1–27, Springer, Berlin
- Gruebel KA, Davis JA, Leckie JO (1988) The feasibility of using sequential extraction techniques for arsenic and selenium in soils and sediments. *Soil Sci Soc Am J* 52, 390-397
- Gunes A, Inal A (2009) Phosphorus efficiency in sunflower cultivars and its relationships with phosphorus, calcium, iron, zinc and manganese nutrition. *J Plant Nutr* 32, 1201-1218
- Gupta SS, Bhattacharyya KG (2011) Kinetics of adsorption of metal ions on inorganic materials: A review. *Adv Colloid Interface Sci* 162, 39-58
- Gupta K, Bhattacharya S, Chattopadhyay D, Mukhopadhyay A, Biswas H, Dutta J, Ray NR, Ghosh UC (2011) Ceria associated manganese oxide nanoparticles: Synthesis, characterization and arsenic(V) sorption behavior. *Chem Eng J* 172, 219-229
- Han Z, Sani B, Mroziak W, Obst M, Beckingham B, Karapanagioti HK, Werner D (2015) Magnetite impregnation effects on the sorbent properties of activated carbons and biochars. *Water Res* 70, 394-403
- Han R, Zou W, Zhang Z, Shi J, Yang J (2006) Removal of copper(II) and lead(II) from aqueous solution by manganese oxide coated sand: I. Characterization and kinetic study. *J Hazard Mater* 137, 384-395
- Hartley W, Edwards R, Lepp NW (2004) Arsenic and heavy metal mobility in iron oxide-amended contaminated soils as evaluated by short- and long-term leaching tests. *Environ Pollut* 131, 495-504
- Hartley W, Lepp NW (2008) Remediation of arsenic contaminated soils by iron-oxide application, evaluated in terms of plant productivity, arsenic and phytotoxic metal uptake. *Sci Total Environ* 390, 35-44
- Hashim MA, Mukhopadhyay S, Sahu JN, Sengupta B (2011) Remediation technologies for heavy metal contaminated groundwater. *J Environ Manag* 92, 2355-2388
- Hattab-Hambli N, Motelica-Heino M, Mench M (2016) Aided phytoextraction of Cu, Pb, Zn, and As in copper-contaminated soils with tobacco and sunflower in crop rotation: Mobility and phytoavailability assessment. *Chemosphere* 145, 543-550
- Hettiarachchi GM, Pierzynski GM, Ransom MD (2000) In Situ Stabilization of Soil Lead Using Phosphorus and Manganese Oxide. *Environ Sci Technol* 34, 4614-4619
- Hiemstra T, Van Riemsdijk WH, Bolt GH (1989a) Multisite proton adsorption modeling at the solid/solution interface of (hydr)oxides: a new approach. I. Model description and evaluation of intrinsic reaction constants. *J Colloid Interface Sci* 133, 91-104

- Hiemstra T, De Wit JCM, Van Riemsdijk WH (1989b) Multisite proton adsorption modeling at the solid/solution interface of (hydr)oxides: a new approach: II. Application to various important (hydr)oxides. *J Colloid Interface Sci* 133, 105-117
- Ho YS (2004) Citation review of Lagergren kinetic rate equation on adsorption reactions. *Scientometrics* 59, 171-177
- Ho YS (2006) Review of second-order models for adsorption systems. *J Hazard Mater* 136, 681-689
- Houba VJG, Temminghoff EJM, Gaikhorst GA, van Vark W (2000) Soil analysis procedures using 0.01 M calcium chloride as extraction reagent. *Commun Soil Sci Plant Anal* 31, 1299-1396
- Houben D, Evrard L, Sonnet P (2013) Mobility, bioavailability and pH-dependent leaching of cadmium, zinc and lead in a contaminated soil amended with biochar. *Chemosphere* 92, 1450-1457
- Houben D, Piricar J, Sonnet P (2012) Heavy metal immobilization by cost-effective amendments in a contaminated soil: Effects on metal leaching and phytoavailability. *J Geochem Explor* 123, 87-94
- Hu J, Chen G, Lo IMC (2005) Removal and recovery of Cr(VI) from wastewater by maghemite nanoparticles. *Water Res* 39, 4528-4536
- Hu J, Lo IMC, Chen G (2004) Removal of Cr(VI) by magnetite nanoparticle. *Water Sci Technol* 50, 139-146
- ICDD, PDF-2 Database, Release 2003, International Centre for Diffraction Data, Newton Square, PA, USA, 2003
- Inaba T, Kobayashi E, Suwazono Y, Uetani M, Oishi M, Nakagawa H, Nogawa K (2005) Estimation of cumulative cadmium intake causing Itai-itai disease. *Toxicol Lett* 159, 192-201
- Johnson JE, Savalia P, Davis R, Kocar BD, Webb SM, Nealson KH, Fisher WW (2016) Real-time manganese phase dynamics during biological and abiotic manganese oxide reduction. *Environ Sci Technol* 50, 4248-4258
- Jönsson J, Sherman DK (2008) Sorption of As(III) and As(V) to siderite, green rust (fougerite) and magnetite: Implications for arsenic release in anoxic groundwaters. *Chem Geol* 255, 173-181
- Jorgensen SE (ed.) (2010) *Ecotoxicology*. Elsevier.
- Kabata-Pendias A (2011) *Trace elements in soils and plants*. Fourth edition. CRC Press. Boca Ranton.
- Kalantari K, Ahmad MB, Masoumi HRF, Shameli K, Basri M, Khandalou R (2015) Rapid and high capacity adsorption of heavy metals by Fe₃O₄/montmorillonite nanocomposite using response surface methodology: preparation, characterization, optimization,

- equilibrium isotherms, and adsorption kinetics study. *J Taiwan Inst Chem Eng* 49, 192-198
- Kandeler E (2007) Activities and locations of enzymes. In: Eldor, A.P. (Ed.), *Soil Microbiology and Biochemistry*. Elsevier, Oxford, pp. 72-77
- Karak T, Abollino O, Bhattacharyya P, Das KK, Paul RK (2011) Fractionation and speciation of arsenic in three tea gardens soil profiles and distribution of As in different parts of tea plant (*Camellia sinensis* L.). *Chemosphere* 85, 948-960
- Karami H (2013) Heavy metal removal from water by magnetite nanorods. *Chem Eng J* 219, 209-216
- Kim BK, Baek K, Ko SH, Yang JW (2011) Research and field experiences on electrokinetic remediation in South Korea. *Sep Purif Technol* 79, 116-123
- Kim K-R, Lee B-T, Kim K-W (2012) Arsenic stabilization in mine tailings using nano-sized magnetite and zero valent iron with the enhancement of mobility by surface coating. *J Geochem Explor* 113, 124-129
- Klaine SJ, Alvarez PJJ, Batley GE, Fernandes TF, Handy RD, Lyon DY, Mahendra S, McLaughlin MJ, Lead JR (2008) Nanomaterials in the environment: behaviour, fate, bioavailability and effects. *Environ. Toxicol Chem* 27, 1825-1851
- Ko MS, Kim JY, Park HS, Kim KW (2015) Field assessment of arsenic immobilization in soil amended with iron rich acid mine drainage sludge. *J Clean Prod* 108, 1073-1080
- Koh, J., Kwon, Y., Pak, Y.N., 2005. Separation and sensitive determination of arsenic species (As^{3+}/As^{5+}) using the yeast-immobilized column and hydride generation in ICP–AES. *Microchem J* 80, 195-199
- Komárek M, Vaněk A, Ettler V (2013) Chemical stabilization of metals and arsenic in contaminated soils using oxides - a review. *Environ Pollut* 172, 9-22
- Komorowicz I, Barańkiewicz D (2011) Arsenic and its speciation in water samples by high performance liquid chromatography inductively coupled plasma mass spectrometry- Last decade review. *Talanta* 84, 247-261
- Koretsky C (2000) The significance of surface complexation reactions in hydrologic systems: a geochemist's perspective. *J Hydrol* 230, 127-171
- Kosmulski M (2004) pH-dependant surface charging and points of zero charge. II. Update. *J Colloid Interface Sci* 275, 214-24
- Kötschau A, Büchel, Einax JW, Fischer C, von Tümpling W, Merten D (2014) Element contents in shoots of sunflower (*Helianthus annuus*): Prediction versus measuring. *Chem Erde Geochem* 74, 385-391
- Kumar S, Chaudhuri S, Maiti SK (2013) Soil Dehydrogenase Enzyme Activity in Natural and Mine Soil - A Review. *Middle-East J Sci Res* 13, 898-906

- Kumpiene J, Fitts JP, Mench M (2012) Arsenic fractionation in mine spoils 10 years after aided phytostabilization. *Environ Pollut* 166, 82-88
- Kumpiene J, Lagerkvist A, Maurice C (2008) Stabilization of As, Cr, Cu, Pb and Zn in soil using amendments - a review. *Waste Manag* 28, 215-225
- Kumpiene J, Ore S, Renella G, Mench M, Lagerkvist A, Maurice C (2006) Assessment of zerovalent iron for stabilization of chromium, copper and arsenic in soil. *Environ Pollut* 144, 62-69
- Kuzyakov Y (2001) Review: Factors affecting rhizosphere priming effects. *J Plant Nutr Soil Sci* 165, 382-396
- Kuzyakov Y, Cheng W (2001) Photosynthesis controls of rhizosphere respiration and organic matter decomposition. *Soil Biol Biochem* 33, 1915-1925
- Lafferty BJ, Ginder-Vogel M, Sparks DL (2010a) Arsenite oxidation by a poorly crystalline manganese-oxide 1. Stirred-flow experiments. *Environ Sci Technol* 44 8460-8466
- Lafferty BJ, Ginder-Vogel M, Zhu M, Livi KJT, Sparks DL (2010b) Arsenite oxidation by a poorly crystalline manganese-oxide 2. Results from X-ray absorption spectroscopy and X-ray diffraction. *Environ Sci Technol* 44, 8467-8472
- Lagergren S (1898) Zur theorie der sogenannten adsorption gelöster stoffe. *Kungliga Svenska vetenskapsakademiens handlingar* 24, 1-39
- Lalhmunsiamia, Lee SM, Tiwari D (2013) Manganese oxide immobilized activated carbons in the remediation of aqueous wastes contaminated with copper(II) and lead(II). *Chem Eng J* 225, 128-137
- Landrot G, Ginder-Vogel M, Livi K, Fitts JP, Sparks DL (2012a) Chromium(III) oxidation by three poorly-crystalline manganese(IV) oxides. 1. Chromium(III)-oxidizing capacity, *Environ Sci Technol* 46, 11594-11600
- Landrot G, Ginder-Vogel M, Livi K, Fitts JP, Sparks DL (2012b) Chromium(III) oxidation by three poorly crystalline manganese(IV) oxides. 2. Solid phase analyses. *Environ Sci Technol* 46, 11601-11609
- Langmuir I (1918) The adsorption of gases on plane surfaces of glass, mica, and platinum. *J Am Chem Soc* 40, 1361-1403
- Lee JC, Kim EJ, Kim HW, Baek K (2015) Oxalate-based remediation of arsenic bound to amorphous Fe and Al hydrous oxides in soil. *Geoderma* 270, 76-82
- Lee SH, Park H, Koo N, Seunghun H, Hwang A (2011) Evaluation of the effectiveness of various amendments on trace metals stabilization by chemical and biological methods. *J Hazard Mater* 188, 44-51
- Lefkowitz JP, Elzinga EJ (2015) Impacts of aqueous Mn(II) on the sorption of Zn(II) by hexagonal birnessite. *Environ Sci Technol* 49, 4886-4893

- Lenoble V, Laclautre C, Serpaud B, Deluchat V, Bollinger J-C (2004) As(V) retention and As(III) simultaneous oxidation and removal on a MnO₂-loaded polystyrene resin. *Sci Total Environ* 326, 197-207
- Li X, Yang Y, Zhang J, Jia L, Li Q, Zhang T, Qiao K, Ma S (2012) Zinc induced phytotoxicity mechanism involved in root growth of *Triticum aestivum* L. *Ecotoxicol Environ Saf* 86, 198-203
- Liang S, Guan DX, Ren JH, Zhang M, Luo J, Ma LQ (2014) Effect of aging on arsenic and lead fractionation and availability in soils: coupling sequential extractions with diffusive gradients in thin-films technique. *J Hazard Mater* 273, 272-279
- Liang Q, Zhao D (2014) Immobilization of arsenate in a sandy loam soil using starch-stabilized magnetite nanoparticles. *J Hazard Mater* 271, 16-23
- Lidelöw S, Ragnvaldsson D, Leffler P, Tesfalidet S, Maurice C (2007) Field trials to assess the use of iron-bearing industrial by-products for stabilisation of chromated copper arsenate-contaminated soil. *Sci Total Environ* 387, 68-78
- Limousin G, Gaudet JP, Charlet L, Szenknect S, Barthes V, Krimissa M (2007) Sorption isotherms: A review on physical bases, modeling and measurement. *Appl Geochem* 22, 249-275
- Lin C, Liu J, Liu L, Zhu T, Sheng L, Wang D (2009) Soil amendment application frequency contributes to phytoextraction of lead by sunflower at different nutrient levels. *Environ Exp Bot* 65, 410-416
- Liphadzi MS, Kirkham MB (2005) Phytoremediation of soil contaminated with heavy metals: a technology for rehabilitation of the environment – A review. *S Afr J Bot* 71(1), 24-37.
- Liu CH, Chuang YH, Chen TY, Tian Y, Li H, Wang MK, Zhang W (2015) Mechanism of arsenic adsorption on magnetite nanoparticles from water: Thermodynamic and spectroscopic studies. *Environ Sci Technol* 49, 7726-7734
- Liu J, He L, Dong F, Hudson-Edwards KA (2016) The role of nano-sized manganese coatings on bone char in removing arsenic(V) from solution: Implications for permeable reactive barrier technologies. *Chemosphere* 153, 146-154
- Liu R, Sun L, Qu J, Li G (2009) Arsenic removal through adsorption, sand filtration and ultrafiltration: In situ precipitated ferric and manganese binary oxides as adsorbents. *Desalination* 249, 1233-1237
- Liu R, Zhao D (2007a) In situ immobilization of Cu(II) in soils using a new class of iron phosphate nanoparticles. *Chemosphere* 68, 1867-1876
- Liu R, Zhao D (2007b) Reducing leachability and bioaccessibility of lead in soils using a new class of stabilized iron phosphate nanoparticles. *Water Res* 41, 2491-2502

- Lombi E, Zhao FJ, Zhang GY, Sun B, Fitz W, Zhang H, McGrath SP (2002). In situ fixation of metals in soils using bauxite residue: chemical assessment. *Environ Pollut* 118, 435-443
- Lovley DR, Phillips EJP (1988) Novel mode of microbial energy metabolism: Organic carbon oxidation coupled to dissimilatory reduction of iron or manganese. *Appl Environ Microbiol* 54, 1472-1480
- Lützenkirchen J (1998) Comparison of 1-pK and 2-pK versions of surface complexation theory by the goodness of fit in describing surface charge data of (hydr)oxides. *Environ Sci Technol* 32, 3149-3154
- Madden AS, Hochella MF, Luxton TP (2006) Insights for size-dependent reactivity of hematite nanomineral surfaces through Cu₂p sorption. *Geochim Cosmochim Acta* 70, 4095-4104
- Mamindy-Pajany Y, Hurel C, Marmier N, Roméo M (2011) Arsenic (V) adsorption from aqueous solution onto goethite, hematite, magnetite and zero-valent iron: Effects of pH, concentration and reversibility. *Desalination* 281, 93-99
- Mandal BK, Suzuki KT (2002) Arsenic round the world: a review. *Talanta* 58, 201-235
- Manning BA, Fendorf SE, Bostick B, Suarez DL (2002) Arsenic(III) oxidation and arsenic(V) adsorption reactions on synthetic birnessite. *Environ Sci Technol* 36, 976-981
- Markovski JS, Marković DD, Đokić VR, Mitrić M, Ristić MĐ, Onjia AE, Marinković AD (2014) Arsenate adsorption on waste eggshell modified by goethite, α -MnO₂ and goethite/ α -MnO₂. *Chem Eng J* 237, 430-442
- Martell AE, Smith RM, Motekaitis RJ (2001) Critically selected stability constants of metal complexes. NIST, Gaithersburg, MD. Version 6.0.
- Massaro EJ (ed.) (1997) *Handbook of Human Toxicology*. CRC Press LLC, Boca Ranton, Florida
- Matos Reyes MN, Cervera ML, Campos RC, de la Guardia M (2008) Non-chromatographic speciation of toxic arsenic in vegetables by hydride generation-atomic fluorescence spectrometry after ultrasound-assisted extraction. *Talanta* 75, 811-816
- Matsumoto S, Kasuga J, Makino T, Arao T (2016) Evaluation of the effects of application of iron materials on the accumulation and speciation of arsenic in rice grain grown on uncontaminated soil with relatively high levels of arsenic. *Environ Exp Bot* 125, 42-51
- McBride MB (1994) *Environmental chemistry of soils*. Oxford University Press, New York.
- McBride MB, Martinez CE (2000) Copper phytotoxicity in a contaminated soil: remediation tests with adsorptive materials. *Environ Sci Technol* 34, 4386-4391
- McCann CM, Gray ND, Tournay J, Davenport RJ, Wade M, Finlay N, Hudson-Edwards KA, Johnson KL (2015) Remediation of a historically Pb contaminated soil using a model natural Mn oxide waste. *Chemosphere* 138, 211-217

- McKay G, Ho YS, Ng JCY (1999) Biosorption of copper from waste waters: A review. *Sep Purif Methods* 28, 87-125
- Meharg AA, Sun G, Williams PN, Adomako E, Deacon C, Zhu YG, Feldmann J, Raab A (2008) Inorganic arsenic levels in baby rice are of concern. *Environ Pollut* 152, 746-749
- Mench M, Renella G, Gelsomino A, Landi L, Nannipieri P (2006a). Biochemical parameters and bacterial species richness in soils contaminated by sludgeborne metals and remediated with inorganic soil amendments. *Environ Pollut* 144, 24-31
- Mench M, Vangronsveld J, Beckx C, Ruttens A (2006b) Progress in assisted natural remediation of an arsenic contaminated agricultural soil. *Environ Pollut* 144, 51-61
- Mench M, Vangronsveld J, Didier V, Clijsters H (1994) Evaluation of metal mobility, plant availability and immobilization by chemical agents in a limed-silty soil. *Environ Pollut* 86, 279-286
- Miyata N, Tani Y, Sakata M, Iwahori K (2007) Microbial manganese oxide formation and interaction with toxic metal ions. *J Biosci Bioeng* 104, 1-8
- Micháľková Z, Komárek M, Šillerová H, Della Puppa L, Joussein E, Bordas F, Vaněk A, Vaněk O, Ettler V (2014) Evaluating the potential of three Fe- and Mn-(nano)oxides for the stabilization of Cd, Cu and Pb in contaminated soils. *J Environ Manag* 146, 226-234
- Micháľková Z, Komárek M, Veselská V, Čihalová S (2016) Selected Fe and Mn (nano)oxides as perspective amendments for the stabilization of As in contaminated soils. *Environ Sci Pollut Res* 23, 10841-10854
- Mohan D, Rajput S, Singh VK, Steele PH, Pittman CU Jr (2011) Modeling and evaluation of chromium remediation from water using low cost bio-char, a green adsorbent. *J Hazard Mater* 188, 319-333
- Mohan D, Sarswat A, Ok YS, Pittman Jr. CU (2014) Organic and inorganic contaminants removal from water with biochar, a renewable, low cost and sustainable adsorbent – a critical review. *Bioresour Technol* 160, 191-202
- Mohan D, Singh P, Sarswat A, Steele PH, Pittman Jr. CU (2015) Lead sorptive removal using magnetic and nonmagnetic fast pyrolysis energy cane biochars. *J Colloid Interface Sci* 448, 238-250
- Morgan JJ (2000) Manganese in natural waters and earth's crust: Its availability to organisms. *Metal Ions Biol Syst* 37, 1-34
- Morin G, Ona-Guema G, Wang Y, Menguy N, Juillot F, Proux O, Guyot F, Calas G, Brown GE Jr (2008) Extended X-ray absorption fine structure analysis of arsenite and arsenate adsorption on maghemite. *Environ Sci Technol* 42, 2361-2366

- Mueller NC, Nowack B (2010) Nanoparticles for remediation: solving big problems with little particles. *Elements* 6, 395-400
- Naderi H, Majles Ara MH, Zebarjadan H, Saydi J, Javidan A (2013) Nonlinear response of nano-particles birnessite-type manganese oxide (γ -MnO₂). *Optik* 124, 1560-1563
- Nagar R, Sarkar D, Makris KC, Datta R (2014) Arsenic bioaccessibility and speciation in the soils amended with organo-arsenicals and drinking-water treatment residuals based on a long-term greenhouse study. *J Hydrol* 518C, 477-485
- Naseri E, Reyhanitabar A, Oustan S, Heydari AA, Alidokht L (2014) Optimization arsenic immobilization in a sandy loam soil using iron-based amendments by response surface methodology. *Geoderma* 232-234, 547-555
- Nelson YM, Lion LW, Ghiorse WC, Shuler ML (1999) production of biogenic Mn oxides by *Leptothrix* discophorass-1 in a chemically defined growth medium and evaluation of their Pb adsorption characteristics. *Appl Environ Microbiol* 65, 175-180
- Ng JC (2005) Environmental contamination of arsenic and its toxicological impact on humans. *Environ Chem* 2, 146-160
- Nielsen SS, Petersen L, Kjedsen P, Jakobsen R (2011) Amendment of arsenic and chromium polluted soil from wood preservation by iron residues from water treatment. *Chemosphere* 84, 383-389
- Noubactep C (2015) Metallic iron for environmental remediation: A review of reviews. *Water Res* 85, 114-123
- Nowack B, Bucheli TD (2007) Occurrence, behaviour and effects of nanoparticles in the environment. *Environ Pollut* 150, 5-22
- Ociński D, Jacukowicz-Sobala I, Mazur P, Raczyk J, Kociołek-Balawejder E (2016) Water treatment residuals containing iron and manganese oxides for arsenic removal from water – Characterization of physicochemical properties and adsorption studies. *Chem Eng J* 294, 210-221
- Okkenhaug G, Grasshorn Gebhardt KA, Amstaetter K, Bue HL, Herzel H, Mariussen E, Rossebø Almås A, Cornelissen G, Breedveld GD, Rasmussen G, Mulder J (2016) Antimony (Sb) and lead (Pb) in contaminated shooting range soils: Sb and Pb mobility and immobilization by iron based sorbents, a field study. *J Hazard Mater* 307, 336-343
- O'Reilly SE, Hochella MF (2003) Lead sorption efficiencies of natural and synthetic Mn and Fe-oxides. *Geochim Cosmochim Acta* 67, 4471-4487
- Oustriere N, Marchand L, Galland W, Gabbon L, Lottier N, Motelica M, Mench M (2016) Influence of biochars, compost and iron grit, alone and in combination, on copper solubility and phytotoxicity in a Cu-contaminated soil from a wood preservation site. *Sci Total Environ* 566-567, 816-825

- Pal S, Tak YK, Song JM (2007) Does the antibacterial activity of silver nanoparticles depend on the shape of the nanoparticle? A study of the gramnegative bacterium *Escherichia coli*. *Appl Environ Microbiol* 73, 1712-1720
- Pantsar-Kallio M, Reinikainen SP, Oksanen M (2001) Interactions of soil components and their effects on speciation of chromium in soils. *Anal Chim Acta* 439, 9-17
- Parkhurst DL, Appelo CAJ (2013) Description of input and examples for PHREEQCversion 3–A computer program for speciation, batch-reaction, one-dimensional transport, and inverse geochemical calculations, U.S. Geol. Surv. Tech. Methods, book 6, chap. A43.
- Paul EA (ed.) (2007) *Soil Microbiology and Biochemistry*, 3rd edition. Elsevier.
- Peña J, Bargar JR, Sposito G (2015) Copper sorption by the edge surfaces of synthetic birnessite nanoparticles. *Chem Geol* 396, 196-207
- Pickering WF (1986) Metal ion speciation - soils and sediments (a review). *Ore Geol Rev* 1, 83-146
- Post JE (1999) Manganese oxide minerals: Crystal structures and economic and environmental significance. *Proc Natl Acad Sci USA* 96, 3447-3454
- Prélot B, Poinignon C, Thomas F, Schouller E, Villiéras F (2003) Structural-chemical disorder of manganese dioxides 1. Influence on surface properties at the solid-electrolyte interface. *J Colloid Interface Sci* 257, 77-84
- Pueyo M, López-Sánchez JF, Rauret G (2004) Assessment of CaCl₂, NaNO₃ and NH₄NO₃ extraction procedures for the study of Cd, Cu, Pb and Zn extractability in contaminated soils. *Anal Chim Acta* 504, 217-226
- Pulford I, Watson C (2003) Phytoremediation of heavy metal-contaminated land by trees – a review. *Environ Int* 29, 529-540
- Qin Q, Wang Q, Fu D, Ma J (2011) An efficient approach for Pb(II) and Cd(II) removal using manganese dioxide formed in situ. *Chem Eng J* 172, 68-74
- Quevauviller P (1998) Operationally defined extraction procedures for soil and sediment analysis I. Standardization. *Trends Anal Chem* 17, 289-298
- Rahman MA, Hasegawa H (2011) High levels of inorganic arsenic in rice in areas where arsenic-contaminated water is used for irrigation and cooking. *Sci Total Environ* 409, 4645-4655
- Rauret G (1998) Extraction procedures for the determination of heavy metals in contaminated soil and sediment. *Talanta* 46, 449-455
- Rauret G, Lopez-Sanchez JF, Sahuquillo A, Barahona E, Lachica M, Ure AM, Davidson CM, Gomez A, Luck D, Bacon J, Yli-Halla M, Muntau H, Quevauviller P (2000) Application of a modified BCR sequential extraction (three-step) procedure for the determination of extractable trace metal contents in a sewage sludge amended soil

- reference material (CRM 483), complemented by a three-year stability study of acetic acid and EDTA extractable metal content. *J Environ Monit* 2, 228-233
- Reeder RJ, Schoonen MAA, Lanzirotti A (2006) Metal speciation and its role in bioaccessibility and bioavailability. *Rev Mineral Geochem* 64, 59-113
- Renella G, Landi L, Ascher J, Ceccherini MT, Pietramellara G, Mench M, Nannipieri P (2008) Long-term effects of aided phytostabilisation of trace elements on microbial biomass and activity, enzyme activities, and composition of microbial community in the Jales contaminated mine spoils. *Environ Pollut* 152, 702-712
- Rivelli AR, De Maria S, Puschenreiter M, Gherbin P (2012) Accumulation of cadmium, zinc, and copper by *Helianthus annuus* L.: impact on plant growth and uptake of nutritional elements. *Int j Phytoremediation* 14, 320-334
- Rogers JE, Li SW (1985) Effects of metals and other inorganic ions on soil microbial activity: soil DH assay as a simple toxicity test. *Bull Environ Contam Toxicol* 34, 858-865
- Rout G, Das P (2003) Effect of metal toxicity on plant growth and metabolism: I. Zinc. *Agronom, EDP Sci* 23, 3-11
- Rudzinski W, Plazinski W (2006) Kinetics of solute adsorption at solid/solution interfaces: a theoretical development of the empirical pseudo-first and pseudo-second order kinetic rate equations, based on applying the statistical rate theory of interfacial transport. *J Phys Chem B* 110, 16514-16525
- Sadiq M (1997) Arsenic chemistry in soils: An overview of thermodynamic predictions and field observations. *Water Air Soil Pollut* 93, 117-136
- Salt DE, Pickering IJ, Prince RC, Gleba D, Dushenkov S, Smith RD, Raskin I (1997) Metal accumulation by aquacultured seedlings of Indian mustard. *Environ Sci Technol* 31, 1636 – 1644
- Scott MJ, Morgan JJ (1995) Reactions at oxides surfaces. 1. Oxidation of As(III) by synthetic birnessite. *Environ Sci Technol* 29, 1898-1905
- Semple KT, Doick KJ, Jones KC, Burauel P, Craven A, Harms H (2004) Defining bioavailability and bioaccessibility of contaminated soil and sediment is complicated. *Environ Sci Technol* 38, 228-231
- Sharma VK, Sohn M (2009) Aquatic arsenic: Toxicity, speciation, transformations, and remediation. *Environ Int* 35, 743-759
- Sharmasarkar S, Vance GF (1997) Extraction and distribution of soil organic and inorganic selenium in coal mine environments of Wyoming, USA. *Environ Geol* 29, 17-22
- Shi W, Shao H, Li H, Shao M, Du S (2009) Progress in the remediation of hazardous heavy metal-polluted soils by natural zeolite. *J Hazard Mater* 170, 1-6

- Shi J, Tang Z, Jin Z, Chi Q, He B, Jiang G (2003) Determination of As(III) and As(V) in soils using sequential extraction combined with flow injection hydride generation atomic fluorescence detection. *Anal Chim Acta* 477, 139-147
- Shuto R (2005) *Encyclopedia of Toxicology (Second Edition)*, Editor in Chief Philip Wexler. Elsevier.
- Simenyuk GY, Zakharov YA, Pavelko NV, Dodonov VG, Pugachev VM, Puzynin AV, Manina TS, Barnakov CN, Ismagilov ZR (2015) Highly porous carbon materials filled with gold and manganese oxide nanoparticles for electrochemical use. *Catal Today* 249, 220-227
- Singh R, Singh S, Parihar P, Singh VP, Prasad SM (2015) Arsenic contamination, consequences and remediation techniques: A review. *Ecotoxicol Environ Saf* 112, 247-270
- Singh M, Thanh DN, Ulbrich P, Strnadová N, Štěpánek F (2010) Synthesis, characterization and study of arsenate adsorption from aqueous solution by α - and δ -phase manganese dioxide nanoadsorbents. *J Solid State Chem* 183, 2979-2986
- Smith AH, Hopenhayn-Rich C, Bates MN, Goeden HM, Hertz-Picciotto IH, Duggan HM, Wood R, Kosnett MJ, Smith MT (1992) Cancer risks from arsenic in drinking water. *Environ Health Perspect* 97, 259-267
- Smolders E, Oorts K, Peeters S, Lanno R, Cheyens K (2015) Toxicity in lead salt spiked soils to plants, invertebrates and microbial processes: Unraveling effects of acidification, salt stress and ageing reactions. *Sci Total Environ* 536, 223-231
- Soares MAR, Quina MJ, Quinta-Ferreira RM (2015) Immobilisation of lead and zinc in contaminated soil using compost derived from industrial eggshell. *J Environ Manag* 164, 137-145
- Sposito G (2008) *The Chemistry of Soils*. Oxford University Press, Oxford, UK
- Spuller C, Weigand H, Marb C (2007) Trace element stabilisation in a shooting range soil: mobility and phytotoxicity. *J Hazard Mater* 141, 378-387
- Stefaniuk M, Oleszczuk P, Ok YS (2016) Review on nano zerovalent iron (nZVI): From synthesis to environmental applications. *Chem Eng J* 287, 618-632
- Steinnes E (2013) in Alloway B.J. (ed.) *Heavy Metals in Soils. Trace Metals and Metalloids in Soils and their Bioavailability*. Third edition. Springer Dordrecht Heidelberg New York London.
- Sun Y, Sun G, Xu Y, Liu W, Liang X, Wang L (2016) Evaluation of the effectiveness of sepiolite, bentonite, and phosphate amendments on the stabilization remediation of cadmium-contaminated soils. *J Environ Manag* 166, 204-210
- Sutherland RA, Tack FMG (2002) Determination of Al, Cu, Fe, Mn, Pb and Zn in certified reference materials using the optimized BCR sequential extraction procedure. *Anal Chim Acta* 454, 249-257

- Tan KH (2011) Principles of Soil Chemistry, Fourth Edition. CRC Press.
- Tang SCN, Lo IMC (2013) Magnetic nanoparticles: essential factors for sustainable environmental applications. *Water Res* 47, 2613-2632
- Tebo BM, Ghiorse WC, van Waasbergen LG, Siering PL, Caspi R (1997) Bacterially mediated mineral formation: Insights into manganese(II) oxidation from molecular genetic and biochemical studies. *Rev Mineral Geochem* 35, 225-266
- Templeton DM, Ariese F, Cornelis R, Danielsson LG, Muntau H, Van Leeuwen HP, Łobiński R (2000) Guidelines for terms related to chemical speciation and fractionation of elements. Definitions, structural aspects, and methodological approaches (IUPAC Recommendations 2000). *Pure Appl Chem* 72, 1453-1470
- Teo BK (1986) EXAFS: Basic principles and data analysis. Springer-Verlag, Berlin Heidelberg New York Tokio
- Tessier A, Campbell PGC, Bisson M (1979) Sequential extraction procedure for the speciation of particulate trace metals. *Anal Chem* 51, 844-851
- Tiberg C, Kumpiene J, Gustafsson JP, Marsz A, Persson I, Mench M, Kleja DB (2016) Immobilization of Cu and As in two contaminated soils with zero-valent iron – Long-term performance and mechanisms. *Appl Geochem* 67, 144-152
- Tiller KG, Gerth J, Brümmer G (1984) The sorption of Cd, Zn and Ni by soil clay fractions: Procedures for partition of bound forms and their interpretation. *Geoderma* 34, 1-16
- Torri S, Lavado R (2009) Plant absorption of trace elements in sludge amended soils and correlation with soil chemical speciation. *J Hazard Mater* 166, 1459-1465
- Tosco T, Papini MP, Viggi CC, Sethi R (2014) Nanoscale zerovalent iron particles for groundwater remediation: a review. *J Clean Prod* 77, 10-21
- Trakal L, Komárek M, Száková J, Tlustoš P, Tejnecký V, Drábek O (2012) Sorption behavior of Cd, Cu, Pb and Zn and their interactions in phytoremediated soil. *Int J Phytoremediat* 14, 806-819
- Trakal L, Bingöl D, Pohořelý M, Hruška M, Komárek M (2014) Geochemical and spectroscopic investigations of Cd and Pb sorption mechanisms on contrasting biochars: engineering implications. *Bioresour Technol* 171, 442-451
- Trakal L, Veselská V, Šafařík I, Vítková M, Číhalová S, Komárek M (2016) Lead and cadmium sorption mechanisms on magnetically modified biochars. *Bioresour Technol* 203, 318-324
- Tratnyek PG, Johnson RL (2006). Nanotechnologies for environmental cleanup. *Nano Today* 1, 44-48
- Tsang DCW, Olds WE, Weber PA, Yip ACK (2013) Soil stabilisation using AMD sludge, compost and lignite. TCLP leachability and continuous acid leaching. *Chemosphere* 93, 2839-2847

- Tsang DCW, Yip ACK (2014). Comparing chemical-enhanced washing and wastebased stabilisation approach for soil remediation. *J Soils Sediments* 14, 936-947
- Tsang DCW, Zhang W, Lo IMC (2007) Copper extraction effectiveness and soil dissolution issues of EDTA-flushing of artificially contaminated soils. *Chemosphere* 68, 234-243
- Tuutijärvi T, Lu J, Sillanpää M, Chen G (2009) As(V) adsorption on maghemite nanoparticles. *J Hazard Mater* 166, 1415-1420
- Tyrovola K, Nikolaidis N (2009) Arsenic mobility and stabilization in topsoils. *Water Res* 43, 1589-1596
- United Nations (1998) Global opportunities for reducing use of leaded gasoline. Inter-Organization for the Sound Management of Chemicals/United Nations Environmental Program/CHEMICALS/98/9, Geneva, Switzerland
- US EPA Method 1312 (2000) Synthetic Precipitation leaching Procedure (SPLP) Leachate Chemistry Data for Solid Minewaste Composite Samples from Southwestern New Mexico, and Leadville, Colorado. U.S. Geological Survey.
- Van Herreweghe S, Swenne R, Cappuyns V, Vandecasteele C (2002) Chemical associations of heavy metals and metalloids in contaminated soils near former ore treatment plants: a differentiated approach with emphasis on pH stat-leaching. *J Geochem Explor* 76, 113-138
- Vangronsveld J, Cunningham SD (1998) Metal contaminated soil: In situ inactivation and phytoremediation. Springer.
- Verma HR (2007) Atomic and nuclear analytical methods. XRF, Mössbauer, XPS, NAA and ion-beam spectroscopic techniques. Springer-Verlag Berlin Heidelberg.
- Villaescusa I, Bollinger J-C (2008) Arsenic in drinking water: sources, occurrence and health effects (a review). *Rev Environ Sci Biotechnol* 7, 307-323
- Villalobos M, Bargar J, Sposito G (2005a) Mechanisms of Pb(II) sorption on a biogenic manganese oxide. *Environ Sci Technol* 39, 569-576
- Villalobos M, Bargar J, Sposito G (2005b) Trace metal retention on biogenic manganese oxide nanoparticles. *Elements* 1, 223-226
- Villalobos M, Escobar-Quiroz IN, Salazar-Camacho C (2014) The influence of particle size and structure on the sorption and oxidation behavior of birnessite: I. Adsorption of As(V) and oxidation of As(III). *Geochim Cosmochim Acta* 125, 564-581
- Wagner CD, Riggs WM, Davis IE, Moulder JF, Muilenberg GE (eds) (1979) Handbook of X-ray photoelectron spectroscopy. Perkin-Elmer Corporation, Minnesota, USA
- Wang P, Du M, Zhu H, Bao S, Yang T, Zou M (2015e) Structure regulation of silica nanotubes and their adsorption behaviors for heavy metal ions: pH effect, kinetics, isotherms and mechanism. *J Hazard Mater* 286, 533-544

- Wang Y, Feng X, Villalobos M, Tan W, Liu F (2012a) Sorption behavior of heavy metals on birnessite: relationship with its Mn average oxidation state and implications for types of sorption sites. *Chem Geol* 292–293, 25–34
- Wang SS, Gao B, Li YC, Mosa A, Zimmerman AR, Ma LQ, Harris WG, Migliaccio KW (2015a) Manganese oxide-modified biochars: preparation, characterization, and sorption of arsenate and lead. *Bioresour Technol* 181, 13–17
- Wang SS, Gao B, Li YC, Wan YS, Creamer AE (2015d) Sorption of arsenate onto magnetic iron-manganese (Fe-Mn) biochar composites. *RSC Adv* 5, 67971–67978
- Wang H, Gao B, Wang S, Fang J, Xue Y, Yang K (2015b) Removal of Pb(II), Cu(II), and Cd(II) from aqueous solutions by biochar derived from KMnO₄ treated hickory wood. *Bioresour Technol* 197, 356–362
- Wang X, He M, Lin C, Gao Y, Zheng L (2012b) Antimony(III) oxidation and antimony(V) adsorption reactions on synthetic manganite. *Chem Erde* 72, S4, 41–47
- Wang Y, Morin G, Ona-Nguema G, Juillot F, Calas G, Brown GE Jr (2011a) Distinctive arsenic(V) trapping modes by magnetite nanoparticles induced by different sorption processes. *Environ Sci Technol* 45, 7258–7266
- Wang S, Mulligan CN (2006) Natural attenuation processes for remediation of arsenic contaminated soils and groundwater. *J Hazard Mater B* 138, 459–470
- Wang S, Mulligan CN (2008) Speciation and surface structure of inorganic arsenic in solid phases: a review. *Environ Int* 34, 867–879
- Wang MC, Sheng GD, Qiu YP (2015c) A novel manganese-oxide/biochar composite for efficient removal of lead(II) from aqueous solutions. *Int J Environ Sci Technol* 12, 1719–1726
- Wang Y, Xionghan F, Villalobos M, Tan W, Liu F (2011b) Adsorption behaviour of heavy metals on birnessite: relationship with its Mn average oxidation state and implications for types of sorption sites. *Chem Geol* 292–293, 25–34
- Warren GP, Alloway BJ, Lepp NW, Singh B, Bochereau FJM, Penny C (2003) Field trials to assess the uptake of arsenic by vegetables from contaminated soils and soil remediation with iron oxides. *Sci Total Environ* 311, 19–33
- Watanabe J, Tani Y, Chang J, Miyata N, Naitou H, Seyama H (2013) As(III) oxidation kinetics of biogenic manganese oxides formed by *Acremonium strictum* strain KR21-2. *Chem Geol* 347, 227–232
- Wenzel WW, Kirchbaumer N, Prohaska T, Stingeder G, Lombi E, Adriano DC (2001a) Arsenic fractionation in soils using an improved sequential extraction procedure. *Anal Chim Acta* 436, 309–323
- Wenzel WW, Wieshammer G, Fitz WJ, Puschenreiter M (2001b) Novel rhizobox design to assess rhizosphere characteristics at high spatial resolution. *Plant Soil* 237, 37–45

- Wilkin RT, Ford RG (2006) Arsenic solid-phase partitioning in reducing sediments of contaminated wetland. *Chem Geol* 228, 156-174
- Woolson EA, Axley JH, Kearney PC (1971) Correlation between available soil arsenic, estimated by 6 methods, and response of corn (*Zea-mays* L.). *Soil Sci Soc Am Proc* 35, 101-107
- Wright DA, Welbourn P (2002) *Environmental Toxicology*. Cambridge University Press, Cambridge.
- Wu P-Y, Jia Y, Jiang Y-P, Zhang Q-Y, Zhou S-S, Fang F, Peng D-Y (2014) Enhanced arsenate removal performance of nanostructured goethite with high content of surface hydroxyl groups. *J Environ Chem Eng* 2:2312–20
- Wu D, Sun S (2016) Speciation analysis of As, Sb and Se. *Trends Environ Anal Chem* 11, 9-22
- Xenidis A, Stouraiti C, Papassiopi N (2010) Stabilization of Pb and As in soils by applying combined treatment with phosphates and ferrous iron. *J Hazard Mater* 177, 929-937
- Yan L, Kong L, Qu Z, Li L, Shen G (2015) Magnetic biochar decorated with ZnS nanocrystals for Pb(II) removal. *ACS Sustainable Chem Eng* 3, 125-132
- Yang S, Liao B, Yang Z, Chai L., Li J (2016) Revegetation of extremely acid mine soils based on aided phytostabilization: A case study from southern China. *Sci Total Environ* 562, 427-434
- Yang L, Watts DJ (2005) Particle surface characteristics may play an important role in phytotoxicity of alumina nanoparticles. *Toxicol Lett* 158, 122-132
- Yari M, Rajabi M, Moradi O, Yari A, Asif M, Agarwal S, Gupta VK (2015) Kinetics of the adsorption of Pb(II) ions from aqueous solutions by graphene oxide and thiol functionalized graphene oxide. *J Mol Liq* 209, 50-57
- Yean S, Cong L, Yavuz CT, Mayo JT, Yu WW, Kan AT, Colvin VL, Tomson MB (2005) Effect of magnetite particle size on adsorption and desorption of arsenite and arsenate. *J Mater Res* 20, 3255-3264
- Yim MH, Joo SJ, Nakane K (2002). Comparison of field methods for measuring soil respiration: a static alkali absorption method and two dynamic closed chamber methods. *For Ecol Manag* 170, 189-197
- Yin H, Zhu J (2016) In situ remediation of metal contaminated lake sediment using naturally occurring, calcium-rich clay mineral-based low-cost amendment. *Chem Eng J* 285, 112-120
- Ying SC, Kocar BD, Fendorf S (2012) Oxidation and competitive retention of arsenic between iron- and manganese oxides. *Geochim Cosmochim Acta* 96, 294-303

- Ying SC, Kocar BD, Griffis DD, Fendorf S (2011) Competitive microbially and Mn oxide mediated redox processes controlling arsenic speciation and partitioning. *Environ Sci Technol* 45, 5572-5579
- Yirsaw BD, Megharaj M, Chen Z, Naidu R (2016) Environmental application and ecological significance of nano-zero valent iron. *J Environ Sci* 44, 88-98
- Yu Z, Zhou L, Huang Y, Song Z, Qiu W (2015) Effects of a manganese oxide-modified biochar composite on adsorption of arsenic in red soil. *J Environ Manag* 163, 155-162
- Zalewska M, Nogalska A (2014) Phytoextraction potential of sunflower and white mustard plants in zinc-contaminated soil. *Chilean J Agric Res* 74, 485-489
- Zaman MI, Mustafa S, Khan S, Xing B (2009) Heavy metal desorption kinetics as affected by anions complexation onto manganese dioxide surfaces. *Chemosphere* 77, 747-755.
- Zhang X, Miao W, Li C, Sun X, Wang K, Ma Y (2015) Microwave-assisted rapid synthesis of birnessite-type MnO₂ nanoparticles for high performance supercapacitor applications. *Mater Res Bull* 71, 111-115
- Zhang L, Qin X, Tang J, Liu W, Yang H (2016) Review of arsenic geochemical characteristics and its significance on arsenic pollution studies in karst groundwater, Southwest China. *Appl Geochem* In press. doi:10.1016/j.apgeochem.2016.05.014
- Zhang G, Qu J, Liu H, Liu R, Qu J (2009) Adsorption behavior and mechanism of arsenate at Fe–Mn binary oxide/water interface. *J Hazard Mater* 168, 820-825
- Zhang G, Qu J, Liu H, Liu R, Wu R (2007) Preparation and evaluation of a novel Fe–Mn binary oxide adsorbent for effective arsenite removal. *Water Res* 41, 1921-1928
- Zhang G, Qu J, Liu H, Qu J, Jefferson W (2012) Arsenate uptake and arsenite simultaneous sorption and oxidation by Fe–Mn binary oxides: Influence of Mn/Fe ratio, pH, Ca²⁺, and humic acid. *J Colloid Interface Sci* 366, 141-146
- Zhao X, Liu W, Cai Z, Han B, Qian T, Zhao D (2016) An overview of preparation and applications of stabilized zero-valent iron nanoparticles for soil and groundwater remediation. *Water Res* 100, 245-266
- Zhou D, Kim DG, Ko SO (2015) Heavy metal adsorption with biogenic manganese oxides generated by *Pseudomonas putida* strain MnB1. *J Ind Eng Chem* 24, 132-139
- Zhu Q, Li Z (2015) Hydrogel-supported nanosized hydrous manganese dioxide: Synthesis, characterization, and adsorption behavior study for Pb²⁺, Cu²⁺, Cd²⁺ and Ni²⁺ removal from water. *Chem Eng J* 281, 69-80
- Zhu M, Paul KW, Kubicki JD, Sparks DL (2009) Quantum chemical study of arsenic (III, V) adsorption on Mn-oxides: Implications for arsenic(III) oxidation. *Environ Sci Technol* 43, 6655-6661

**Curriculum vitae
&
List of publications**

Zuzana Michálková

Born: 4th December, 1987, Cheb (Czech Republic)

Address: Mimoňská 627, 19000, Prague 9, Czech Republic

E-mail: michalkovaz@fzp.czu.cz

Education

- 2012 – present: Ph.D. studies
Applied and landscape ecology, Faculty of Environmental Sciences
Czech University of Life Sciences, Prague, Czech Republic
Thesis: *The use of (nano)oxides for metal and metalloid stabilization in contaminated soils*
- 2010 – 2012: Master programme
Sustainable Biosphere Development, Faculty of Agrobiolgy, Food and Natural Resources
Czech University of Life Sciences, Prague, Czech Republic
Thesis: *Bioavailability of Cu and main soil cations in contaminated soils amended with EDDS*
- 2007 – 2010: Bachelor programme
Sustainable Use of Natural Resources, Faculty of Agrobiolgy, Food and Natural Resources
Czech University of Life Sciences, Prague, Czech Republic
Thesis: *Use of fast-growing trees for phytoremediation of soils contaminated with metals*

Publications

- Michálková Z.**, Komárek M., Veselská V., Číhalová S. (2016) Selected Fe and Mn (nano)oxides as perspective amendments for the stabilization of As in contaminated soils. *Environmental Science and Pollution Research* 23: 10841-10854.
- Martínez-Fernández, D., Vítková, M., **Michálková, Z.**, Komárek, M. (2016) Engineered nanomaterials for phytoremediation of metal/metalloids contaminated soils: implications for plant physiology. In: Anasari A.A., Gill S.S., Gill R., Lanza G.R., Newman L. (eds.): *Phytoremediation: Management of Environmental Contaminants Vol. 5*, Springer International Publishing Switzerland. In press.
- Vítková M., Rákosová S., **Michálková Z.**, Komárek M. (2016) Metal(loid)s behaviour in soils amended with nano zero-valent iron as a function of pH and time. *Journal of Environmental Management*, in press, <http://dx.doi.org/10.1016/j.jenvman.2016.06.003>.
- Ettler V., Tomášová Z., Komárek M., Mihaljevič M., Šebek O., **Michálková Z.** (2015) The pH-dependent long-term stability of an amorphous manganese oxide in smelter-polluted soils: Implication for chemical stabilization of metals and metalloids. *Journal of Hazardous Materials* 286: 386-394.
- Michálková Z.**, Komárek M., Šillerová H., Della Puppa L., Joussein E., Bordas F., Vaněk A., Vaněk O., Ettler V. (2014) Evaluating the potential of three Fe- and Mn-(nano)oxides for the stabilization of Cd, Cu and Pb in contaminated soils. *Journal of Environmental Management* 146: 226-234.
- Komárek M., **Michálková Z.**, Száková J., Vaněk A., Grygar T. (2011) Evolution of bioavailable copper and major soil cations in contaminated soils treated with ethylenediaminedisuccinate: A two-year experiment. *Bulletin of Environmental Contamination and Toxicology* 86: 525-530.

Submitted articles and manuscripts in preparation

Micháلكová Z., Komárek M., Vítková M., Řečínská M., Ettler V. (2016) Stability, transformations and stabilizing potential of an amorphous manganese oxide and its surface-modified form in contaminated soils. Manuscript submitted to Applied Geochemistry.

Micháلكová Z., Martínez-Fernández D., Komárek M. (2016) The application of an amorphous manganese oxide effectively reduces metal(loid) uptake by sunflower (*Helianthus annuus* L.). Manuscript in preparation.

Trakal L., **Micháلكová Z.**, Piqueras Barceló A., Vítková M., Komárek M. (2016) Biochar coated by amorphous manganese oxide efficiently remove various metal(loid)s from aqueous solution. Manuscript in preparation.

Grants and projects

- Co-worker on grant: Stabilization of metals/metalloids in contaminated soils using novel synthetic manganese oxide: Comparison with other stabilizing amendments.

P503/11/0840 (Czech Science Foundation)

- Co-worker on grant: Modelling the competitive adsorption of metals and As onto Fe-nanooxides: Implications for soil remediation

15-07117S (Czech Science Foundation)

- Principal investigator on grant: The use of (nano)oxides for metal and metalloid stabilization in contaminated soils

CIGA 20134209 (Czech University of Life Sciences)

- Co-investigator on grant: Synthesis and use of innovative adsorbents for stabilization of metals and metalloids in contaminated soils

CIGA 20154202 (Czech University of Life Sciences)

- Co-investigator on grant: Simulation of Zn sorption processes in soil using geochemical modelling

IGA 4240013123159 (Internal Grant Agency of the Faculty of Environmental Sciences, CULS Prague)

Teaching activities

- Environmental Soil Chemistry – laboratory course
- Supervision of 14 bachelor theses